designs

MDPI

*Article*

# Strength of Composite Columns Consists of Welded Double CF Sigma-Sections Filled with Concrete—An Experimental Study

**Mohamed A. Reda [1,2], Ahmed M. Ebid [2,*], Sherif M. Ibrahim [1] and Mohamed A. El-Aghoury [1]**

[1] Structural Engineering Department, Faculty of Engineering, Ain Shams University, Cairo 11535, Egypt
[2] Structural Engineering & Construction Management Department, Faculty of Engineering & Technology, Future University in Egypt, Cairo 11865, Egypt
* Correspondence: ahmed.abdelkhaleq@fue.edu.eg

**Abstract:** In-filled tubes section is a very successful configuration for axially loaded members such as columns and struts. Steel shell tube filled with concrete has many advantages, such as eliminating the need for shuttering, reinforcement bars or ties besides increasing both flexural and axial capacities and enhancing the ductility. The main disadvantage of in-filled tubes is the need for a shell thick enough to prevent the local buckling and hence the local decomposition. Previous studies tried to solve this problem using intermediate stiffeners or shear connectors. This research presents another approach to solve this problem using double cold-formed sigma-sections (face to face) as steel shell tubes. Sixteen specimens with different lengths, cross section dimensions and shell thicknesses were tested under both concentric and eccentric compression loads. Ultimate capacities, lateral deformations and normal strains were recorded. The theoretical capacities were calculated using AISC-LRDF-94, EN-1994-04 and CSI-COL software considering full composite action, and the deviations from the experimental results were 24%, 24% and 13%, respectively.

**Keywords:** cold formed; composite columns; sigma sections; in-filled column

**Citation:** Reda, M.A.; Ebid, A.M.; Ibrahim, S.M.; El-Aghoury, M.A. Strength of Composite Columns Consists of Welded Double CF Sigma-Sections Filled with Concrete—An Experimental Study. *Designs* **2022**, *6*, 82. https://doi.org/10.3390/designs6050082

Academic Editor: Farshid Aram

Received: 23 August 2022
Accepted: 13 September 2022
Published: 21 September 2022



## 1. Introduction

Composite steel and concrete members, such as Concrete-filled Steel Tubes (CFST), have been widely used since the early decades of the 20th century in constructing both buildings and bridges [1]. Combining the high tensile strength of steel with the high compressive strength of concrete gives the (CTSF) members the advantages of low cost, high ductility and hence high performance under seismic loads [2,3]. Several research studies were carried out to study the behavior (CFST) columns with different cross sections (circular, square and rectangular).

Lin et al., 2005 [4] carried out an experimental study using 50 (CFST) specimens to investigate the effect of cross-sectional shape (circular or square), dimensions, yield strength and local slenderness ratio (D/t) on the axial capacity of the column. They developed an equation to predict the axial capacity considering the studied factors. The results of this research were valid for short columns only. Zhang and Guo, 2007, 2011 [5,6] tested 26 rectangular section (CFST) specimens with different slenderness ratios (L/r), aspect ratios (b/d), steel to concrete ratios (As/Ac) and relative eccentricity ratios (e/d) to figure out the effect of each parameter on the capacity of the column. They compared the test results with international codes. However, the study considered only rectangular sections. Bahrami et al., 2011 [7] presented a theoretical study using non-linear finite element analysis models to investigate the behavior and capacity of (CFST) columns under axial compressive loading. Different cross sections, number of stiffeners and thicknesses of steel sheets were tested to investigate their effects on both behavior and capacity. The study was concerned with square columns only. Ren et al., 2014 [8] tested 44 axially loaded short (CFST) columns with special cross sections (triangular, fan-shaped, D-shaped, 1/4 circular and semi-circular).

They reported the failure mode and ultimate capacity for each column, but their conclusions are valued for stub (short) columns only.

Double-tube composite sections were investigated by Wang et al., 2017 [9], Ding et al., 2019 [10] and Ci et al., 2020 [11]. They presented experimental studies to investigate the capacity of concrete-filled double-tube circular columns under axial compression loads considering the effect of concrete strength, yield strength, inner and outer tube thickness, and the ratio between the diameters of inner and outer tubes. The tested samples were simulated using 3D-FEM models, and the experimental results were compared with both numerical models and international design codes. The tested samples were only short circular and rectangular columns.

Cold-formed short, square composite columns were studied by Tao et al., 2009 [12]. They suggested a design procedure for stiffened concrete-filled thin-walled steel tubular columns based on experimental study results. They found that adding fibers to concrete can effectively increase ductility.

Stainless-steel shells were used instead of traditional steel shells in (CFST) members to increase the corrosion resistance and add some architectural effects. Young and Ellobody, 2005 [13] tested a number of rectangular cold-formed stainless-steel tubes filled with concrete under axial compression and suggested design recommendations for such short columns. Dai et al., 2020 [14] tested and analyzed the compressive behavior of 18 specimens of stainless-steel short and circular columns filled with concrete. He et al., 2020 [15] studied the buckling effect on slender circular (CFST) with stainless-steel shell and high-strength concrete using 12 experimental tests. They identified different failure modes and presented a set of load deformation curves. In the same context, Kazemzadeh et al., 2020 [16] presented a series of experimental and numerical investigations on the local and post local buckling of stainless-steel composite columns to investigate the axial slenderness limit of different column cross sections (box, circular and I-section).

El-Aghoury et al., 2016 [17,18] studied both the ultimate capacity and buckling behavior of axially loaded columns consisting of combined CFS sigma pure steel sections (empty shells). They used 3D numerical modeling to investigate both the global and local buckling behavior of the double sigma section.

This research presented a novel composite cross section that has never been tested before; this novel section consists of double cold-formed sigma-sections (face to face) filled with concrete. The aim of this study is to experimentally investigate the ultimate capacity of the previously described composite column considering the effect of the global slenderness ratio of the column (L/r), aspect ratio of the cross section (b/d), local slenderness ratio (c/t) and relative eccentricity ratio (e/d). Besides that, the experimental capacities were compared with theoretical capacities calculated using AISC-LRFD, EN-1994 and CSI-COL software, considering full composite action behavior.

## 2. Materials and Methods

### *2.1. Concrete*

Table 1 presents the mix proportions of the used concrete, where the fineness modulus of the used sand was 2.30 and the measured slump was 37 mm. Figure 1 summarizes the grain size distribution and the physical properties of both coarse and fine aggregates. The design strength of the concrete mix was 20 Mpa. The actual compressive cube strength and elastic modulus of concrete were measured by testing 150 mm size cubes and 150 × 150 × 300 mm size prisms, respectively. The average cube compressive strengths were 17.2 and 21.1 Mpa after 7 and 28 days, respectively. The measured concrete elastic modulus (Ec) after 28 days was 21.3 Gpa.

**Table 1.** The concrete mix proportions (by weight/$m^3$).

| Item | OPC Grade R42.5 | Coarse Aggregate (Crushed Stone) | Fine Aggregate (Natural Sand) | Potable Water |
|---|---|---|---|---|
| Unit | kg | kg | kg | Liter |
| Value | 250 | 1300 | 650 | 125 |

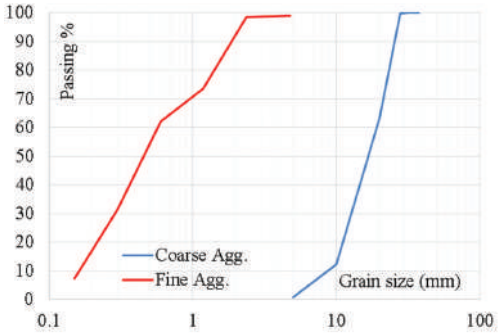


**Figure 1.** Grain size distribution of fine and coarse aggregates.

*2.2. Steel*

All sigma sections were fabricated using 1.5, 2.0 and 2.5 mm thick steel sheets. Three coupon samples for each thickness were tested according to ASTM E8 [19], using a displacement-controlled servo-hydraulic tensile testing machine. The loading rate was 0.8 mm/min to measure yield stress (Fy) and ultimate strength (Fu). Table 2 summarizes the test results.

**Table 2.** Steel properties.

| Sample | Thickness (mm) | Fy (Mpa) | Fu (Mpa) |
|---|---|---|---|
| 1 | 1.5 | 336 | 445 |
| 2 | 2.0 | 329 | 438 |
| 3 | 2.5 | 322 | 431 |

*2.3. Test Specimens*

The experimental program was designed to study the effect of global slenderness ratio (λ), local slenderness ratio (c/t), aspect ratio (d/b) and load eccentricity ratio (e/d), where © is the longest straight portion of the steel shell. Accordingly, 16 specimens were fabricated and tested in the labs of the Housing and Building National Research Center (HBRC), Giza, Egypt. Each specimen consists of two cold-formed sigma sections welded face to face using a single bevel butt weld and filled with concrete. The specimen's dimensions were selected within the shown ranges in Table 3.

**Table 3.** Considered values for studied variables.

| Variable | Considered Values |
|---|---|
| Column height (L) | 1000, 2000 and 2500 mm |
| Cross section depth (d) | 100, 150 and 200 mm |
| Load eccentricity ratio (e/d) | 0.00, 0.125 and 0.25 |
| Steel shell thickness (t) | 1.5, 2.0 and 2.5 mm |

All specimens have the same cross section width (b) of 100 mm. Table 4 summarizes the configurations of each specimen, while Figure 2 shows the specimens manufacturing process and all fabricated steel shells tube.

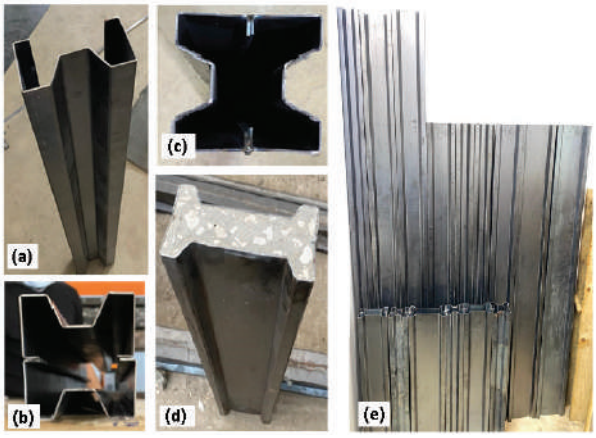


**Figure 2.** Specimens manufacturing process (**a**) Forming sigma sections, (**b**) assembling column section, (**c**) welding the two stigmas, (**d**) casting concrete and (**e**) all fabricated steel shells.

**Table 4.** Summary of tested specimens' configurations.

| Spec. ID | L (mm) | b (mm) | d (mm) | t (mm) | c (mm) | e (mm) | $r_{min}$ (mm) | $\lambda_{max}$ | d/b | c/t | e/d |
|---|---|---|---|---|---|---|---|---|---|---|---|
| 1 | 2500 | 100 | 150 | 1.5 | 75 | 37.5 | 29 | 86 | 1.5 | 50 | 0.25 |
| 2 | 2500 | 100 | 100 | 2.0 | 50 | 12.5 | 32 | 78 | 1.0 | 25 | 0.13 |
| 3 | 2500 | 100 | 200 | 2.5 | 125 | 0.0 | 29 | 86 | 2.0 | 50 | 0.00 |
| 4 | 2500 | 100 | 150 | 2.5 | 75 | 0.0 | 31 | 82 | 1.5 | 30 | 0.00 |
| 5 | 2000 | 100 | 150 | 1.5 | 75 | 37.5 | 29 | 69 | 1.5 | 50 | 0.25 |
| 6 | 2000 | 100 | 200 | 1.5 | 125 | 25.0 | 28 | 72 | 2.0 | 83 | 0.13 |
| 7 | 2000 | 100 | 100 | 2.0 | 50 | 0.0 | 32 | 63 | 1.0 | 25 | 0.00 |
| 8 | 2000 | 100 | 150 | 2.5 | 75 | 37.5 | 31 | 66 | 1.5 | 30 | 0.25 |
| 9 | 2000 | 100 | 100 | 2.5 | 50 | 12.5 | 32 | 62 | 1.0 | 20 | 0.13 |
| 10 | 2000 | 100 | 200 | 2.5 | 125 | 0.0 | 29 | 69 | 2.0 | 50 | 0.00 |
| 11 | 1000 | 100 | 100 | 2.0 | 50 | 25.0 | 32 | 31 | 1.0 | 25 | 0.25 |
| 12 | 1000 | 100 | 150 | 1.5 | 75 | 20.0 | 29 | 34 | 1.5 | 50 | 0.13 |
| 13 | 1000 | 100 | 100 | 1.5 | 50 | 0.0 | 31 | 32 | 1.0 | 33 | 0.00 |
| 14 | 1000 | 100 | 150 | 2.0 | 75 | 0.0 | 30 | 33 | 1.5 | 38 | 0.00 |
| 15 | 1000 | 100 | 100 | 2.5 | 50 | 12.5 | 32 | 31 | 1.0 | 20 | 0.13 |
| 16 | 1000 | 100 | 200 | 2.5 | 125 | 25.0 | 29 | 34 | 2.0 | 50 | 0.13 |

### *2.4. Test Setup and Instrumentation*

Each specimen was equipped with two strain gauges at mid height of the column on the 100 mm width faces measuring the maximum and minimum axial strains due to concentric and eccentric loads. In addition, two LVTDs were used to measure the lateral deformations at mid height of the column in both major and minor directions of the cross section. Finally, the testing frame is equipped with a load cell to measure the applied load. Figure 3 illustrates test setup and instrumentation.

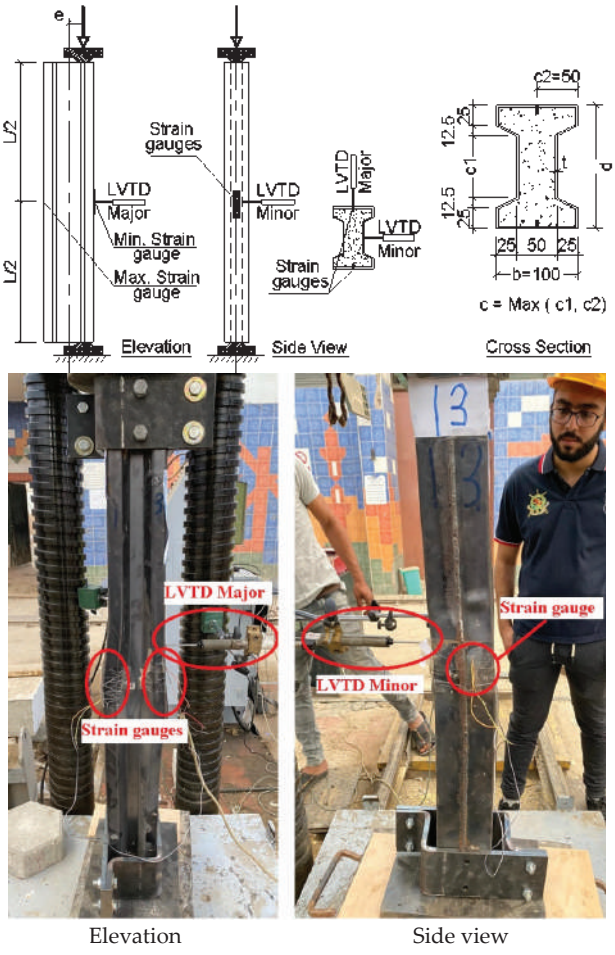


**Figure 3.** Testing setup, instrumentation and typical dimensions of specimen cross section.

*2.5. Test Procedure*

All specimens were tested under axial compression (concentric or eccentric) load up to failure using an AMSLER compression testing machine with 5000 kN capacity. To ensure full contact between the column head and loading plate, the top and bottom 20 mm was cut from each specimen using a concrete saw to obtain a smooth and leveled loading surface.

Two-ball seats were welded to the upper and lower steel loading heads at the required eccentricity to achieve the hinged support. The lower ball seating was fixed to the lower machine head to prevent any displacement of the specimens during testing. The upper plate is allowed to rotate around a fixed sphere. This ensures that the applied load is always passing through the desired location (concentric or eccentric) and perpendicular to the specimen cross section. The specimens were loaded up to failure with a loading rate of 50 kN per minute.

## 3. Experimental Results

For each specimen, failure load, failure mode, maximum lateral deformations and axial strains were recorded as summarized in Table 5, where LVTD minor and major readings are the lateral movements of the mid-height specimen in minor and major cross section axis,

respectively. Negative strain and positive strain values correspond to compressive stresses and tensile stresses, respectively. Figure 4 shows the failure modes of tested specimens.

**Table 5.** Summary of experimental program results.

| Spec. ID | P Exp | Δ Minor Measured | Δ Minor Calc. | Δ Major Measured | Δ Major Calc. | Strain-Min | Strain-Max | Mode of Failure |
|---|---|---|---|---|---|---|---|---|
| | (KN) | (mm) | (mm) | (mm) | (mm) | (με) | (με) | |
| 1 | 226 | **18** | **25** | 5 | 20 | −1062 | 10 | GB |
| 2 | 233 | **40** | **21** | **53** | **6** | −935 | −329 | GB, F |
| 3 | 394 | **29** | **25** | 7 | 0 | −731 | −661 | GB |
| 4 | 464 | **28** | **23** | 2 | 0 | −968 | −891 | GB |
| 5 | 243 | 3 | 16 | **13** | **14** | −952 | −293 | F |
| 6 | 353 | 3 | 18 | 7 | 12 | −1080 | −373 | LB |
| 7 | 285 | **31** | **13** | 15 | 0 | −807 | −788 | GB, F |
| 8 | 383 | **29** | **14** | **19** | **15** | **−1709** | −2 | GB, F and C |
| 9 | 442 | 1 | 13 | **29** | **6** | **−1497** | −518 | F, C |
| 10 | 580 | **79** | **16** | 68 | 0 | −937 | −922 | GB, F |
| 11 | 278 | 2 | 3 | **9** | **3** | **−1611** | 16 | F, C |
| 12 | 350 | 1 | 4 | **2** | **3** | −1260 | −371 | F |
| 13 | 324 | **4** | **3** | 1 | 0 | −935 | −827 | GB |
| 14 | 405 | **3** | **3** | 1 | 0 | −913 | −891 | GB |
| 15 | 451 | 2 | 3 | **7** | **2** | **−1749** | −519 | F, C |
| 16 | 586 | **8** | **4** | **6** | **4** | −1028 | −881 | GB, F |

GB: global buckling; LB: local buckling; C: compression failure; F: flexural failure.

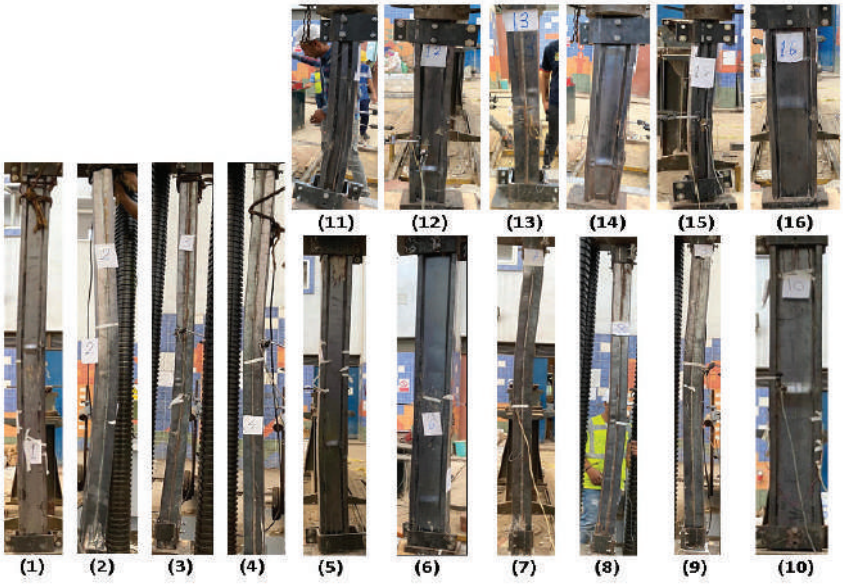


**Figure 4.** Failure modes of tested specimens.

The failure mode of each specimen was investigated based on the measured axial strains and lateral deformations as follows:

- The lateral deformation due to eccentricity (in major direction) is estimated for each specimen using Equation (1):

$$\Delta_{major} = \frac{P_{exp}\, e\, L^2}{8\, EI} \quad (1)$$

where (EI) is the fully bonded composite flexural stiffness; hence, if the measured Δ-major was close to or exceeded this value, that indicated flexural failure.

- The lateral deformation due to global buckling (in a minor direction) is estimated for each specimen using Equation (2):

$$\Delta_{minor} = \frac{\lambda^2 \, b}{30,000} \tag{2}$$

where (λ) is the fully bonded composite global slenderness ratio. If the measured Δ-minor was near or more than this value, that indicated global buckling failure.

- Yield strain equals (Fy/Es) which is (0.33/210 = 1570 μ-strain). If the minimum measured strain was within this range or more, this value indicated overstressing failure.
- Finally, if none of the above conditions occurred, this indicated a local buckling failure.

The marked numbers in Table 5 illustrate the critical values used in classifying the failure mode.

## 4. Theoretical Analysis

The ultimate capacities of the 16 tested columns were estimated according to the AISC-LRFD-94 code [20] and EN-1994-04 code [21] using the well-known CSI-COL. The capacities from the three theoretical methods were compared to experimental capacities. Table 6 summarizes these results.

**Table 6.** Summary of theoretical analysis results.

| Spec. | EXP. | AISC | Error | EN-1994 | Error | CSI-COL. | Error |
|---|---|---|---|---|---|---|---|
| ID | (kN) | (kN) | (%) | (kN) | (%) | (kN) | (%) |
| 1 | 226.0 | 172.0 | −24% | 225.0 | 0% | 246.0 | 9% |
| 2 | 233.0 | 233.0 | 0% | 284.0 | 22% | 253.0 | 9% |
| 3 | 394.0 | 393.0 | 0% | 489.0 | 24% | 422.0 | 7% |
| 4 | 464.0 | 365.0 | −21% | 423.0 | −9% | 404.0 | −13% |
| 5 | 243.0 | 268.0 | 10% | 300.0 | 23% | 263.0 | 8% |
| 6 | 353.0 | 310.0 | −12% | 354.0 | 0% | 392.0 | 11% |
| 7 | 285.0 | 329.0 | 8% | 347.0 | 13% | 328.0 | 7% |
| 8 | 383.0 | 351.0 | −8% | 324.0 | −15% | 379.0 | −1% |
| 9 | 442.0 | 336.0 | −24% | 350.0 | −21% | 431.0 | −2% |
| 10 | 580.0 | 539.0 | −7% | 570.0 | −2% | 516.0 | −11% |
| 11 | 278.0 | 301.0 | 8% | 250.0 | −10% | 269.0 | −3% |
| 12 | 350.0 | 343.0 | −2% | 332.0 | −5% | 343.0 | −2% |
| 13 | 324.0 | 328.0 | 1% | 350.0 | 8% | 332.0 | 3% |
| 14 | 405.0 | 494.0 | 9% | 517.0 | 14% | 496.0 | 9% |
| 15 | 451.0 | 406.0 | −10% | 385.0 | −15% | 400.0 | −11% |
| 16 | 586.0 | 690.0 | 18% | 714.0 | 22% | 655.0 | 12% |

### *4.1. AISC-LRFD-94 Code*

The design philosophy of this code depends on estimating the equivalent strength of the composite column ($F_{ym}$) and equivalent elastic modulus ($E_m$), as shown in Equations (3) and (4), while the equivalent radius of gyration is the same as an empty steel shell.

$$F_{ym} = F_y + c_1 \, f_{yr} \, (A_r/A_s) + c_2 \, F_c \, (A_c/A_s) \tag{3}$$

$$E_m = E_s + c_3 \, E_c \, (A_c/A_s) \tag{4}$$

where

- $f_s$ and $A_s$ are yield strength and cross sectional area of steel section
- $F_c$ and $A_c$ are compressive strength and cross sectional areas of concrete
- $f_{yr}$ and $A_r$ are yield strength and cross sectional area of reinforcement bars
- $c_1 = 1.00$, $c_2 = 0.68$ and $c_3 = 0.40$ for in-filled composite columns.

For a small eccentric load, where the vertical load is more than 20% of the axial capacity of the section, the well-known interaction formula shown in Equation (5) is used.

$$(P/P_n) + 0.89\,(M_x/M_{xn}) + 0.89\,(M_y/M_{yn}) = 1.0 \quad (5)$$

where

- P, $M_x$ and $M_y$ are the actual vertical load and bending moments in X and Y directions
- $P_n$ is the axial capacity of a section considering buckling, as shown in Equations (6) and (7)
- $M_{xn}$ and $M_{yn}$ are the flexural capacity of column section in X and Y directions without axial load and considering plastic stress distribution

$$P_n = F_{cr}\,A_s \quad (6)$$

$$F_{cr-} = (1 - 0.348\,\lambda_m{}^2)\,F_{ym} \text{ for } \lambda_m \leq 1.1 \\ = 0.648\,F_{ym}/\lambda_m{}^2 \text{ for } \lambda_m > 1.1 \quad (7)$$

where

- $\lambda_m$ is the normalized slenderness ratio = $\frac{L\sqrt{(Fy/Em)}}{\pi r}$.

*4.2. EN-1994-04 Code*

Unlike the AICS-LRFD code, EN-1994 depends on drawing an interaction diagram for the composite section with vertical load, considering the buckling effect on *Y*-axis and the bending moment on *X*-axis, as shown in Figure 5a.

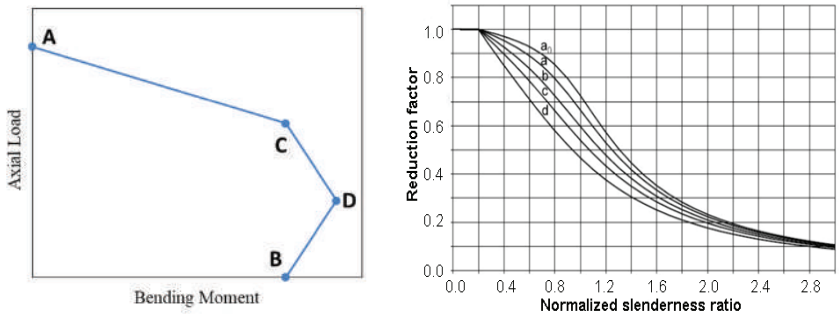


(**a**) (**b**)

**Figure 5.** (**a**) Typical interaction diagram of EN-1994. (**b**) Buckling reduction factor of EN-1994.

Point (A) presents the pure axial capacity of the composite section considering the buckling effect as shown in Equation (8)

$$P_n = X\,(0.85\,f_{c'}\,A_c + F_{yr}\,A_r + F_y\,A_s) \quad (8)$$

where X is the buckling reduction factor from curve "b" (for in-filled hollow sections) in Figure 5b.

Point (B) presents the pure plastic flexural capacity of the composite section without axial load. Point (C) has the same moment value as (B), and axial load equals the axial capacity of only the concrete section. Finally, point (D) has half the axial capacity of (C) and the plastic flexural capacity of the composite section, considering the effect of the corresponding axial load.

Once the interaction diagram is generated, the capacity of the section at a certain eccentricity could be determined by drawing a straight line from the origin with a slope equals to (N/M = 1/e) and finding its intersection with the interaction diagram.

*4.3. Using CSI-COL Software (Computers & Structures INC., California, USA)*

A 3D-interaction diagram (PMM-interaction diagram) was generated for each specimen using the well-known CSI-COL Ver. 6.2 software considering the built-in Mander model for unconfined concrete behavior and the built-in structural steel model. The stress–strain curve of the Mander model [22] is automatically generated for certain (fc′ and Ec) values, while the structural steel model requires (Fy and Fu) to generate the stress–strain curve. Figure 6 presents both the generated and the experimental stress–strain curves for steel and concrete and a typical 3D-interaction diagram.

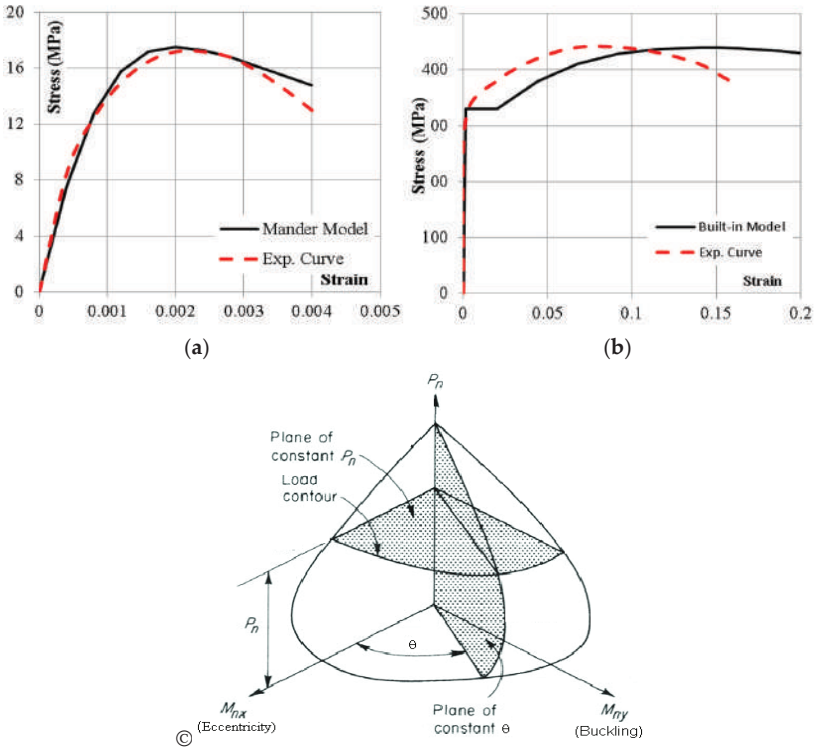


(**a**) (**b**)

(**c**) Typical 3D-inetraction diagram

**Figure 6.** Used material modes (**a**) for concrete, (**b**) for steel and (**c**) typical 3D interaction diagram.

In order to present both experimental and theoretical capacities graphically as shown in Figure 7, a certain section in the 3D interaction diagram is constructed. The angle of this section (θ) depends on the value of eccentricity moment ($M_{major} = P \times e$) and buckling moment ($M_{minor} = P \times \Delta_{minor}$), as shown in Equation (9):

$$\theta = \tan^{-1} (M_{minor}/M_{major}) \quad (9)$$

In the constructed 2D interaction diagram, the presented bending moment is the resultant moment as shown in Equation (10):

$$M_{result} = (M_{minor}{}^2 + M_{major}{}^2)^{0.5} \quad (10)$$

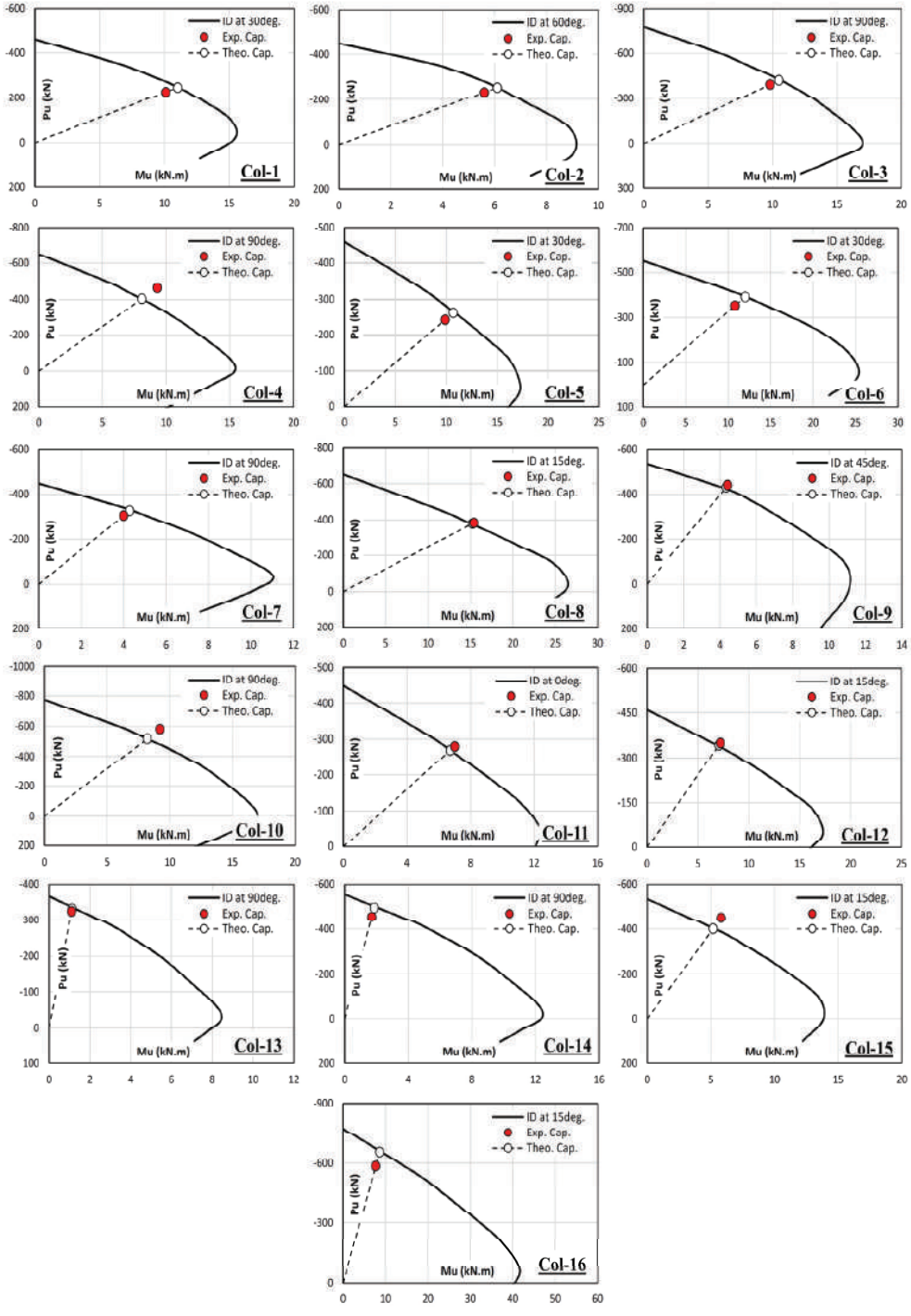


**Figure 7.** CSI-COL interaction diagrams for the tested specimens.

## 5. Discussion

The summarized experimental results in Section 3 included the measured failure loads, maximum lateral deformations, extreme axial strains and the investigated models of failure. However, in order to study the impact of each considered parameter on the axial capacity and failure mode, the reduction factor ($P_{exp}/P_{max}$) was calculated for each specimen, where $P_{max}$ is the maximum axial capacity of the composite section without considering the buckling effect as per Equation (11).

$$P_{max} = 0.85\, f_{c'}\, A_c + F_y\, A_s \quad (11)$$

Figure 8a presents the relation between the buckling reduction factor and the global normalized slenderness ratio for different relative eccentricities. The best fitting curves indicated the following:

- The reduction factor ($P_{exp}/P_{max}$) decreases with increasing the global normalized slenderness ratio regardless of the relative eccentricity.
- For centric loading (e/d = 0) the reduction factor ranged between 90% and 60% for global normalized slenderness ratio of 0.4–1.1, respectively, which matches (EN-1994) curve "b" in Figure 5b.
- For small eccentricity (e/d = 0.13), where the axial force acts inside the core of the section, the reduction factor is slightly less than the centric case, which indicates that plastic failure due to vertical load dominates the behavior.

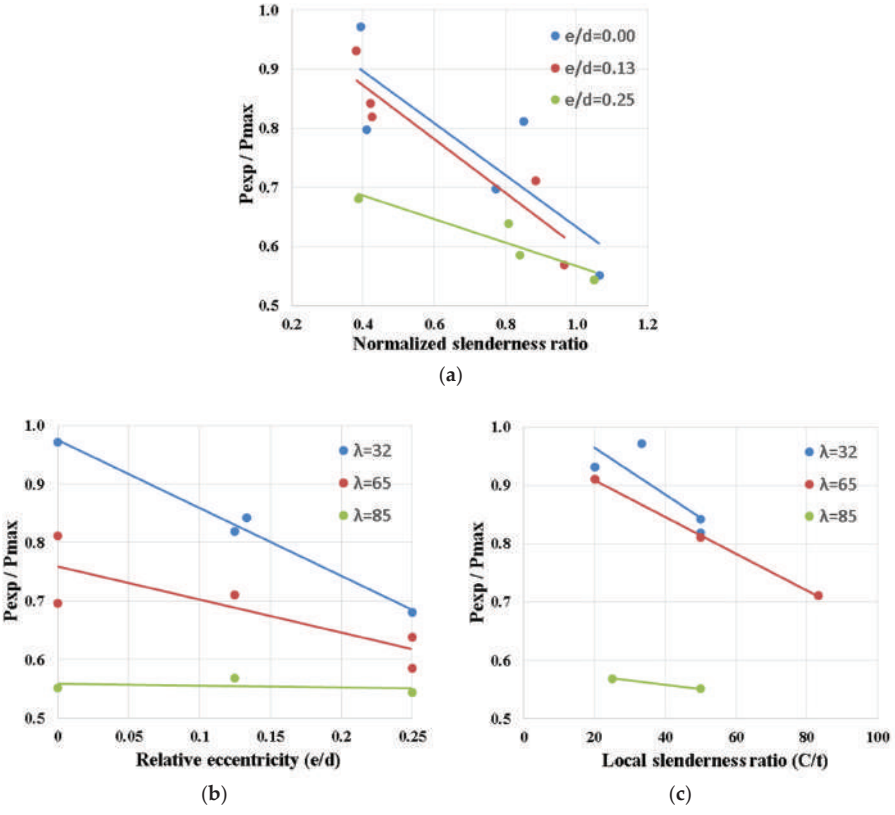


**Figure 8.** Relation between ($P_{exp}/P_{max}$) and (**a**) normalized slenderness ratio, (**b**) relative eccentricity and (**c**) local slenderness ratio.

- For critical eccentricity (e/d = 0.25), where the axial force acts on the core edge of the section, the reduction factor is significantly reduced, which indicates that flexural plastic failure dominates the behavior.
- Finally, all fitting lines almost intersected at a normalized slenderness ratio of 1.1, which matches the elastic buckling limit of AISC that showed in Equation (7).

Figure 8b illustrates the relationship between the buckling reduction factor and relative eccentricities for different global slenderness ratios. The best fitting curves indicated the following:

- The rate of reduction factor decreasing is decreased with increasing the slenderness ratio. The maximum decreasing rate was observed for the lowest slenderness ratio ($\lambda$ = 32 or $\lambda$ = 0.4), while the reduction factor was almost constant for the highest slenderness ratio ($\lambda$ = 85 or $\lambda$ = 1.05).
- The slenderness limit that separates plastic failure from elastic buckling is about ($\lambda$ = 90 or $\lambda$ = 1.10), which matches the recommendations of the AISC code.

Figure 8c shows the relation between buckling reduction factor and local slenderness ratio for different global slenderness ratios. It could be noted that the impact of the local slenderness ratio (C/t) is clearly observed in the case of low and medium global slenderness ratios ($\lambda$ = 32, 65 or $\lambda$ = 0.4, 0.8), where the failure occurred due to overstressing. On the other hand, for high global slenderness ratios ($\lambda$ = 85 or $\lambda$ = 1.05), the effect of local buckling was very minor as the columns failed due to elastic buckling.

The comparison between both experimental results from Section 3 and theoretical analysis from Section 4 indicates the following points:

- Both experimental and analytical results showed that the core of the considered composite section lies at e/d = 0.25. At this relative eccentricity, the minimum normal stress is almost zero (as shown in Table 5, specimens 1, 8 and 11).
- The summarized results in Table 6 and Figure 9 show wed deviation of 24% between the experimental capacities and the calculated ones using AISC and EN-1994 codes, while the deviation was about 13% for the CSI-COL capacities.
- The enhanced accuracy of CSI-COL may be justified as follows:
  - CSI-COL considered the Mander model for concrete behavior, which is so close to the experimental one (as shown in Figure 6a). On the other hand, most design codes (including AISC and EN-1994) considered a simplified equivalent block distribution to simulated concrete behavior.
  - CSI-COL considered a non-linear stress–strain relation for steel sections, while design codes used simplified bilinear elastic–perfect plastic relation.
  - The formulas in design codes were developed based on regular cross sections (rectangular or circular in-filled tubes), while CSI-COL considered the actual non-regular cross section of double sigma face-to-face.
  - The software used generates a 3D-interaction diagram, while AISC uses an interaction formula and EN-1994 uses a simplified polygon 2D interaction diagram.
- Although CSI-COL showed better accuracy than design codes, it still has a significant deviation from the experimental results. This deviation could be justified as follows:
  - The built-in stress–strain curve for steel sections in CSI-COL has a significant deviation from the actual one, as shown in Figure 6b.
  - CSI-COL does not consider the effect of local buckling of the thin steel shell.
  - There must be some imperfections and random errors in manufacturing and testing the samples, which cannot be considered in any theoretical analysis.

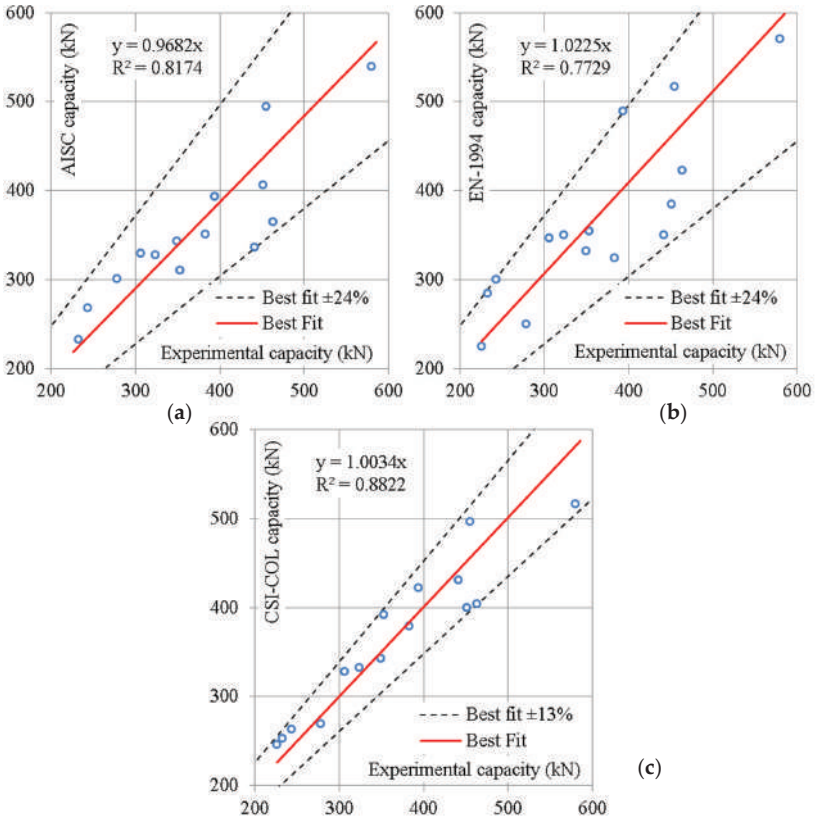


**Figure 9.** Comparison between both experimental and theoretical capacities. (**a**) Using AISC-LRFD, (**b**) Using EN-1994, (**c**) Using CSI-COL software.

## 6. Conclusions

This paper studied both experimental and theoretical behaviors of composite columns consisting of two cold-formed sigma sections welded face to face and filled with concrete. The study considered axial and eccentric compression loading for different slenderness ratios. The results of this study could be summarized in the following points.

- Experimental tests, design codes and CSI-COL software results indicated that over-stressing plastic failure is distinguished from elastic buckling failure at a normalized slenderness ratio of about 1.1 ($\lambda \approx 90$).
- Both theoretical calculations and strain measurements showed that the core edge of this section is located at relative eccentricity (e/d) equals 0.25.
- The calculated capacities using CSI-COL software, AISC-LRFD-94 and EN-1994-04 had deviations of (13%, 24% and 24%) from the experimental capacities, respectively.
- Although the local buckling failure was experimentally observed for local slenderness ratio (c/t = 80), none of the three used theoretical methods was able to capture this behavior. An advanced non-linear 3D FEM modeling may be needed to simulate this phonon.
- The good matching between experimental and CSI-COL capacities indicated that the studied section could achieve full composite behavior without using any shear connectors.
- The results of this study are limited by the size of the tested sample; more full-scale samples should be tested to verify the accuracy of the concluded results.

- Further studies may be carried out using more advanced 3D-FEM modeling to investigate the local buckling behavior of this section.

**Author Contributions:** Conceptualization, M.A.E.-A.; methodology and editing, A.M.E.; formal analysis and investigation, M.A.R.; supervision, S.M.I. All authors have read and agreed to the published version of the manuscript.

**Funding:** This research received no external funding.

**Data Availability Statement:** Not applicable.

**Conflicts of Interest:** The authors declare no conflict of interest.

## References

1. Alimohammadi, H.; Hesaminejad, A.; Yaghin, M.L. Effects of different parameters on inelastic buckling behavior of composite concrete-filled steel tubes. *Int. Res. J. Eng. Technol.* **2019**, *6*, 603–609.
2. Liu, D.; Gho, W.; Yuan, J. Ultimate capacity of high-strength rectangular. *J. Constr. Steel Res.* **2003**, *59*, 1499–1515. [CrossRef]
3. Zhu, L.; Ma, L.; Bai, Y.; Li, S.; Song, Q. Large diameter concrete-filled high strength steel tubular stub. *Thin-Walled Struct.* **2016**, *108*, 12–19. [CrossRef]
4. Han, L.; Yao, G.; Zhao, X. Tests and calculations for hollow structural steel (HSS) stub columns filled with self-consolidating. *J. Constr. Steel Res.* **2005**, *61*, 1241–1269. [CrossRef]
5. Zhang, S.; Guo, L. Behavior of High Strength Concrete-Filled Slender RHS Steel Tubes. *Adv. Struct. Eng.* **2007**, *10*, 337–351. [CrossRef]
6. Guo, L.; Zhang, S.; Xu, Z. Behavior of Filled Rectangular Steel HSS Composite Columns under Bi-Axial Bending. *Adv. Struct. Eng.* **2011**, *14*, 295–306. [CrossRef]
7. Bahrami, A.; Badaruzzaman, W.H.W.; Osman, S.A. Finite Element Analysis of Ultimate Load Capacity of Slender Concrete-Filled Steel Composite Columns. In Proceedings of the International Conference on Advanced Science, Engineering and Information Technology 2011, Bangi-Putrajaya, Malaysia, 14–15 January 2011. [CrossRef]
8. Ren, Q.X.; Han, L.H.; Lam, D.; Hou, C. Experiments on special-shaped CFST stub columns under axial compression. *J. Constr. Steel Res.* **2014**, *98*, 123–133. [CrossRef]
9. Wang, Z.B.; Tao, Z.; Yu, Q. Axial compressive behavior of concrete-filled double-tube stub columns with stiffeners. *Thin-Walled Struct.* **2017**, *120*, 91–104. [CrossRef]
10. Ding, F.X.; Wang, W.J.; Lu, D.R.; Liu, X.M. Study on the behavior of concrete-filled square double-skin steel tubular stub columns under axial loading. In *Structures*; Elsevier: Amsterdam, The Netherlands, 2020; pp. 665–676. [CrossRef]
11. Ci, J.; Jia, H.; Chen, S.; Yan, W.; Song, T.; Kim, K.S. Performance analysis and bearing capacity calculation on circular concrete filled double steel tubular stub columns under axial compression. In *Structures*; Elsevier: Amsterdam, The Netherlands, 2020; pp. 554–565. [CrossRef]
12. Tao, Z.; Uy, B.; Han, L.H.; Wang, Z.B. Analysis and design of concrete-filled stiffened thin-walled steel tubular columns under axial compression. *Thin-Walled Struct.* **2009**, *47*, 1544–1556. [CrossRef]
13. Young, B.; Ellobody, E. Experimental investigation of concrete-filled cold-formed high strength stainless steel tube columns. *J. Constr. Steel Res.* **2005**, *62*, 484–492. [CrossRef]
14. Dai, P.; Yang, L.; Wang, J.; Zhou, Y. Compressive strength of concrete-filled stainless steel tube stub columns. *Eng. Struct.* **2020**, *205*, 110106. [CrossRef]
15. He, A.; Liang, Y.; Zhao, O. Flexural buckling behaviour and resistances of circular high strength concrete-filled stainless steel tube columns. *Eng. Struct.* **2020**, *219*, 110893. [CrossRef]
16. Azad, S.K.; Li, D.; Uy, B. Axial slenderness limits for austenitic stainless steel-concrete composite columns. *J. Constr. Steel Res.* **2020**, *166*, 105856. [CrossRef]
17. El Aghoury, M.A.; Hana, M.T.; Amoush, E.A. Axial stability of columns composed of combined sigma CFS. In Proceedings of the Annual Conference of Structural Stability Research Council, Orlando, FL, USA, 12–15 April 2016.
18. el Aghoury, M.A.; Hana, M.T.; Amoush, E.A. Strength of combined sigma cold formed section columns. In Proceedings of the EUROSTEEL 2017, Copenhagen, Denmark, 13–15 September 2017.
19. *ASTM E8/E8M−13a*; Standard Test Methods for Tension Testing of Metallic Materials. ASTM International: West Conshohocken, PA, USA, 2022. [CrossRef]
20. American Institute of Steel Construction (AISC). *Manual of Steel Construction-Load & Resistance Factor Design-Volume I-Structural Members, Specifications, & Codes*; American Institute of Steel Construction: Chicago, IL, USA, 1994; ISBN 1-56424-042-8.
21. *EN 1994-1-1:2004*; Eurocode 4: Design of Composite Steel and Concrete Structures–Part 1-1: General Rules and Rules for Buildings. European Committee for Standardization (CEN): Brussels, Belgium, 2004.
22. Mander, J.B.; Priestley, M.J.N.; Park, R. Theoretical stress-strain model of confined concrete. *J. Struct. Eng.* **1988**, *114*, 1804–1826. [CrossRef]

designs

MDPI

*Article*

# Estimating the Buckling Load of Steel Plates with Center Cut-Outs by ANN, GEP and EPR Techniques

**Jagan Jayabalan [1], Manju Dominic [2], Ahmed M. Ebid [3,*], Atefeh Soleymani [4], Kennedy C. Onyelowe [5] and Hashem Jahangir [6]**

[1] Department of Civil Engineering, Galgotias University, Greater Noida 203201, India
[2] Department of Civil Engineering, Rajadhani Institute of Engineering and Technology, Thiruvananthapuram 695102, India
[3] Department of Structural Engineering, Future University in Egypt, New Cairo 11865, Egypt
[4] Department of Structural Engineering, Shahid Bahonar University of Kerman, Kerman 76169-14111, Iran
[5] Department of Civil Engineering, Michael Okpara University of Agriculture, Umudike 440101, Nigeria
[6] Department of Civil Engineering, University of Birjand, Birjand 97174-31349, Iran
* Correspondence: ahmed.abdelkhaleq@fue.edu.eg

**Abstract:** Steel plates are used in the construction of various structures in civil engineering, aerospace, and shipbuilding. One of the main failure modes of plate members is buckling. Openings are provided in plates to accommodate various additional facilities and make the structure more serviceable. The present study examined the critical buckling load of rectangular steel plates with centrally placed circular openings and different support conditions. Various datasets were compiled from the literature and integrated into artificial intelligence techniques like Gene Expression Programming (GEP), Artificial Neural Network (ANN) and Evolutionary Polynomial Regression (EPR) to predict the critical buckling loads of the steel plates. The comparison of the developed models was conducted by determining various statistical parameters. The assessment revealed that the ANN model, with an $R^2$ of 98.6% with an average error of 10.4%, outperformed the other two models showing its superiority in terms of better precision and less error. Thus, artificial intelligence techniques can be adopted as a successful technique for the prediction of the buckling load, and it is a sustainable method that can be used to solve practical problems encountered in the field of civil engineering, especially in steel structures.

**Keywords:** cut-outs; buckling load; artificial intelligence; steel plates; axial loading

**Citation:** Jayabalan, J.; Dominic, M.; Ebid, A.M.; Soleymani, A.; Onyelowe, K.C.; Jahangir, H. Estimating the Buckling Load of Steel Plates with Center Cut-Outs by ANN, GEP and EPR Techniques. *Designs* **2022**, *6*, 84. https://doi.org/10.3390/designs6050084

Academic Editor: Farshid Aram

Received: 26 August 2022
Accepted: 19 September 2022
Published: 22 September 2022



## 1. Introduction

### *1.1. Background*

Plate buckling analysis has a wide range of applications in a variety of engineering domains, such as civil and structural engineering, mechanical engineering, marine, aerospace engineering, etc. [1], particularly when a lightweight design is the main objective [2]. Plate buckling is a type of destabilization that occurs when a sudden deflection occurs under compressive load. Plates buckle when exposed to compressive stresses greater than the critical limit [3,4]. A critical level of stress develops whenever the plates are subjected to compressive load, causing this to occur. The origin of plate buckling is governed by partial differential equations, which makes the interpretation exceedingly difficult [5,6]. A plate with cut-outs has a more sophisticated buckling analysis than a plate without cut-outs [7]. Cut-outs in box girders and certain load-bearing spars save material, can be used as windows or doors, or simply improve the design aesthetics. They also provide ventilation, accessibility for maintenance, installation, and damage assessment. As a result, an in-depth understanding of perforated and non-perforated plate buckling is necessary [8–13]. Perforated plates have lower structural strength than plates without

holes, and buckling behavior is one of the most significant failures to be considered in these systems' safe and reliable operation.

### *1.2. Literature Review*

The existence of cut-outs of varied sizes results in the formation of free edges in steel plates, which causes high stresses, resulting in plate stiffness degradation and early fracture [14–16]. Therefore, for effective design, it is critical for the design engineer to comprehend the stability, overall strength, and failure parameters of steel plates with cut-outs of varied shapes and sizes. A full grasp of buckling stresses and corresponding mode shapes is the cornerstone of dependable structural designs and constructing a straightforward technique can give an acceptable method. Because of the issue's difficulty, most academics investigated the buckling performance of rectangular sheets with perforations and isotropic support using the FEM or Rayleigh-Ritz techniques [17–20].

Numerical, experimental, and analytical methods and their combinations have been used in several important investigations. The impact of a rectangular cut-out on a plate was studied by Suneel Kumar et al. [21]. Several cut-out dimensions, slenderness ratios, and area ratios were employed to get the required result. The impact of changing different factors on the ultimate strength of a plate subjected to axial compression was determined. Ansys simulation was used to verify the findings. The consequences of perforations on the buckling behavior of planes in a linear manner were investigated by Maiorana et al. [22]. Under compressive stresses, the boundary condition completely supported all edges, and circular and square holes were studied. The findings were reported on graphs for circular and square perforations with variations in the position of the cut-outs. Sandeep Singh et al. [23] investigated the effect of partial edge compression, modification in aspect ratio, and the effects of cut-outs on buckling load, discovering that partial edge compression had a larger effect on buckling strength than uniform edge compressive load, and panels without holes had a greater critical load than panels with perforation. Although the effect of partial edge compression on buckling load was less clear. Dadrasi [24] investigated the buckling performance of punctured steel plates with rectangular shapes when subjected to uniaxial compressive stress. Cut-outs in a circle or square were utilized in a variety of loading bands, numeral, and empirical findings. For finite element analysis, ABAQUS software was employed, and for an experimental study, a group of servo-hydraulic INSTRON8802 was utilized. The findings for plates with or without cut-outs were inspected. They found that the critical buckling load ascended as the loading band broadened and, furthermore, that the buckling load for plates with a circular cut-out was higher than for plates with square cut-outs. Djelosevic et al. [25] investigated the elastic stability of panels with varied perforation geometry. For circular, square, and rectangular apertures, several variables' influence on the plate's elastic stability, such as opening form, size, and direction, was investigated, and a sensitivity factor was constructed. The presence of holes, they found, decreased the deformation energy. Whenever thin rectangular plates with cut-outs in the shape of a circle were uniaxially loaded, instability arose far before the yield point, and it occurred prior to the yield point of the panel material when the plates were thick, according to Mauro et al. [26]. The effect of change in plate thickness with a hole regarding plate buckling was investigated by Mohamazadeh and Noh [27]. The buckling coefficient and buckling stresses were determined using the Gerard and Becker formulas. They compared plates with cut-outs against plates without perforations and discovered that if there was an increase in the thickness of the plate, the buckling load and stress also increased. They [28] also examined the effect of perforations on the buckling of thin plates. ABAQUS was used to perform the simulations, and critical values for buckling load and corresponding stress were computed for variations in hole diameter and plate thickness. Shariati et al. [29] studied the buckling behavior of a panel in the shape of a rectangle with a circular hole at various points on the panel under various boundary circumstances, and found that the boundary circumstances had a substantial effect on the buckling behavior. For different aspect ratios, Jana [30] investigated the buckling performance of a rectangular sheet composed of a simple

support border for uniform axial compressive loads with a circular cut-out. For changes in perforation size, aspect ratio, and thickness of the plate, eigenvalue buckling analysis was performed. Using Ansys and MATLAB, he discovered that the ideal perforation location for the highest buckling load is in the middle of the axis on which the stress is applied. Giulio Lorenzini et al. [31] investigated the impact of several types of cut-outs on the buckling of the plate and discovered that by selecting the right cut-out method, a high performance might be achieved, i.e., performance could be improved by eliminating a similar quantity of material. Using the Ritz energy equation, Adah et al. [32] develop MATLAB software to determine the critical buckling load for a rectangular plate with an axial compression force. Researchers determined critical buckling coefficients for a variety of boundary conditions and then compared their results to existing literature. By examining the increase in buckling stress caused by cut-outs, Blesa, Gracia, and Rammerstorfer [33] determined that cut-outs can enhance plate buckling strength while decreasing weight. Caio César Cardoso da Silva and colleagues [34] looked into the impact of hexagonal opening geometric arrangements on buckling mechanical characteristics and found that a longitudinally hexagonal cut-out outperforms an oblique hexagonal cut-out. The basic buckling of annular and circular plates with guided edges [12,35] and elastic edges [36,37] was investigated by Rao and Rao. They did not, however, consider the perforation in their research. Using the finite element approach, Sinha et al. [5] performed a buckling study on stainless-steel plates either with or without perforation. The influence of plate length, thickness, and diamond-shape hole-size on buckling load values was investigated. The purpose of Gore and Lokavaraput's research [1] was to explore how material characteristics and geometrical modifications influenced the buckling load bearing capacity of rectangular flat sheets joined on both sides. A comparison was made between a solid plate and a plate with a perforation. Variations in the orientation of the elliptical perforation and the greatest buckling load that could be attained were explored. Fu and Wang [38] devised a new phenomenological galaxy formation model for the critical buckling load of perforated plates with characteristic equations based on the Timoshenko shear beam theory. The suggested model's results were compared to those produced using FEM and found to be in excellent agreement. Using FEM, Hosseinpour et al. [39] investigated the behavior of steel plates with a central circular cut-out when exposed to compressive axial force. As a consequence, an ANN-based formula for determining perforated steel plate's ultimate strength was developed, and its reliability was contrasted to that of previous research formulas.

As stated above, the buckling examination of plates with varied perforation shapes, sizes, orientations, and locations has been the subject of various research. Their findings showed that plate buckling is influenced by perforations' form, size, and direction. Yet, there are several opportunities to investigate the influence of these factors in various combinations [5]. Plates are integral structural members with wide applications in civil engineering, aerospace, and shipbuilding. They are used in construction as it reduces the weight of structures considerably. They are used as the main load-carrying structural member in all these applications. Columns are one-dimensional load-carrying members and plates are two-dimensional load-carrying members used in buildings, bridges, airplanes, and ships. Buckling is the major failure phenomenon observed in plates. Buckling happens when plates are subjected to axial compressive loads. It is important to ensure that plates fail by yielding rather than by buckling. This can be done by keeping the critical buckling stress above yield stress. The support conditions of the plates affect the critical buckling load. The width-thickness ratio of the plates can be adjusted to ensure that buckling stress is above yield stress for different support conditions. Analytical formulas are available for calculating the critical buckling load in plates with different support conditions [40]. Openings or cut-outs are provided in plate elements for increasing the serviceability of the plate structural elements used in structures. The presence of openings always changes the load-carrying capacity and structural stability of plate structures. Openings create a redistribution of stresses and change the buckling behavior. It develops stress concentration

around the openings. Openings reduce the mass of the plates, and it has been found that the presence of openings increases the critical buckling load capacity of plates [41,42].

Analysis of plates with openings is very complex, and due to this complexity, finite element methods (FEM) are usually sought after for such analyses, which are validated using experimental methods. Many FEM and experimental studies have been conducted to study the behavior of plates with openings [43,44]. While experimental studies are destructive and costly, FEM studies are less costly, non-destructive, and less time-consuming. Using the data sets from experimental and FEM studies, the critical buckling load of plates with openings has been calculated using the buckling coefficient method [45] and predicted using various statistical methods [46]. Meanwhile, Wu et al. [47] deployed the differential quadrature method (DQM) to analyze the isotropic and composite laminated plates and shells with particular consideration to the hierarchical finite element method (HFEM). This research utilized the layer-wise theory with linear expansion in each layer to develop a p-version curved laminated composite. It was found that this method used fewer degrees of freedom and less input data to model a complicated case based on interpolation on arc length coordinates. The Bezier method was also used by Kabir et al. [48] for nonlinear vibration and post-buckling of random checkerboard composites reinforced with graphene nano-platelets. This robust Bezier-based solution recommended a probabilistic model to determine a matrix modulus of the graphene nano-platelets reinforced composite.

Artificial intelligence (AI) has many applications to the civil engineering field, specifically in predicting the buckling load of stiffened panels, imperfect reticulates shells, and thin cylindrical shells [49–52]. It can reduce the complexity of practical civil engineering problems to a large extent by making use of already existing experimental studies and results. Civil engineering design practices have moved from their infancy to a state of maturity through the development of design codes. These design codes have been developed based on years of exhaustive experimental studies conducted in relevant areas. AI is one step ahead of these methods due to its capacity to handle large data sets [53,54]. This will bring more accuracy to the results predicted. In this research paper, the critical buckling load of rectangular steel plates with circular cut outs loaded with uniaxial compressive load was predicted with different AI techniques.

## 2. Materials and Methods

### *2.1. Steel Setup and Experimental Data Collection*

In the present study, a critical buckling load of rectangular steel plates with circular cut-outs loaded with uniaxial compressive load as depicted in Figure 1 was studied.

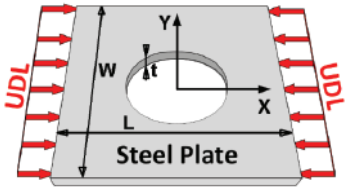


**Figure 1.** Uniaxial loaded steel plate with a centrally placed circular opening under uniformly distributed loading (UDL).

The support conditions considered are simply supported on all four sides (SSSS), clamped free clamped free (CFCF) and simply supported clamped simply supported clamped (SCSC). Figure 2 depicts the various support conditions.

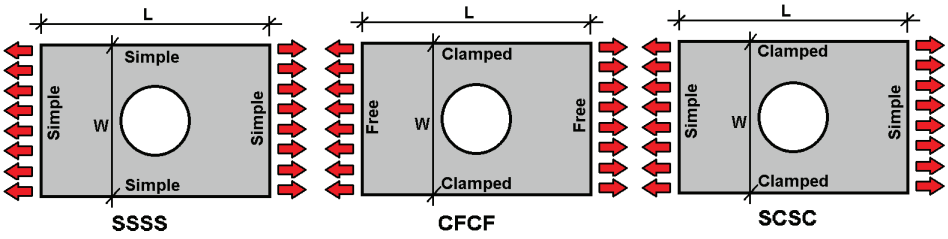


**Figure 2.** Support conditions of the steel plate.

The independent variables considered are the aspect ratio (length/breadth ratio) of the plate, the thickness of the plate, and the radius of the circular opening, whereas the dependent variable is the buckling load. AI techniques like genetic programming, artificial neural network, and evolutionary polynomial regression have been used to predict the critical buckling loads of steel plates.

### *2.2. Collected Database and Statistical Analysis*

At the end of the loading exercise, 103 experimental test results were collected for rectangular steel plates with centrally placed circular holes with different configurations as presented in the Appendix A to determine their buckling load. Each record contains the following data:

- Aspect ratio (length/width) (L/W),
- Slenderness ratio (width/thickness) (W/t),
- Loss ratio (hole diameter/width) (D/W),
- Boundary conditions (buckling coefficient in width dir. x buckling coef. in length dir.) (Kx.Ky), where K = 2.00 for clamp-free, 1.00 for simple-simple, 0.75 for simple-clamp, and 0.50 for clamp-clamp,
- Relative buckling stress (buckling stress/yielding stress) (Fb/Fy), where buckling stress = buckling load/net area = $\frac{Pb}{(L-D)t}$

The collected records were divided into training (73 records) and validation sets (30 records). The validation set (testing set) was randomly selected and it was the hold-out of the training process and used to test the trained model. Tables 1 and 2 summarized their statistical characteristics and the Pearson correlation matrix. Finally, Figure 3 shows the histograms for both inputs and outputs.

**Table 1.** Statistical analysis of collected database.

| | (L/W) | (W/t) | (D/W) | (Kx.Ky) | (Fb/Fy) |
|---|---|---|---|---|---|
| | | | Training set | | |
| Min. | 1.00 | 41.67 | 0.08 | 0.50 | 0.01 |
| Max. | 10.00 | 700.00 | 0.90 | 4.00 | 1.02 |
| Avg | 1.80 | 92.10 | 0.21 | 2.51 | 0.36 |
| SD | 1.51 | 113.76 | 0.17 | 1.60 | 0.32 |
| Var | 0.83 | 1.24 | 0.82 | 0.64 | 0.88 |
| | | | Validation set | | |
| Min. | 1.0 | 20.0 | 0.1 | 0.5 | 0.0 |
| Max. | 10.0 | 500.0 | 0.6 | 4.0 | 1.0 |
| Avg | 2.1 | 90.0 | 0.2 | 2.0 | 0.3 |
| SD | 1.8 | 98.5 | 0.2 | 1.6 | 0.3 |
| Var | 0.82 | 1.09 | 0.83 | 0.79 | 0.91 |

**Table 2.** Pearson correlation matrix.

| | L/W | W/t | D/W | Kx.Ky | Fb/Fy |
|---|---|---|---|---|---|
| L/W | 1.00 | | | | |
| W/t | 0.04 | 1.00 | | | |
| D/W | −0.14 | −0.21 | 1.00 | | |
| Kx.Ky | −0.28 | −0.44 | 0.28 | 1.00 | |
| Fb/Fy | −0.31 | −0.27 | −0.11 | −0.23 | 1.00 |

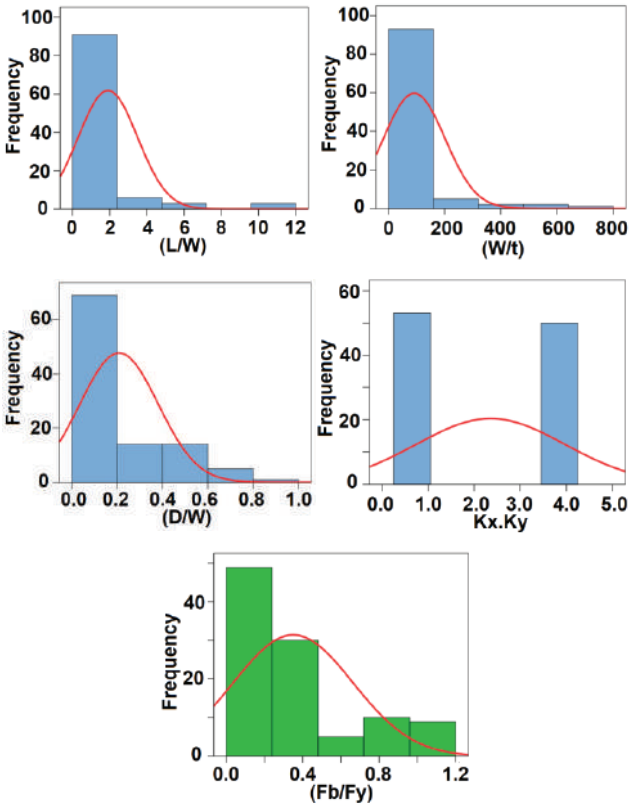


**Figure 3.** Distribution histograms for inputs (in blue) and outputs (in green).

*2.3. Research Program*

Three different artificial intelligence (AI) techniques were used to predict the buckling stress of perforated plates or plates with cut outs. These techniques are gene expression programming (GEP), artificial neural network (ANN) and polynomial linear regression optimized using a genetic algorithm which is known as evolutionary polynomial regression (EPR). All three developed models were used to predict the values of relative buckling stress (Fb/Fy) using an aspect ratio (L/W), slenderness ratio (W/t), loss ratio (D/W), and boundary conditions (Kx.Ky). Each model of the three developed models was based on a different approach (evolutionary approach for GEP, mimicking biological neurons for ANN, and optimized mathematical regression technique for EPR). However, for all developed models, prediction accuracy was evaluated in terms of the sum of squared errors (SSE).

The following section discusses the results of each model. The performance accuracies of developed models were evaluated by comparing the (SSE) between predicted and calculated (Fb/Fy) values.

## 3. Results and Discussion

### *3.1. Prediction of Relative Buckling Stress (Fb/Fy)*

#### 3.1.1. Model (1)—Using GEP Technique

The developed GP model started with 50 gene/chromosomes and settled at 250 gene/chromosomes. The population size, survivor size, and number of generations were 1000, 300, and 200, respectively. Equation (1) presents the output formulas for Fb/Fy,. The average error percentage of the total set is 22.7%, while the $R^2$ value is 0.932.

$$\frac{Fb}{Fy} = 0.9\left(\frac{W}{L}\right)^{\exp\left(\frac{W}{C.L}\right)} + \left(\frac{\sqrt{W/D}}{Kx.Ky} + \frac{W}{5.6D}\right)\left(\frac{t}{W}\right)\left(1 - \frac{D}{W}\right)$$
$$\text{where } C = 0.422\left(\frac{\sqrt{D/W}}{(W/D) - \log(0.42\ Kx.Ky)} + 1\right) \quad (1)$$

#### 3.1.2. Model (2)—Using ANN Technique

A GRG-trained ANN with one hidden layer and a HyperTanh activation function was used to predict the same Fb/Fy values. The used network layout of a 4-4-1 ANN model and its connation weights are illustrated in Figure 4 and Table 3. The developed ANN was created and trained using SPSS software. It was sequentially trained with a learning rate of 0.05, the model stopped training when the reduction in errors between two successive epochs was less than 1%. Since ANN has a nonlinear activation function, it cannot be converted into an equivalent equation. The average error percentage of the total dataset for this network is 10.4% and the $R^2$ value is 0.986. The relative importance values for each input parameter are illustrated in Figure 5, which indicated that the aspect ratio (L/W) was the most important factor, followed by the sereneness ratio (W/t), while other factors have less influence, which agrees with a previous work [55].

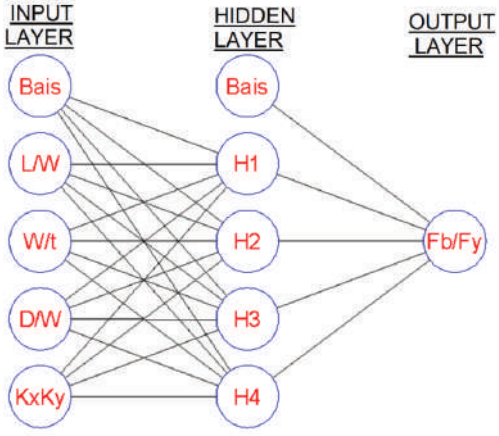


**Figure 4.** Layout for the developed ANN and its connection weights.

**Table 3.** Weight matrix for the developed ANN model.

| | **H1** | **H2** | **H3** | **H4** | |
|---|---|---|---|---|---|
| (Bias) | 13.70 | 1.37 | 9.75 | 8.58 | |
| L/W | 10.88 | −6.93 | 2.93 | 13.16 | |
| W/t | −3.84 | 3.82 | 21.04 | −3.67 | |
| D/W | −0.63 | −0.49 | −1.57 | 0.85 | |
| Kx.Ky | −5.89 | 7.93 | −3.19 | −3.07 | |
| | H1 | H2 | H3 | H4 | (Bias) |
| Fb/Fy | −5.23 | −10.61 | −27.02 | −10.32 | −22.31 |

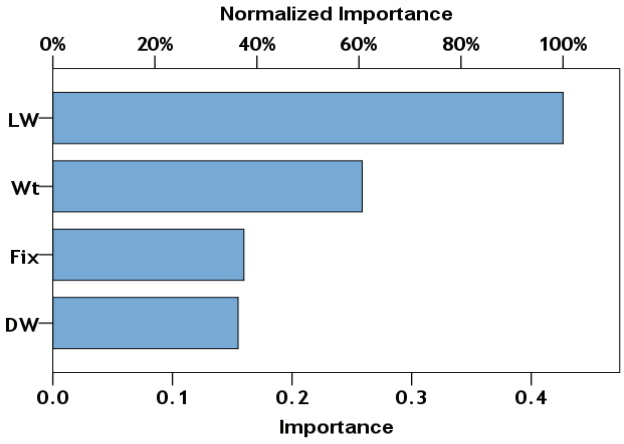


**Figure 5.** Relative importance of input parameters.

3.1.3. Model (3)—Using EPR Technique

Finally, the developed EPR model was limited to quadrilateral level, for 4 inputs; there are 70 possible terms (35 + 20 + 10 + 4 + 1 = 210) as follows:

$$\sum_{i=1}^{i=4}\sum_{j=1}^{j=4}\sum_{k=1}^{k=4}\sum_{l=1}^{l=4} X_i.X_j.X_k.X_l + \sum_{i=1}^{i=4}\sum_{j=1}^{j=4}\sum_{k=1}^{k=4} X_i.X_j.X_k + \sum_{i=1}^{i=4}\sum_{j=1}^{j=4} X_i.X_j + \sum_{i=1}^{i=4} X_i + C$$

The GA technique was applied to these 70 terms to select the most effective 10 terms to predict the values of Fb/Fy. The outputs are illustrated in Equation (2). The average error percentage and $R^2$ values were 15.3% & 0.970 for the total datasets. The results of all developed models are summarized in Table 4.

$$\frac{Fb}{Fy} = \frac{Kx.Ky.L^2}{4165\ W.D} + \frac{Kx.Ky.W.D + 53540\ t^2}{605\ L.t} + \frac{1.7W(2.1Kx.Ky - 1)}{L(Kx.Ky)^3} - \left(\frac{W}{L}\right)^2\left(\frac{30760\ t + W}{41565\ t}\right) + \frac{28.9\ t\left[1-(2\ Kx.Ky)^2\right]}{W(Kx.Ky)^3} - 0.25 \quad (2)$$

**Table 4.** Accuracies of developed models.

| Technique | Developed Eq. | SSE | Error % | $R^2$ |
|---|---|---|---|---|
| GEP | Equation (1) | 0.65 | 22.7 | 0.932 |
| ANN | Figure 2 | 0.14 | 10.4 | 0.986 |
| EPR | Equation (2) | 0.30 | 15.3 | 0.970 |

The relations between calculated and predicted values for all developed models are shown in Figure 6.

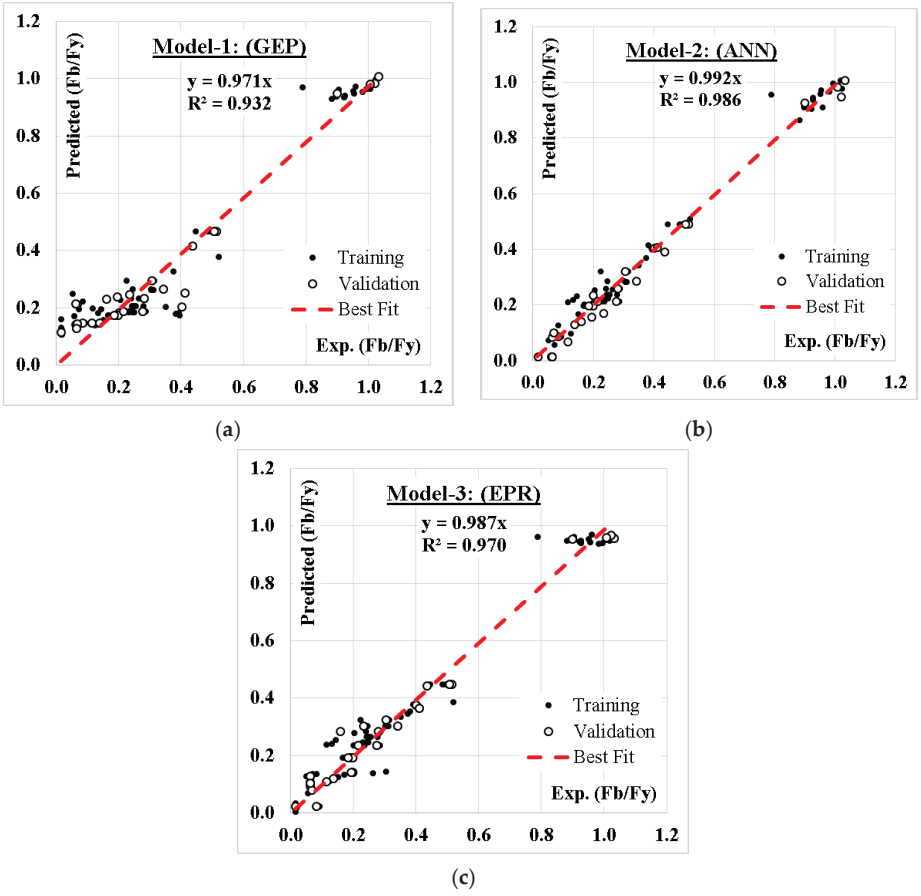


**Figure 6.** Relation between predicted and calculated Fb/Fy values using the developed models. (**a**) using GEP, (**b**) using ANN & (**c**) using EPR.

## 4. Conclusions

This research presented three models using three AI techniques (GEP, ANN and EPR) to predict the values of relative buckling stress (Fb/Fy) using an aspect ratio (L/W), slenderness ratio (W/t), loss ratio (D/W), and boundary conditions (Kx.Ky). The results of comparing the accuracies of the developed models can be concluded in the following points:

- Both ANN and EPR have the most similar prediction accuracy, 89.6% and 84.7%, respectively, while the GEP model has the lowest prediction accuracy (77.3%).
- Although, the error percentage of the ANN and EPR models were so close, the output of the EPR model was closed form equations which could be manually used or as software unlike the ANN output which cannot be manually used.
- The summation of the absolute weights of each neuron in the input layer of the developed (ANN) model indicated that aspect ratio (L/W) had major influences on the relative buckling stress rather than the slenderness ratio (W/t), while the loss ratio (D/W) and boundary conditions (Kx.Ky) had less impact on (Fb/Fy).
- The GA technique successfully reduced the 70 terms of conventional polynomial regression quadrilateral formula to only 10 terms without significant impact on its accuracy.

- Like any other regression technique, the generated formulas were valid within the considered range of parameter values, beyond this range the prediction accuracy should be verified.

**Author Contributions:** Conceptualization, K.C.O.; methodology, A.M.E.; formal analysis, A.S.; investigation, M.D.; data curation, J.J.; supervision, H.J. All authors have read and agreed to the published version of the manuscript.

**Funding:** This research received no external funding.

**Institutional Review Board Statement:** Not applicable.

**Informed Consent Statement:** Not applicable.

**Data Availability Statement:** Utilized data are available in the Appendix A.

**Conflicts of Interest:** The authors declare no conflict of interest.

## Appendix A. Utilized Database

| L/W. | W/t. | D/W. | Kx.Ky | Fb/Fy. | L/W. | W/t. | D/W. | Kx.Ky | Fb/Fy. |
|---|---|---|---|---|---|---|---|---|---|
| 1.5. | 48. | 0.20. | 4.0. | 0.25. | 1.5. | 48. | 0.35. | 1.0. | 0.08. |
| 1.5. | 48. | 0.50. | 4.0. | 0.25. | 1.5. | 48. | 0.20. | 4.0. | 0.25. |
| 1.5. | 48. | 0.40. | 4.0. | 0.24. | 5.0. | 200. | 0.10. | 0.5. | 0.02. |
| 1.0. | 63. | 0.08. | 1.0. | 1.02. | 1.5. | 48. | 0.10. | 4.0. | 0.23. |
| 1.5. | 48. | 0.10. | 4.0. | 0.29. | 1.7. | 600. | 0.10. | 0.5. | 0.02. |
| 1.5. | 48. | 0.40. | 4.0. | 0.26. | 1.5. | 48. | 0.30. | 4.0. | 0.28. |
| 1.5. | 48. | 0.25. | 1.0. | 0.07. | 1.5. | 48. | 0.50. | 4.0. | 0.30. |
| 1.0. | 83. | 0.11. | 1.0. | 0.95. | 1.5. | 48. | 0.70. | 4.0. | 0.37. |
| 1.5. | 48. | 0.50. | 4.0. | 0.30. | 1.5. | 48. | 0.10. | 4.0. | 0.24. |
| 1.0. | 50. | 0.16. | 1.0. | 0.90. | 1.0. | 42. | 0.16. | 1.0. | 0.96. |
| 1.6. | 48. | 0.10. | 4.0. | 0.17. | 2.5. | 400. | 0.10. | 0.5. | 0.02. |
| 1.0. | 63. | 0.14. | 1.0. | 0.95. | 2.0. | 100. | 0.50. | 1.0. | 0.17. |
| 1.1. | 48. | 0.10. | 4.0. | 0.45. | 10.0. | 50. | 0.10. | 0.5. | 0.07. |
| 1.5. | 48. | 0.30. | 4.0. | 0.24. | 1.5. | 48. | 0.30. | 4.0. | 0.25. |
| 1.0. | 63. | 0.11. | 1.0. | 1.01. | 1.5. | 48. | 0.15. | 4.0. | 0.13. |
| 2.5. | 80. | 0.10. | 0.5. | 0.39. | 1.5. | 48. | 0.08. | 1.0. | 0.05. |
| 1.5. | 48. | 0.30. | 4.0. | 0.26. | 3.3. | 300. | 0.10. | 0.5. | 0.02. |
| 1.5. | 48. | 0.50. | 4.0. | 0.31. | 1.5. | 48. | 0.10. | 4.0. | 0.20. |
| 1.0. | 50. | 0.14. | 1.0. | 0.79. | 1.4. | 700. | 0.10. | 0.5. | 0.01. |
| 2.0. | 100. | 0.10. | 0.5. | 0.39. | 10.0. | 100. | 0.10. | 0.5. | 0.02. |
| 1.0. | 83. | 0.14. | 1.0. | 0.93. | 1.5. | 48. | 0.60. | 4.0. | 0.22. |
| 1.1. | 48. | 0.10. | 4.0. | 0.49. | 2.0. | 100. | 0.60. | 1.0. | 0.20. |
| 1.0. | 100. | 0.08. | 1.0. | 0.98. | 1.1. | 48. | 0.10. | 4.0. | 0.51. |
| 1.7. | 120. | 0.10. | 0.5. | 0.38. | 2.0. | 100. | 0.30. | 1.0. | 0.14. |
| 2.0. | 100. | 0.40. | 1.0. | 0.15. | 1.5. | 48. | 0.10. | 4.0. | 0.28. |
| 1.5. | 48. | 0.10. | 4.0. | 0.23. | 1.5. | 48. | 0.50. | 4.0. | 0.34. |
| 1.5. | 48. | 0.20. | 4.0. | 0.23. | 2.0. | 250. | 0.10. | 0.5. | 0.06. |
| 1.0. | 83. | 0.08. | 1.0. | 0.99. | 1.1. | 48. | 0.10. | 4.0. | 0.51. |
| 2.1. | 48. | 0.10. | 4.0. | 0.09. | 2.0. | 100. | 0.10. | 1.0. | 0.11. |
| 2.1. | 48. | 0.10. | 4.0. | 0.09. | 1.5. | 48. | 0.40. | 4.0. | 0.28. |
| 2.1. | 48. | 0.10. | 4.0. | 0.09. | 3.3. | 60. | 0.10. | 0.5. | 0.40. |
| 1.0. | 83. | 0.16. | 1.0. | 0.90. | 1.5. | 48. | 0.40. | 1.0. | 0.16. |
| 1.5. | 48. | 0.08. | 4.0. | 0.12. | 2.1. | 48. | 0.10. | 4.0. | 0.08. |
| 1.4. | 350. | 0.10. | 0.5. | 0.06. | 1.0. | 50. | 0.08. | 1.0. | 1.03. |
| 3.3. | 150. | 0.10. | 0.5. | 0.07. | 2.0. | 500. | 0.10. | 0.5. | 0.02. |
| 1.5. | 48. | 0.40. | 4.0. | 0.29. | 10.0. | 20. | 0.10. | 0.5. | 0.44. |
| 1.5. | 48. | 0.60. | 4.0. | 0.31. | 1.6. | 48. | 0.10. | 4.0. | 0.19. |
| 1.0. | 100. | 0.11. | 1.0. | 0.93. | 1.7. | 300. | 0.10. | 0.5. | 0.06. |
| 2.1. | 48. | 0.10. | 4.0. | 0.09. | 1.0. | 63. | 0.16. | 1.0. | 0.90. |

| L/W. | W/t. | D/W. | Kx.Ky | Fb/Fy. | L/W. | W/t. | D/W. | Kx.Ky | Fb/Fy. |
|---|---|---|---|---|---|---|---|---|---|
| 1.4. | 140. | 0.10. | 0.5. | 0.35. | 1.6. | 48. | 0.10. | 4.0. | 0.20. |
| 1.0. | 42. | 0.11. | 1.0. | 1.02. | 1.5. | 48. | 0.15. | 1.0. | 0.06. |
| 1.5. | 48. | 0.10. | 4.0. | 0.22. | 1.5. | 48. | 0.60. | 4.0. | 0.31. |
| 1.6. | 48. | 0.10. | 4.0. | 0.17. | 1.5. | 48. | 0.45. | 1.0. | 0.20. |
| 1.5. | 48. | 0.20. | 4.0. | 0.25. | 1.5. | 48. | 0.50. | 1.0. | 0.23. |
| 2.0. | 100. | 0.20. | 1.0. | 0.12. | 1.5. | 48. | 0.10. | 4.0. | 0.22. |
| 1.5. | 48. | 0.25. | 4.0. | 0.14. | 5.0. | 100. | 0.10. | 0.5. | 0.07. |
| 1.5. | 48. | 0.90. | 4.0. | 0.52. | 1.0. | 42. | 0.14. | 1.0. | 1.02. |
| 1.5. | 48. | 0.10. | 4.0. | 0.21. | 2.5. | 200. | 0.10. | 0.5. | 0.06. |
| 1.0. | 100. | 0.14. | 1.0. | 0.92. | 1.0. | 50. | 0.11. | 1.0. | 1.01. |
| 1.1. | 48. | 0.10. | 4.0. | 0.49. | 1.6. | 48. | 0.10. | 4.0. | 0.19. |
| 1.5. | 48. | 0.38. | 4.0. | 0.21. | 5.0. | 40. | 0.10. | 0.5. | 0.41. |
| 1.0. | 100. | 0.16. | 1.0. | 0.88. | . | . | . | . | . |

## References


1. Gore, R.; Lokavarapu, B.R. Effect of Elliptical Cutout on Buckling Load for Isotropic Thin Plate. In *Innovations in Mechanical Engineering*; Narasimham, G.S.V.L., Babu, A.V., Reddy, S.S., Dhanasekaran, R., Eds.; Springer: Singapore, 2022; pp. 51–69.
2. Al Qablan, H. Applicable Formulas for Shear and Thermal Buckling of Perforated Rectangular Panels. *Adv. Civ. Eng.* **2022**, *2022*, 3790462. [CrossRef]
3. Dehadray, P.M.; Alampally, S.; Lokavarapu, B.R. Buckling Analysis of Thin Isotropic Square Plate with Rectangular Cut-Out. In *Innovations in Mechanical Engineering*; Narasimham, G.S.V.L., Babu, A.V., Reddy, S.S., Dhanasekaran, R., Eds.; Springer: Singapore, 2022; pp. 71–86.
4. Taherian, I.; Ghalehnovi, M.; Jahangir, H. Analytical Study on Composite Steel Plate Walls Using a Modified Strip Model. In Proceedings of the 10th International Congress on Civil Engineering, Abriz, Iran, 5–7 May 2015.
5. Sinha, V.; Patel, R.; Ghetiya, K.; Nair, M.; Trivedi, T.; Rao, L.B. Impact of Diamond-Shaped Cut-Out on Buckling Nature of Isotropic Stainless-Steel Plate. In *Innovations in Mechanical Engineering*; Narasimham, G.S.V.L., Babu, A.V., Reddy, S.S., Dhanasekaran, R., Eds.; Springer: Singapore, 2022; pp. 119–146.
6. Soleymani, A.; Reza Esfahani, m. Effect of concrete strength and thickness of flat slab on preventing of progressive collapse caused by elimination of an internal column. *J. Struct. Constr. Eng.* **2019**, *6*, 24–40. [CrossRef]
7. Hosseini-Hashemi, S.; Khorshidi, K.; Amabili, M. Exact solution for linear buckling of rectangular Mindlin plates. *J. Sound Vib.* **2008**, *315*, 318–342. [CrossRef]
8. Orun, A.E.; Guler, M.A. Effect of hole reinforcement on the buckling behaviour of thin-walled beams subjected to combined loading. *Thin-Walled Struct.* **2017**, *118*, 12–22. [CrossRef]
9. Singh, T.G.; Chan, T.-M. Effect of access openings on the buckling performance of square hollow section module stub columns. *J. Constr. Steel Res.* **2021**, *177*, 106438. [CrossRef]
10. Hasrati, E.; Ansari, R.; Rouhi, H. A numerical approach to the elastic/plastic axisymmetric buckling analysis of circular and annular plates resting on elastic foundation. *Proc. Inst. Mech. Eng. Part C J. Mech. Eng. Sci.* **2019**, *233*, 7041–7061. [CrossRef]
11. Russell, M.J.; Lim, J.B.; Roy, K.; Clifton, G.C.; Ingham, J.M. Welded steel beam with novel cross-section and web openings subject to concentrated flange loading. *Structures* **2020**, *24*, 580–599. [CrossRef]
12. Rao, L.B.; Rao, C.K. Buckling of Circular Plates with an Internal Elastic Ring Support and Elastically Restrained Guided Edge Against Translation. *Mech. Based Des. Struct. Mach.* **2009**, *37*, 60–72. [CrossRef]
13. Jahangir, H.; Daneshvar Khorram, M.H.; Ghalehnovi, M. Influence of geometric parameters on perforated core buckling restrained braces behavior. *J. Struct. Constr. Eng.* **2019**, *6*, 75–94. [CrossRef]
14. Daneshvar, M.H.; Saffarian, M.; Jahangir, H.; Sarmadi, H. Damage identification of structural systems by modal strain energy and an optimization-based iterative regularization method. *Eng. Comput.* **2022**, *37*, 1–21. [CrossRef]
15. Jahangir, H.; Khatibinia, M.; Kavousi, M. Application of Contourlet Transform in Damage Localization and Severity Assessment of Prestressed Concrete Slabs. *Soft Comput. Civ. Eng.* **2021**, *5*, 39–67. [CrossRef]
16. Muddappa, P.P.Y.; Rajanna, T.; Giridhara, G. Effect of reinforced cutouts on the buckling and vibration performance of hybrid fiber metal laminates. *Mech. Based Des. Struct. Mach.* **2021**, *49*, 1–21. [CrossRef]
17. Mohammadzadeh, B.; Choi, E.; Kim, W.J. Comprehensive investigation of buckling behavior of plates consider-ing effects of holes. *Struct. Eng. Mech.* **2018**, *68*, 261–275. [CrossRef]
18. Abolghasemi, S.; Eipakchi, H.; Shariati, M. An analytical solution for buckling of plates with circular cutout subjected to non-uniform in-plane loading. *Arch. Appl. Mech. Vol.* **2019**, *89*, 2519–2543. [CrossRef]
19. Kim, J.-H.; Park, D.-H.; Kim, S.-K.; Kim, J.-D.; Lee, J.-M. Lateral Deflection Behavior of Perforated Steel Plates: Experimental and Numerical Approaches. *J. Mar. Sci. Eng.* **2021**, *9*, 498. [CrossRef]
20. Yidris, N.; Hassan, M. The effects of cut-out on thin-walled plates. In *Modelling of Damage Processes in Biocomposites, Fibre-Reinforced Composites and Hybrid Composites*; Woodhead Publishing: Philadelphia, PA, USA, 2019. [CrossRef]

21. Kumar, M.S.; Alagusundaramoorthy, P.; Sundaravadivelu, R. Ultimate strength of square plate with rectangular opening under axial compression. *J. Nav. Arch. Mar. Eng.* **2007**, *4*, 15–26. [CrossRef]
22. Maiorana, E.; Pellegrino, C.; Modena, C. Linear buckling analysis of perforated plates subjected to localised symmetrical load. *Eng. Struct.* **2008**, *30*, 3151–3158. [CrossRef]
23. Singh, S.; Kulkarni, K.; Pandey, R.; Singh, H. Buckling analysis of thin rectangular plates with cutouts subjected to partial edge compression using FEM. *J. Eng. Des. Technol.* **2012**, *10*, 128–142. [CrossRef]
24. Shariati, M.; Dadrasi, A. Numerical and Experimental Investigation of Loading Band on Buckling of Perforated Rectangular Steel Plates. *Res. J. Recent Sci.* **2012**, *1*, 63–71.
25. Djelosevic, M.; Tepic, J.; Tanackov, I.; Kostelac, M. Mathematical Identification of Influential Parameters on the Elastic Buckling of Variable Geometry Plate. *Sci. World J.* **2013**, *2013*, 268673. [CrossRef]
26. De Mauro Vasconcellos, R.; Liércio André, I.; Alexandra Pinto, D.; Daniel, H. Elastic and Elasto-Plastic Buckling Analysis of Perforated Steel Plates. Repositório Inst. 2013. Available online: https://repositorio.furg.br/handle/1/4929 (accessed on 1 May 2022).
27. Behzad, M.; Noh, H.-C. Use of Buckling Coefficient in Predicting Buckling Load of Plates with and without Holes. *J. Korean Soc. Adv. Compos. Struct.* **2014**, *5*, 1–7. [CrossRef]
28. Mohammadzadeh, B.; Noh, H.C. Investigation into the buckling coefficients of plates with holes considering variation of hole size and plate thickness. *Mechanika* **2016**, *22*, 167–175. [CrossRef]
29. Shariati, M.; Faradjian, Y.; Mehrabi, H. Numerical and Experimental Study of Buckling of Rectangular Steel Plates with a Cutout. *J. Solid Mech.* **2016**, *8*, 116–129.
30. Jana, P. Optimal design of uniaxially compressed perforated rectangular plate for maximum buckling load. *Thin-Walled Struct.* **2016**, *103*, 225–230. [CrossRef]
31. Lorenzini, G.; Helbig, D.; Silva, C.; Real, M.; Santos, E.; Rocha, L. Numerical evaluation of the effect of type and shape of perforations on the buckling of thin steel plates by means of the constructal design method. *Int. J. Heat Technol.* **2016**, *34*, S9–S20. [CrossRef]
32. Adah, D.E.; Onwuka, O.M. Ibearugbulem, Matlab Based Buckling Analysis of Thin Rectangular Flat Plates. *Am. J. Eng. Res.* **2019**, *8*, 224–228.
33. Gracia, J.B.; Rammerstorfer, F.G. Increase in buckling loads of plates by introduction of cutouts. *Acta Mech.* **2019**, *230*, 2873–2889. [CrossRef]
34. Da Silva, C.C.C.; Helbig, D.; Cunha, M.L.; dos Santos, E.D.; Rocha, L.A.O.; Real, M.D.V.; Isoldi, L.A. Numerical buckling analysis of thin steel plates with centered hexagonal perforation through constructal design method. *J. Braz. Soc. Mech. Sci. Eng.* **2019**, *41*, 309. [CrossRef]
35. Rao, L.B.; Rao, C.K. Fundamental Buckling of Annular Plates with Elastically Restrained Guided Edges Against Translation. *Mech. Based Des. Struct. Mach.* **2011**, *39*, 409–419. [CrossRef]
36. Rao, L.B.; Rao, C.K. Buckling of circular plate with foundation and elastic edge. *Int. J. Mech. Mater. Des.* **2015**, *11*, 149–156. [CrossRef]
37. Rao, L.B.; Rao, C.K. Buckling of Annular Plates with Elastically Restrained External and Internal Edges. *Mech. Based Des. Struct. Mach.* **2013**, *41*, 222–235. [CrossRef]
38. Fu, W.; Wang, B. A semi-analytical model on the critical buckling load of perforated plates with opposite free edges. *Proc. Inst. Mech. Eng. Part C J. Mech. Eng. Sci.* **2022**, *236*, 4885–4894. [CrossRef]
39. Hosseinpour, P.; Hosseinpour, M.; Sharifi, Y. Artificial neural networks for predicting ultimate strength of steel plates with a single circular opening under axial compression. *Ships Offshore Struct.* **2022**, *17*, 1–16. [CrossRef]
40. Timoshenko, S.P.; Gere, J.M. *Theory of Elastic Stability*; Tata McGraw-Hill Education Pvt. Ltd.: New Delhi, India, 2010.
41. Ebid, A.M.; El-Aghoury, M.A.; Onyelowe, K.C. Estimating the Optimum Weight for Latticed Power-Transmission Towers Using Different (AI) Techniques. *Designs* **2022**, *6*, 62. [CrossRef]
42. Reda, M.A.; Ebid, A.M.; Ibrahim, S.M.; El-Aghoury, M.A. Strength of Composite Columns Consists of Welded Double CF Sigma-Sections Filled with Concrete—An Experimental Study. *Designs* **2022**, *6*, 82. [CrossRef]
43. Nemeth, M.P. Buckling behavior of compression-loaded symmetrically laminated angle-ply plates with holes. *AIAA J.* **1988**, *26*, 330–336. [CrossRef]
44. Faradjian Mohtaram, Y.; Taheri Kahnamouei, J.; Shariati, M.; Behjat, B. Experimental and numerical investigation of buckling in rectangular steel plates with groove-shaped cutouts. *J. Zhejiang Univ. Sci. A* **2012**, *13*, 469–480. [CrossRef]
45. Kelpša, Š.; Peltonen, S. Local Buckling Coefficient Calculation Method of Thin Plates with Round Holes. *ce/Papers* **2019**, *3*, 841–846. [CrossRef]
46. Shi, J.; Guo, L.; Gao, S. Study on the buckling behavior of steel plate composite walls with diamond ar-ranged studs under axial compression. *J. Build. Eng.* **2022**, *50*, 2352–7102.
47. Wu, Y.; Xing, Y.; Liu, B. Analysis of isotropic and composite laminated plates and shells using a differential quad-rature hierarchical finite element method. *Compos. Struct.* **2018**, *205*, 11–25. [CrossRef]
48. Kabir, H.; Aghdam, M. A robust Bézier based solution for nonlinear vibration and post-buckling of random checkerboard graphene nano-platelets reinforced composite beams. *Compos. Struct.* **2019**, *212*, 184–198. [CrossRef]

49. Sun, Z.; Lei, Z.; Bai, R.; Jiang, H.; Zou, J.; Ma, Y.; Yan, C. Prediction of compression buckling load and buckling mode of hat-stiffened panels using artificial neural network. *Eng. Struct.* **2021**, *242*, 112275. [CrossRef]
50. Zhu, S.; Ohsaki, M.; Guo, X. Prediction of non-linear buckling load of imperfect reticulated shell using modified consistent imperfection and machine learning. *Eng. Struct.* **2020**, *226*, 111374. [CrossRef]
51. Badarloo, B.; Jafari, F. A Numerical Study on the Effect of Position and Number of Openings on the Performance of Composite Steel Shear Walls. *Buildings* **2018**, *8*, 121. [CrossRef]
52. Tahir, Z.U.R.; Mandal, P.; Adil, M.T.; Naz, F. Application of artificial neural network to predict buckling load of thin cylindrical shells under axial compression. *Eng. Struct.* **2021**, *248*, 113221. [CrossRef]
53. Abambres, M.; Rajana, K.; Tsavdaridis, K.D.; Ribeiro, T.P. Neural Network-Based Formula for the Buckling Load Prediction of I-Section Cellular Steel Beams. *Computers* **2018**, *8*, 2. [CrossRef]
54. El-Aghoury, M.A.; Ebid, A.M.; Onyelowe, K.C. Optimum Design of Fully Composite, Unstiffened, Built-Up, Hybrid Steel Girder Using GRG, NLR, and ANN Techniques. *J. Eng.* **2022**, *2022*, 7439828. [CrossRef]
55. Kadry, A.A.; Ebid, A.M.; Mokhtar, A.-S.A.; El-Ganzoury, E.N.; Haggag, S.A. Parametric study of Unstiffened multi-planar tubular KK-Joints. *Results Eng.* **2022**, *14*, 100400. [CrossRef]

designs

MDPI

*Article*

# Prospects of Triangular Modular Structures for Roadside Service Buildings

**Konstantin Samoilov [1,*], Bolat Kuspangaliyev [1], Gaukhar Sadvokasova [2] and Nurlytan Kuanyshbekov [2]**

[1] Institute of Architecture and Construction, Satbayev University, 22 Satbayev Str., Almaty 050000, Kazakhstan
[2] International Education Corporation/KazGASA, 28 Ryskulbekov Str., Almaty 050043, Kazakhstan
* Correspondence: samconiv@mail.ru; Tel.: +7-701-357-68-93

**Abstract:** The need for a relatively quick solution to the problem of providing highways with roadside service facilities necessitates the development of a series of appropriate standard projects. To increase the efficiency of these series, it is advisable to carry out the interconnection of space-planning solutions based on a particular module. Taking into account the variety of planning and landscape characteristics of the sites for the placement of objects of the mainline service, it seems advisable to choose as a module not a square or rectangular, but a triangular configuration, which allows in most cases to harmoniously block the modules. The proposed roof module in the form of a "regular" triangle facing the tetrahedron has a structural basis in the form of a single-tier rod spatial plate. The principal space-planning solutions of all four dozen objects from the approved nomenclature of the mainline service performed in the process of analyzing the possibilities show the real possibility of solving the development tasks on the basis of this system. The use of the proposed modular system makes it possible to successfully solve a number of tasks to reduce the harmful impact on the environment and effectively use renewable energy sources. The work is devoted specifically to the field of design.

**Keywords:** roadside service buildings; modular buildings; sustainable architecture; spatial grid plates; reusable structures; base module; collapsible buildings

**Citation:** Samoilov, K.; Kuspangaliyev, B.; Sadvokasova, G.; Kuanyshbekov, N. Prospects of Triangular Modular Structures for Roadside Service Buildings. *Designs* **2022**, *6*, 90. https://doi.org/10.3390/designs6050090

Academic Editors: Joshua M. Pearce and Tiago Pinto Ribeiro

Received: 20 June 2022
Accepted: 28 September 2022
Published: 2 October 2022



## 1. Introduction

Modern facilities of the mainline service demonstrate a wide variety of planning solutions and architectural and artistic forms. The problem that has arisen at this stage of roadside service development (including in Kazakhstan, where there are a number of promising opportunities in the construction sector, per B.Torgautov, A. Zhanabayev, A. Tleuken, A. Turkyilmaz, M. Mustafa, F. Karaca, F. [1], who point to challenges and opportunities in the construction sector of Kazakhstan in the aspect of a closed-cycle economy), the problem of accelerated, almost one-time construction of a large number of facilities puts forward a number of peculiar tasks that have not yet received appropriate research work (the relevance of the development of architecture of roadside service facilities in Kazakhstan is emphasized N.N. Kuanyshbekov, A.K. Tuyakaeva [2]).

The objects of roadside service naturally began to arise with the development of communication routes. With the advent of motor transport, the nomenclature of objects has increased somewhat, but the functional specifics of their work has not changed much. Accordingly, space-planning solutions, having a centuries-old practice of application and improvement, have a significant degree of study. The totality is formed in the mutual influence of several aspects important for the ongoing research. So, the general assessment of the roadside service system is covered in the works T. Cui, Y. Ouyang, Z.J.M. Shen [3], where the design of a reliable placement of an object under the risk of failures is considered. D. Ettema, T. Gärling, L.E. Olsson, M. Friman and S. Moerdijk analyze the satisfaction of Dutch drivers with roadside service [4]; M.K. Bostani, F. Hashemzehi and M.R. Anvari

evaluate roadside service centers on the example of a separate highway [5]; Z. Dvorak, E. Sventekova, D. Rehak, Z. Cekerevac [6] analyze the quality of the most important elements of infrastructure in transport; H.Z. Rahman, A. Andreas, D. Perwitasari, J.S. Petroceany [7] paid attention to the development of the typology of the social infrastructure of roadside stations; M.M. Hasan, A. Alam, A.M. Mim, A. Das [8] analyzed the features of determining the level of satisfaction of users with road services; the economic assessment of the construction of roadside service facilities was carried out by such researchers as O. Makovetskaya-Abramova, A. Ivanov, Y. Lazarev, M. Shakhova, and A. Rozov [9].

Certain types of roadside service facilities and the specifics of their location are considered in various regulatory documents and research papers (A. Hurley, J.A. Jakle, K.A. Sculle [10–13] actualized the problem of roadside restaurants, taking into account the peculiarities of road transport; M. Magdic, P. Sjöstrand [14] drew attention to the key role of gas stations; K. Wolfe, R. Holland, J. Jeff Aaron [15] conducted marketing of agricultural products sold in roadside stores; K. Shanahan drew attention to the degree of correspondence between the advertising on roadside billboards and the attributes of motels in demand by tourists [16]; M. Kendrick analyzed the history of the development of models [17]; Y.W. Wang and C.R. Wang calculated the optimal scheme of the location of passenger vehicle refueling stations [18]; L. Henderson [19] drew attention to the change in the range of services provided by motels; A.F. Al-Kaisy, Z. Kirkemo, D. Veneziano and C. Dorrington examined the use of recreation areas on rural highways [20]; K.J. Sheng, A.S. Baharudin, K. Karkonasasi [21] studied the system for determining the location of a car service station in case of a breakdown; I. Xanthopoulos, G. Goulas, C. Gogos, P. Alefragis and E. Housos drew attention to the relationship between optimizing energy consumption and user satisfaction with roadside recreation areas [22]; A. Plovnick, A. Berthaume, C. Poe, T. Hodges [23] studied the problem of designing and operating sustainable recreation areas in the transport system; P. Karanja, C.W. Gathitu [24] illustrated the strategy of placing gas stations on a concrete example of an important highway; M. Rubeis, S. Groves, T. Portera and G. Bonaccorsi discuss the prospects for further development and the feasibility of operating roadside service stations [25]; D. Green, P. Roper, L. Steinmetz, L. Latter, K. Lewis, D. Gaynor [26] detailed the issue of equipment of recreation areas for heavy vehicles; A. Quito drew attention to the prospects for the development of roadside chapels [27]).

Special attention is paid to the points where alternative fuels are refueled (I. Capar, M. Kuby, V.L. Leon, Y.J. Tsai [28,29], S.H. Chung, C. Kwon [30], S.F. Bhatti, M.K. Lim, H.Y. Mak [31], M. Ghamami, A. Zockaie, Y.M. Nie [32], T.H. Tran, T.B.T. Nguyen [33]).

Accordingly, the potential of the modularity of structures, which is realized in objects of different volume and shape, looks promising (G.Angelucci, F.Mollaioli, R.Tardocchi [34]). The rapid construction of a large number of typologically different objects, technologically linked into a roadside service complex, suggests the possibility of using end-to-end modularity (A. Subbotin, S. Grigoryan [35], K.I. Samoilov [36]).

However, despite the considerable degree of study of certain aspects of the problem of roadside maintenance, the problem of interaction of objects in the complex has not been studied enough. Particularly noteworthy is the idea of unification and standardization of roadside service facilities, which provides a quick visual identification of the function of each object in the process of moving along the highway, as well as an understanding of its planning features, which makes it convenient to navigate in the service process.

The scientific novelty of the study is as follows:

- for the first time, the possibility of spatial-planning linking of typologically diverse roadside service facilities with a large-sized structural module is demonstrated;
- for the first time, the possibility of forming roadside service complexes based on multi-configuration blocking of modules, taking into account both the uniqueness of the typology of an individual object and the complex as a whole is shown;
- for the first time, a triangular module was used to solve the above problems.

Thus, the proposed material shows a set of new scientific results that determine the possibility of effective use of a modular system based on a triangular rod spatial plate

with appropriate planning adaptation of the entire nomenclature of individual objects and roadside service complexes.

At the beginning, the specifics of buildings and structures that solve individual tasks that form a set of roadside service needs are considered. Then, the application of the triangular module is justified and the possibility of an integrated approach to solving these problems based on this configuration is shown. The advantages of the proposed system from the point of view of the organization of production, construction, and operation, including issues of energy efficiency and environmental protection, are indicated below. In conclusion, the prospects for further study of this topic are shown.

## 2. Materials and Methods

The research method used in the work is the general scientific dialectical way of cognition from observation through generalizations to practice. In its context, the following are applied:

- an integral-differential approach, which allows dividing the array of roadside service facilities on the principle of similarity of typological forms into many components, combining them into a set reflecting the possibility of planning unification;
- a formal approach that allows to trace the development of various typological forms of roadside service facilities;
- an iconographic approach that allows to explore the manifestation of the features of various historical prototypes in the modern layout of roadside service facilities;
- a structural-semiotic approach that allows modeling the development and prospects of the planning unification of roadside service facilities.

The methodology determined the techniques and sequence of work: selection and analysis of literature; field surveys; differentiation of the array of data obtained; comparison and analysis of options; formation of a unified layout design model based on a triangular module.

Having the character of mass use, road service objects are organically predisposed to typification and unification. On the one hand, this ensures their rapid visual recognition in conditions of the complexity of high-speed traffic, and on the other hand, it allows them to be built optimally quickly, taking into account the working methods. The need to improve roadside services and increase traffic flow adds to the need to expand existing single or complex structures. This naturally actualizes the need for modularity of elements, which makes it possible to increase the structure using, among other things, the initial design solutions. Among the nomenclature of roadside service facilities, the most dynamic element is filling stations of various types of fuel. Checkpoints and individual parking lots are also interesting from this point of view.

The nomenclature of roadside facilities for servicing vehicles includes: refueling with various types of fuel, washing motorcycles and cars of various sizes, service stations. Gas stations differ both in the types of fuel being refueled and in the specifics of their work. Automatic self-service filling stations are gradually becoming more widespread. Externally, they are usually a small canopy over the control panel. The main problem of common solutions is the lack of comfort during use, since the minimized surface of the canopy protects not only the car being refueled, but in most examples even the process control panel from precipitation. Moreover, if this is just an inconvenience for urban conditions, then it is a critical disadvantage for highways. Large gas stations are usually characterized by a fairly wide canopy, usually uniform for the complex, providing partial or complete shelter of the refueling car from atmospheric precipitation. In the operator's pavilion located in the immediate vicinity, there are sometimes small shops of related products and buffets of tonic drinks, as well as toilets, which imply the use of not only staff, but also road users.

Trading operations for refueling and selling products in the store, depending on the size of the complex, are carried out by one or more people. One or several people are also engaged in servicing the refueling columns themselves, for whom an appropriate

set of rooms is provided in the structure of the complex: dressing rooms with showers, a recreation room. The complex also has an administration office, rooms for engineering support systems, and storerooms for technical, technological, and cleaning equipment. The architectural and artistic solution of the canopy reflects the preferences of customers interpreted by the author of the project or the corporate identity of the supplier of a particular type of fuel. The technological peculiarity of gas as a type of automobile fuel has determined the spatial solution of the corresponding gas stations, which are either included in the complex of conventional diesel-gasoline gas stations in the form of a separate structure or as independent complexes with an appropriate set of main and auxiliary rooms. The main technological feature of gas filling stations is the ground location of tanks, which ensures high explosion and fire safety of the complex. Sometimes, there are solutions with an underground location of gas tanks, but this entails the need to ensure the constant operation of a special ventilation system. Such gas stations operate both in normal and automatic mode according to the self-service system. Electric filling stations usually operate in automatic mode using a self-service system. The main problem of the formation of such structures as elements of roadside service is to provide leisure time for drivers and passengers during the refueling process, which takes from one and a half to several hours. This entails the need to create an appropriate pavilion with a set of services for short-term rest. This practice is almost not found now.

Car washes vary both by system of operation and by means of transport. Self-service car washes are often formed for passenger cars and motorcycles, which are covered posts partially fenced off by stationary or transformable partitions with control panels for pipelines of hose supply of water, detergents, compressed air, as well as waste disposal suction. Depending on the number of washing stations and placement, the structure includes an operator's pavilion with an appropriate set of main and auxiliary rooms. If a small structure of this type is included in the complex of a large car wash for trucks and buses, then the operator's pavilion is usually not made, being combined with the corresponding rooms of the main car wash. Quite often, self-service car washes are combined in one facility with automatic contactless car washes. Since the process of contactless washing involves the in-line execution of several technological processes, the pavilion itself has a longer length than for a conventional washing, providing through movement even of a passenger car, which determines the peculiarity of its position in the layout of the complex. Depending on the customer's wishes, during the contactless washing process, he can either stay in the car or stay outside. For the convenience of visual control of the process, in some examples, stained glass glazing of the washing line room is used. For trucks and buses, automatic open portal-type sinks are often used, moving along the vehicle. The limitation of the use of such sinks is their convenience only for the relatively warm season, which determines their location in a complex with closed sinks for year-round operation. The most common because of the convenience of use are pavilion sinks for cars, trucks and buses. They are mostly with a dead-end arrival or through passage. The main room of the sink is usually divided by stationary or mainly transformable curtain partitions. Auxiliary rooms are located compactly from above as an independent floor or on the mezzanine, in the middle part, on the side or symmetrically. They include a complex of rooms for customers with a room for receiving orders, a rest room, a buffet and toilets; administration—with one or more offices. A group of rooms for staff is specially planned: a control room, dressing rooms with toilets, showers and storerooms of clean and used workwear; a meal room with a built-in kitchen, storerooms of cleaning and technological equipment, cleaning materials. There is also a group of rooms for engineering support systems, panel rooms, ventilation chambers, a heat point, a water measuring unit, pumping stations. In combination with various types of sinks, there are recycling water treatment facilities. They are located in various places: in the basement space directly under the washing posts, on the side or behind in an annex or in a free-standing structure.

A separate, less often built-in, facility is a car service station. Usually, technological operations are performed by specialized personnel. However, there are self-service stations

for minor repairs. Usually, the complexes are pavilions with the main room, fenced off by stationary partitions for repair posts, having independent dead-end entrances and exits to each post. The doors in the partitions provide a consistent connection of the repair rooms with each other. The repair room has a technologically determined height that ensures the maintenance of the car on the lift. Adjacent to the repair posts are storage rooms for spare parts, parts, consumables, tools and technological equipment. The complex of rooms for repair personnel, located on the same level with the repair posts or on the mezzanine, includes dressing rooms with toilets and showers, storerooms of clean and used workwear, a meal room with a built-in kitchen, a recreation room, a classroom. The administrative and clerical part includes: a document processing room, a rest room, a buffet, toilets, a control room, administration offices. Depending on the layout, the premises of engineering support systems are located compactly or dispersed.

The nomenclature of traffic control structures includes: points of traffic control services, checkpoints, points of dimensional and weight control of vehicles.

Primary traffic control is carried out at small points of traffic police services. They are usually located near populated areas. Relative to the highway, posts are of island and coastal types. The structure of such points usually includes a small canopy and partially isolated areas for the placement of duty officers. Sometimes, the item includes a separate heated pavilion, which houses a toilet, duty rooms and utility rooms. To improve visual control, the duty rooms in such pavilions are sometimes located on the second level. At the same time, the first level is used mainly as a covered parking place for a special car on duty. For extended sections between settlements, it is advisable to use structures with an expanded composition of premises. In the case of an island position on the highway, in a two-story pavilion on the ground floor, there are operator traffic control rooms, rooms for checking documents of detained cars, and toilets. Parking places for special cars on duty with the possibility of direct or rotary exit to the highway in the right direction are arranged under the end canopies. In the sequel, already in an open area, detained cars are parked in the direction of direct traffic. On the sides under the canopies, there are lanes of slow-motion free passage of vehicles. The second floor includes symmetrically located offices of operational visual control, oriented to the incoming section of the highway, staff wardrobes with toilets and showers, the office of the head of the shift on duty, a study room, a meal room with a built-in kitchen, a room for administratively detained drivers and passengers, storerooms of special and cleaning equipment, technical communication rooms.

Checkpoints with controlled passage are provided for entry and exit to toll sections of highways. At the same time, each lane has a barrier and a payment machine under the canopy. Vehicles stop for a short time only for carrying out payment transactions. The facility is located across the highway and has duty personnel pavilions located along the coastal or island scheme. In one- or two-storey pavilions, there are operator's rooms, control rooms, staff wardrobes with toilets and showers, meal rooms with built-in kitchens, the office of the shift supervisor, storerooms of special and cleaning equipment, rooms of technical means of communication and alarm systems. The pavilions are directly adjacent to the canopies for parking special cars with a direct or rotary exit in the appropriate direction. In a simplified version, the pavilions of the personnel of such checkpoints are small buildings with two or three small rooms only for operational duty officers.

Large structures with enhanced operator control of each lane are provided for specialized control of travel to the relevant road sections or entry-exit to the relevant zones. At the same time, vehicles stop at the post for the time necessary for conducting an external inspection of the rolling stock and checking the documents of the drivers. In accordance with this, each lane has a separate pavilion for accommodating an operational duty officer and a shift worker, as well as a toilet. The room on duty has a height that allows you to see the vehicle through the stained glass to the full height of the road dimension—4.5 m. In the underground level, there are rooms with anti-aircraft openings for visual inspection of the bottom of vehicles. Further, on top of the room on duty, there are bridges for inspection

of the upper part of the car. All three levels of each pavilion are connected by a stairwell. The underground observation rooms through the gallery and observation bridges are directly sequentially connected to each other and to the administrative pavilion located in the middle (island version) or to the side (coastal version). This ensures an operational visually isolated passage of personnel to a specific post. In this pavilion, on the ground floor, there are duty rooms, offices for paperwork, toilets. The second floor is occupied by visual control rooms of access areas, staff wardrobes with toilets and showers, a meal room with a built-in kitchen, a classroom, technical rooms for special communications and alarm systems. Storerooms of special and cleaning equipment, warehouses of workwear, and technical rooms of engineering support systems are located in the basement. The complex includes covered parking lots for special cars with the possibility of direct or rotary exit in the appropriate direction, as well as open parking lots for detained vehicles.

A typical example of such a structure is the complex on the Narol-Naroda Road in Gujarat. It was built according to the project of the company "Archohm" (architect S. Gupta, 2010) [37]. Having an area of 3860.0 sq.m, it is planned to represent 16 (8 + 8) control and toll collection posts connected by an underground gallery with each other and with two blocks of administrative and office purpose. The buildings are elongated volumes with blind side walls and a fully glazed central cylindrical block. On the ground floor of the office block, there are: lobby, security post, elevator, waiting hall, stairs, passage, toilet, equipment storage room, garden, cash register, archive, shop, document verification room, security room. On the second floor, there are: toilet and shower for staff, locker room, elevator, passage, kiosk, cafe, guest hall, cleaning room, manager's office, women's toilet, men's toilet, staff room, classroom. On the third floor, there are: the dispatchers' pavilion, the exploited sections of the roof. The posts have sufficient height for lateral visual control. An iconic element of the architectural and artistic solution are awnings with geometry that varies depending on the weather and the location of the sun. The dominant color of the complex is red. This color has blind sections of the walls of the administrative and office pavilions, awnings and tubular bumpers stretched to the full height of the truck.

The auxiliary object of traffic control complexes are the points of weight and dimensional control of vehicles. They can be formed either in an open version or in the form of a pavilion with canopies. When closed, they include canopies with equipment for parametric control, as well as a pavilion for staff accommodation and registration of relevant documents. The pavilion's premises include toilets, storerooms for special and cleaning equipment, rooms for engineering support, and communication systems.

The nomenclature of roadside service facilities for drivers and passengers includes: public transport stops, retail and catering outlets, public toilets and showers, laundries, medical and rescue service points, wellness pavilions, picnic and recreation areas, scenic areas, playgrounds and pavilions, roadside temples of various denominations, heating points, post offices, motels, warehouses, supermarkets.

The difference between public transport stops in the city and on intercity routes is based on a much longer waiting time and a stronger impact of precipitation and wind. In addition, unlike city stops, suburban stops, due to the open space around, practically do not block the view of suitable transport. Accordingly, for city stops, it is necessary to ensure "transparency" that creates end-to-end visibility. For suburban stops, however, a larger canopy and the creation of a partially enclosed pavilion with blind rear and side walls are advisable. Roadside retail and catering outlets have different capacities depending on the intensity of cargo-passenger flow on the highway. Usually, they consist of a dining room with several tables and an adjacent kitchen with a cutting room and a dishwasher. Free access to goods is provided in the trading floor, some small goods are sold from behind the counter. The premises include a toilet for visitors and staff, an administrative office, and a number of utility rooms.

In order to avoid duplication of structures, ensuring the possibility of using the services of travelers moving in opposite directions leads to the need to create crossings across the

highway. At the same time, parking is arranged on both sides, and the bridge in some places is used as a passing shopping or dining hall.

Public toilets are a very important element of roadside service. In most cases, these are small container-type structures. However, this is not very convenient, since, for example, when a regular bus stops, a queue of passengers is created, which is critically unacceptable. Accordingly, it seems appropriate to create more spacious facilities, including two compartments with vestibules-washrooms, rooms of the actual restroom with ordinary booths and booths for disabled visitors, a pantry of cleaning equipment. In some cases, it is optimal to expand the composition of the premises for the organization of a shower.

The modern practice of creating roadside medical and rescue service facilities in most cases demonstrates mobile container roadside emergency medical aid stations. However, the need to improve services determines the need to create stationary facilities, including reception rooms, dressing rooms, storerooms of medicines and equipment, toilets with large vestibules for changing clothes, tool rooms, rest rooms for duty crews, dispatching rooms, staff reception rooms, administrative rooms, workwear storerooms, wardrobes with showers, and covered parking spaces for special cars. In some cases, separate dentist and therapist offices are needed. Roadside heating points are part of the medical and rescue service complexes. Currently, in most cases they are mobile in the form of equipped cars or tents. In some cases, containers are used. However, taking into account the places of possible accumulation of cars in winter known from long-term operation practice, it is advisable to form stationary heating points in addition to mobile points. As part of their premises, wardrobes with toilets and places for drying clothes, a small buffet for hot food and drinks, a rest room, a control room, a staff room and the necessary set of rooms for engineering support systems are provided.

In the most picturesque places of the route or as part of large roadside service complexes, places for organizing picnics are provided, designed for several unrelated companies of vacationers. At the same time, the possibility of placing customers both in the open air and under the canopies of free-standing gazebos and pavilions is provided. Gazebos and pavilions are designed for a different number of vacationers. Of course, it is necessary to set up toilets, places for washing dishes, as well as containers for collecting garbage and food waste. Usually, places for cooking food on an open fire with wood warehouses are organized. Electric grills with the appropriate equipment are also provided.

To ensure the spiritual needs of those passing by, roadside structures of a cult nature are formed. They have different sizes depending on local characteristics. The space-planning solution is built depending on the canons of a particular denomination. However, the general set of rooms and spaces largely coincides. These are: a common or divided into male and female parts prayer hall, lobby, clergy room, library. There are also open courtyards or spaces under canopies for pre-prayer and post-prayer concentration. The orientation of prayer halls is created depending on the canons. Historically, there was also a type of small roadside chapels or chapels, consisting of one or two rooms for one or more travelers to pray without the participation of a clergyman.

As part of roadside complexes for long-term recreation, children's playgrounds with heated pavilions are being built, in which game rooms, utility and storage rooms and toilets are arranged. Next to the pavilion, it is advisable to arrange a large canopy for games during rain or bright sun.

The roadside service system includes small post offices associated mainly with the function of receiving correspondence and providing telephone communication in various formats. Roadside laundries are an integral part of the service. These facilities provide for both self-service and taking things to the laundry for a short-term or long-term stop. As part of their premises, there is usually a lobby, a cash register, a toilet for customers, self-service laundry rooms and laundry items, laundry pantries, self-service ironing and ironing items, inventory rooms, a laundry reception point, staff wardrobes with toilet and shower, cleaning equipment storerooms, a laundry pick-up point, engineering support systems rooms.

The complex of roadside entertainment includes various sizes of summer theaters, variety shows and stage platforms. They have open and canopied spaces for spectators and artists. The composition of the stage premises sometimes includes artistic rooms with toilets and storerooms of scenery. In places of long-term recreation, it is planned to build fitness clubs with a different set of rooms for gymnastics and water-entertainment procedures. The premises of such facilities may include: a lobby, a reception desk with a cash register and a utility room, a men's and women's department (wardrobe, linen closet, toilet, vestibule, shower room, corridor, steam room, gym, equipment pantry, coaching room, toilet), a hall with a swimming pool (swimming bath, bubble baths, children's splashing pool), a bar for light drinks, rooms of engineering systems, a playground for recreation and gymnastics under a canopy.

Along with gas stations, the most important object of roadside service are motels. They are mainly solved as one- or two-storey buildings with rooms representing an entrance hall, a bathroom and a room with a built-in kitchen. Sometimes, a bathroom with a kitchen is located in the back at the back wall, and the entrance is organized directly into the room. Three- or four-storey motels are quite rare. The main planning requirement for the models is the organization of parking the client's car opposite the entrance to his room or in the immediate vicinity of it. Some models are formed from detached houses with parking lots. Then the administration room is located in a separate pavilion. Sometimes, a vacation in motels turns into a kind of ethnographic attraction. As part of the motels, recreation areas with swimming pools are provided.

Ensuring the function of responsible storage of goods of various sizes is implemented by roadside warehouses. Usually these are large rooms, some of which are occupied by racks. Administrative and technical premises are located in the side parts. The buildings have numerous gates for the arrival of customer transport.

The largest objects of roadside service are supermarkets. The main requirement for the location of the store is the presence of a multi-seat parking lot, which determines its placement usually in the depth of the designated area. The most common is the rectangular shape of the plan, but there are other solutions. Their premises usually include: a lobby with one or two entrances with storage chambers; trolley placement zones; flow-distribution zones with areas for short-term rest of visitors; information desk; security point; currency exchange offices; branches of banks and telephone companies; pharmacy, perfume, jewelry, book and newspaper kiosks; workshops for small express repairs of shoes, bags, umbrellas, watches, phones and gadgets; buffets for light snacks; bars for soft drinks; public toilets; cash register; the main trading hall with shelving, display, counter and container-stand placement of goods. In the auxiliary compartment, there are: auxiliary and storage rooms with cold storage rooms; administrative and household premises for personnel; a reception area for goods with places for unloading trucks; a zone for pre-sale preparation of goods; a zone for storing recycled containers; a zone for storing used packaging, garbage and waste; the parking and maintenance room for electric cars, the room for cleaning machines, mechanisms and inventory, as well as the premises of engineering support systems (ventilation chambers, pumping, panel, heating points, communication nodes). Part of the auxiliary and technical rooms is located on the mezzanine.

One of the most interesting examples is the Repsol gas station, built in Madrid under the project of "Foster + Partners" in 1998). Despite the 20 years that have passed since its commissioning, its volumetric and spatial solution, implying the possibility of significant expansion while preserving the figurative and stylistic character, continues to attract the attention of researchers [38–40]. A special aspect is the figurative recognition of the object. The conceptual prototype of such an umbrella solution is, for example, Pegasus filling stations designed by E.F. Noyce in 1960 for the company "Mobile", where round umbrellas are used (Red Hill Filling Station, Leicestershire, UK) [41]. At the same time, the umbrella idea for gas stations itself has a longer history—for example, the classic gas station designed by A. Jacobsen in 1937. The continuation of the story is the Munich gas station with translucent membrane awnings, designed in 2006 by T. Frank and T. Probst, the firm

"Frank and Probst architects". In general, as for membranes and awnings, there is a wide field for modularity. An example is the structures supplied by the company "Guanzhou Faith Trass awning" for road service facilities [42]. There are not only gas stations, but also checkpoints and individual parking. The company "Travelpark Ulyanovsk" offers to implement large modules in the complexes of roadside service of the Ulyanovsk region [43]. A typical complex consists of seven volumes sequentially located parallel to the highway for various purposes, having the same spatial solution. The outer contour has a beveled elongated U-shape, forming a roof, rounded into blind end walls. The side surfaces have solid stained glass glazing. A typical complex includes a refueling station for several types of fuel with eight lanes (including buses and trucks—a kind of "fuel hypermarket"), retail outlets, catering, a motel, warehouses. The refueling unit itself is longer to provide convenient through passage along the complex. Each block has its own color, providing quick visual recognition of the function, which allows users to conveniently park in close proximity to the selected object. This, of course, improves the orientation conditions of drivers when driving on the highway.

These examples show the prospects of using a modular system for roadside service facilities, as they allow you to vary the modularity not only depending on the size of the roadside complex, but also take into account a variety of natural and climatic conditions of the region. In accordance with the regulations of some countries [44], these facilities, depending on the volume and range of services, can be divided into four categories. So, the objects of category "D" include: gas stations, toilets, points of sale. There is no gas station in the objects of category "C", but a food point and parking are added. The nomenclature of objects of category "B" includes: a gas station, a motel, a toilet, a shower, points of trade and catering, a service station, a car wash, a medical center, a parking lot and a picnic area. The largest nomenclature has objects of category "A", which include: gas stations, a motel, a toilet, a shower, points of trade and catering, a medical center, a service station, a car wash, a parking lot, a shopping and entertainment area, a picnic area. A separate object is the "Heating point". As an addition, you can also specify the need to equip checkpoints of road safety and control services. It is also advisable to include in the nomenclature, for example, objects of category "A", small structures for performing religious rites of the main religious denominations. A separate category of objects are points of ordinary and special traffic control, located, depending on the specific situation, at a distance of 50–70 km from each other, as well as in close proximity to large settlements. And, of course, it is necessary to build supermarkets mainly in the suburbs, which will ensure satisfaction of the demand not only of users of the transcontinental highway, but also of citizens, since due to good transport infrastructure (access roads, large parking lots) it will allow for prompt delivery of a wide range of goods.

Taking into account the significant number of objects and the expediency of their rapid construction, one of the possible ways to implement this is the unification of space-planning and design solutions of objects based on a modular system. As the basis of this system, it is proposed to use the construction of a rod spatial plate on angular supports. Similar constructions, the idea of which is partly based on the research of the "Geodesic Dome" by R.B. Fuller (1947), have been actively studied and widely used since the second half of the last century [45].

Usually these are one- or two-tiered structures with parallel belts formed by triangles, squares or hexagons. The support of the structural plates is nodular or with a developed core capital. Sometimes there is a perimeter support in the form of the same spatial lattice structure. There is also a solution with cable-stayed fastening of plates with supports brought up. However, the optimal solution of the tightness of the fastening unit from the point of view of isolation from precipitation is difficult here. The structure is usually formed by rods of one-dimensional length from pipes or rolled profiles of various cross-sections, depending on the location of the plate in the structure. The nodal connection is welded or bolted. Elements in the form of a group of plates, a ball or a polyhedron are used as a basis. In the vast majority of cases, the plate has a square or rectangular shape. There are

variants with a triangular or hexagonal shape, depending on the structure of the actual lattice. Single or interlocked modules usually form a covering of rectangular buildings and structures.

The use of rectangular configurations for plates, for example, with a belt structure of regular triangles leads to the appearance of an additional standard size of the rod and the corresponding nodal element, which reduces the effect of uniformity of the design. This situation occurs in complexes of diverse objects, which include objects of road service. The basis of most of these facilities is a developed roof with canopies that provide comfortable boarding and disembarking of drivers and passengers of various vehicles (buses, trucks, cars) in places of road control, refueling with various types of fuel and recreation of road users. For this whole group of objects, it is proposed to use a modular single-tiered, triangular spatial plate formed on the basis of a tetrahedron. According to the regulatory recommendations [46], it is possible to use triangular-shaped plates with a discharged internal structure, when the discharged lower grid forms hexagonal cells in plan.

This is effectively used in areas of open canopies. However, in the areas where heated pavilions are located, a standardly filled lower belt allows you to fix on it (in the nodes) the suspensions of the insulated upper unused ceiling, which removes the problem of forming an independent overlap of the heated pavilion. At the same time, technologically justified episodic movements of personnel for the control of cable systems, pipelines and air ducts are provided along the appropriate bridges, also fixed to the nodes of the lower belt of the structural plate, but on top of the rod system. Given the absence of suspended equipment at the road service facilities under consideration, this solution can be successfully implemented, giving significant savings in the field of basic load-bearing structures.

The basic size is the width of two-lane traffic, 7.5 m (3.75 × 2), provided by a common tunnel size of 9.0 m. This corresponds to a "right triangle" with a side of 14.0 m. In it, the median/bisector/height is ~12.12 m (14.0 × 0.866). Accordingly, the columns located with these axial dimensions provide a full-fledged two-lane passage and sidewalks/sidewalks of ~1.56 m (taking into account the diameter of the columns of 0.4 m is 1.36 m for free passage). That is, the module is formed by rods with a conditional (calculated axial) length of 2.0 m. The lower belt is 7 triangles on the side (14.0 m), the upper belt is 8 triangles on the side (16.0 m). The height of the spatial plate will be 2.0 $(2/3)^{1/2}$ = 1.63 m, which with a margin, according to the ratio of span and section, provides spatial rigidity for this type of structures (Figure 1). Cables and pipelines of engineering support systems are conveniently located in the resulting space from the point of view of access and control. The height from the roadway is 6.0 m, which corresponds to the tunnel dimension of 5.0 m and ensures the placement of the necessary signaling devices and road signs above it. For some objects, the height can be changed according to technological parameters, which will be discussed later. The area of the room under the roof of the module is 84.0 sq.m (Figure 2).

The regional winter temperature regime allows you to leave the metal structures of the module open. The heated parts are formed as independent blocks that are not connected to the main supporting structure. It is the triangular shape of the module that makes it convenient from an architectural and planning point of view to block it in configurations corresponding to the landscape relief and functional planning features of a particular construction site.

The placement of related engineering and technological structures (underground or ground-based fuel tank farms for liquid or gaseous mixtures, transformer, pumping, fire-fighting and technological tanks, sewage treatment plants, wind generators, masts and poles of outdoor lighting, communication systems, etc.) is determined in each specific case and does not affect the space-planning solution of the object.

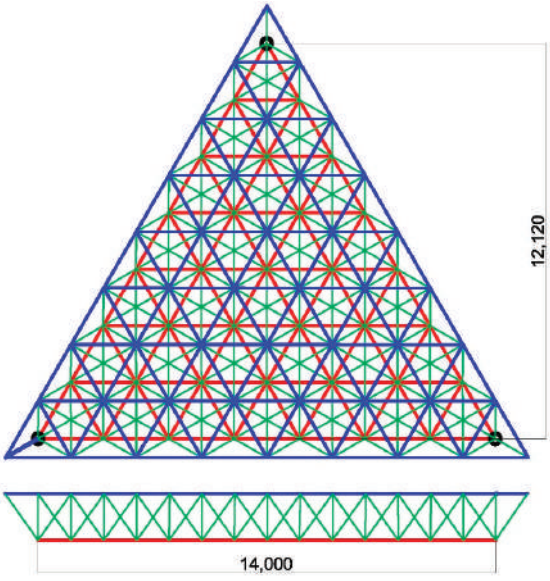


**Figure 1.** The scheme of the modular structural plate: a plan, a section (Dimensions are given in mm).

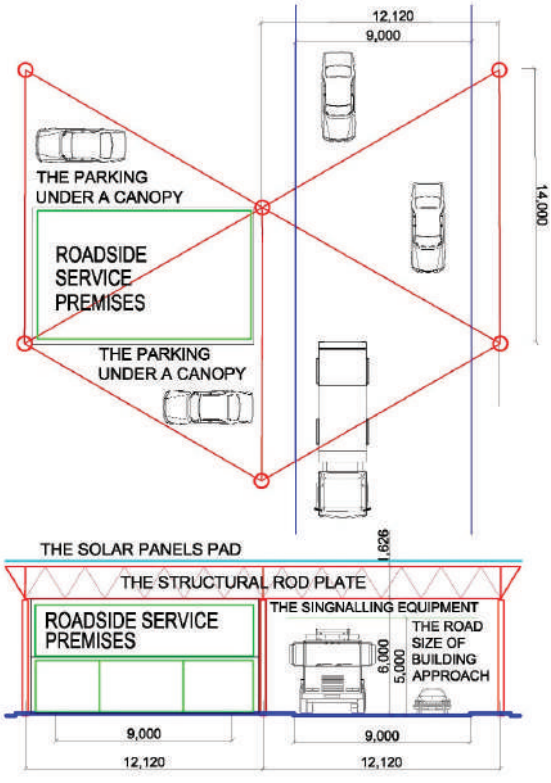


**Figure 2.** Module parameters: a plan, a section (Dimensions are given in mm).

Various quantitative and configurative combinations of these modules make it possible to provide an optimal architectural and planning solution for any object from the proposed nomenclature in both single and interlocked locations. The unification of the main load-bearing structures gives an advantage in ensuring the regulated quality of construction and installation work in the absence of an accessible developed construction and technical base and highly qualified personnel along most road sections. Equally promising from the point of view of quality is the possibility of centralized manufacturing of the main elements, the convenience of packaging and delivery of elements of two standard sizes (rods with nodal elements and racks), as well as the relative simplicity of their uniform assembly and subsequent installation of a large-sized structure. Depending on the accepted technological scheme of the organization of construction and production of works, section-by-section pre-assembly with delivery of individual sections in finished form is possible.

The uniformity of the space-planning appearance of structures is also of significant importance, which ensures rapid visual recognition of objects by drivers from distant perception plans in a tense situation of high-speed traffic. However, in the field of architectural and artistic solutions, there is the possibility of color-graphic differentiation of objects, for example, by regions of the region within the framework of stylistic unity and a kind of "corporate identity" of the highway. This is not only geographically oriented, but also important from a cultural and propaganda point of view.

### *2.1. A Set of Modular Roadside Service Facilities*

In the proposed set of modular objects, the height to the bottom of the structural coating plate in accordance with the planning and technological requirements is 4.5 m (for small single-storey structures with a side entrance of buses or trucks); 6.0 m (for travel canopies, two-storey pavilions and religious buildings); 7.5 m (for special control points, warehouses and supermarkets). According to this parameter, the proposed sets of modules for 39 types of objects are grouped (Figure 3). The sequence of objects shown in the figure corresponds to the number of interlocked modules (incrementally). All objects, except for traffic control service points located across the highway and entry and exit to special sections (positions 24, 29, 32, 33, 38), are placed on the side of highways.

It is advisable to place all objects in pairs or in a staggered order. The exception is religious buildings (positions 12, 13, 14, 15, 21, 27) and supermarkets (position 40). Depending on the specific conditions, it is advisable to place them singly, providing, due to road interchanges at different levels, the possibility of entry and departure in any direction. In addition, religious buildings are oriented in accordance with the canonical requirements of each of the religions. At the same time, it is advisable to avoid the layout of complexes in which the canonical direction of one denomination has a view of the temple of another denomination. In the vicinity of religious buildings, it is advisable to place pavilions of public toilets and showers for pre-prayer procedures (position 5).

The objects have the following operationally and technologically sound spatial planning solution, linked to the adopted modular system.

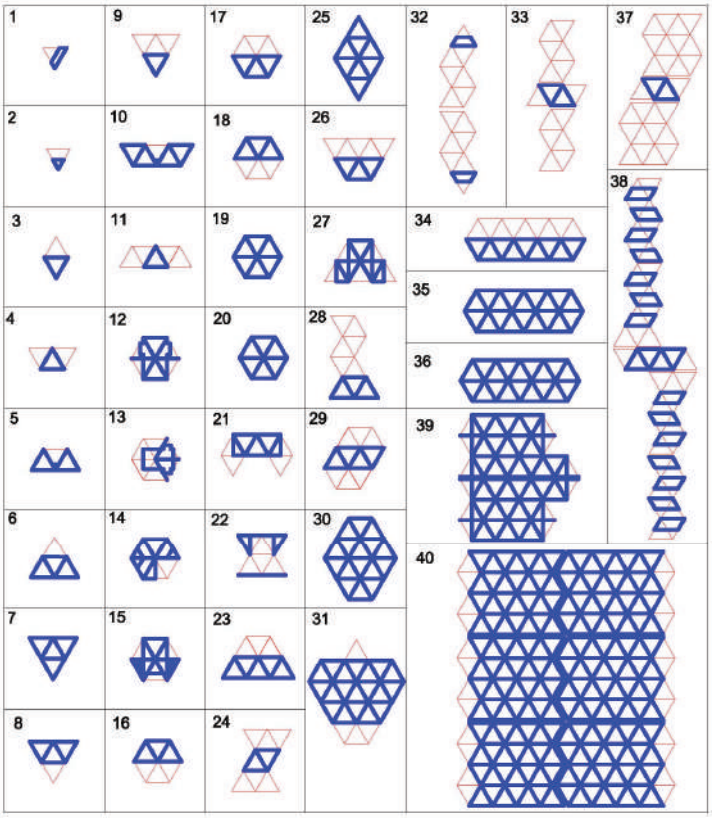


**Figure 3.** Modular buildings—layout schemes: 1—public transport stop; 2, 9, 26, 28—car refueling; 3, 4, 23—point of retail trade and public catering; 5, 10—public toilet and shower; 6, 8—medical center; 7, 25, 37, 39—car wash; 11—picnic area; 12, 13, 14, 15, 21, 27—temples of various denominations; 16—children's play pavilion; 17—heating point; 18—post office; 19, 30—car service station; 20—laundry; 22—scene; 24, 29, 32, 33, 38—point of traffic control; 31—Wellness Pavilion; 34, 35—motel; 36—warehouse; 40—supermarket (drawing of the authors).

Consider the planning solutions of such objects as the Public transport stop, the Automatic gas station, the Catering point, the Public toilet, the Public toilet and shower, the Picnic area and the Wellness pavilion (Figure 4). The public transport stop (Figure 4(1)): 1 module (50% canopy + 50% heated contour), dimensions 12.12 × 14.0 m (in axes), height to the bottom of the structural plate 4.5 m. The structure is a one-block one-storey structure: a platform under a canopy (42.0 sq.m) and a pavilion of a comfortable waiting area glazed from the inside in the direction of suitable transport, consisting of a hall and a toilet (42.0 sq.m).The automatic car refueling (self-service) gas or gasoline-diesel, or electric—(Figure 4(2)): 1 module (70% canopy + 30% heated contour), dimensions 12.12 × 14.0 m (in axes), height to the bottom of the structural plate 6.0 m. The structure is a one-block one-storey structure: a platform under a canopy (59.0 sq.m) for two refueling cars, a through passage, as well as a pavilion with a two-part isolated technical room (25.0 sq.m) and an external panel for self-service. The catering point (16 seats) (Figure 4(3)): 3 modules (2 canopies + 1 heated), dimensions 12.12 × 28.0 m (in axes), height to the bottom of the structural plate 4.5 m is a single-block one-story structure: central heated pavilion (84.0 sq.m) with a dining room for four four-seater tables, a kitchen, a dishwasher, a utility room, a wardrobe for staff, a toilet for visitors and staff. On the sides of the pavilion, there are canopies (84.0 sq. m each) for eating and relaxing in the warm season. The public toilet

(Figure 4(4)): 3 modules (0.8 canopy + 2.2 heated), dimensions 12.12 × 28.0 m (in axes), height to the bottom of the structural plate 4.5 m is a single-block single-storey structure with a central canopy (70.0 sq.m.) and side pavilions (91.0 sq.m + 91.0 sq.m), in which there are male and female public toilets (vestibule-washroom, a restroom with 6 ordinary booths and 1 for disabled visitors, a storage room for cleaning equipment). Having a connection with both branches, there is a cash register in the middle. The public toilet and shower (Figure 4(5)): 5 modules (0.8 canopy + 4.2 heated), dimensions 12.12 × 42.0 m (in axes), height to the bottom of the structural plate 4.5 m is a one-block single-storey structure with a central canopy (70.0 sq.m.) and side pavilions (175.0 sq.m + 175.0 sq.m.), in which there are male and female public toilets (vestibule-washroom, a restroom with 6 ordinary cabins and 1 for disabled visitors, a pantry of cleaning equipment) and showers (vestibule, the actual shower room with 6 ordinary closed booths and 2 closed booths for disabled visitors). Having a connection with both branches, there is a cash register in the middle. The picnic area (Figure 4(6)): 5 modules (80% canopy + 20% heated contour), dimensions 12.12 × 42.0 m (in axes), height to the bottom of the structural plate 4.5 m. The structure is a one-block, one-story structure with side canopies (168.0 + 168.0 sq.m) for isolated eating and recreation of two companies of clients at the same time, as well as a central pavilion (84.0 sq.m), divided into two parts. In each of them there is: a storeroom of inventory, a kitchen, a utility room and a toilet. The fitness complex (Figure 4(7)): 23 modules (17% canopy + 83% heated contour), dimensions 60.60 × 56.0 m (in axes), height to the bottom of the structural plate 6.0 m. The structure is a single-block structure with a canopy for short-term car parking in front of the main entrance. The pavilion (1596.0 sq.m.) includes: a lobby, a reception with a cash desk and an utility room, a men's department (a wardrobe, a linen closet, a toilet, a vestibule, a shower, a corridor, a steam room, a gym, a storage room, a trainer's room, a toilet), a women's department (a wardrobe, a laundry closet, a toilet, a vestibule, a shower room, a corridor, a steam room, a gym, a storage room, a trainer's room, a toilet), hall with swimming pool (swimming bath −25.0 × 7.0 m; two bubble baths, children's a splashing pool), a light drinks bar, a heating point, a water measuring unit, a recreation area under a canopy.

Consider the planning solutions of such objects as the Point of medical and rescue service, the Car Service station, the Car wash and the Point of weight and dimensional control (Figure 5). The medical and rescue service point (Figure 5(1)): 4 modules (25% canopy + 75% heated contour), dimensions 24.24 × 28.0 m (in axes), height to the bottom of the structural plate 6.0 m. The structure is a single-block structure with a canopy (84.0 sq.m) for two special cars and a two-storey pavilion (504.0 sq.m). On the ground floor, there are: two reception rooms, two dressing rooms, a corridor, a heating point with a water measuring unit, a medicine pantry, a storage room for inventory, men's and women's toilets with large vestibules for changing clothes, an instrumental, a storage room for cleaning equipment. On the second floor (level +3000), there are: a corridor, a rest room for duty crews, a control room, a server room, a panel room, a staff meal room, an administrative room, a pantry of clean workwear, a women's wardrobe with toilet and shower, a men's wardrobe with a toilet and a shower, a pantry of used workwear, a utility room. The pavilion has one internal and two external stairs leading to an open parking of special cars. The car service station (4 posts) (Figure 5(2)): 6 modules (100% heated contour), dimensions 24.24 × 28.0 m (in axes), height to the bottom of the structural plate 6.0 m. The structure is a single-block structure with a one-storey two-light side section (252.0 sq.m) and a two-storey side pavilion (504.0 sq.m) in accordance with the technical and technological parameters of the equipment. In the one-story part, in an open space, technologically separated, if necessary, by inventory blind and mesh partitions, there are 4 posts for repair and maintenance of passenger cars (3 posts), trucks and buses (1 post). Each post has an independent entrance and exit in opposite directions. The two-storey pavilion houses: on the ground floor—a room for customers, a utility room, a corridor, a toilet, a storage room for cleaning equipment, a tool room, a storage room for consumables, a storage room for equipment, a heating point with a water measuring unit, a storage rooms, a panel room; on

the second floor (level +3000), male and female wardrobes with showers, storerooms of clean and used workwear, toilets, an office, a meal room with a buffet, a classroom with inventory. The two-storey pavilion has one internal and one external staircase. The car wash (3 posts—3 cars, 1 bus or truck) (Figure 5(3)): 4 modules (100% heated contour), dimensions 24.24 × 28.0 m (in axes), height to the bottom of the structural plate 6.0 m. The structure is a single-block structure. In the central, two-light part (252.0 sq.m), there are washing posts, technologically shielded by curtains. The posts have independent entrances and exits in opposite directions. In the side two-storey pavilion (168.0 sq.m), there are rooms for customers, toilets, a water metering unit, a heating station, a staff room, a storage room for inventory, a stairwell—on the first floor; hall, toilets, men's wardrobe with shower, women's wardrobe with shower, office, utility room, stairwell—on the second floor. The point of weight and dimensional control of vehicles (2 posts) (Figure 5(4)): 8 modules (75% canopy + 25% heated contour), dimensions 36.36 × 35.0 m (in axes), height to the bottom of the structural plate 7.5 m. The structure is a single-block structure. In the central pavilion, there are: vestibule, men's toilet, reception room, operator's room, document storage room, server room, vestibule, women's toilet, reception room, operator's room, water metering unit, heat point. On both sides, under the canopies, there are zones of dimensional and weight control with observation bridges.

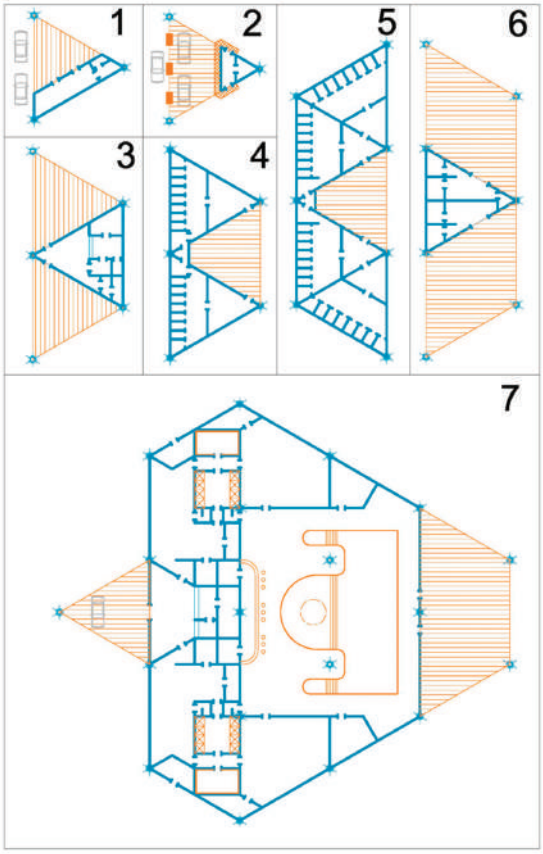


**Figure 4.** Planning solutions: 1—the Public transport stop; 2—the Automatic gas station (self-service); 3—the Catering point (16 seats); 4—the Public toilet; 5—the Public toilet and shower; 6—the Picnic area; 7—the Wellness pavilion.

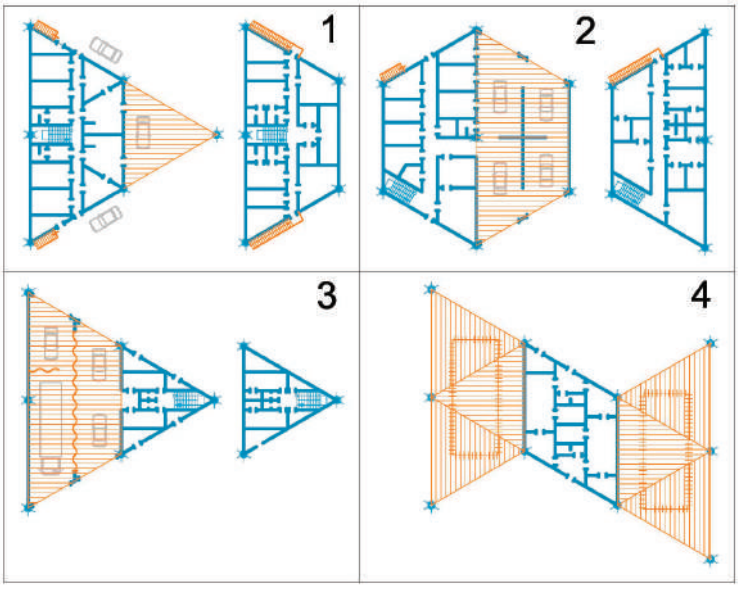


**Figure 5.** Planning solutions: 1—the Point of medical and rescue service—1st, 2nd floors; 2—the Car Service station—1st, 2nd floors; 3—the Car wash (4 posts)—1st, 2nd floors; 4—the Point of weight and dimensional control.

Consider the planning solutions of such objects as the Heating point, the Children's play area, the Post office, the Laundry, the First aid post, the Auditorium, the Retail and catering point, the Car refueling, the Car refueling and the Retail point (Figure 6). The heating point for drivers and passengers (Figure 6(1)): 6 modules (50% canopy + 50% heated contour), dimensions 24.24 × 28.0 m (in axes), height to the bottom of the structural plate 6.0 m. The structure is a one-block one-storey structure with canopies (252.0 sq.m) for parking cars (4 posts), trucks and buses (1 post), as well as a pavilion (252.0 sq.m) with a rest room, a panel, a heating point, a water measuring unit, a storage room for cleaning equipment, a hall, a dining room, a buffet, a dishwasher, a buffet utility room, male and female bathrooms, including dressing rooms, drying rooms, and a toilet. The children's play pavilion (Figure 6(2)): 6 modules (50% canopy + 50% heated contour), dimensions 24.24 × 28.0 m (in axes), height to the bottom of the structural plate 4.5 m. The structure is a one-block, one-story structure with canopies (252.0 sq.m) for outdoor games and recreation and an enclosed room with two game rooms, a buffet, buffet utility rooms, a corridor, men's and women's toilets. The post office (Figure 6(3)): 6 modules (50% canopy + 50% heated contour), dimensions 24.24 × 28.0 m (in axes), height to the bottom of the structural plate 6.0 m. The structure is a one-block one-story structure with canopies (252.0 sq.m) for short-term parking of cars. In the heated part (252.0 sq.m), there are: a hall, a storage room for inventory, a men's toilet, a corridor, a server room, a heating point, two special storerooms, a vestibule, a water measuring unit, a storage room for special inventory, an operator's room (4 posts), a pantry, a women's toilet, a storage room for cleaning equipment. The laundry—(Figure 6(4)): 6 modules (100% heated contour), dimensions 24.24 × 28.0 m (in axes), height to the bottom of the structural plate 4.5 m. The structure is a one-block one-storey building (504.0 sq.m), including: a lobby, a cash register, a toilet for customers, a self-service laundry room, a pantry for washing products, a self-service ironing room, an inventory room, a corridor, a laundry room, a men's staff wardrobe with a toilet and a shower, a women's staff wardrobe with a toilet and a shower, a laundry room, a detergent pantry, an ironing room, a corridor, a cleaning equipment pantry, a laundry pick-up point, a heat point, a water meter unit. The medical center (Figure 6(5)): 4 modules (25% canopy

+ 75% heated contour), dimensions 24.24 × 28.0 m (in axes), height to the bottom of the structural plate 6.0 m. The structure is a one-block, one-storey structure with a canopy (84.0 sq.m.) for short-term parking of a car and a platform in front of the entrance, and a block of premises including: a lobby, toilets for visitors, a reception, a document storage, a dentist's office, a dentist's utility room, a dentist's medicine pantry, a corridor, toilets for staff, a therapist's medicine pantry, a therapist's utility room, a water meter unit, a heat point. The auditorium/the stage area (Figure 6(6)): 6 modules (83% canopy + 17% heated contour), dimensions 24.24 × 28.0 m (in axes), height to the bottom of the structural plate 6.0 m. The structure is a one-block, one-story structure with an indoor auditorium for 400 seats, a stage box (14.0 × 14.0 m—in axes), side heated pavilions (42.0 + 42.0 sq.m) with a vestibule, toilet and an artistic room. In the corners of the hall, in closed rooms, there are sound and panel rooms. The point of trade and catering (40 seats) (Figure 6(7)): 8 modules (37% canopy + 63% heated contour), dimensions 24.24 × 42.0 m (in axes), height to the bottom of the structural plate 6.0 m. The structure is a one-block, one-story structure with a canopy (252.0 sq.m) for parking 1 bus or truck and 4 passenger cars. In the pavilion (420.0 sq.m), there are: a shopping and dining room, a shop, a toilet, a technical room, a corridor, a wardrobe, a toilet, a shower room, a kitchen with a transfer room, a distribution area, a dishwasher, a pantry, a technical room. The gas car refueling (Figure 6(8)): 4 modules (75% canopy + 25% heated contour), dimensions 24.24 × 28.0 m (in axes), height to the bottom of the structural plate 6.0 m. The structure is a one-block one-story structure with a canopy (252.0 sq.m), providing refueling on four columns, and a pavilion (84.0 sq.m) with an operating room, an operator's room, a toilet, a utility room, a technical room. The electric car refueling (Figure 6(9)): 8 modules (63% canopy + 37% heated contour), dimensions 24.24 × 42.0 m (in axes), height to the bottom of the structural plate 6.0 m. The structure is a one-block, one-story structure with a canopy (420 sq.m) for nine refueling stations for electric vehicles and hybrids. Taking into account the real time of operational (from 40 min) and full (from 75 min) electric refueling for the leisure of drivers and passengers in the immediate vicinity of cars, in the pavilion (252.0 sq.m) there is: a customer rest room, a buffet, a dishwasher, a utility room, an electrical switchboard, a toilet, a water meter and a heating point. The retail point of sale (Figure 6(10)): 2 modules (50% canopy + 50% heated contour), dimensions 24.24 × 14.0 m (in axes), height to the bottom of the structural plate 4.5 m. The structure is a one-block, one-storey structure: a platform under a canopy (84.0 sq.m) with the possibility of parking four cars in two rows and a heated pavilion (84.0 sq.m) with a sales hall, a utility room, a corridor and a toilet.

Consider the planning solutions of such objects as the Checkpoint, the Service station, and the Traffic control point (Figure 7). The coastal-type checkpoint (6 + 6 posts) (Figure 7(1)): 14 modules (86% canopy + 14% heated contour), dimensions 98.96 × 21.0 m (in axes), height to the bottom of the structural plate 6.0 m. The structure is a structure, according to antiseismic measures, divided into two symmetrical blocks. It is located across the highway and is designed to control entry and exit to special (including paid) sections. It provides passage through barriers with control panels under canopies (504.0 + 504.0 sq.m) of cars in twelve lanes in both directions. Control and support services are located in side two-storey pavilions (168.0 sq.m each). In the pavilions, there are: an operator's room, a corridor, a toilet, a technical room, a hall, a shower room, a toilet, a staff room, an office. The height of the floor is 3.0 m. The connection between the floors is carried out by an external staircase. From the outside of the pavilions under canopies (21.0 + 21.0 sq. m), it is possible to park a car of control services and special services with the possibility of direct access to the highway in the appropriate direction. The car service station (8 posts) (Figure 7(2)): 16 modules (100% heated contour), dimensions 48.48 × 42.0 m (in axes), height to the bottom of the structural plate 6.0 m. The structure is a single-block structure with a one-storey two-light central part (840.0 sq.m) and two-storey side pavilions (504.0 + 504.0 sq.m) in accordance with the technical and technological parameters of the equipment. In the central part, in an open space, there are eight posts for repair and maintenance of passenger cars (4 posts), trucks and buses (4 posts). Each post has an independent entrance and exit in

opposite directions. In the two-storey side pavilions, there are rooms for customers, toilets, administrative, household and sanitary rooms for staff, storerooms of cleaning equipment, warehouses of parts, tools, materials, cleaning equipment, rooms of engineering support systems (ventilation chambers, pumping, panel, heating points, communication nodes). The height of the floor is 3.0 m. Each pavilion has one internal and one external staircase. The point of traffic control services (Figure 7(3)): 10 modules (60% canopy + 40% heated contour), dimensions 36.36 × 35.0 m (in axes), height to the bottom of the structural plate 6.0 m. The structure is a single-block structure with side canopies (252.0 + 252.0 sq.m) for controlled passage of four traffic lanes in both directions. In the central two-storey pavilion (672.0 sq.m), on the ground floor, there are: a document processing room, a corridor, a toilet, a control room, a water meter unit, a document processing room, a corridor, a toilet, a control room, a heat point. On the second floor (level +3000), there are: a corridor, a men's toilet, a men's shower room, a room for detainees, an office, an inventory room, a server room, a meal room, a men's wardrobe, an office for operational visual control, an office, an inventory room, a women's wardrobe, a women's toilet, a women's shower room, a staff training room, a shift supervisor's office, an office for operational visual control. The pavilion has one internal and two external stairs. At the ends, under the canopies, there are parking lots for special cars with the possibility of direct access to the highway in the appropriate direction.

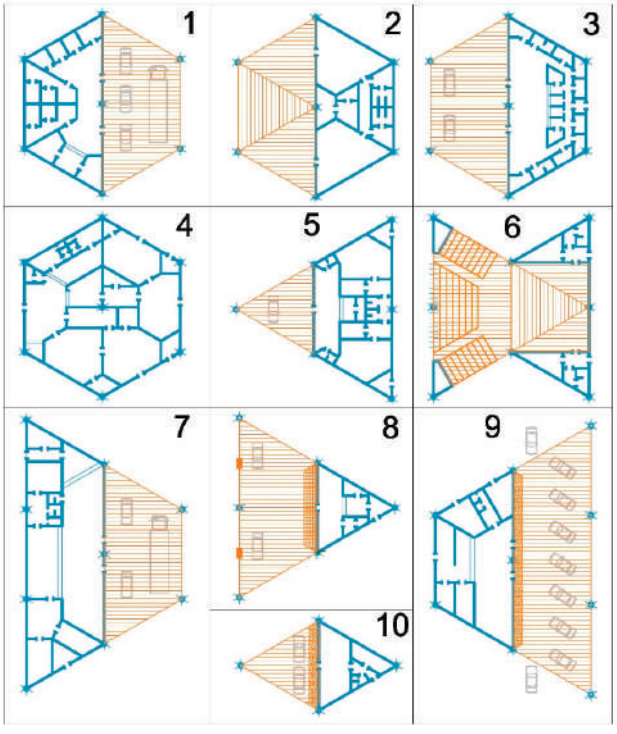


**Figure 6.** Planning solutions: 1—the Heating point; 2—the Children's play area; 3—the Post office; 4—the Laundry; 5—the First aid post; 6—the Auditorium; 7—the Retail and catering point; 8—the Car refueling (gas); 9—the Car refueling (electric); 10—the Retail point.

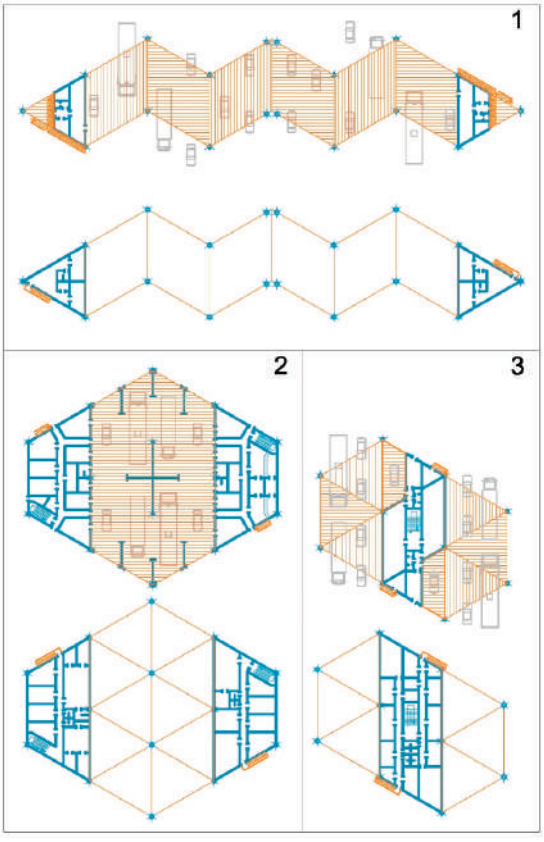


**Figure 7.** Planning solutions: 1—the Checkpoint (6 + 6 posts)—1st, 2nd floors; 2—the Service station (8 posts)—1st, 2nd floors; 3—the Traffic control point—1st, 2nd floors.

Consider the planning solutions of such objects as the Car wash and the Car refueling (Figure 8). The car wash (6 posts—4 cars, 2 buses or trucks) (Figure 8(1)): 8 modules (100% heated contour), dimensions 48.48 × 28.0 m (in axes), height to the bottom of the structural plate 6.0 m. The structure is a single-block structure. In the central two-light part (504.0 sq.m), there are washing posts, technologically shielded by curtains. The posts have independent exits in opposite directions; for trucks and buses, the passage is through. In the side two-storey pavilions (168.0 + 168.0 sq.m), there are: on the ground floor—a client room, a control room, a pantry, a stairwell, a heating point, an electric switchboard, an inventory room, a detergent pantry, a water meter unit, a stairwell, a pantry; on the second floor—toilets, a men's and women's wardrobe with showers and drying rooms, an office, a hall, storerooms. The petrol-diesel car refueling (Figure 8(2)): 9 modules (67% canopy + 33% heated contour), dimensions 48.48 × 28.0 m (in axes), height to the bottom of the structural plate 6.0 m. The structure is a one-block one-storey structure with a canopy (504.0 sq.m), providing refueling for ten columns, and a pavilion (252.0 sq.m) with a client and a mini-store of related products, an operator's room, a utility room, showers, a passage, a toilet, a staff room, a pantry, a water measuring unit and a heating point.

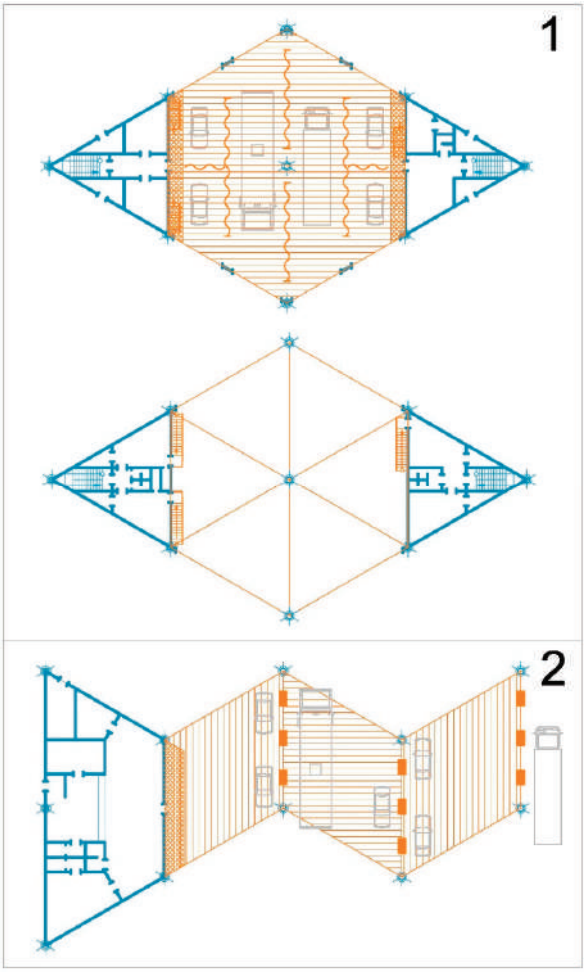


**Figure 8.** Planning solutions: 1—the Car wash (6 posts)—1st, 2nd floors; 2—the Car refueling (petrol-diesel).

Consider the planning solutions of such objects as the Checkpoint and the Self-service car wash (Figure 9). The island-type checkpoint (6 + 6 posts) (Figure 9(1)): 16 modules (88% canopy + 12% heated contour), dimensions 88.84 × 35.0 m (in axes), height to the bottom of the structural plate 6.0 m. The structure is a structure divided into three blocks, located across the highway, in accordance with antiseismic measures, for controlling entry and exit to special (including paid) sections. It provides passage through barriers with control panels under canopies (504.0 + 504.0 sq.m) of cars in twelve lanes in both directions. Control and support services are located in a central two-storey pavilion (168.0 sq.m on each floor) with canopies. The pavilion has: on the ground floor—a corridor, a heat point, a control room, a corridor, a water measuring unit, a control room; on the second floor (level +3000), a corridor, a men's wardrobe with toilet and shower, a server room, a shift supervisor's office, a corridor, a women's wardrobe with toilet and shower, a meal room, an inventory room. The two-storey pavilion has one internal and two external stairs. From the outside of the pavilion under canopies (84.0 + 84.0 sq.m), it is possible to park cars of control services and special services with the possibility of direct or rotary exit to the highway in the right direction. The self-service car wash (Figure 9(2)): 28 modules (93% canopy + 7%

heated contour), dimensions 88.84 × 49.0 m (in axes), height to the bottom of the structural plate 4.5 m. The structure is a complex of three blocks, the dimensions of which take into account regional antiseismic measures. In the central part there is a heated pavilion with an operator's room, a toilet, a corridor and technical rooms. Canopies are located at the ends of the pavilion. On both sides, there are symmetrically arranged canopies, under which there are 24 car and motorcycle washing stations using the self-service system. In the alignment of the main supports, there are panels with hoses for water supply for washing, liquid detergents and compressed air for drying and cleaning, as well as cabinets with cleaning materials. The posts have independent departures. Each post is shielded by curtains.

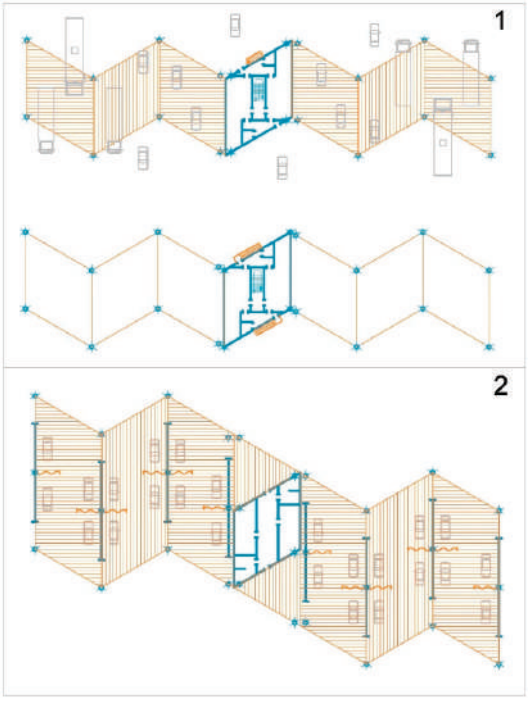


**Figure 9.** Planning solutions: 1—the Checkpoint (6 + 6 posts)—1st, 2nd floors; 2—the Self-service car wash (24 posts).

Consider the planning solutions of such objects as the Contactless car wash and the Warehouse (Figure 10). The contactless car washing (4 posts) (Figure 10(1)): 46 modules (13% canopy + 87% heated contour), dimensions 38.36 × 70.0 m (in axes), height to the bottom of the structural plate 7.5 m. The structure is a complex of two symmetrical blocks. In each of them, there are: a car washing line (reception post, washing post, drying post), a corridor, an operator's room with a toilet, a technical room, an inventory storeroom, an electric switchboard, a complex washing line for buses and trucks. The warehouse—(Figure 10(2)): 18 modules (100% heated contour), dimensions 24.24 × 70.0 m (in axes), height to the bottom of the structural plate 7.5 m. The structure is a one-block, one-story structure. The premises include a storage area, an administrative room, a corridor, a toilet, a storage room for inventory, a heating point, an electrical switchboard, a charging room for electric cars, a water meter unit.

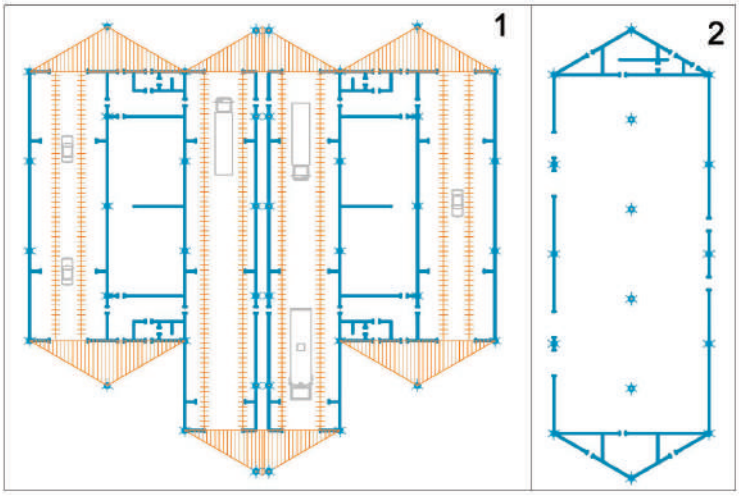


**Figure 10.** Planning solutions: 1—the Contactless car wash (4 posts); 2—the Warehouse.

Consider the planning solutions of such objects as the highly comfortable motel with parking under a canopy (Figure 11) and the ordinary motel (Figure 12). The luxury motel (10 apartments with individual parking site) (Figure 11): 18 modules (50% canopy + 50% heated contour), dimensions 24.24 × 70.0 m (in axes), height to the bottom of the structural plate 6.0 m. The facility is a single-block structure with a high canopy for parking ten customer cars opposite the entrance to the corresponding room (588.0 sq.m.). In the two-storey part (588.0 + 588.0 sq.m), there are 10 highly comfortable duplex rooms. The height of the floor is 3.0 m. On the ground floor, there are: a lobby (two-light), a registration service, a toilet, a utility room, a water measuring unit, a panel room, a heating point, a storage room for inventory, a storage room for clean linen, a storage room for dirty linen, rooms. The set of rooms consists of: 6 pieces of type A rooms (ordinary)—a living room, a bathroom, a staircase, a bedroom with a bathroom, a bedroom with a bathroom: 2 pieces of type B rooms (central)—a living room, a bathroom, a staircase, a bedroom, a bedroom with a bathroom, a bedroom with a bathroom and a loggia: 2 pieces of type C rooms (at the end)—a living room, a bathroom, a bedroom, a staircase, a bedroom with a bathroom, a bedroom with a bathroom, a loggia. The motel (36 rooms) (Figure 12): 18 modules (100% heated contour), dimensions 24.24 × 70.0 m (in axes), height to the bottom of the structural plate 6.0 m. The structure is a single-block structure in the form of a two-storey volume (1176.0 + 1176.0 sq.m) with a corridor layout scheme. On the ground floor, there are: a porch, a two-light lobby, a registration service, a toilet, a utility room, a corridor, a stairwell, a storage room of inventory, a utility room, a panel room, a storage room of street cleaning equipment, a corridor, a stairwell, a storage room of equipment, a water meter unit, a heating point, 10 rooms with a bedroom, a bathroom and a built-in kitchen, 10 rooms with a bedroom and a bathroom. On the second floor (level +3000), there are: a corridor with a central gallery, a stairwell, a pantry of clean linen, a pantry of dirty linen, a stairwell, a pantry of furniture, a pantry of inventory, 10 rooms with a bedroom, a bathroom and a built-in kitchen, 10 rooms with a bedroom and a bathroom.

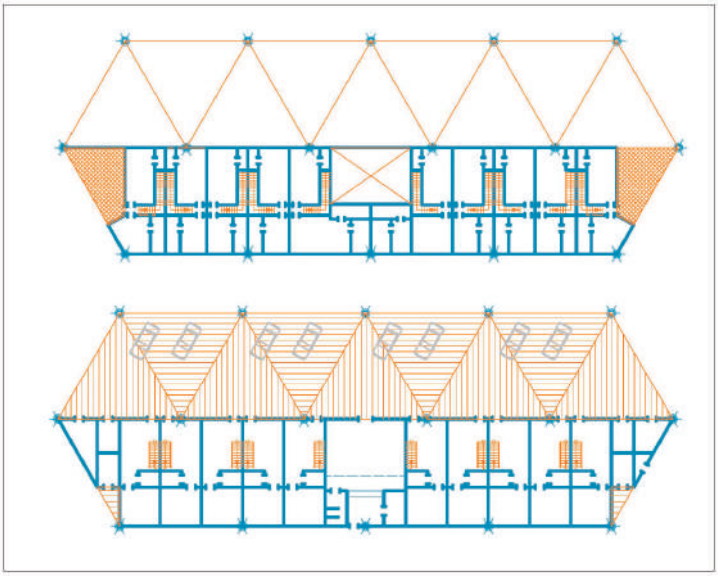

**Figure 11.** Planning solutions: the Highly comfortable motel (10 apartments) with parking under a canopy—1st, 2nd floors.

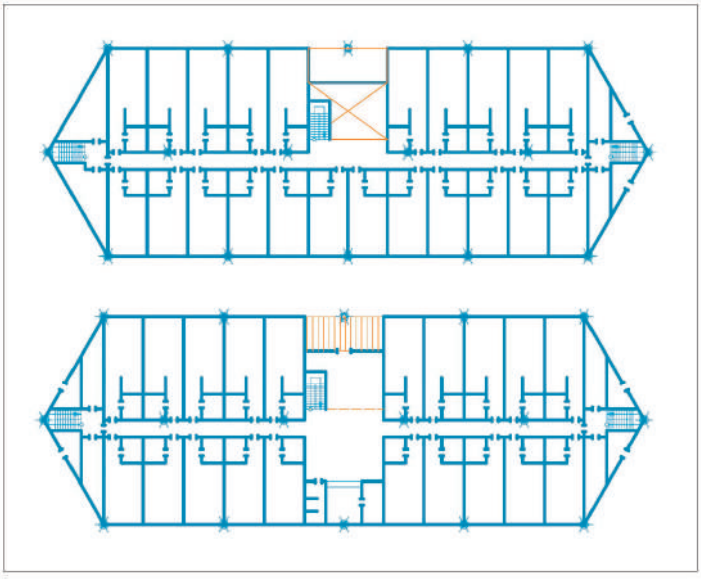

**Figure 12.** Planning solutions: the Ordinary Motel (24 rooms)—1st, 2nd floors.

Consider the planning solution of such an object as the Special traffic control point (Figure 13): 40 modules (55% canopy + 45% heated contour), dimensions 210.04 × 49.0 m (in axes), height to the bottom of the structural plate 7.5 m. The structure is a complex of five blocks, the dimensions of which take into account regional antiseismic measures. In the central part, there is an administrative four-level building of 6 blocks. In the basement (level −4950) there is a water measuring unit, a heat point, an electrical switchboard and passages with viewing chambers at each control post. In the side volumes, there are

storerooms of cleaning equipment, storerooms of clean and used workwear, storerooms of appliances and tools. On the ground floor, duty rooms, document processing offices, men's and women's toilets, inventory storerooms are located in a symmetrical layout. Under the canopies, there are parking lots for special cars on duty with the possibility of direct or rotary exit in the right direction. On the second floor (level +3300), there are: male and female wardrobes with showers, toilets, a meal room, a classroom, a room for special equipment, an office of the head of the duty shift, offices of the visual control officers. On the third level (level +5.200), there are exits to the platform for passage to the observation bridges at each inspection post. The connection between the levels is carried out by two stairwells. In the canopies adjacent to the central block, there are two lanes of emergency free passage. On both sides, pavilions of special control posts are linearly placed under paired canopies. Each post is a three-level structure. In the basement (level −4950), there is a special control camera with a hole in the ceiling that provides inspection of the bottom of the passing vehicle control. All pavilions are sequentially connected to each other and to the central block to ensure optimal passage of personnel to the appropriate post. On the ground floor there is a high (4.6 m) duty room with stained glass windows on the side of the passage, a toilet, a shift staff room. On the third level (level +5.200), there are pavilions of stairwells that provide staff exits to observation bridges. All observation bridges are connected in series with each other and with the central unit.

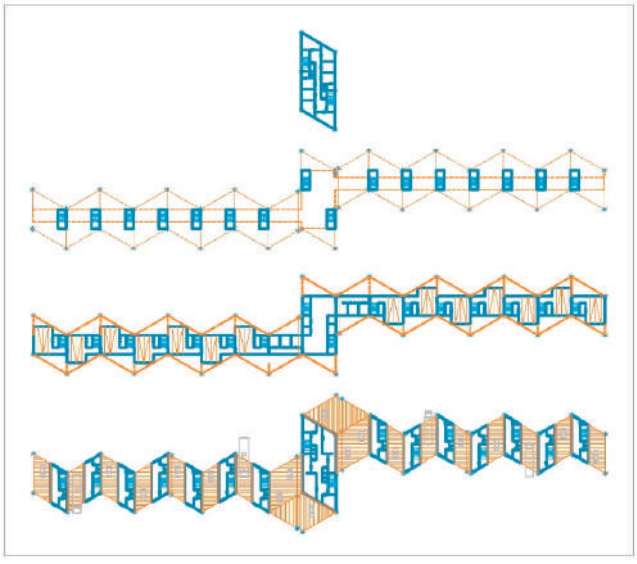

**Figure 13.** Planning solutions: the Special vehicle control point (levels 1, 2, 3, 4).

Consider the planning solution of such object as the Supermarket (Figure 14): 204 modules (12% canopy + 88% heated contour), dimensions 149.44 × 128.0 m (in axes), height to the bottom of the structural plate 7.5 m. The structure is a complex of six blocks, the dimensions of which take into account regional antiseismic measures. The overall dimensions are determined from the most common standardized supermarket parameters ~90 × 140 m. The heated contour (15,120.0 sq.m) accommodates: a lobby with storage chambers; trolley placement areas; flow-distribution zones with areas for short-term rest of visitors; an information desk; a security point; currency exchange offices; branches of banks and telephone companies; a pharmacy, a perfume, an jewelry, book and newspaper kiosks; workshops for small express repairs of shoes, bags, umbrellas, watches, phones and gadgets; buffets for light snacks; bars for soft drinks; public toilets; a cash register; a main trading hall with shelving, a display, counter and container-stand placement of goods.

In the two-level auxiliary compartment (mezzanine at level +4.500), there are: auxiliary and storage rooms with cold rooms; administrative and household premises for personnel; goods reception area with unloading places for trucks; goods pre-sale preparation area; a storage area for recycled packaging; a storage area for used packaging, a garbage and a waste; a parking and maintenance of electric cars, cleaning machines, mechanisms and inventory, as well as engineering support systems (ventilation chambers, pumping, panel, heating points, communication nodes). A part of the auxiliary and technical rooms is located on the mezzanine, where internal and external stairs lead. The canopies located on the sides (2016.0 sq.m) provide for the possibility of covered parking of cars (48 seats), supermarket personnel, and special services of legal, financial, sanitary-epidemiological, fire control.

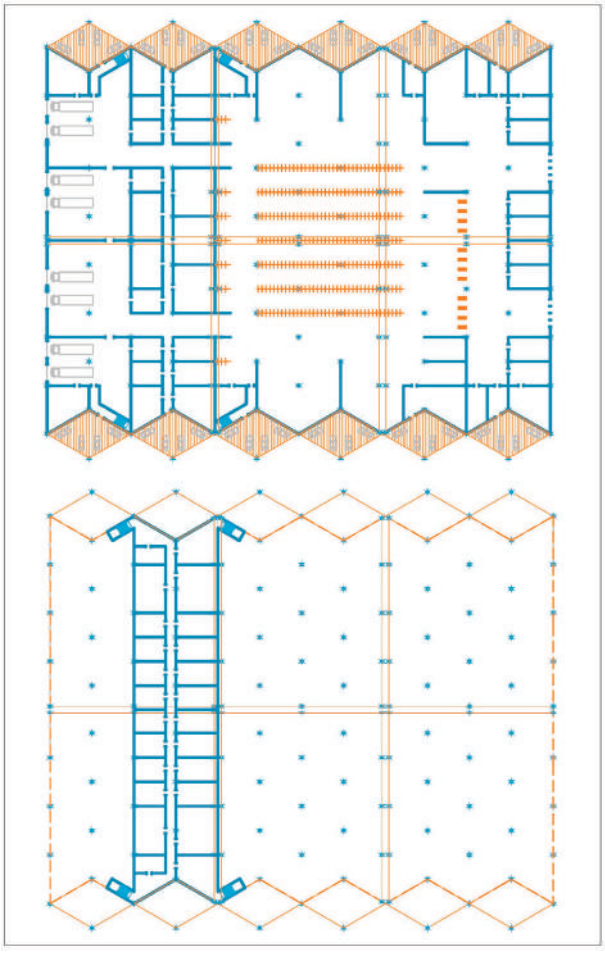

**Figure 14.** Planning solutions: the Supermarket—1st, 2nd floors.

A complex of appropriate buildings is designed to fulfill the religious needs of drivers and passengers. Consider planning solutions of such objects as: the Mosque, the Buddhist temple, the Protestant temple, the Orthodox temple, the Catholic temple, the Synagogue (Figure 15). The Mosque (Figure 15(1)): 8 modules (50% canopy + 50% heated contour), dimensions 24.24 × 42.0 m (in axes), height to the bottom of the structural plate 6.0 m. The structure is a one-block, one-story structure with a heated part (336.0 sq.m), a two-part

(male and female parts) domed prayer hall with a mihrab niche, a covered courtyard, a reading room, a library, an imam's office, and servants' rooms located in the middle. Under the canopy (336.0 sq.m.), there are places for pre-prayer and after prayer concentration and rest. Orientation of the mihrab canonically to the Kaaba in Mecca city. The Buddhist temple (Figure 15(2)): 7 modules (43% canopy + 57% heated contour), dimensions 24.24 × 42.0 m (in axes), height to the bottom of the structural plate 6.0 m. The structure is a one-block, one-story structure with a prayer ("golden") hall placed in the middle of the heated part (336.0 sq.m), covering its gallery, a reading room and a concentration room. Under the side canopies (252.0 sq. m), there are places for pre-prayer and after prayer concentration and rest. The building is preceded by a courtyard with pagodas, the actual entrance is in the form of a canonical "Middle Gate". The entrance to the temple is canonically from the East side. The Protestant church (Figure 15(3)): 6 modules (41% canopy + 59% heated contour), dimensions 24.24 × 28.0 m (in axes), height to the bottom of the structural plate 6.0 m. The structure is a one-block, one-story structure with a heated part (294.0 sq.m), a prayer hall with an altar part placed in the middle, a block with a library, a hall and a utility room located on the side. Under the front and side canopies (210.0 sq.m), there are places for pre-prayer and after prayer concentration and rest. The altar is canonically oriented to the East. The Orthodox church (Figure 15(4)): 6 modules (25% canopy + 75% heated contour), dimensions 24.24 × 28.0 m (in axes), height to the bottom of the structural plate 6.0 m. The structure is a one-block one-story structure with a heated part (378.0 sq.m) placed in the middle of a prayer hall with a dome, a three-apse altar part and side chapels, a porch, an office, a reception room, a shop, a utility room, a pantry. Under the side canopies (126.0 sq.m), there are places for pre-prayer and after prayer concentration and rest. The altar is canonically oriented to the East. The Catholic church (Figure 15(5)): 6 modules (50% canopy + 50% heated contour), dimensions 24.24 × 28.0 m (in axes), height to the bottom of the structural plate 6.0 m. The structure is a one-block, one-story structure with a prayer hall in the heated part (252.0 sq.m) placed in the middle with a dome over the transept, a three-apse altar part, a narthex, an office and a utility room located on the sides. Under the front and side canopies (252.0 sq.m), there are places for pre-prayer and after prayer concentration and rest. The altar is canonically oriented to the East. The Synagogue (Figure 15(6)): 6 modules (33% canopy + 67% heated contour), dimensions 24.24 × 28.0 m (in axes), height to the bottom of the structural plate 6.0 m. The structure is a one-block, one-story structure with a heated part (336.0 sq.m) in the middle of a two-part (male and female parts) prayer hall, lobby, clerical offices located on the sides and auxiliary rooms. Under the front and side canopies (168.0 sq.m), there are places for pre-prayer and after prayer concentration and rest. The orientation of the altar is canonically on the city of Jerusalem.

From the same rod elements, it is possible to form supports for information boards both in front of individual structures (for example, fuel filling stations; indication of type and prices) and in front of complexes of roadside service facilities. The lattice structure also provides convenient access for technical personnel to service the back of the LED panel. The dimensions of the supports can be different depending on the specific tasks—including the possibility of installing sufficiently large screens. An example of the solution of a rod structure as a support for an information board is shown in the Figure 16.

The proposed modularity allows for both single and lockable placement of various objects as part of complexes of various categories. Blocking allows in some cases to reduce the size of buildings due to the possibility of excluding some duplicated sanitary or engineering premises. At the same time, blocking can be performed both directly, forming a single volume (for small objects), and through a seam (for large objects), ensuring compliance with antiseismic measures. The configuration of the lock is determined by the individual landscape features of the territory of the complex and the creative preferences of the authors of the project.

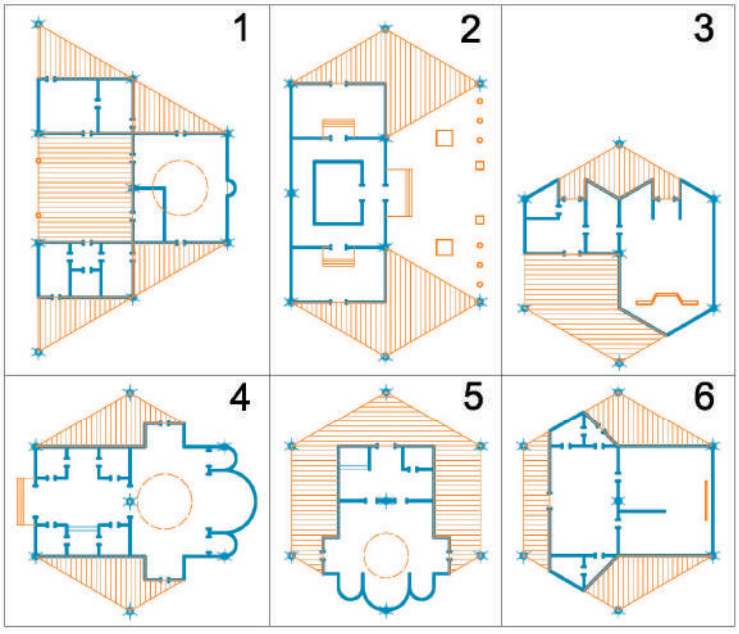


**Figure 15.** Planning solutions: 1—the Mosque; 2—the Buddhist temple; 3—the Protestant temple; 4—the Orthodox temple; 5—the Catholic temple; 6—the Synagogue.

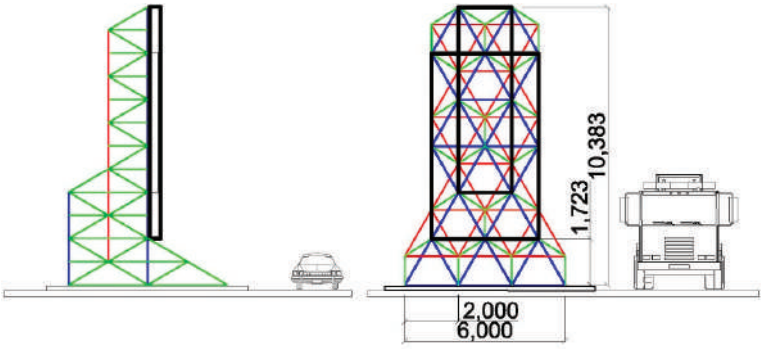


**Figure 16.** The Diagram (side view, front view) of the rod structure as a support for the information board (Dimensions are given in mm).

*2.2. Ensuring Energy Efficiency and Reducing the Harmful Environmental Impact of Road Service Facilities*

The formation of a complex of maintenance facilities along highways, as an essential part of the system of sustainable development of territories, implies the implementation of a set of measures to improve processes in all aspects, from creation to operation. The proposed modular system for the formation of objects for various purposes based on a triangular cell with an overlap of a core spatial plate makes it possible to improve a number of indicators of the complexes being created according to the basic parameters of sustainable development.

Firstly, it is the level of production. It is the uniformity of structural elements, a small number of standard sizes and the need for mass production that immediately improve a number of indicators related to energy efficiency. Centralized mass production is naturally more economical than scattered piece production in all parameters in terms of unit output.

Moreover, importantly, significantly stricter product quality control is provided at all stages of manufacturing.

Secondly, transportation of building elements and parts. The presence of only three main standard sizes (rod, nodal polyhedron, rack) allows them to be compactly packaged and tightly placed on vehicles for transportation to the installation site. Under certain conditions, it becomes possible to partially assemble, for example, pyramids on specialized sites and package several pyramids already nested in each other for transportation. This reduces the number of necessary vehicles and leads, among other things, to a reduction in the harmful impact on the environment due to exhaust emissions. At the same time, fuel is saved.

Thirdly, the construction of groups of modules on various dispersed sites. The uniformity of the assembly processes of the main elements of high factory readiness makes it possible to significantly reduce the construction time of the main structures due to the acquisition and use of skills by teams of installers. The need to use cranes is limited by a small set of works on lifting the modular element of the structural plate mounted at the bottom to the design position. The main volume of installation work does not require crane equipment. Accordingly, it becomes possible to use the in-line method of constructing objects based on the use of highly specialized construction and installation teams. This, as the successful practice of domestic construction in the second half of the last century has shown, significantly reduces the time of construction and installation work, leading, accordingly, to the saving of energy resources. A significant advantage of using a modular canopy system is that after the installation of the coating, all other construction and finishing work on the creation of pavilions with rooms for various purposes is carried out in relatively comfortable conditions under the roof, which protects builders from precipitation and excessive insolation. It also reduces energy consumption, improves the quality of work and reduces their time. The reduction of time is achieved, among other things, due to the possibility of organizing round-the-clock three-shift work, because the core structure of the canopy allows you to harmoniously place in it and move, as necessary, floodlight lighting of both the entire construction site and its individual sections.

Fourth, the materials proposed for use for the structures of the built-in heated pavilions are: steel racks and beams of the main frame, steel bent profiles and corrugated sheets for floors and staircase structures, sandwich panels for exterior walls, magnesite and gypsum cardboard plates for partitions with a frame of bent thin-sheet steel profiles and mineral wool filling, as well as ceiling linings (in rooms with high humidity or high requirements for fire-fighting indicators, special surface finishing is performed),wood-fibrous plates for the underlying layers of floors, extruded foam and foam insulation for thermal insulation of non-modular sections of structures and pipelines of engineering systems, metal-plastic windows with double-glazed filling, which entail a high degree of industry in terms of of manufacturing, packaging, warehousing, delivery, and installation, ensuring high energy efficiency in these areas. In addition, energy-consuming "wet processes" at the construction site are almost completely excluded (the exception is the device of monolithic reinforced concrete foundations. However, this can also be significantly reduced by switching to prefabricated monolithic or fully prefabricated reinforced concrete foundations of factory manufacture).

Fifth, the possibility of active use of mainly solar and to a small extent wind energy, as well as biofuels, which makes it possible to compensate for some of the total costs of electric energy complexes. The most common way of using solar photo energy generators is associated with the maximum filling of the roof space, leaving only technologically necessary passages. Sometimes it is filling the adjacent territory with generators (as, for example, at one of the Beijing gas stations). An additional source of saving artificial lighting in the interior spaces of the pavilions is the use of transparent photogenerators on the roof. In addition to the solution of replacing part of the electricity costs for lighting, photogenerators are also included in the system of operation of gas station pumps.

Gradually, a kind of "direct" use of the electricity generated by photogenerators for refueling electric vehicles is becoming more widespread. However, a purely technical problem is the time to refuel the batteries of an electric car or hybrid, which is three hours for a 70-km trip. This limits the use of such refueling stations on highways, where refueling time is essential. Accordingly, the scope of their application so far extends to parking for employees of various enterprises and educational institutions who have the opportunity to leave the car for several hours. Sometimes, these are systems for individual parking at residential buildings. At the same time, the supply of electricity from photogenerators is included in the general electrical supply system of the house, from which the electric car or hybrid is then charged. The modular electric filling stations offered for roads provide for the presence of a special pavilion for leisure activities by drivers and passengers of the corresponding vehicles.

In the aspect of the modular system proposed for roadside service facilities, it can be noted that an important advantage of this module is the possibility of placing on the roof, using the same (although, of course, smaller cross-section) core and node elements, solar panels that can be optimally oriented based on a structurally secured three-sector direction. The approximate area of the active surface of stationary batteries is 144.0 sq.m on each module. As an addition to the electrical supply system of the facility, it is recommended to place weathervane wind generators, which are fixed in the area of the module supports. Naturally, when blocking groups of modules through a seismic seam with paired columns, the weathervane wind generator is placed only on one of the columns. It is advisable to place small vertical wind turbines on side platforms, as it is used, for example, at the previously considered SEPSA gas station, Adanero (architect "Saffron Brand Consultants + Malka + Portus", 2015). Large-blade wind turbines are optimally located on relatively isolated sites. The sites for the placement of wind generators, of course, are fields for photo generators. The location of large-bladed wind generators next to road maintenance complexes and the device of their illumination at night makes it possible to improve the visual orientation of drivers, who from a sufficiently long distance will be able to see the presence of the object of interest to them.

The sixth position of increasing energy efficiency and compensating for the harmful impact on the environment of roadside service complexes is a system for collecting and cleaning rain and meltwater, as well as domestic sewage effluents for use for watering green spaces in the structure of the complex. An important component in this area is also the system of circulating water supply of vehicle washing points operating in the system of sewage treatment plants.

Some indicators can also be improved by organizing a system of differentiated collection and packaging of food waste, household and technological garbage, and used containers and packaging.

## 3. Results

The need for a relatively quick solution to the problem of providing all highways in the country with roadside service facilities in accordance with the directives of the nomenclature specified, taking into account historical experience, necessitates the development of a series of relevant standard projects. In order to increase the efficiency of these series, it is advisable to link up space-planning decisions based on one or another module. Considering the variety of planning and landscape characteristics of the areas of placement of objects for mainline maintenance, it seems appropriate to choose as a module not a square or rectangular, but a triangular configuration, which in most cases allows harmoniously blocking the modules. The proposed roofing module in the form of a "regular" triangle extending to a tetrahedron has a structural basis in the form of a single-tier rod spatial plate. Half a century of extensive practice in the use of such structures (mainly with a cell in the form of an equilateral pyramid with a square base), including in the Central Asian region, minimizes the construction and technological difficulties in the manufacture, delivery and installation. The height characteristics of the location of the core spatial plate are linked to

the normalized road dimensions and features of the technology of functioning of each of the typologically different objects. The principle space-planning solutions of all four dozen objects from the approved nomenclature of primary maintenance services carried out in the process of the analysis of opportunities show the real possibility of solving development tasks based on this system. For large-sized complexes, in accordance with normalized anti-seismic measures, seismic cutting was performed by arranging the pair supports of the modular plate. The use of the proposed modular system allows us to successfully solve a number of tasks to reduce the harmful effects on the environment and to effectively use renewable energy sources.

## 4. Discussion

The lack of uniformity in approaches to the design and construction of roadside service facilities, pronounced in today's practice, slows down the design process and complicates construction. In these conditions, it seems appropriate to adapt a system of design and construction based on standard series that has a long history and good practical results. One of the approaches can be the interconnection of space-planning solutions based on a particular spatial module. The advantages of a triangular module based on a structural basis of a single-tier rod spatial plate on three supports revealed in the course of research allow us to solve a number of space-planning and spatial-layout problems for individual objects and their complexes in a harmonious way. In addition, the uniformity of design solutions and construction methods in combination with other measures allows us to successfully solve a number of tasks to reduce the harmful impact on the environment and effectively use renewable energy sources. The studied topic presents a significant prospect for expansion with further research. Thus, it is promising to detail the level of standard for projects of the proposed schemes of space-planning solutions for individual objects. It is very important to consider possible options for blocking objects of various types in complexes of various sizes that have a single roof. Moreover, of course, it is advisable to consider the possibility of using small-scale panel structures for the formation of external walls and partitions of objects.

## 5. Conclusions

Roadside service facilities have a long history. Their space-planning specifics reflect the specifics of cargo and passenger transportation along the road near which they are located and the level of administration in the surrounding territories. A separate issue remains passenger transport. Within the framework of this service, given its specificity and the need for almost simultaneous construction of almost identical objects on vast territories, the idea of using reusable projects first, and then standard projects for this class of objects grows. The expansion of the nomenclature of primary-line service facilities was determined by the appearance and intensive development of automobile transport, which led to a significant increase in the territory occupied by each complex due to the need to provide parking and convenient maneuvering of cars of various classes. Grouped by function: car service (refueling of various types of fuel, washing of motorcycles and cars of various sizes, service stations), road control (points of traffic control services, checkpoints, points of dimensional and weight control of vehicles), passenger service (public transport stops, retail and catering points, public toilets and showers, laundries, medical and rescue service points, health pavilions, picnic and recreation areas, stage platforms, playgrounds and pavilions, roadside temples of various faiths, heating points, post offices, motels, warehouses, supermarkets), these objects are constantly integrated into large complexes or differentiated by individual functions, depending on the actual territorial conditions.

Taking into account the variety of planning and landscape characteristics of the sites for the placement of objects of the mainline service, it seems advisable to choose as a module not a square or rectangular, but a triangular configuration, which allows in most cases to harmoniously block the modules. The proposed roof module in the form of a "regular" triangle facing the tetrahedron has a structural basis in the form of a single-tier core

spatial plate. The half-century-old extensive practice of using such structures minimizes construction and technological difficulties in the manufacture, delivery, and installation. The principal space-planning solutions of all four dozen objects of the nomenclature of objects of the mainline service performed in the process of analyzing the possibilities show the real possibility of solving the development tasks based on this system. The use of the proposed modular system makes it possible to successfully solve a number of tasks to reduce the harmful impact on the environment and effectively use renewable energy sources.

**Author Contributions:** Conceptualization, K.S., B.K., G.S. and N.K.; methodology, K.S., B.K. and G.S.; software, K.S. and N.K.; validation, K.S., G.S. and N.K.; formal analysis, K.S., B.K. and G.S.; investigation, K.S., B.K., G.S. and N.K.; resources, K.S., B.K. and N.K.; data curation, B.K. and K.S.; writing—original draft preparation, K.S., B.K., G.S. and N.K.; writing—review and editing, K.S., B.K. and G.S.; visualization, N.K. and K.S.; supervision, K.S. and G.S.; project administration, K.S. and B.K.; funding acquisition, K.S. and B.K. All authors have read and agreed to the published version of the manuscript.

**Funding:** This research received no external funding.

**Institutional Review Board Statement:** Not applicable.

**Informed Consent Statement:** Not applicable.

**Data Availability Statement:** Not applicable.

**Acknowledgments:** Authors express their gratitude to the Google search engine, the USA Library of Congress, the British Library, whose resources are used for the selection of theoretical material.

**Conflicts of Interest:** The authors declare no conflict of interest.

## References

1. Torgautov, B.; Zhanabayev, A.; Tleuken, A.; Turkyilmaz, A.; Mustafa, M.; Karaca, F. Circular Economy: Challenges and Opportunities in the Construction Sector of Kazakhstan. *Buildings* **2021**, *11*, 501. [CrossRef]
2. Kuanyshbekov, N.N.; Tuyakaeva, A.K. *Aktual'nost' Razvitiya Arhitektury ob"Ektov Pridorozhnogo Servisa v Kazahstane [The Relevance of the Development of Architecture of Roadside Service Facilities in Kazakhstan]/Sbornik Nauchnykh Trudov XIII Mezhdunarodnaya Nauchno-Prakticheskaya Konferenciya Imeni V.Tatlina*; PGUiAS: Penza, Russia, 2018; pp. 95–98.
3. Cui, T.; Ouyang, Y.; Shen, Z.J.M. Reliable facility location design under the risk of disruptions. *Oper. Res.* **2010**, *58*, 998–1011. [CrossRef]
4. Ettema, D.; Gärling, T.; Olsson, L.E.; Friman, M.; Moerdijk, S. The road to happiness: Measuring Dutch car drivers' satisfaction with travel. *Transp. Policy* **2013**, *27*, 171–178. [CrossRef]
5. Bostani, M.K.; Hashemzehi, F.; Anvari, M.R. Evaluation of roadside service centers. Case study: Zahedan to Khash Road. *Ukr. J. Ecol.* **2017**, 7, 374–381. Available online: https://www.researchgate.net/publication/322752928_Evaluation_of_roadside_service_centers_Case_study_Zahedan_to_Khash_Road (accessed on 15 January 2022). [CrossRef]
6. Dvořák, Z.; Sventekova, E.; Řehák, D.; Čekerevac, Z. Assessment of Critical Infrastructure Elements in Transport. *Procedia Eng.* **2017**, *187*, 548–555. [CrossRef]
7. Rahman, H.Z.; Andreas, A.; Perwitasari, D.; Petroceany, J.S. Developing a typology for social infrastructure (Case study: Roadside station infrastructure). *EDP Sci.* **2019**, *276*, 02020. [CrossRef]
8. Hasan, M.M.; Alam, A.; Mim, A.M.; Das, A. Identifying User Satisfaction Level of Road services: A Focus on Rajshahi City Bypass Road, Bangladesh. *Transp. Res. Procedia* **2020**, *48*, 3132–3152. [CrossRef]
9. Makovetskaya-Abramova, O.; Ivanov, A.; Lazarev, Y.; Shakhova, M.; Rozov, A. Economic assessment of construction of the roadside service facilities. *E3S Web Conf.* **2020**, *157*, 04035. [CrossRef]
10. Guidelines for Service Stations. RTS 13. Land Transport Safety Authority: Wellington, New Zealand, 2001; 42p. Available online: https://www.nzta.govt.nz/assets/resources/road-traffic-standards/docs/rts-13.pdf (accessed on 15 January 2022).
11. Hurley, A.; Jakle, J.A.; Sculle, K.A. Fast Food: Roadside Restaurants in the Automobile Age. *J. Am. Hist.* **2001**, *87*, 1576. Available online: https://www.researchgate.net/publication/275844041_Fast_Food_Roadside_Restaurants_in_the_Automobile_Age (accessed on 15 January 2022). [CrossRef]
12. Filling Station Developments Access- & Building Line Management Technical Overview & Guidelines. Department of Police, Roads and Transport. Free State Province. 22p. Available online: http://www.energy.gov.za/files/PPA-Campaigns/free-state/Filling-Station-Developments-Access-and-Building-Line-Management.pdf (accessed on 15 January 2022).

13. Rest Areas: Mounting Costs and Increased Expectations Create the Perfect Opportunity for Exploring New Public Private Partnerships/Virginia Department of Transportation/Prepared by Ken Winter. June 2008. 21p. Available online: http://vtrc.virginiadot.org/rsb/RSB17.pdf (accessed on 15 January 2022).
14. Magdic, M.; Sjöstrand, P. The Petrol Station—A Hot Spot along the Road. Master's Thesis, IA7400/Department of Informatics School of Economics and Commercial Law University of Gothenburg, Gothenburg, Sweden, 2002; 81p. Available online: https://gupea.ub.gu.se/bitstream/2077/4587/1/magdic_sjostrand.pdf (accessed on 15 January 2022).
15. Wolfe, K.; Holland, R.; Jeff Aaron, J. Road Side Stand Marketing of Fruits and Vegetables. The University of Georgia. Center for Agribusiness and Economic Development. College of Agricultural and Environmental Sciences. September 2002; 42p. Available online: https://sustainagga.caes.uga.edu/content/dam/caes-subsite/sustainable-agriculture/documents/CR-02-09.pdf (accessed on 15 January 2022).
16. Shanahan, K. The degree of congruency between roadside billboard advertisements and sought attributes of motels by US drive tourists. *J. Vacat. Mark.* **2003**, *9*, 381–395. Available online: https://www.researchgate.net/publication/247764549_The_degree_of_congruency_between_roadside_billboard_advertisements_and_sought_attributes_of_motels_by_US_drive_tourists (accessed on 15 January 2022). [CrossRef]
17. Kendrick, M. Roadside Motels. Society of Architectural Historians Archipedia. Available online: https://sah-archipedia.org/essays/CA-01-ART-01 (accessed on 15 January 2022).
18. Wang, Y.W.; Wang, C.R. Locating passenger vehicle refueling stations. *Transp. Res. Part E Logist. Transp. Rev.* **2010**, *46*, 791–801. [CrossRef]
19. Henderson, L. America's Roadside Lodging: The Rise and Fall of the Motel. Historia 2010. 11p. Available online: https://www.eiu.edu/historia/2010Henderson.pdf (accessed on 15 January 2022).
20. Al-Kaisy, A.F.; Kirkemo, Z.; Veneziano, D.; Dorrington, C. Traffic Use of Rest Areas on Rural Highways. *Transp. Res. Rec. J. Transp. Res. Board* **2011**, *2255*, 146–155. Available online: https://www.researchgate.net/publication/272774521_Traffic_Use_of_Rest_Areas_on_Rural_Highways (accessed on 15 January 2022). [CrossRef]
21. Sheng, K.J.; Baharudin, A.S.; Karkonasasi, K. A Car Breakdown Service Station Locator System. *Int. J. Appl. Eng. Res.* **2016**, *11*, 11037–11040. Available online: https://www.researchgate.net/publication/311795116_A_Car_Breakdown_Service_Station_Locator_System (accessed on 15 January 2022).
22. Xanthopoulos, I.; Goulas, G.; Gogos, C.; Alefragis, P.; Housos, E. Highway Rest Areas simultaneous energy optimization and user satisfaction. In Proceedings of the 20th Pan-Hellenic Conference on Informatics, Patras, Greece, 10–12 November 2016; pp. 1–4. [CrossRef]
23. Plovnick, A.; Berthaume, A.; Poe, C.; Hodges, T. Sustainable Rest Area Design and Operations. U.S. Department of Transportation. Federal Highway Administration. October 2017 (DOT-VNTSC-FHWA-17-20 FHWA-HEP-18-006). 31p. Available online: http://www.bv.transports.gouv.qc.ca/mono/1204435.pdf (accessed on 15 January 2022).
24. Karanja, P.; Gathitu, C.W. Strategic Location Considerations for Fuel Filling Stations along Thika Super Highway-Kenya. *Int. J. Acad. Res. Bus. Soc. Sci.* **2018**, *8*, 220–230. Available online: https://hrmars.com/papers_submitted/4460/Strategic_Location_Considerations_for_Fuel_Filling_Stations_along_Thika_Super_Highway-Kenya.pdf (accessed on 15 January 2022). [CrossRef]
25. Rubeis, M.; Groves, S.; Portera, T.; Bonaccorsi, G. Is There a Future for Service Stations. // Boston Consulting Group. 12 July 2019. Available online: https://www.bcg.com/publications/2019/service-stations-future (accessed on 15 January 2022).
26. Green, D.; Roper, P.; Steinmetz, L.; Latter, L.; Lewis, K.; Gaynor, D. Guidelines for the Provision of Heavy Vehicle Rest Area Facilities. Edition 1.1. Austroad Research Report AP-R591-19. July 2019. 58p. Available online: https://austroads.com.au/__data/assets/pdf_file/0025/160648/AP-R591-19_Guidelines_for_the_Provision-of_HVRA_Facilities-1.1.pdf (accessed on 15 January 2022).
27. Quito, A. Roadside chapels gain traction in Western Europe as church attendance declines. QZ. 22 February 2020. Available online: https://qz.com/1805065/autobahnkirche-the-surprising-rise-of-roadside-chapels-in-europe/ (accessed on 15 January 2022).
28. Capar, I.; Kuby, M. An efficient formulation of the flow refueling location model for alternative-fuel stations. *IIE Trans.* **2012**, *44*, 622–636. [CrossRef]
29. Capar, I.; Kuby, M.; Leon, V.J.; Tsai, Y.J. An arc cover-path-cover formulation and strategic analysis of alternative-fuel station locations. *Eur. J. Oper. Res.* **2013**, *227*, 142–151. [CrossRef]
30. Chung, S.H.; Kwon, C. Multi-period planning for electric car charging station locations: A case of Korean expressways. *Eur. J. Oper. Res.* **2015**, *242*, 677–687. [CrossRef]
31. Bhatti, S.F.; Lim, M.K.; Mak, H.Y. Alternative fuel station location model with demand learning. *Ann. Oper. Res.* **2014**, *230*, 105–127. [CrossRef]
32. Ghamami, M.; Zockaie, A.; Nie, Y.M. A general corridor model for designing plug-in electric vehicle charging infrastructure to support intercity travel. *Transp. Res. Part C Emerg. Technol.* **2016**, *68*, 389–402. [CrossRef]
33. Tran, T.H.; Nguyen, T.B.T. Alternative-fuel station network design under impact of station failures. *Ann. Oper. Res.* **2018**, *279*, 151–186. [CrossRef]
34. Angelucci, G.; Mollaioli, F.; Tardocchi, R. A New Modular Structural System for Tall Buildings Based on Tetrahedral Configuration. *Buildings* **2020**, *10*, 240. [CrossRef]

35. Subbotin, A.; Grigoryan, S. Road service facilities for improving the ecological state using the PPP mechanism. *E3S Web Conf.* **2019**, *91*, 08007. Available online: https://www.e3s-conferences.org/articles/e3sconf/pdf/2019/17/e3sconf_tpacee2019_08007.pdf (accessed on 15 January 2022). [CrossRef]
36. Samoilov, K.I. The triangular module for roadside service buildings/Education materials. Almaty. 2020. 120p. Available online: https://znanio.ru/media/samoilov-ki-the-triangular-module-for-roadside-service-buildings--education-materials---almaty-2020-120-p-2711058 (accessed on 15 January 2022).
37. Toll Plaza/Archohm.—ArchDaily: The World's Most Visited Architecture Website. 26 January 2013. Available online: https://www.archdaily.com/322127/toll-plaza-archohm (accessed on 15 January 2022).
38. Repsol Service Stations.—Foster + Partners. Available online: https://www.fosterandpartners.com/projects/repsol-service-stations/ (accessed on 15 January 2022).
39. Parasol Paraíso (Repsol Filling Stations, Spain and Portugal).—The Beauty of Transport: Transport Design, Transport Architecture, and Transport's Influence on Art and Culture. 24 February 2016. Available online: https://thebeautyoftransport.com/2016/02/24/parasol-paraiso-repsol-filling-stations-spain-and-portugal/ (accessed on 15 January 2022).
40. "Foster + Partners" Repsol service station.—Divisare: The Atlas of Contemporary Architecture. 23 June 2016. Available online: https://divisare.com/projects/320787-foster-partners-nigel-young-repsol-service-station (accessed on 15 January 2022).
41. Spin Me Right Round (Red Hill Filling Station, Leicestershire, UK)—The Beauty of Transport: Transport Design, Transport Architecture, and Transport's Influence on Art and Culture. 21 August 2013. Available online: https://thebeautyoftransport.com/2013/08/21/spin-me-right-round-red-hill-filling-station-leicestershire-uk/ (accessed on 15 January 2022).
42. Shell Shape High-Speed Way Entrance Tent PTFE Membrane Structure/Guangzhou Feite Truss Tent Co., Ltd. Available online: https://www.truss-tent.com/product/shell-shape-high-speed-way-entrance-tent-ptfe-membrane-structure/ (accessed on 15 January 2022).
43. Ulyanovskie Dorogi "Ukrasyat" 3h-Zvezdnymi Gostinicami I Mnogotoplivnymi Zapravkami [Ulyanovsk Roads will be "Decorated" with Three-Star Hotels and Multi-Fuel Gas Stations]. Finance. 18 April 2017. Available online: http://1ul.ru/finance/biznes/news/ulyanovskie_dorogi_ukrasyat_3h_zvezdnymi_gostinicami_i_mnogotoplivnymi_zapravkami/ (accessed on 15 January 2022).
44. Standart Respubliki Kazakhstan 2476-2014 «Dorogi Avtomobilnye Obshego Polzovania. Trebovania k Obiektam Dorojnogo servisa i ih Uslugam» [Standard of the Republic of Kazakhstan 2476-2014 "Public Roads. Requirements for Road Service Facilities and Their Services"]. Astana, Komitet Tekhnicheskogo Regulirovaniya i Metrologii Ministerstva po Investiciyam i Razvitiyu Respubliki Kazahstan (Gosstandart), 2014. 106 s. Available online: https://ru.qaj.kz/upload/medialibrary/255/%D0%A1%D0%A2%D0%A0%D0%9A%202476-2014.pdf (accessed on 15 January 2022).
45. Mikhailov, V.V.; Sergeev, M.S. *Spatial Core Construction of Coatings (Structures)*; Izdatelstvo Vladimirskogo Gosudarstvennogo Universiteta: Vladimir, Russia, 2011; 56 s.
46. Rekomendatsii po Proektirovaniyu Strukturnykh Konstruktsii [Recommendations for the Design of Structural Constructions]/TSNIISK im.Kucherenko Gosstroia SSSR [Recommendations for the Design of Structural Constructions]. Moskwa: Stroiizdat. 1984. 416 s. Available online: http://www.complexdoc.ru/ntdpdf/537365/rekomendatsii_po_proektirovaniyu_strukturnykh_konstruktsii.pdf (accessed on 15 January 2022).

designs

MDPI

*Article*

# A Systematic Review of Architectural Design Collaboration in Immersive Virtual Environments

**Rongrong Yu [1,*], Ning Gu [1], Gun Lee [2] and Ayaz Khan [1]**

[1] UniSA Creative, Australian Research Centre for Interactive and Virtual Environment, University of South Australia, Adelaide, SA 5000, Australia
[2] UniSA STEM, Australian Research Centre for Interactive and Virtual Environment, University of South Australia, Adelaide, SA 5000, Australia
* Correspondence: rongrong.yu@unisa.edu.au

**Abstract:** Emerging applications of immersive virtual technologies are providing architects and designers with powerful interactive environments for virtual design collaboration, which has been particularly beneficial since 2020 while the architecture, engineering and construction (AEC) industry has experienced an acceleration of remote working. However, there is currently a lack of critical understanding about both the theoretical and technical development of immersive virtual environments (ImVE) for supporting architectural design collaboration. This paper reviewed recent research (since 2010) relating to the topic in a systematic literature review (SLR). Through the four steps of identification, screening, eligibility check, and inclusion of the eligible articles, in total, 29 journal articles were reviewed and discussed from 3 aspects: ImVE in the AEC industry, ImVE for supporting virtual collaboration, and applications of ImVE to support design collaboration. The results of this review suggest that future research and technology development are needed in the following areas: (1) ImVE support for design collaboration, particularly at the early design stage; (2) cognitive research about design collaboration in ImVE, toward the adoption of more innovative and comprehensive methodologies; (3) further enhancements to ImVE technologies to incorporate more needed advanced design features.

**Keywords:** architectural design collaboration; immersive virtual environments; systematic literature review

**Citation:** Yu, R.; Gu, N.; Lee, G.; Khan, A. A Systematic Review of Architectural Design Collaboration in Immersive Virtual Environments. *Designs* **2022**, *6*, 93. https://doi.org/10.3390/designs6050093

Academic Editor: Farshid Aram

Received: 12 September 2022
Accepted: 8 October 2022
Published: 11 October 2022

**Publisher's Note:** MDPI stays neutral with regard to jurisdictional claims in published maps and institutional affiliations.



## 1. Introduction and Background

Traditionally, most architects work and collaborate in face-to-face environments, and virtual collaboration only occurs occasionally, mainly during the latter design stages such as design review. Although the concept of computer-supported cooperative work (CSCW) in the design field has emerged and been extensively studied during the past few decades, in actuality, the area has not seen significant advances throughout that time. With emerging technologies such as immersive virtual environments (ImVE), architects and designers are able to collaborate virtually with more convenience and power. Since 2020, there has been an urgent global acceleration of remote working, leading to a rush of adoption of virtual technologies across most industries, including in the architecture and design sectors.

Design collaboration refers to team-based design activities working toward achieving the shared design goals. Effective collaboration during the initial design stage will lead to fewer problems during the latter, more complex design and construction stages [1]. Design collaboration with multiplicate problem-solving approaches can align different stakeholders' opinions toward a common baseline that can more optimally result in valuable project insights [2]. Tan [3] argues that design collaboration enhances reflection upon the actions of architects within a team. Citing the need for remote collaboration during pandemic times, Kim et al. [4] note that social networking services can increase idea clarification and the sharing of information to support active design collaboration. Combrinck and Porter [5]

found that initial stages of design benefit directly from the collaboration between architects and end-users. Design collaboration occurring at the early design stage is significant for achieving design innovation and ultimately optimal design solutions.

Researchers have emphasised that digital modalities and collaboration affect the quality, efficiency, and accuracy of design [6–8]. Virtual collaboration environments enable distributed remote design collaboration, facilitating greater time and cost efficiency in design, and have become increasingly relevant and crucial since 2020. Early studies have explored the application of shared digital environments in design collaboration during the design phase [9–11], including the effects of those environments on designers. For example, Gu et al. [12] suggested that 3D virtual worlds support the production of considerable perceptual events during synchronous design collaboration. Recent developments in ImVE facilitate intuitive virtual interactions between designers, and also between designers and the design environments [13], leading to better spatial perception [14] that may be beneficial for the design process. ImVE refers to virtual environments in which the users can "immerse" themselves inside the computer-generated world and feel they are in fact an integral part [15]. This can be achieved by using head-mounted displays (HMD) or multiple projections [16]. Virtual reality (VR), augmented reality (AR), and mixed reality (MR) are typical categories of ImVE systems that allow different degrees of interactions between the physical and the virtual worlds supporting building projects with different complexity and diversity [17]: VR is a computing technique that immersively manipulates the user's senses to make him/her feel present in a simulated virtual environment [18,19]; AR on the other hand superimposes virtual information upon the real world in a graphical manner via digital computing platforms to deliver enhanced experiences of the real world [20]; and MR is a combination of AR and augmented virtuality (AV), with the potential to integrate virtual and augmented realities together [21].

In light of the increasing application of ImVE within the architecture, engineering and construction (AEC) industry, it is important to critically understand how ImVE supports design collaboration. This study has reviewed the recent (since 2010) research in this area, to reveal the current body of knowledge and different applications of ImVE for supporting design collaboration, as well as potential future research directions to further advance the field.

## 2. Research Method- Systematic Literature Review

This study adopts the research method of systematic literature review (SLR) to review current research on design collaboration in ImVE and synthesise further knowledge about the field. SLR is an authoritative procedural method that synthesises and delineates the boundaries of knowledge in a research domain [22,23]. In accordance with common SLR research conventions, this study adopted a four-stage SLR to review the published articles related to design collaboration in ImVE, comprising a widespread literature search, full text assessment, meta-synthesis, and critical content analysis. The following sections elaborate on the details and steps of SLR. The article retrieval process is shown in Figure 1 below. Through the 4 steps of identification, screening, eligibility check, and inclusion of the eligible articles, ultimately 29 articles were selected for analysis from the initial 1106 papers identified. The relatively small number of articles that were closely related to the topic shows that architectural design collaboration in immersive virtual environments has not been extensively explored in the field, and this in turn supports the needs for this review and for future research.

### *2.1. Selection of Databases and Literature Search*

The SLR process should be reinforced by a detailed and impartial search in specifying relevant research. A choice of database selection that ensures a broad coverage of research must be identified and used. In this regard, this study uses Scopus and Web of Science (WoS), the two most significant platforms for article retrieval. These two databases offer a wide coverage of literature and are feasible for conducting organised queries. Past

reviews have used similar databases for article selection in the AEC industry [24,25]. Firstly, prominent keywords related to architectural design collaboration and ImVE were identified, and in the next step, a number of keywords having similar semantic meanings were merged. The resulting search string used for this study was as follows:

[TITLE-ABS-KEY ("architectural design" OR architecture) AND TITLE-ABS-KEY ("collaboration" OR "design collaboration") AND TITLE-ABS-KEY ("virtual reality" OR "augmented reality" OR "mixed reality" OR "immers* techn*" OR "virtual environment*")]. A total of 689 articles from *Scopus* and 417 articles from *WoS* were identified via the search.

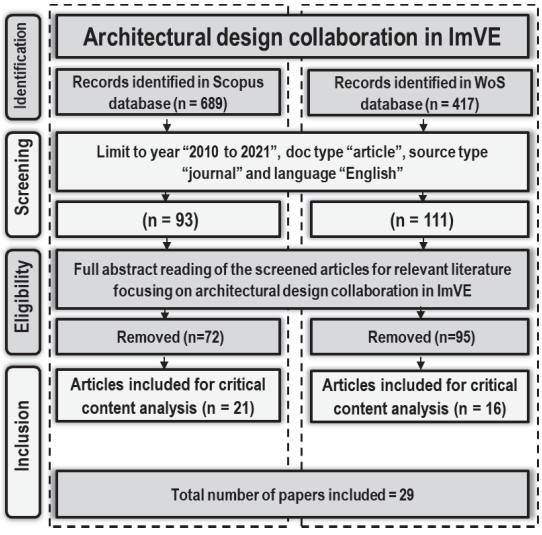


**Figure 1.** Article retrieval process (data was collected in March 2022).

### 2.2. Screening of Articles

The screening of the articles provides and constitutes the benchmark utilised in the SLR process for filtering the pool of articles. At this stage, this filtering was performed based on year, document type, source type, and the language of articles. The applied filtering procedure is as follows: [(LIMIT-TO (YEAR, "2010-present") AND (LIMIT-TO (DOCTYPE, "ar") AND (LIMIT-TO (SRCTYPE, "j") AND (LIMIT-TO (LANGUAGE, "English")]. The articles considered for this study were limited to recent ones (from 2010, in accordance with the prominent boom of ImVE). In relation to document type and source type, only peer-reviewed journals articles were considered for the study; since journal articles go through a more rigorous peer review process and provide more in-depth knowledge than other research articles such as conference papers. Finally, non-English language articles were filtered out. This stage resulted in a total of 93 articles from Scopus and 111 articles from WoS.

### 2.3. Eligibility and Inclusion Criteria of Articles

In this step, eligibility and inclusion criteria were developed to narrow down the articles relevant to the specific focus of this study: criteria such as abstract review, keywords, evaluation of conclusions, and results were applied to the articles from the previous step. Papers with a focus on ImVE but for health care, manufacturing, and other domains were removed at this stage. This stage resulted in a total of 21 articles from Scopus and 16 articles from WoS. Articles which were identified as duplicates in both search engines were then merged. In the end, a total of 29 articles were for this study, which is a significant number for critical content analysis. This sample size is favourable compared with other similar reviews.

### *2.4. Meta-Synthesis and Critical Content Analysis of Articles*

Meta-synthesis refers to the analysis of metadata within the pool of articles in the SLR process [26]. It augments the SLR process by extracting the metadata from each article and is utilised to provide a basis for organising a framework for the study [27]. Information such as journal name, year of publication, focus of research, and limitations constitutes metadata and was organised in a tabular format into an Excel file. This comprehensive table can be described as an "idea thought matrix supplemented by components of analysis" [26]. The articles were then categorised further into research themes, emphasising commonalities among them to form clusters from among the retrieved articles; this process is called critical content analysis, and it facilitates establishing the current status quo and developing future trends in the domain of study [28].

## 3. Results

### *3.1. Publication Trend of Architectural Design Collaboration in ImVE*

The articles in this study were limited to those from the year 2010 to present, due to the rise of ImVE only being significantly noticeable over the last decade, and this focus is more likely to deliver the latest advancements and status quo in the specific subject area. Figure 2 depicts the annual trends in research publications on the topic. From the figure, we can see that the period of time between 2010 to 2013 only has up to 3 articles per year, as this period marks the inception of ImVE in the architecture field (where architects found ImVE to be a novel design collaboration tool and could engage clients and other stakeholders in a more intuitive way). In 2014, the social media company Meta promoted its Oculus VR headset, which resulted in a substantial amount of awareness to the public. However, this did not result in increasing number of research publications in this area, due to a number of reasons; firstly, there were significant barriers encountered by the AEC industry for adopting ImVE devices including low battery life, tracking issues, interoperability concerns, and relatively high degree of skills required from users [17], and secondly the AEC industry comprises of large number of small and medium-sized enterprises (SMEs) that lacked interests in adopting ImVE due to the relatively high costs, capital required for training, and other significant obstacles [24]. A surge in the number of papers is seen from 2017 on the use of ImVE for design collaboration. This is because technological advancements seen in the latest ImVEs have resolved major prior concerns and issues. Further surge in demand resulting from the COVID-19 pandemic has brought such applications of ImVE to the broader industry. Virtual collaboration has never carried more necessity and meaning than in the recent times of the COVID-19 pandemic, which saw a general upwelling of interest among researchers since 2020 [29]. Such upward trends in this area makes this study especially timely and valuable in its analysis of the status quo, emergent themes, and future research directions for design collaboration in ImVE. Note that in Figure 2 the upward trend is not seen in the 2022 data point, as this study's data collection was only completed in March 2022.

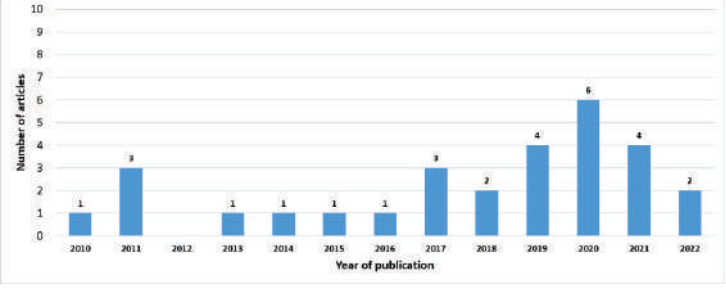


**Figure 2.** Annal publication trend of articles for design collaboration in ImVE.

### *3.2. Distribution of Journals for Publishing the Topic*

The 29 articles included in this study were published across a total of 17 journals. Table 1 lists the journals, and the number of articles published. Six journals published at least two articles each, with the top contributing journals being *Automation in Construction* (7) and *Journal of Information Technology in Construction* (4). The analysis of journals provides a summary for researchers who may conduct similar kinds of studies. Other main journals include *Visualisation in Engineering*, *Frontiers in Robotics and AI,* and *Journal of Higher Education Theory and Practice*. Together, they have illustrated the applications and benefits of ImVE from a wide range of perspectives, such as automating the design collaboration process, providing better visualisations for end users, and promoting the use of information technologies within the AEC field.

Table 1 categorises the 29 articles about architectural design collaboration in ImVE that have been reviewed. The table also organises these current studies in terms of the type of technology, focus of design collaboration, main research content, and project stage in which ImVE has supported design collaboration. The results of the review are further discussed in Section 4.

**Table 1.** Reviewed articles on design collaboration in ImVE.

| No. | Journal | Author & Year | Article Title | Type of ImVR | Focus of Design Collaboration | Main Research Content | Project Stage |
|---|---|---|---|---|---|---|---|
| 1 | Automation in Construction | [30] | A multi-user collaborative BIM-AR system to support design and construction | BIM and AR | Multi-stakeholder collaboration | Presented a BIM-AR system that provides the ability to view, interact with, and collaborate with 3D and 2D BIM data via AR with geographically dispersed teams. | Multiple stages |
| 2 | Automation in Construction | [31] | From BIM to extended reality in AEC industry | Extended reality | Technologies for construction collaboration between stakeholders | Explored outsourcing patterns for technologies among construction project stakeholders. | Multiple stages |
| 3 | Automation in Construction | [32] | Virtual reality applications for the built environment: Research trends and opportunities | VR | Design collaboration, multi-user virtual construction | Review paper; reviewed VR applications in AEC. | Multiple stages |
| 4 | Automation in Construction | [33] | OpenBIM-Tango integrated virtual showroom for offsite manufactured production of self-build housing | BIM, VR, and AR | Early involvement of stakeholders and end-users | Streamlined the design process and provided a pared-down agnostic openBIM system with low latency and included concurrent user accessibility. | Design stage |
| 5 | Automation in Construction | [34] | Zero latency: Real-time synchronization of BIM data in Virtual Reality for collaborative decision-making | BIM and VR | Improvement of collaboration in AEC industry | Proposed a BIM VR real-time synchronisation system based on an innovative cloud-based BIM metadata interpretation and communication method. | Design stage |
| 6 | Automation in Construction | [35] | Immersive virtual environments versus physical built environments: A benchmarking study for building design and user-built environment explorations | Immersive virtual environments | End-user involvement | Explored the use of immersive virtual environments during the design, construction, and operation phases of AEC projects. | Multiple stages |

**Table 1.** *Cont.*

| No. | Journal | Author & Year | Article Title | Type of ImVR | Focus of Design Collaboration | Main Research Content | Project Stage |
|---|---|---|---|---|---|---|---|
| 7 | Automation in Construction | [12] | Technological advancements in synchronous collaboration: The effect of 3D virtual worlds and tangible user interfaces on architectural design | 3d virtual worlds and tangible user interface | Design collaboration | Presented and evaluated two current advancements of collaborative technologies for architectural design. | Design stage |
| 8 | Journal of Information Technology in Construction | [36] | The impact of avatars, social norms and copresence on the collaboration effectiveness of AEC virtual teams | VR | Virtual team collaboration on AEC project | Review paper; examined collaboration effectiveness of global virtual engineering project teams. | Multiple stages |
| 9 | Journal of Information Technology in Construction | [37] | Virtual Reality for the built environment: A critical review of recent advances | VR and virtual environment applications | Benefits for collaboration | Review paper; presented a classification framework to reveal the scholarly coverage of VR and virtual environment. | Multiple stages |
| 10 | Journal of Information Technology in Construction | [38] | Case studies using multiuser virtual worlds as an innovative platform for collaborative design | Multi-user virtual worlds | Collaboration between designers | Investigated the innovative use of emerging multiuser virtual world technologies for supporting human–human collaboration and human–computer co-creativity in design. | Design stage |
| 11 | Journal of Information Technology in Construction | [39] | Framework for model-based competency management for design in physical and virtual worlds | Virtual worlds | Design collaboration | Explored differences and commonalities in competencies for design in the physical and virtual worlds by examining design input, process, and outcome. | Design stage |
| 12 | Journal of Construction Engineering and Management | [24] | State-of-the-Art review on Mixed Reality applications in the AECO industry | MR | Multi-user collaboration | Review paper; reviewed MR technology applications in the AECO industry. | Multiple stages |

**Table 1.** *Cont.*

| No. | Journal | Author & Year | Article Title | Type of ImVR | Focus of Design Collaboration | Main Research Content | Project Stage |
|---|---|---|---|---|---|---|---|
| 13 | Journal of Construction Engineering and Management | [40] | Virtual collaborative design environment: Supporting seamless integration of multitouch table and immersive VR | VR | Multi-stakeholder collaboration | Presented the design and evaluation of a virtual collaborative design environment. | Design stage |
| 14 | Applied Sciences (Switzerland) | [41] | Developing a BIM-based MUVR treadmill system for architectural design review and collaboration | BIM based Multi-user VR | High-level immersion in architectural design review and collaboration | Presented a system framework that integrates multi-user virtual reality (MUVR) applications into omnidirectional treadmills. | Design review |
| 15 | Applied Sciences (Switzerland) | [25] | End-Users' Augmented Reality utilization for architectural design review | AR | End-user involvement in design review | Investigated how the AR system affects architectural design review from users' perspectives. | Design review |
| 16 | Applied Sciences (Switzerland) | [42] | Trends and research issues of Augmented Reality studies in architectural and civil engineering education—A review of academic journal publications | AR | Collaboration between academia and practice | Review paper; reviewed AR in AEC education, with a focus on collaboration promoting optimal connection between general pedagogy and domain-specific learning. | Multiple stages |
| 17 | Journal of Engineering, Design and Technology | [43] | Multiuser immersive Virtual Reality application for real-time remote collaboration to enhance design review process in the social distancing era | Immersive VR | Collaboration in design review | Explored design review process conducted among participants remotely located. | Design review |
| 18 | International Journal of Digital Earth | [44] | Immersive Virtual Reality for extending the potential of building information modeling in architecture, engineering, and construction sector: systematic review | Building Information Modelling (BIM) and Immersive VR | Communication and collaboration in design, construction, operation, and maintenance phases | Review paper; reviewed most commonly adopted technologies, applications, and evaluation methods of VR. | Multiple stages |

**Table 1.** *Cont.*

| No. | Journal | Author & Year | Article Title | Type of ImVR | Focus of Design Collaboration | Main Research Content | Project Stage |
|---|---|---|---|---|---|---|---|
| 19 | Journal of Computational Design and Engineering | [45] | Evaluation framework for BIM-based VR applications in design phase | BIM and VR | Multi-user collaboration | Developed an evaluation framework for BIM-based VR applications focused on the design phase of projects. | Design stage |
| 20 | Journal of Higher Education Theory and Practice | [46] | Innovation in architecture education: Collaborative learning method through Virtual Reality | VR | Collaborative learning | Review paper; reviewed VR encounters and long-term collaborative learning approaches. | Design education |
| 21 | Construction Innovation | [47] | Using Virtual Reality to facilitate communication in the AEC domain: A systematic review | VR | Multi-stakeholder collaboration | Review paper; explored how VR has been applied for communication purposes in AEC. | Multiple stages |
| 22 | Environment and Planning B-Urban Analytics and City Science | [48] | Architectural design creativity in multi-user virtual environment: A comparative analysis between remote collaboration media | VR | Multi-user virtual environments | Investigated the affordance of multi-user virtual environments for the production of novel and appropriate solutions in remote collaboration. | Design stage |
| 23 | Frontiers in Robotics and AI | [49] | Laypeople's collaborative immersive Virtual Reality design discourse in neighborhood design | VR | Virtual participatory urban design | Protocol study; explored design communication and participation of laypeople in a virtual participatory urban design process. | Design stage |
| 24 | Advanced Engineering Informatics | [50] | Overlay design methodology for virtual environment design within digital games | VR | Design collaboration | Protocol study; explored the use of overlay design methodology for the creation of virtual environments within digital gaming contexts. | Design stage |
| 25 | Visualization in Engineering | [51] | Virtual Reality-integrated workflow in BIM-enabled projects collaboration and design review: A case study | BIM and VR | Collaboration in design review | Developed and tested a VR integrated collaboration workflow. | Design review |

**Table 1.** *Cont.*

| No. | Journal | Author & Year | Article Title | Type of ImVR | Focus of Design Collaboration | Main Research Content | Project Stage |
|---|---|---|---|---|---|---|---|
| 26 | Journal of Digital Landscape Architecture | [52] | Using Virtual Reality as a design input: Impacts on collaboration in a university design studio setting | Immersive VR | Student learning and group collaboration | Presented the application of immersive VR to assist landscape architecture students in design. | Design education |
| 27 | Co-Design | [53] | Enablers and barriers of the multi-user virtual environment for exploratory creativity in architectural design collaboration | Multi-user virtual environment | Architectural design collaboration | Explored the design collaboration process using multi-user virtual environment and sketching media in face-to-face and remote collaboration modes. | Design stage |
| 28 | Computers in Industry | [54] | Mutual awareness in collaborative design: An Augmented Reality integrated telepresence system | AR | Design collaboration | Proposed a new computer-mediated remote collaborative design system, TeleAR, to enhance the distributed cognition among remote designers. | Design stage |
| 29 | IEEE Transactions on Visualization and Computer Graphics | [55] | A spatially Augmented Reality sketching interface for architectural daylighting design | AR | Collaboration between designers and end-users | Presented an application of interactive global illumination and spatially augmented reality to architectural daylight modelling. | Design stage |

## 4. Discussion

During past decades, emerging immersive virtual technologies have significantly changed the nature of collaboration in the AEC industry at various stages of a building project including design. Technological advancements create new design environments for designers and make virtual collaboration possible, which also have an impact on designers' thinking processes as well as on the design solutions they produced [56]. This section discusses the current state of theoretical and technical developments about immersive virtual technologies, and their applications in supporting design collaboration from various perspectives, as revealed from the critical review.

### *4.1. Immersive Virtual Technologies and It's Attributes in the AEC Industry*

One of the most significant obstacles for current design technologies has been the immersion of the relevant stakeholder in the design representation during different stages of the project. Table 1 shows that the term "immersive" is increasingly being seen in design collaboration research since 2015. Prior to 2015, researchers used alternative terms such as "virtual worlds", and "multi-user virtual worlds". Despite possessing numerous advantages for streamlining the process of design, design technologies have not provided adequate immersive presence for its users. The importance of presence when visualising a design solution is significant in the AEC industry for realising the aesthetic appearance of a space, simulating the functionality of the design, and enabling users to effectively experience the place in terms of other factors such as safety and ergonomics. Advancements in digital design technologies including ImVE have supplied architects with a myriad of opportunities, for visualising the appearance and performance of their designs [57].

Recent broader adoption of computing technologies have enabled designers to more readily utilise ImVE in practice. Conceptually, an ImVE system can be predominantly classified into four categories of elements, namely devices, platforms, applications, and tools (Figure 3).

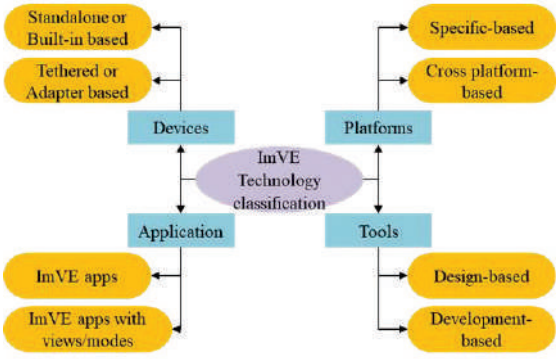


**Figure 3.** The conceptual model of an ImVE system.

The first category elements in the model is devices, which can be subdivided into standalone or built-in, and tethered or adapter based. The VR Quest series by Meta is a typical example of a standalone VR device, although it can also be optionally tethered to give it more rendering power. The Oculus Rift seriesis a more recent tethered models that needs to be connected to a computer through a cable. One of the earliest examples of adapter-based devices is Google Cardboard, which simply wraps around a smartphone. In relation to AR, examples such as Microsoft HoloLens act as a standalone device incorporating high-level computing capabilities. On the other hand, Holokit act as adapter based AR device using Apple ARKit enabled smartphones. There has been continuous advancement among ImVE devices with companies such as HTC, Microsoft, and Meta developing high-end devices with significant enhancements to the visual field of view,

storage capacities, ergonomics, and graphics rendering to name a few. The second category of elements relates to the software platforms that serve as the basis for devices to work; such platforms can be subdivided further into specific and cross platforms. Companies such as Meta, HTC, and Magic Leap provide their own proprietary software platforms for their devices to function, while cross platforms (sometimes referred to as open platforms) allow different hardware devices to function on the same software platform. Steam VR, Windows Mixed Reality (WMR), and WebXR are examples of such open or cross platforms. The third category pertains to ImVE applications, which are subdivided into ImVE applications alone and ImVE applications with views and modes. The difference between those two relates to their real-world integration and communication. Most typically, VR applications are without real-world integration, while AR/MR applications possess real-world interaction capabilities. Finally, the fourth-category elements relate to ImVE tools that are either design based or development based. Tools such as Tilt Brush, Quill, and Aero are design oriented and are common among designers such as architects. Development tools such as Unity and Unreal Engine are significant tools for creating VR and AR visualisations respectively.

Based on data from the online market data portal Statista, the market size of ImVE is predicted to increase vastly in the coming years, from 30.7 billion USD in 2021 to 296.9 billion USD in 2024. This is indicative of the future demand for ImVE and its related technologies and applications across many industries. Figure 4 shows the main ImVE types and their usage comparison data obtained from Statista for actual 2020 and predicted 2024. From the figure, we can see that in 2020, all VR-related technologies were utilised more than AR-related technologies. Among them the VR standalone HMDs were the most popular immersive technology (accounted for 43.76%). However, for 2024 the prediction is that AR-related technologies combined will be utilised more than VR combined, and among the AR technologies the AR standalone HMDs will have the highest usage (accounted for 31.28%). AR represents the superimposition of the virtual information over the real world to construct the synthetic environment aiming to enrich reality [58]), and the growing trend of research shifting away from VR and toward AR/MR can also be noticed in the ImVR literature that was reviewed (Figure 5). In the figure, we can see that although most of the reviewed articles focused on VR-related ImVE technologies, in recent years, there is a visible increase of AR/MR utilisation in design collaboration. The growing application of AR technologies for design collaboration may due to the fact that AR technologies were based on early VR technologies that had been developed to extend VR technologies, focusing on the capability of augmenting the real world with virtual information, allowing real and virtual information to coexist and at a same time making user interactions more intuitive through references to reality [59].

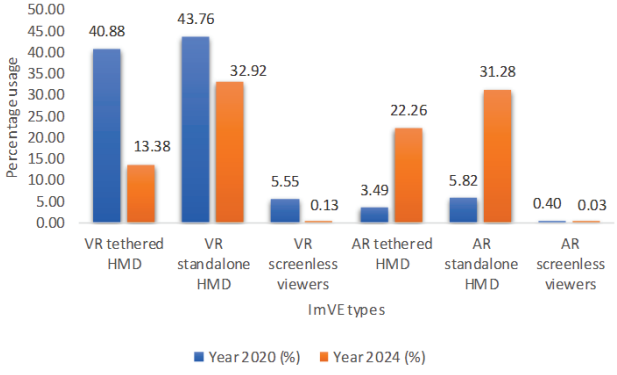


**Figure 4.** Main ImVE types and their usage comparison (Source: Statista).

Some of the main attributes of ImVE include presence, immersion, and interactivity [60,61]. Presence describes the complete feeling of being in an immersive simulated

space, wherein the user is psychologically immersed in the virtual environment in a manner that they temporarily escape their real world [62–64]. The immersion level is affected by the sophistication of the simulation in terms of the quality of its visual representation, consistency, freedom of movement of the user, and physical interaction/feedback functionality within the ImVE. The interactivity level indicates to what extent a user is able to alter the ImVE in real-time [65]. Additionally, immersive AR technologies are able to augment real world spaces with overlayed virtual information in a manner such that real and virtual information can coexist simultaneously to enable enhanced intuitive user interactions [59].

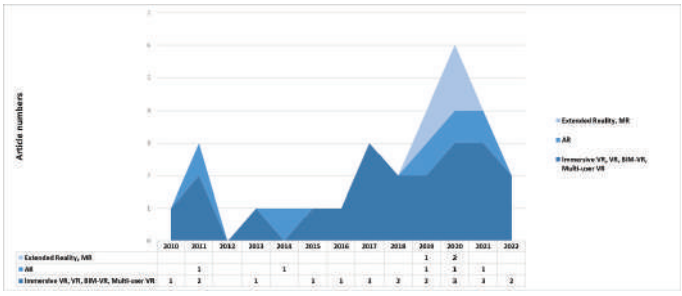


**Figure 5.** Types of ImVE technologies the review articles focused on.

### *4.2. ImVE in Supporting Virtual Collaboration*

Virtual collaboration tools currently in use within the AEC industry largely focus on design review or construction scheduling, such as Unity Reflect Review, Resolve, Trezi, Fuzor, and BIM 360. A few recently emerging tools are intended for use in the design ideation stage, including Wild, Mindesk, and Arkio. For design ideation purposes, most tools support importing 3D models from commonly used architectural design software such as Revit and SketchUp. Mindesk and Arkio support the use of Grasshopper, which is a popular parametric design tool for design ideation in architecture. Arkio provides functions including real-time Boolean operations, sun studies, smart guides for geometry alignment and creation, integrated street maps, etc., which can support a range of design ideation purposes. For design collaboration, Wild provides native digital sketching tools for both ideation and as (speech to text) annotation for design review. Mindesk allows teams to collaborate on the same parametric model in multi-user VR sessions. Arkio on the other hand focuses on supporting multi-user model modification during design collaboration. All of the aforementioned virtual collaboration tools enable access via VR including desktop VR options that are convenient for users without headsets. Wild and Arkio also allow mobile access for users. Another virtual collaboration tool Hyve 3D, is primarily focused on providing 3D sketching in immersive design environments, to support both ideation and remote collaboration. Hyve 3D requires a Macbook, iPad Pros, and a 4K projector but a VR headset is not needed to have the immersive experience. Table 2 summarises the main ImVE used for virtual design collaboration in the AEC industry. In addition, generic communication and collaboration tools are also used in the AEC practice, including Teams, Zoom, Slack, etc. Some of those generic tools also provides certain visual collaboration functions, for example, Miro has a 2D digital whiteboard for supporting brainstorming, Asana can assist with project workflow planning with a visual timeline and calendar, and as Jira can be linked to Navisworks and allow the display of 3D models. From the table, we can see that there are recently developed design collaboration tools utilising ImVE technologies, some of which are focused on application at the early design stage. However, they are not yet widely adopted throughout the AEC industry. Furthermore, the review results suggest that academic research has fallen behind the technological advancement, and there is a lack of understanding of how the recently developed ImVE technologies support design collaboration, particularly at the early design stage.

**Table 2.** Virtual design collaboration tools in the AEC industry (Source: respective official website of each individual platform).

| Virtual Design Collaboration Tools | Project Stages | Collaboration Means | Interoperability | Accessibility | Design Support |
|---|---|---|---|---|---|
| The Wild (https://thewild.com/) | Multiple stages | Annotation (speech to text) for design review | Revit, SketchUp, BIM 360 | VR, desktop or mobile | Sketching, Inspection of object BIM data |
| IrisVR (joined Wild) (https://irisvr.com/) | Multiple stages | Optimised *Revit* to VR workflow, multi-user meetings, collaborative tracking, annotation, other user controls, BIM coordination. | Revit, Sketchup, Navisworks, Rhino | VR or desktop | Inspection of elements, tape measure, scale model mode, sun studies |
| Generic communication tools such as Zoom (https://zoom.us/), Teams (https://www.microsoft.com/en-au/microsoft-teams/log-in (accessed on 12 September 2022)), Slack (https://slack.com/intl/en-au/in (accessed on 12 September 2022)), Miro (https://miro.com/), Asana (https://asana.com/). | Multiple stages | Multi-user meeting, 3D model viewing, 2D shared white board, visual timeline, calendar, chat box | - | - | 3D model viewing, 2D drawing sharing. |
| Fuzor (https://www.kalloctech.com/) | Multiple stages with a focus on construction | Multi-user view | Revit, Rhino | VR, desktop or mobile | Flythrough and walkthrough videos |
| BIM 360 (https://www.autodesk.com/bim-360/in (accessed on 12 September 2022)) | Multiple stages with a focus on construction | Multi-user model modification | BIM | Desktop | Model modification |
| Hyve3D (https://www.hyve3d.com/) | Ideation | Multi-user model modification, sketching | Can import model from Revit, SketchUp, but primarily focus on sketching | Need iPad Pro, Macbook Pro, and 4K projector, but does not require a headset | 3D sketching simultaneously in complementary (orthogonal) representations. |

**Table 2.** *Cont.*

| Virtual Design Collaboration Tools | Project Stages | Collaboration Means | Interoperability | Accessibility | Design Support |
|---|---|---|---|---|---|
| Arkio (https://www.arkio.is/) | Ideation, modelling | Multi-user model modification, sketching | Revit, SketchUp, BIM 360, Rhnio | AR/VR or mobile | Parametric design, sketching, real-time Boolean operations and parametric volumes, sun studies, PC spectator mode, see inside with sections, smart guides, integrated street map, and instantly enable 3D buildings from OpenStreetMap, etc. |
| Mindesk (https://mindeskvr.com/) | Ideation, design review | 3D/surface modelling, multi-user model modification, navigation, selection, review and co-presence and use of body language for communication | Revit, Rhino, Grasshopper, Solid works | VR or desktop | Parametric design, Unreal Studio and OBS Studio for VR |
| Theia BigRoom (upcoming) (https://www.theia.io/bigroom/in (accessed on 12 September 2022)) | Design review | Multi-user meeting, 3D sketching tools, whiteboard drawing tools, ideation boards, task lists and post-it notes | BIM | VR, desktop or mobile | Unreal engine, interactive sun + sky. |
| Unity Reflect review (https://unity.com/products/unity-reflect-reviewin (accessed on 12 September 2022)) | Design review | Walkthroughs in VR and AR, annotation, and filter BIM data to effectively communicate design intent to stakeholders | Revit, SketchUp, BIM 360, Navisworks, Rhino | AR/VR, desktop, or mobile | Sun studies, overlay models in 1:1 AR at scale (marker-based or tabletop) |
| Resolve (https://www.resolvebim.com/) | Design review, facility management | Annotation (speech to text), multi-user meeting | BIM | VR or desktop | Annotate by measuring and sketching, issue tracking integration with BIM 360, inspect BIM properties |
| Trezi (https://trezi.com/) | Manufacturing | Multi-user meeting | BIM | VR or desktop | Model modification, design review |

*4.3. Applications of ImVE in Supporting Design Collaboration*

ImVE provides opportunities for designers and other stakeholders to work collaboratively in a shared virtual environment. In the AEC industry, ImVE combining with standard design and collaboration platforms specific to the sector such as BIM have significantly enhanced communication and collaboration across design, construction, operation, and maintenance stages [44]. This study reviewed recent research on design collaboration in ImVE. As shown in Figure 6, 15 out of 29 articles focus on the design stage, 10 articles discuss collaboration across multiple stages including design of a building project, and 4 articles focus on design review. Collaboration research focussing on the design stage in ImVE covers a wide range of topics including the development of various VR environments or frameworks to support design collaboration [40,45], cognitive exploration on how designers collaborate in VR environments [49,50], and in an education context, virtual design studio through VR collaboration [46,52]. Articles focussing on design review discuss various directions including developing a BIM-based multi-user VR system for architectural design review and collaboration [41], investigating how AR affects architectural design reviews based on the user's perspectives [25], and integrating VR into collaboration workflow [51]. For articles focussing on collaboration in ImVE across multiple stages or in the general AEC context, some present relevant ImVE applications [44,47] and other advance technical developments of ImVE, especially by combining with BIM, to facilitate collaboration [30,35]. The review of the 29 articles has identified 3 main application areas of ImVE in supporting design collaboration: (1) design review with end-users and other stakeholders in ImVE; (2) visual data in BIM-based ImVE for supporting design collaboration; and (3) cognition and education in collaborative ImVE. These three application areas will be further discussed as follows.

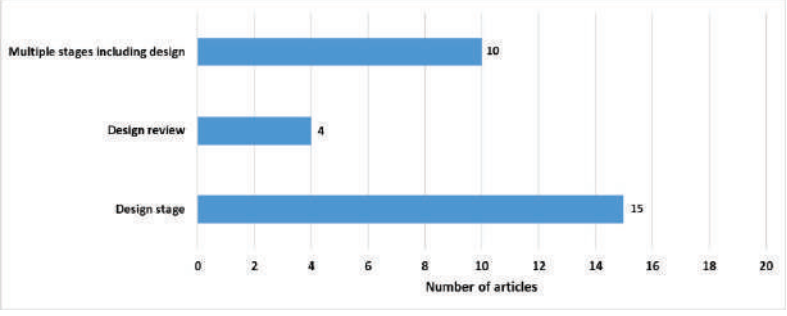


**Figure 6.** Number of articles focusing on different project stages.

4.3.1. Design Review with End-Users and Other Stakeholders in ImVE

In current practice, architects have embraced ImVE in the participatory process to engage with end-users and to obtain their feedback. For instance, Pour Rahimian et al. [33] consider VR an effective tool for end-user engagement due to the advanced visual communication of building design, and a dynamic feedback initiator. Whether by simulating the realistic scale of the building, or functional aspects of the design, or other end-users experiences such as safety, ImVE has enabled telepresence for different stakeholders including clients, end-users and authorities [56]. ImVE can be intimidating initially for new users especially outside the professional project team, as it involves various hardware and software setup. However, the benefits of ImVR are enormous, as it can leverage the showcase of virtual models to clients in a superior way [66], enabling them with a more thorough understanding of the design and better align the business- client requirements. As a result, design professionals including architects are increasingly using VR for design showcase [67].

ImVE delivers spatial information and at the same time allows collaborative communication. In the AEC disciplines, the goal of including clients during the design process

beyond the final showcase—clients who often have limited spatial comprehension and limited specialist knowledge—is to improve both design quality and client satisfaction [33,68], and has gained increasing popularity in the sector. Similarly, Heydarian et al. [35] also find that ImVE is an effective tool in the design phase of a building project in terms of acquiring performance feedback from end users. These benefits are evident in all types of ImVE. For example, VR has been considered to engage clients to the project in an inclusive way [35], and could be more effective than the traditional approach for design review [43]. Lee et al. [25] suggest that AR is effective in reviewing the visual elements of a building and leads to a higher degree of satisfaction in terms of user experience. AR could be an effective platform to investigate evaluate the appearances of a virtual model and to examine the user experience in the design review process [25]. Sheng et al. [55] present an application of an interactive AR application to architectural daylight modelling in which designers and end users can review and have their input on the daylighting design. The involvement of end users leads to higher performing design and end user satisfaction. MR has shown potential in increasing the spatial understanding of end users [69], to allow the interpretation and translation of virtual content through wearable devices [70]. Enabling an end user to experience a realistic and immersive visualisation of a building project, has a different effect on an end user's cognition, and can reveal new possibilities. Unlike AEC professionals, end users are unable to be effectively related to two-dimensional drafting documents. Standard BIM models, despite having multiple advantages over drawings, still lack in leveraging the experiences of the end users to critically understand the design. It is therefore necessary to utilise BIM combing with immersive technologies in participatory design to adequately support end users' decision-making processes [71]. Combining BIM and immersive technologies can also bring many other benefits. For example, the ability to allow collaborators to interact with BIM models without being physically together at different stages of a building project, can be achieved via VR. Zaker and Coloma [51] further suggest that VR collaboration in the design review is beneficial for a wide range of disciplines involved.

Early design review and visualisation, optimisation of building performance analysis, and building maintenance and operations, are possible areas where MR integration can improve the delivery of the building project [24]. The rapid development in MR technologies has significant potential for the AEC industry by combining digital- and real-world information, which is beneficial for design collaboration [69]. MR collaboration can be face-to-face or remote. Face-to-face MR collaboration is achieved by using a shared coordinate system, where collaborators interact with the same set of virtual data information in person [72]. In remote MR collaboration, remote data sharing and remote collaboration are both accomplished utilising the MR platform [73]. Currently, MR collaboration has not been widely adopted within the AEC industry, and there is especially a lack of applications for remote MR collaboration, despite that such applications are likely to benefit AEC professionals to communicate and interact across distributed locations, due to its strong capability of integrating both digital- and physical-world information [24].

#### 4.3.2. Data Visualisation in BIM-Based ImVE for Supporting Design Collaboration

BIM combining with ImVE enable collaboration among multiple parties via both two dimensional and three-dimensional models [74]. Data visualisation in BIM-based ImVE can effectively support and improve design collaboration; in particular, the data visualisation in immersive BIM-based VR environments during the design process can potentially facilitate a deeper understanding among collaborators [75], which can make real-time visualisation and communication more accurate during design [76,77]. Additionally, studies suggest that the barriers in BIM-VR data exchange need further exploration, which may otherwise limit applications of VR within the AEC industry [44]. For example, Du et al. [34] introduced a real-time synchronisation system for BIM-based VR, which is cloud-based, and updates changes to the BIM model and VR model simultaneously to facilitate effective data exchange.

BIM-based AR enriches the real world with digital data by providing more dynamic outcomes with real-time visualisations through a seamless management process [78], hence BIM-based AR environments have potential to benefit design collaboration, by supporting richer interactions and media representations [79]. Visualising and sharing of information by multiple users through AR can augment the real environment by embedding relevant digital data for supporting design decision-making. Overall, by combining the real and the digital, AR can improve designers' information processing and communication [80] and offer subsequent benefits in terms of project visualisation, monitoring, and control [81]. One example of a BIM-based AR system was developed by Garbett et al. [30], which allows distributed teams to view, interact and collaborate on both 3D and 2D BIM data via AR. The other immersive technology—MR—can also be used to enhance BIM model information and its visualisation, feeding mixed-reality representations back to the original BIM model during the design process [82]. BIM-MR integration can potentially further enhance the visualisation of the BIM model, along with supporting more context-aware interactions between the designers and between the designers and the design environment [33]. However, one of the main limitations in BIM-MR integration is the amount of data and details of a BIM model, which is at times not required and not appropriate for an effective corresponding MR application. Therefore, timely data-keeping, and dropping of non-required BIM data, should be addressed in future studies to improve the performance of BIM-based MR applications for design collaboration. Future data storage technologies supported by cloud computing will also help addressing this issue, and can expand the potential utilisation of BIM-based MR applications, to include large-scale collaborative projects, which tend to produce significant amounts of data. Data storage and transfer, together with other issues such as the accuracy of spatial registration, user interface, and multi-user collaboration have been suggested to be key areas for future MR research [24].

#### 4.3.3. Design Cognition and Education in Collaborative ImVE

The exploration of design perception, design physiology, and design cognition and neurocognition in a collaborative environment can generate the knowledge needed in order to support improved design patterns, creativity, and reasoning among multiple users to support their designing and collaboration [83]. Research shows that ImVE aids designers' cognitive processes such as those related to working memory, design data search and access, spatial cognition, and attention allocation. Particularly, ImVE has a positive effect on users' perception and memory [75,77]. Hermund et al. [84] determined that immersive VR representations during the design process were less demanding on designers' cognitive load than traditional 3D visualisation on desktop computers. Design is not a linear process, since designers typically formulate a design problem and develop a design solution in parallel [85]. Studies indicate that ImVE can potentially lead to higher performance of designers particularly in problem finding [86], which can have positive effect in both the problem and solution spaces. In another study focusing on collaboration, Hong et al. [53] developed a multi-user virtual environment and track users' problem-solving measures in a shared design setting. Their results suggest positive effective of ImVE especially in increasing inspiration for new approaches to problem-solving among design collaborators.

Advances in design computing and cognition research have provided a number of methodological approaches to studying both human–human and human–agent communications and interactions in ImVE [38]. For example, Roupe et al. [40] developed a virtual collaborative design environment that enhances the communication, collaboration, understanding, and knowledge sharing of participants. They conducted two collaborative design workshops to explore the collaboration behaviours of designers in a virtual collaborative environment, utilising direct documented observations and semi-structured interviews with participants, to explore their experiences and views about their collaborative design processes. Leon et al. [1] developed a pre-BIM conceptual design stage protocol for cognitive design studies in collaborative virtual environments, and its coding scheme included team formation, introduction of the brief, discussion of project requirements, solution synthesis

and brainstorming, solution evaluation, consensus, and final solution. For design collaboration in ImVE, communication tools have mainly consisted of a few forms of text-based tools, voice chat tools, visual sharing tools and avatars, which can potentially improve the communication efficiency of design collaboration in the AEC industry [47]. In one example, based on participatory observation in a virtual collaboration environment it has been found [36] that the use of avatar movement is effective for communicating non-verbal information that enhances the effectiveness of collaboration. Other studies focusing on various communication approaches during collaboration in ImVE, include Kim et al. [50] which applied an overlay design methodology in studying virtual environments based on protocol studies of participants' collaborative design process, and found that method can effectively assist with communication, doubling the collaboration segments among team members and reducing the overall time needed to complete their design compared to use of traditional design method. Another example is Wang et al. [54] development of a computer-mediated remote collaborative design system TeleA. Via measurement of participants' physiological movements such as gestures, facial expressions, fine motor movements and bodily postures and distances, as well as observation of their emotional states, that study suggested that developed system had a positive effect on designers' communication and collaboration, especially for distributed cognition and mutual awareness.

Furthermore, previous studies have also explored design collaboration in ImVE in the context of architectural education focusing on teaching and learning. For instance, Rauf et al. [46] discussed the application of VR in architectural education to support collaborative learning, and identified the effect of VR applications from various collaborative levels including student-instructor, student-client and student-industry. Similarly, Diao and Shih [42] reviewed AR applications in the broader AEC education and suggested that collaborative learning enabled by AR can promote the connection between general pedagogy and domain-specific learning. George et al. [52] studied students' design processes in ImVE and found that VR is effective in enhancing students' understanding of design decisions by assisting them with rapid design prototyping.

Among various design studies, especially cognitive design studies on collaboration techniques and frameworks, the dominant majority have the overarching aim of streamlining the collaboration process to produce more optimal design output. ImVE has the potential to assist in producing creative design solutions during the collaboration. Particularly, design solutions appeared to be more creative in terms of both novelty and appropriateness in multi-user virtual environments than in traditional sketching environments due to the explicit communication cues for sharing the collaborative procedure and spatial information provided by the former [48]. Similarly, Chowdhury and Schnabel [49] also found that the more spontaneous exchange of visual information in a shared virtual environment is beneficial for producing optimal design solutions.

## 5. Conclusions and Future Research

This study has reviewed recent research on design collaboration in ImVE from the past ten years. The results demonstrate an increasing research focus on this area through the past decade. From a technical development perspective, immersive technologies are being rapidly developed and applied within the AEC industry to facilitate collaboration at various design and construction stages. Recent research on design collaboration in ImVE has focused on design review with end users and other stakeholders in ImVE, visual data/information in BIM-based ImVE in supporting design collaboration, and cognitive studies of design collaboration in ImVE. To date, current research provides us with some early understandings of design collaboration in ImVE as applied in the above-mentioned ways. However, academic research about ImVE support for design collaboration, is not keeping pace with the accelerating rate of its technological advancement. Generally there is a lack of critical understanding about design collaboration in ImVE, thus the following future research is needed.

First, additional studies regarding ImVE support for design collaboration, especially at the early design stage, are needed. Commonly used design collaboration platforms in the AEC industry such as BIM tend to be tailored to the later design and management stages rather than providing support for the conceptualising, interacting, and sharing of design concepts at the early stage [7,87]. Most virtual collaboration tools are focused on visualisation [31,88,89]. A few recent tools that support design ideation (such as Wild, Mindesk, and Arkio) provide limited design functions of sketching or parametric modelling, etc., and they have not yet been widely applied and tested throughout the design industry. Effective collaboration during the initial concept design stage will lead to fewer problems during the later stages such as developed design, detailed design, and design documentation [1]. In addition, effective collaboration is often supported by digital and network tools, for example, through social networking services for enhancing remote design collaboration [4]. There is currently a lack of critical understanding about the effectiveness of these virtual technologies and various emerging add-on tools for meeting the needs of design collaboration, especially at the early design stage [90].

Secondly, further cognitive research on design collaboration in ImVE adopting more innovative and comprehensive methodologies is needed. Current research has explored the design collaboration process in ImVE from various cognitive perspectives, including the creativity of design solutions (i.e., novelty and appropriateness) in multi-user virtual environments [48], design collaborators' problem-solving measures in multi-user virtual environments [53], and various explorations from design teaching and learning perspectives [42,46]. More comprehensive understandings about how architects collaborate in ImVE from a cognitive perspective, compared with face-to-face or more traditional computer-based collaboration, will allow us to identify the barriers of adopting ImVE for design collaboration, and designers' needs for future tools to better support design collaboration. Very recently, more innovative and comprehensive cognitive studies such as by adopting or combining design and neuroscience perspectives could possibly lead to a deeper understanding of designers' collaboration, through measurements of designers' biometric responses such as eye-tracking and electroencephalogram (EEG), to complement the existing knowledge about the impact of ImVE on designers' collaboration process.

Finally, the continuing development of new ImVE technologies with more advanced design features (such as intuitive parametric and generative design functions) is needed to better assist with designing during collaboration. Current limitations of collaborative ImVE in terms of design support include insufficient conceptual sketching and overly simplified modelling functions. The parametric design functions provided by some tools rely mostly upon external add-ons rather than within the collaboration environment itself. There is a clear need for an algorithmic design feature in collaborative ImVE [89]. Furthermore, there is also a lack of advanced design features such as those for analysing building performance, cost, and land use, which are essential for making more informed design decisions during architectural design collaboration.

**Author Contributions:** R.Y., conceptualization, methodology, formal analysis, original draft preparation, supervision; N.G., conceptualization, writing-review and editing, supervision; G.L., conceptualization, writing-review and editing, supervision; A.K., conceptualization, methodology, formal analysis. All authors have read and agreed to the published version of the manuscript.

**Funding:** This research received no external funding.

**Data Availability Statement:** Not applicable.

**Conflicts of Interest:** The authors declare no conflict of interest.

## References

1. Leon, M.; Laing, R.; Malins, J.; Salman, H. Making collaboration work: Application of A conceptual design stages protocol for pre-BIM stages. *WIT Trans. Built Environ.* **2015**, *149*, 205–216.
2. Feast, L. Professional perspectives on collaborative design work. *CoDesign* **2012**, *8*, 215–230. [CrossRef]
3. Tan, L. Collaborative Cultures of Architecture Teams: Team Learning and Reflective Practice. *Des. J.* **2021**, *24*, 489–498. [CrossRef]

4. Kim, M.J.; Hwang, Y.S.; Hwang, H.S. Utilising social networking services as a collective medium to support design communication in team collaboration TT—SNS as a collective medium. *ArchNet-IJAR* **2020**, *14*, 409–421. [CrossRef]
5. Combrinck, C.; Porter, C.J. Co-design in the architectural process. *Archnet-IJAR* **2021**, *15*, 738–751. [CrossRef]
6. Froese, T.M. The impact of emerging information technology on project management for construction. *Autom. Constr.* **2010**, *19*, 531–538. [CrossRef]
7. Garber, R. *BIM Design: Realising the Creative Potential of Building Information Modelling*; John Wiley & Sons, Inc.: Hoboken, NJ, USA, 2014.
8. Succar, B. Building information modelling framework: A research and delivery foundation for industry stakeholders. *Autom. Constr.* **2009**, *18*, 357–375. [CrossRef]
9. McCall, R.; Johnson, E. Using argumentative agents to catalyze and support collaboration in design. *Autom. Constr.* **1997**, *6*, 299–309. [CrossRef]
10. Kalay, Y.E.; Khemlani, L.; Choi, J.W. An integrated model to support distributed collaborative design of buildings. *Autom. Constr.* **1998**, *7*, 177–188. [CrossRef]
11. Gross, M.D.; Yi-Luen Do, E.; McCall, R.J.; Citrin, W.V.; Hamill, P.; Warmack, A.; Kuczun, K.S. Collaboration and coordination in architectural design: Approaches to computer mediated team work. *Autom. Constr.* **1998**, *7*, 465–473. [CrossRef]
12. Gu, N.; Kim, M.J.; Maher, M.L. Technological advancements in synchronous collaboration: The effect of 3D virtual worlds and tangible user interfaces on architectural design. *Autom. Constr.* **2011**, *20*, 270–278. [CrossRef]
13. Pour Rahimian, F.; Seyedzadeh, S.; Oliver, S.; Rodriguez, S.; Dawood, N. On-demand monitoring of construction projects through a game-like hybrid application of BIM and machine learning. *Autom. Constr.* **2020**, *110*, 103012. [CrossRef]
14. Paes, D.; Arantes, E.; Irizarry, J. Immersive environment for improving the understanding of architectural 3D models: Comparing user spatial perception between immersive and traditional virtual reality systems. *Autom. Constr.* **2017**, *84*, 292–303. [CrossRef]
15. Mostafavi, A. Architecture, biometrics, and virtual environments triangulation: A research review. *Archit. Sci. Rev.* **2021**, 1–18. [CrossRef]
16. Furht, B. Immersive Virtual Reality. In *Encyclopedia of Multimedia*; Springer: Boston, MA, USA, 2008; pp. 345–346.
17. Khan, A.; Sepasgozar, S.; Liu, T.; Yu, R. Integration of BIM and Immersive Technologies for AEC: A Scientometric-SWOT Analysis and Critical Content Review. *Buildings* **2021**, *11*, 126. [CrossRef]
18. Diemer, J.; Alpers, G.W.; Peperkorn, H.M.; Shiban, Y.; Mühlberger, A. The impact of perception and presence on emotional reactions: A review of research in virtual reality. *Front. Psychol.* **2015**, *6*, 1–9. [CrossRef] [PubMed]
19. Serrano, B.; Baños, R.M.; Botella, C. Virtual reality and stimulation of touch and smell for inducing relaxation: A randomized controlled trial. *Comput. Hum. Behav.* **2016**, *55*, 1–8. [CrossRef]
20. Behzadan, A.H.; Kamat, V.R. Visualization of construction graphics in outdoor augmented reality. In Proceedings of the Winter Simulation Conference, Orlando, FL, USA, 4 December 2005.
21. Milgram, P.; Kishino, F. A Taxonomy of Mixed Reality Visual Displays. *EICE Trans. Inf. Syst.* **1994**, *E77-D*, 1321–1329.
22. Linnenluecke, K.M.; Marrone, M.; Singh, A.K. Conducting systematic literature reviews and bibliometric analyses. *Aust. J. Manag.* **2020**, *45*, 175–194. [CrossRef]
23. Pickering, C.; Grignon, J.; Steven, R.; Guitart, D.; Byrne, J. Publishing not perishing: How research students transition from novice to knowledgeable using systematic quantitative literature reviews. *Stud. High. Educ.* **2015**, *40*, 1756–1769. [CrossRef]
24. Cheng, J.C.P.C.P.; Chen, K.; Chen, W. State-of-the-Art Review on Mixed Reality Applications in the AECO Industry. *J. Constr. Eng. Manag.* **2020**, *146*, 03119009. [CrossRef]
25. Lee, J.; Seo, J.; Abbas, A.; Choi, M. End-Users' Augmented Reality Utilization for Architectural Design Review. *Appl. Sci.* **2020**, *10*, 5363. [CrossRef]
26. Lachal, J.; Revah-Levy, A.; Orri, M.; Moro, M.R. Metasynthesis: An Original Method to Synthesize Qualitative Literature in Psychiatry. *Front. Psychiatry* **2017**, *8*, 269. [CrossRef] [PubMed]
27. Hedges, L.V. Meta-Analysis. *J. Educ. Stat.* **1992**, *17*, 279–296. [CrossRef]
28. Stemler, S. An overview of content analysis. *Pract. Assess. Res. Eval.* **2000**, *7*, 17. [CrossRef]
29. Matthews, B.; See, Z.S.; Day, J. Crisis and extended realities: Remote presence in the time of COVID-19. *Media Int. Aust.* **2020**, *178*, 198–209. [CrossRef]
30. Garbett, J.; Hartley, T.; Heesom, D. A multi-user collaborative BIM-AR system to support design and construction. *Autom. Constr.* **2021**, *122*, 103487. [CrossRef]
31. Alizadehsalehi, S.; Hadavi, A.; Huang, J.C. From BIM to extended reality in AEC industry. *Autom. Constr.* **2020**, *116*, 103254. [CrossRef]
32. Zhang, Y.; Liu, H.; Kang, S.; Al-hussein, M. Automation in Construction Virtual reality applications for the built environment: Research trends and opportunities. *Autom. Constr.* **2020**, *118*, 103311. [CrossRef]
33. Rahimian, F.P.; Chavdarova, V.; Oliver, S.; Chamo, F.; Amobi, L.P. OpenBIM-Tango integrated virtual showroom for offsite manufactured production of self-build housing. *Autom. Constr.* **2019**, *102*, 1–16. [CrossRef]
34. Du, J.; Zou, Z.; Shi, Y.; Zhao, D. Zero latency: Real-time synchronization of BIM data in virtual reality for collaborative decision-making. *Autom. Constr* **2018**, *85*, 51–64. [CrossRef]

35. Heydarian, A.; Carneiro, J.P.; Gerber, D.; Becerik-Gerber, B.; Hayes, T.; Wood, W. Immersive virtual environments versus physical built environments: A benchmarking study for building design and user-built environment explorations. *Autom. Constr.* **2015**, *54*, 116–126. [CrossRef]
36. Anderson, A.; Dossick, C.S.; Iorio, J.; Taylor, J.E. The impact of avatars, social norms and copresence on the collaboration effectiveness of AEC virtual teams. *J. Inf. Technol. Constr.* **2017**, *22*, 287–304.
37. Kim, M.J.; Wang, X.; Love, P.E.D.; Li, H.; Kang, S.C. Virtual reality for the built environment: A critical review of recent advances. *J. Inf. Technol. Constr.* **2013**, *18*, 279–305.
38. Merrick, K.E.; Gu, N.; Wang, X. Case studies using multiuser virtual worlds as an innovative platform for collaborative design. *Electron. J. Inf. Technol. Constr.* **2011**, *16*, 165–188.
39. Cerovšek, T.; Zupančič, T.; Kilar, V. Framework for model-based competency management for design in physical and virtual worlds. *Electron. J. Inf. Technol. Constr.* **2010**, *15*, 1–22.
40. Roupe, M.; Johansson, M.; Maftei, L.; Lundstedt, R.; Viklund-Tallgren, M. Virtual Collaborative Design Environment: Supporting Seamless Integration of Multitouch Table and Immersive VR. *J. Constr. Eng. Mangement* **2020**, *146*, 1–31. [CrossRef]
41. Keung, C.C.W.; Kim, J.I.; Ong, Q.M. Developing a bim-based muvr treadmill system for architectural design review and collaboration. *Appl. Sci.* **2021**, *11*, 6881. [CrossRef]
42. Diao, P.H.; Shih, N.J. Trends and research issues of augmented reality studies in architectural and civil engineering education-A review of academic journal publications. *Appl. Sci.* **2019**, *9*, 1840. [CrossRef]
43. Tea, S.; Panuwatwanich, K.; Ruthankoon, R.; Kaewmoracharoen, M. Multiuser immersive virtual reality application for real-time remote collaboration to enhance design review process in the social distancing era. *J. Eng. Des. Technol.* **2022**, *20*, 281–298. [CrossRef]
44. Safikhani, S.; Keller, S.; Schweiger, G.; Pirker, J. Immersive virtual reality for extending the potential of building information modeling in architecture, engineering, and construction sector: Systematic review. *Int. J. Digit. Earth* **2022**, *15*, 503–526. [CrossRef]
45. Kim, J.I.; Li, S.; Chen, X.; Keung, C.; Suh, M.; Kim, T.W. Evaluation framework for BIM-based VR applications in design phase. *J. Comput. Des. Eng.* **2021**, *8*, 910–922. [CrossRef]
46. Rauf, H.L.; Shareef, S.S.; Othman, N.N. Innovation in Architecture Education: Collaborative Learning Method Through Virtual Reality. *J. High. Educ. Theory Pract.* **2021**, *21*, 33–40. [CrossRef]
47. Wen, J.; Gheisari, M. Using virtual reality to facilitate communication in the AEC domain: A systematic review. *Constr. Innov.* **2020**, *20*, 509–542. [CrossRef]
48. Hong, S.W.; El Antably, A.; Kalay, Y.E. Architectural design creativity in Multi-User Virtual Environment: A comparative analysis between remote collaboration media. *Environ. Plan. B Urban Anal. City Sci.* **2019**, *46*, 826–844. [CrossRef]
49. Chowdhury, S.; Schnabel, M.A. Laypeople's Collaborative Immersive Virtual Reality Design Discourse in Neighborhood Design. *Front. Robot. AI* **2019**, *6*, 1–10. [CrossRef]
50. Kim, I.; Hong, S.; Lee, J.H.; Bazin, J.C. Overlay Design Methodology for virtual environment design within digital games. *Adv. Eng. Inform.* **2018**, *38*, 458–473. [CrossRef]
51. Zaker, R.; Coloma, E. Virtual reality-integrated workflow in BIM-enabled projects collaboration and design review: A case study. *Vis. Eng.* **2018**, *6*, 1–15. [CrossRef]
52. George, B.H.; Sleipness, O.R.; Quebbeman, A. Using virtual reality as a design input: Impacts on collaboration in a university design studio setting. *J. Digit. Landsc. Archit.* **2017**, *2017*, 252–259. [CrossRef]
53. Hong, S.W.; Jeong, Y.; Kalay, Y.E.; Jung, S.; Lee, J. Enablers and barriers of the multi-user virtual environment for exploratory creativity in architectural design collaboration. *CoDesign* **2016**, *12*, 151–170. [CrossRef]
54. Wang, X.; Love, P.E.D.; Kim, M.J.; Wang, W. Mutual awareness in collaborative design: An Augmented Reality integrated telepresence system. *Comput. Ind.* **2014**, *65*, 314–324. [CrossRef]
55. Sheng, Y.; Yapo, T.C.; Young, C.; Cutler, B. A Spatially Augmented Reality Sketching Interface for Architectural Daylighting Design. *IEEE Trans. Vis. Comput. Graph.* **2011**, *17*, 38–50. [CrossRef] [PubMed]
56. Yu, R.; Gu, N.; Ostwald, M.J. *Computational Design: Technology, Cognition and Environments*, 1st ed.; CRC Press, Taylor & Francis Group: Boca Raton, FL, USA, 2021.
57. Yu, R.; Ostwald, M.J. Comparing Architects' Perceptions of the Usefulness of Digital Design Environments with their Aspirations for Sustainable Design in Australia. *J. Sustain. Archit. Civ. Eng.* **2021**, *2021*, 5–20. [CrossRef]
58. Azuma, R.T. A Survey of Augmented Reality. *Presence Teleoperators Virtual Environ.* **1997**, *6*, 355–385. [CrossRef]
59. Billinghurst, M.; Clark, A.; Lee, G. A survey of augmented reality. *Found. Trends Hum. -Comput. Interact.* **2014**, *8*, 73–272. [CrossRef]
60. Ryan, M.-L. *Narrative as Virtual Reality 2: Revisiting Immersion and Interactivity in Literature and Electronic Media*; Johns Hopkins University Press: Baltimore, MD, USA, 2015.
61. Walsh, K.R.; Pawlowski, S.D. Virtual reality: A technology in need of IS research. *Commun. Assoc. Inf. Syst.* **2002**, *8*, 20. [CrossRef]
62. Schubert, T.; Friedmann, F.; Regenbrecht, H. The experience of presence: Factor analytic insights. *Presence Teleoperators Virtual Environ.* **2001**, *10*, 266–281. [CrossRef]
63. Slater, M.; Steed, A. A virtual presence counter. *Presence Teleoperators Virtual Environ.* **2000**, *9*, 413–434. [CrossRef]
64. Sundar, S.S.; Xu, Q.; Bellur, S. Designing interactivity in media interfaces: A communications perspective. *Conf. Hum. Factors Comput. Syst. Proc.* **2010**, *4*, 2247–2256. [CrossRef]

65. Steuer, J. Defining virtual reality: Dimensions determining telepresence. *J. Commun.* **1992**, *42*, 73–93. [CrossRef]
66. Sidani, A.; Dinis, F.M.; Sanhudo, L.; Duarte, J.; Santos Baptista, J.; Poças Martins, J.; Soeiro, A. Recent Tools and Techniques of BIM-Based Virtual Reality: A Systematic Review. *Arch. Comput. Methods Eng.* **2021**, *28*, 449–462. [CrossRef]
67. Hilfert, T.; König, M. Low-cost virtual reality environment for engineering and construction. *Vis. Eng.* **2016**, *4*, 1–18. [CrossRef]
68. Asgari, Z.; Rahimian, F.P. Advanced Virtual Reality Applications and Intelligent Agents for Construction Process Optimisation and Defect Prevention. *Procedia Eng.* **2017**, *196*, 1130–1137. [CrossRef]
69. Wang, X.; Dunston, P.S. User perspectives on mixed reality tabletop visualization for face-to-face collaborative design review. *Autom. Constr* **2008**, *17*, 399–412. [CrossRef]
70. Piroozfar, P.; Essa, A.; NewSchool, E.R.P.F. The application of Augmented Reality and Virtual Reality in the construction industry using wearable devices. In Proceedings of the 9th International Conference on Construction in the 21st Century, Dubai, United Arab Emirates, 5–7 March 2017.
71. Damen, T.; MacDonald, M.; Hartmann, T.; Giulio, R.D.; Bonsma, P.; Luig, K.; Sebastian, R.; Soetanto, D. Bim based collaborative design technology for collective self-organised housing. In Proceedings of the 40th IAHS World Congress on Housing: Sustainable Housing Construction, Funchal, Portugal, 16–19 December 2014.
72. Billinghurst, M.; Kato, H.; Kiyokawa, K.; Belcher, D.; Poupyrev, I. Experiments with Face-To-Face Collaborative AR Interfaces. *Virtual Real.* **2002**, *6*, 107–121. [CrossRef]
73. Cidota, M.; Lukosch, S.; Datcu, D.; Lukosch, H. Workspace Awareness in Collaborative AR using HMDs: A User Study Comparing Audio and Visual Notifications. In Proceedings of the 7th Augmented Human International Conference 2016, Geneva, Switzerland, 25–27 February 2016; p. 3.
74. Dunston, P.S.; Wang, X.; Lecturer, S.; Program, P. A hierarchical taxonomy of aec operations for mixed reality applications. *J. Inf. Technol. Constr.* **2011**, *16*, 433–444.
75. Roupé, M.; Johansson, M.; Tallgren, M.V.; Jörnebrant, F.; Tomsa, P.A. Immersive visualization of Building Information Models. *In Living Systems and Micro-Utopias: Towards Continuous Designing, Proceedings of the 21st International Conference of the Association for Computer-Aided Architectural Design Research in Asia (CAADRIA 2016), New Delhi, India, 28–30 April 2016*; pp. 673–682.
76. Johansson, M.; Roupé, M.; Bosch-Sijtsema, P. Real-time visualization of building information models (BIM). *Autom. Constr.* **2015**, *54*, 69–82. [CrossRef]
77. Calderon-Hernandez, C.; Paes, D.; Irizarry, J.; Brioso, X. Comparing Virtual Reality and 2-Dimensional Drawings for the Visualization of a Construction Project. In Proceedings of the ASCE International Conference on Computing in Civil Engineering 2019, Atlanta, GA, USA, 17–19 June 2019; pp. 17–24.
78. Hou, L.; Wang, X. Experimental framework for evaluating cognitive workload of using AR system in general assembly task. In Proceedings of the 28th International Symposium on Automation and Robotics in Construction (ISARC 2011), Seoul, Korea, 29 June–2 July 2011; pp. 625–630. [CrossRef]
79. Wang, X.; Love, P.E.D.; Kim, M.J.; Park, C.S.; Sing, C.P.; Hou, L. A conceptual framework for integrating building information modeling with augmented reality. *Autom. Constr.* **2013**, *34*, 37–44. [CrossRef]
80. Shin, D.H.; Dunston, P.S. Technology development needs for advancing Augmented Reality-based inspection. *Autom. Constr.* **2010**, *19*, 169–182. [CrossRef]
81. Chi, H.L.; Kang, S.C.; Wang, X. Research trends and opportunities of augmented reality applications in architecture, engineering, and construction. *Autom. Constr.* **2013**, *33*, 116–122. [CrossRef]
82. Lee, J.; Kim, J.; Ahn, J.; Woo, W. Context-aware risk management for architectural heritage using historic building information modeling and virtual reality. *J. Cult. Herit.* **2019**, *38*, 242–252. [CrossRef]
83. Shealy, T.; Gero, J.; Hu, M.; Milovanovic, J. Concept generation techniques change patterns of brain activation during engineering design. *Des. Sci.* **2020**, *6*, e31. [CrossRef]
84. Hermund, A.; Klint, L.; Bundgaard, T. BIM with VR for Architectural Simulations Building Information Models in Virtual Reality as an Architectural and Urban Designtool. In Proceedings of the ACE 2018, Singapore, 14–15 May 2018.
85. Dorst, K.; Cross, N. Creativity in the design process: Co-evolution of problem-solution. *Des. Stud.* **2001**, *22*, 425–437. [CrossRef]
86. Wu, T.-H.; Wu, F.; Kang, S.-C.; Chi, H.-L. Comparison of Virtual Communication Environment for Remote BIM Model Review Collaboration. In Proceedings of the 36th International Symposium on Automation and Robotics in Construction (ISARC), Banff, AB, Canada, 21–24 May 2019; pp. 1149–1154.
87. Okeil, A. Hybrid design environments: Immersive and non-immersive architectural design. *ITcon* **2010**, *15*, 202–216.
88. Davila Delgado, J.M.; Oyedele, L.; Demian, P.; Beach, T. A research agenda for augmented and virtual reality in architecture, engineering and construction. *Adv. Eng. Inform.* **2020**, *45*, 101122. [CrossRef]
89. Castelo-Branco, R.; Leitão, A. Algorithmic Design in Virtual Reality. *Architecture* **2022**, *2*, 31–52. [CrossRef]
90. Idi, D.B.; Khaidzir, K.A.M. Critical perspective of design collaboration: A review. *Front. Archit. Res.* **2018**, *7*, 544–560. [CrossRef]

*designs*

MDPI

*Article*

# Influence of Microclimate on Older Peoples' Outdoor Thermal Comfort and Health during Autumn in Two European Cities

**María Teresa Baquero Larriva * and Ester Higueras García**

Escuela Técnica Superior de Arquitectura, Universidad Politécnica de Madrid, Av. Juan de Herrera, 2, 28040 Madrid, Spain
* Correspondence: m.t.baquero.larriva@upm.es

**Abstract:** Public spaces and green areas have been proven to influence people's mental and physical health, thermal comfort being one of the main indicators. The growing trend of an ageing population globally led this research to analyse the outdoor thermal comfort of older adults in public spaces from two cities in Europe: Madrid in Spain and Newcastle upon Tyne in the United Kingdom during autumn. A mixed methodology through environmental measurements and surveys was performed in situ. In addition, the UTCI (Universal Thermal Climate Index) and PET (Physiological Equivalent Temperature) outdoor thermal comfort indices were applied. The results highlighted the risk of thermal stress and the vulnerability of this group of the population to the effects of climate on their health. Although most older people had 'neutral' thermal sensation, 86.3% of them would be at risk of cold stress in Newcastle, whilst in Madrid 31.5% would be at risk of cold stress and 35.7% of heat stress. Those results could be a starting point for the design of more comfortable and healthy public spaces that improve the quality of life of all citizens within the guidelines of active ageing and healthy cities.

**Keywords:** outdoor thermal comfort; older people; thermal stress; health risk; urban public spaces

**Citation:** Baquero Larriva, M.T.; Higueras García, E. Influence of Microclimate on Older Peoples' Outdoor Thermal Comfort and Health during Autumn in Two European Cities. *Designs* **2023**, *7*, 27. https://doi.org/10.3390/designs7010027

Academic Editor: Tomohiko Sakao

Received: 23 December 2022
Revised: 13 January 2023
Accepted: 18 January 2023
Published: 1 February 2023



## 1. Introduction

The Intergovernmental Panel on Climate Change (IPCC) forecasts an increase in the intensity, number, and duration of extreme weather events, so it is expected that the extreme temperature will increase [1]. This affects normal temperatures in autumn and spring; in some cases, the change in season is imperceptible [2]. Parallel to this, according to the World Health Organization (WHO), the ageing population in 2050 will triple. In addition, more than half of the world's population lives in urban habitats. By 2030, six out of ten people in the world will live in a city, of which 900 million would be older adults [3].

One of the characteristics of ageing is its diversity among people over 65 years old. Thus, health depends on various factors such as genetic predisposition, lifestyle and quality of life, and at the same time is influenced by the physical and social environment. However, statistics indicate that a large percentage of older people tend to present multimorbidity and are also more sensitive to environmental effects on health (noise pollution, heat waves, cold waves, etc.) [4]. Some physiological changes that occur with ageing affect the thermal sensitivity, perception, adaptation and preferences of older adults [5]. For instance, muscle strength, work capacity, activity level, metabolic rate, vascular reactivation, thermoregulation capacity, sweating and hydration levels decrease and affect their ability to detect and respond to temperature changes, making them vulnerable to thermal extremes [6].

Public spaces are determinants for people's health [7]. Thermal comfort depends on several factors including: geographical (latitude, altitude); microclimatic (temperature, humidity, wind, radiation); personal (activity, clothing, age, gender, state of health, among others); psychological factors (aptitude, experience, expectation, memory, etc.) and built

environment factors (vegetation, shade, surface material, SVF, microclimate, etc.) [8]. Therefore, a good urban design based on bioclimatic criteria influences the quality of these spaces and the well-being of their users and the environment [9].

Most studies on thermal comfort are based on the physical and physiological characteristics of the 'type person' (a man, 35 years, 1.70 m in height, 75 kg in weight, level of shelter and standard metabolic rate [10–12], without taking into account the physiological conditions of older people or other vulnerable groups [13]. Novieto and Zhang [6] applied the IESD-Fiala model to represent the ageing human body considering the metabolic rate, heart rate and weight. They found that these factors differ between 10 and 19.2% of the characteristics of an average young person. Additionally, through sensitivity tests and simulations to establish the impact of these factors on the thermal comfort of older people, they discovered that the most influential factor was the basal metabolic rate. In a literature review of the existing literature on the thermal comfort of older adults [5], it was found that there are differences between 0.2 °C to 4 °C between the comfort ranges of the elderly and the rest of the age groups, the latter groups being more tolerant of the outside environment [5]. However, most of these studies refer to indoors and are heterogeneous in terms of methodologies, sample sizes and climatic zones, evidencing the need for more research in this area [13].

Until the early years of the twenty-first century, not much attention had been paid to the study of exterior thermal comfort and most evaluation systems had been developed for interiors, in stable conditions, that is, without considering the multiple factors that affect the urban microclimate [14,15]. Some authors have tried to adapt the interior thermal comfort indices such as PMV [16], SET [17] and ET [18]. Subsequently, other methods have been developed to establish the sensation of thermal comfort for open spaces, such as the case of PET (Physiological Equivalent Temperature) [19] and UTCI (Universal Thermal Climate Index) [20]. These are the most used in outdoor assessment [21].

Different climatic zones have specific characteristics that influence thermal comfort conditions and thermal adaptation among diverse seasons [22,23]. Thermal adaptation refers to the ability to adapt to the microclimate conditions, and this could be physical, physiological or psychological [24]. For instance, some aspects are related to cultural and social factors specific to each locality and context that affect thermal adaptation, including physiological conditions (health status, gender, age and metabolic rate), psychological issues (origin, expectation, personal experience, attitude, etc.) and clothing insulation levels [25,26].

In this context, the objectives of the present study are as follows:

- To evaluate how microclimate variables (air temperature, wind speed, mean radiant temperature, relative humidity and sky view factor) affect the thermal comfort of older people in public spaces during autumn in different climatic zones (Csa—Mediterranean Climate and Cfb—oceanic climate).
- To identify thermal comfort ranges for older adults in outdoor public spaces during autumn.
- To identify health risk via thermal stress (due to extrem cold or heat) for older adults in different climates during autumn according to PET and UTCI indexes.

## 2. Materials and Methods

To evaluate the influence of outdoor microclimate on the thermal comfort of older people, five public spaces were selected within two different cities corresponding to different climatic zones in Europe, Madrid (continental Mediterranean climate) and Newcastle upon Tyne (humid temperate oceanic) (Figure 1). Fieldwork was performed in the months of autumn 2018 in Madrid and autumn 2019 in Newcastle upon Tyne (September, October, and November 2019).

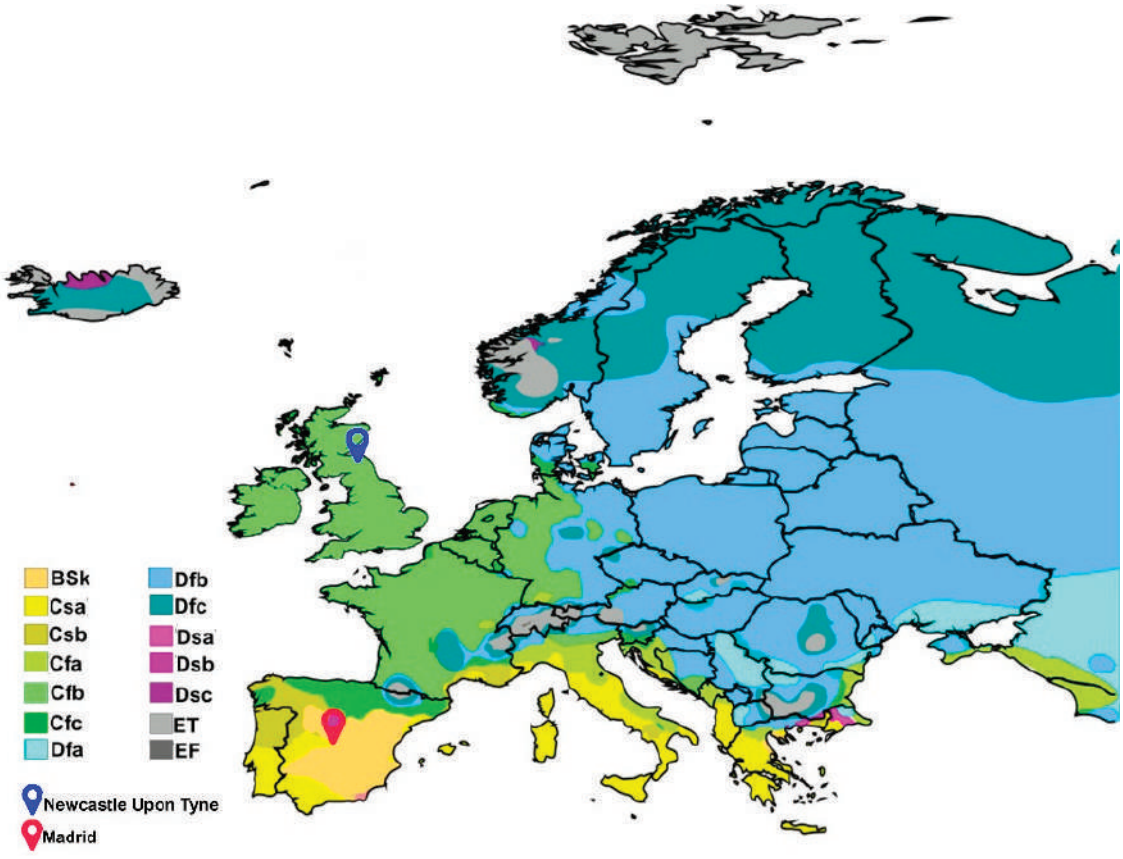


**Figure 1.** Case studies location in the Köppen–Geiger's climate classification map of Europe. (BSk, cold semi-arid; Csa, hot summer Mediterranean; Csb, warm-summer Mediterranean; Cfa, humid subtropical; Cfb, oceanic climate west coast; Cfc, oceanic climate subpolar; Dfa, hot summer humid continental; Dfb, warm summer humid continental; Dfc, regular subarctic; Dsa, dry and hot summer humid continental; Dsb, dry and warm summer humid continental; Dsc, dry summer, regular subarctic; ET, tundra; EF, ice cap climate).

### *2.1. Description of Case Studies*

#### 2.1.1. Madrid, Spain

The city of Madrid is in central Spain, at latitude 40°26′ N and longitude 3°41′ W at an altitude of 667 metres above sea level (Figure 2). According to the Köppen–Geiger climate classification, its climate corresponds to 'Csa' Mediterranean (temperate climate with dry and hot summers). In summer, it is characterised by its low average relative humidity of 37% and an average temperature of 25–32 °C. In winter, it presents a moderate–high humidity of around 71% and average temperatures of 2–11°C. The average annual temperature is around 14.1 °C [27,28].

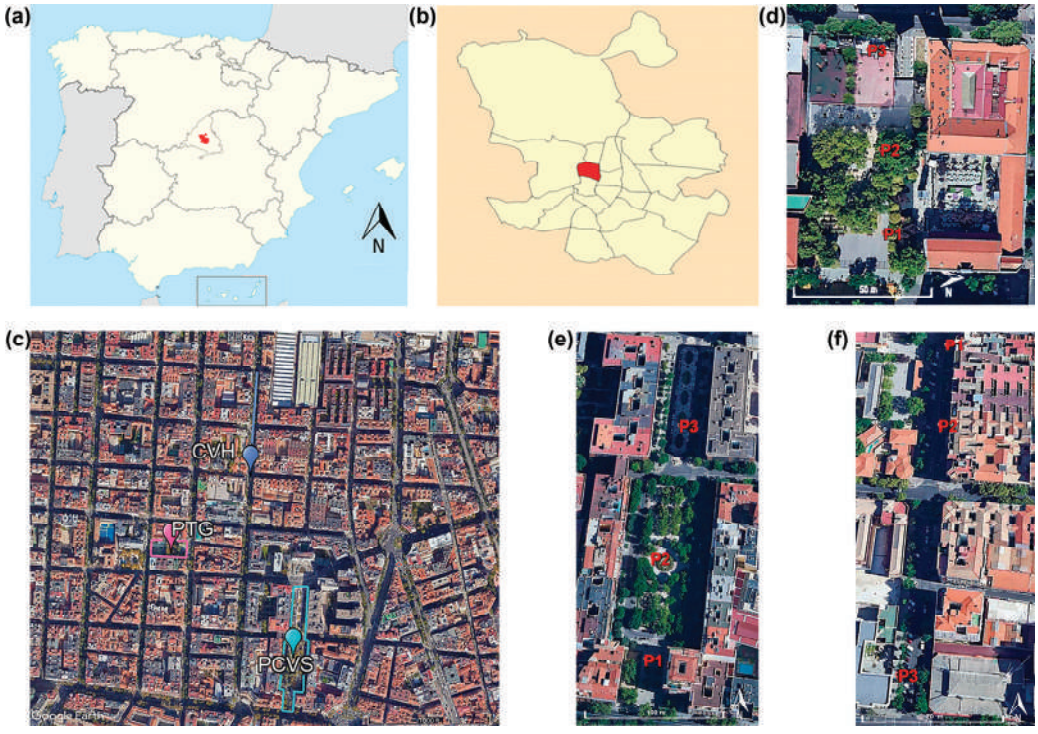


**Figure 2.** Case study of Madrid. (**a**) Location of Madrid in Spain; (**b**) location of Chamberi district in Madrid; (**c**) location of Park Galileo Theatre (PTG), *Conde del Valle de Schill* Square (PCVS) and *Vallehermoso* street (CVH); (**d**) aerial view of PTG and location of measurement points; (**e**) aerial view of PCVS and location of measurement points, (**f**) aerial view of CVH and location of measurement points.

A park (PTG), a square (PCVS) and a street (CVH) in a high-density, mainly residential neighbourhood (Arapiles, Chamberi) were selected as case studies due to their diverse characteristics. Figure 2 shows the location of these case studies.

2.1.2. Newcastle upon Tyne, United Kingdom

Newcastle upon Tyne is in the northeast of England, in the metropolitan borough of Tyne and Wear, situated at an altitude of 30 m above sea level, at latitude 54°58′40″ N and longitude 1°36′48″ W. Its climate corresponds to 'Cfb' humid temperate oceanic, characterised by cool summers, with abundant and well-distributed rainfall throughout the year (Figure 1). The mean temperature in summer is 15 °C and the mean in winter is 4 °C. The average annual temperature is 8.5 °C, with an average annual precipitation of 655 mm [29].

In the city of Newcastle, two public spaces are located in the centre of the city in an area of mainly commercial use (Westgate), a square (OES) and a pedestrian street (NS), and were taken as case studies because of observations of the concentration of older people. Figure 3 shows the location of those case studies.


**Figure 3.** Case study of Newcastle upon Tyne. (**a**) Location of Newcastle in the UK; (**b**) location of Westgate in Newcastle upon Tyne; (**c**) location of Old Eldon Square (OES) and Northumberland Street (NS); (**d**) aerial view of OES and location of measurement points; (**e**) aerial view of NS and location of measurement points.

### *2.2. Environmental Measurements*

The fieldwork was conducted one day per month, between 10:00 and 18:00, the hours for the concentration of older people in those public spaces during September, October and November (2018 and 2019) on calm weather days. Three sample points were selected for environmental measurements in each public space, where equipment was located and fixed for 15 min (i.e., it remained stationary), whilst at the same time surveys were performed for people who were around those sample points. Figure 4 presents an example of the measurement process.

**Figure 4.** Measurement and survey at point 2 in CVH Street, Madrid.

The environmental variables including the relative humidity (RH), air temperature (Ta), wind speed (Ws) and sky view factor (SVF) were measured at 15-min intervals at each

point at 1.1 m above floor level corresponding to the centre of gravity of the human body as recommended in ISO 7726 [30]. Characterisation of the measurement equipment can be found in Table 1.

**Table 1.** Environmental measuring equipment specifications.

| Variable | Equipment | Measurement Range | Accuracy |
|---|---|---|---|
| Ta (°C) | Thermohydrometer data logger HOBO UX100 (HOBO, MA USA) | −20–70 °C | ±0.2 °C |
| RH (%) | | 1–95% | ±2.5% |
| Ws (m/s) | Anemometer Proster Digital MS6252a (Proster, Hong Kong) | 0.4–30 m/s | ±2% |
| SVF | Rayman 1.2 software | | |
| Tmrt (°C) | | | |

Ta = air temperature; RH = relative humidity; WS = wind speed; Tmrt = mean radiant temperature; SVF = sky view factor.

The mean radiant temperature (Trm) that represents the combination of air temperature and short- and long-wave radiation fluxes has been calculated using Rayman 1.2 software, in which environmental variables measured in situ, such as the air temperature, relative humidity and wind speed, in addition to the geographic data of the site, date and time, are entered. This method has been used by several authors [31–33]. Similarly, for the sky-view factor (SVF) fisheye lens (180°) pictures were taken during each measurement with a Sigma 8 mm circular lens in the north direction and then calculated in Rayman 1.2 software [31,33,34].

### *2.3. Thermal Perception Assessment and Sample Selection*

The sample was selected using simple random methods. Simultaneously with the urban environmental measurements, older people (who visually appeared to be older than 65 years of age) present (people who passed by and people who stayed) at each measured point in the assessed public spaces were asked about their willingness to answer the survey, which consisted of a two-part questionnaire.

The first part was related to personal demographics and behavioural characteristics (age, sex, level of clothing insulation, time and frequency of the visit). The second part was focused on their thermal perception through a seven-point scale of (−3. cold; −2. cool; −1. slightly cold; 0. neutral; 1. slightly warm; 2. warm; 3. hot) for thermal sensation (TSV) assessment [35] and the McIntyre three-point scale (1. warmer; 2. would not change; 3. colder) [36] for thermal preference (TP) assessment. For humidity and wind perception, a four-point scale was used (1. Very pleasant—4. Very unpleasant) [37].

### *2.4. Thermal Comfort Indices*

Whilst the UTCI index was computed using the official program version 0. 002 [20], the PET index was derived using Rayman. The features of a 'typical adult', as used in most research, were used in the PET standard calculation (a man, 35 years old, weight 75 kg, 1.75 m tall, 0.9 clo and 80 W). In this study, the data on the average older person in the UK and in Spain has included separating men from women, as well as the appropriate degree of activity (W) and clothing (clo) corresponding to each interviewed person.

### *2.5. Statistical Analysis*

All the collected data were processed in IBM SPSS statistics software and analysed with a significance of 5%. As the decision of which statistical test to use depends on the distribution of the data and the type of variable, a prior normality test (Kolmogoroy–Smirnov) was applied, if data were normally distributed, a parametric test such as a Pearson correlation was performed, otherwise, non-parametric tests were employed (Mann–Whitney, Kruskal–Wallis, Spearman correlation, chi-squared). The thermal sensation and thermal preference (qualitative/ordinal) were considered dependent variables for this

study, whilst environmental, personal and others were independent. Additionally, linear regression was applied between thermal-sensation vote and air temperature to identify the neutral temperature at which more older people felt comfortable.

## 3. Results and Discussion

### 3.1. Outdoor Environmental Conditions

Outdoor microclimatic conditions varied across both climates. Table 2 presents the environmental measurement data from autumn 2018 in Madrid and autumn 2019 in Newcastle. As regards the average air temperature, there is a difference of 4.8 °C, with Newcastle being colder. However, Madrid presented lower minimum and higher maximum temperatures, with a greater daily thermal amplitude, and the average radiant temperature was higher in Madrid, whilst relative humidity and wind speed were higher in Newcastle.

**Table 2.** Summary of environmental data measured in situ in public spaces in Madrid and Newcastle upon Tyne.

| City | Public Space | Ta °C | RH % | Ws m/s | Mrt °C | SVF |
|---|---|---|---|---|---|---|
| | | Mean | Mean | Mean | Mean | Mean |
| Madrid | PCVS | 20.9 | 38.3 | 1.5 | 35.0 | 0.04 |
| | CVH | 17.5 | 50.0 | 1.1 | 28.3 | 0.02 |
| | PTG | 19.4 | 50.5 | 1.2 | 30.5 | 0.03 |
| | Mean | 19.3 | 46.2 | 1.3 | 31.2 | 0.03 |
| Newcastle upon Tyne | OES | 13.3 | 60.8 | 1.6 | 22.7 | 0.01 |
| | NS | 15.9 | 54.7 | 1.9 | 20.3 | 0.02 |
| | Mean | 14.6 | 57.8 | 1.7 | 21.5 | 0.01 |

Ta = air temperature; RH = relative humidity; Ws = wind speed; Mrt = mean radiant temperature; SVF = sky view factor.

### 3.2. Sample Description

The sample size in both cases was similar, seventy people in Madrid and seventy-three in Newcastle upon Tyne.

In Madrid, 56% were women. Regarding the level of clothing insulation (clo), 60% corresponds to 1 clo and 34.3% to 1.5 clo, as this is considered normal for autumn (about 1 clo) [10]. The rest (5.7%) had worn around 0.5 clo, whilst in Newcastle, 47% were women, and 74% of the interviewees wore around 1 clo of clothing insulation.

No statistical relationship was found between gender or age and the level of clothing ($p > 0.05$) using the Kruskal–Wallis test. However, the older they were, the higher the level of clothing they wore, especially in the case of Madrid, with men wearing the most clothing. Figure 5 presents the sample distribution regarding gender, age and city.

### 3.3. Thermal Sensation of Older Adults in Outdoor Public Spaces

The thermal sensation of the people is a result of the extrinsic conditions of the place in addition to the subjective ones of the people. In this case, in Madrid, 63% of older people stated to have a 'neutral' thermal sensation, whilst 14.3% of the interviewees perceived it between 'slightly hot and hot', 22.8% between 'slightly cold and cold'. About 69% selected 'no change' as the thermal preference.

Regarding the humidity, 87% of the interviewees perceived this, whilst the perception of the wind speed was between 'pleasant' and 'very pleasant' for 83% of them.

In Newcastle, just 32% of older people had a 'neutral' thermal sensation whilst 31% of the interviewees perceived it as between 'slightly cool and cold' and just 10% between 'slightly hot and hot'.

Regarding preference, 42% preferred 'no change' and 31% would like it to be 'warmer'.

The humidity was perceived as between 'pleasant' and 'very pleasant' for 57% of older people, whilst the wind speed was pleasant for 53% of them.

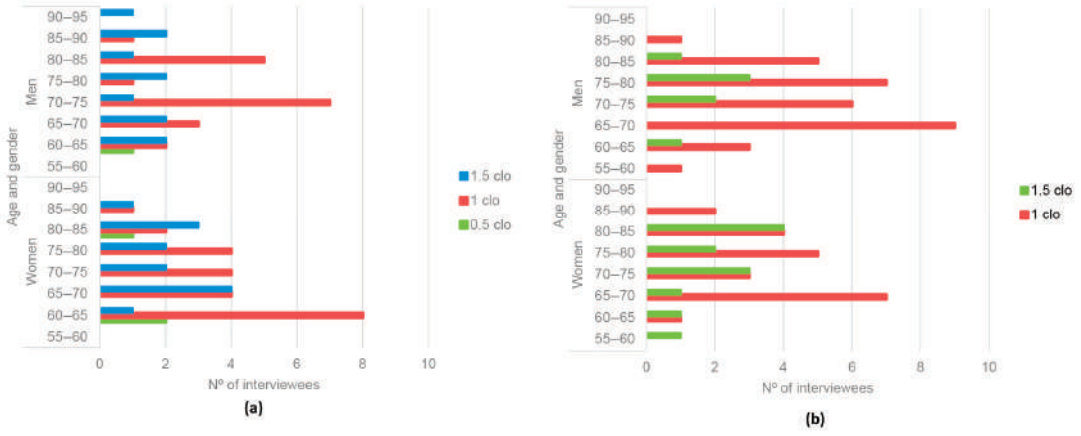


**Figure 5.** Sample characteristics. (**a**) Madrid; (**b**) Newcastle upon Tyne.

A chi-squared test was performed to identify the association between gender, thermal comfort and thermal preference for both cities, and results showed that there was no statistical relation. Figure 6 shows that thermal comfort votes were similar between both genders, even though in the case of Madrid a greater percentage of men felt colder, whilst in Newcastle men felt warmer than women. In the case of thermal preference, in both cities women were more dissatisfied with the thermal environment. In the case of Madrid, more women would have liked to be warmer and the same amount colder, whilst in Newcastle more women would have liked it to be warmer. These findings are in line with some studies that have found statistical differences between thermal comfort for men and women, where men were more satisfied with the thermal environment and women were more sensitive, especially in cooler conditions [38–40].

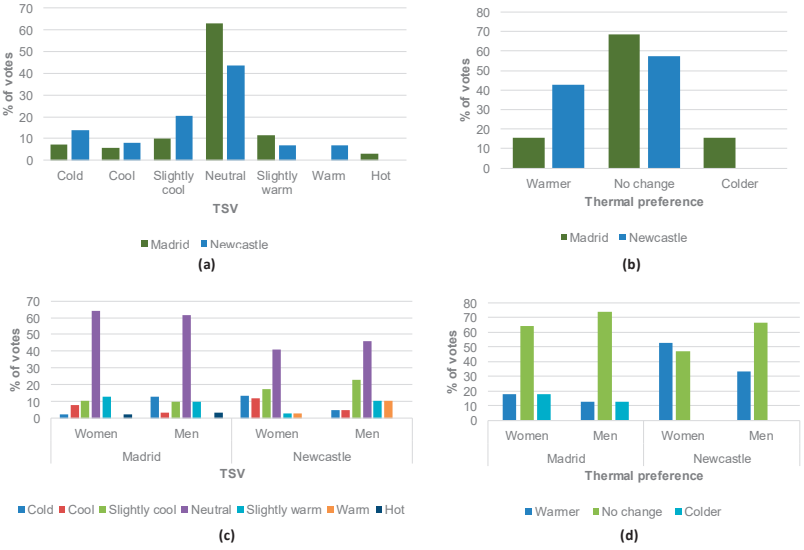


**Figure 6.** Thermal perception. (**a**) Thermal sensation (TSV) by city; (**b**) thermal preference by city; (**c**) thermal sensation by gender and city; (**d**) thermal preference by gender and city.

### *3.4. Influence of the Microclimate on Thermal Perception*

To identify statistical differences between the two case studies, the t-Student test for environmental variables, the Kruskal–Wallis test for the level of clothing (clo), age and visit time, and the chi-squared test for gender and thermal comfort (TSV = 0), were applied. A summary of these tests is presented in Table 3. Significant differences between all the environmental variables were measured except for the sky view factor. Additionally, there is a distinction between activity, time and frequency of visits. Regarding thermal perception and thermal sensation, those varied among both cities, but the thermal preference and thermal acceptability did not differ.

**Table 3.** Statistical differences between Madrid climate (Csa) and Newcastle upon Tyne climate (Cfb).

| | | **Statistical Test** | | |
|---|---|---|---|---|
| **Variable** | | **Chi-Squared** | **Kruskal-Wallis** | **Student's-t** |
| | | **Sig (Bilateral)** | **Sig (Bilateral)** | **Sig (Bilateral)** |
| Microclimatic | Ta (°C) | | | 0.000 ** |
| | HR (%) | | | 0.000 ** |
| | Ws (m/s) | | | 0.000 ** |
| | SVF | | | 0.080 |
| | Trm (°C) | | | 0.000 ** |
| Personal | clo | | 0.611 | |
| | Age | | 0.415 | |
| | Gender | 0.274 | | |
| | Visit time | | 0.001 ** | |
| | Activity | 0.000 ** | | |
| | Frequency of visit | 0.000 ** | | |
| Perception | Humidity perception | 0.239 | | |
| | Wind perception | 0.000 ** | | |
| | TSV | 0.023 * | | |
| | PT | 0.172 | | |
| Thermal index | UTCI 'Wellbeing' | 0.0246 * | | |
| | PET 'no thermal stress' | 0.007 ** | | |

Ta = air temperature; RH = relative humidity; Ws = wind speed; Mrt = mean radiant temperature; SVF = sky view factor. * The correlation is significant at level 0.05 (2 tails); ** The correlation is significant at level 0.01 (2 queues).

Although clothing insulation was not statistically different between both cities, it was higher in Madrid, and this could be attributed to the behavioural and adaptative cultural differences between both cities [25].

Additionally, the Pearson's correlation test was performed to identify the main environmental variables that influence thermal comfort for both cities (Table 4). In the case of Madrid, all the environmental variables were correlated to thermal comfort ($p \leq 0.00$) less than the SVF. Whist in the case of Newcastle, just the wind speed ($\leq$0.01) was related to thermal comfort, similar to other study findings [40]. Madrid presented a higher percentage of people in comfort (Figure 6) and the perception of ventilation was also more pleasant there.

**Table 4.** Correlation between thermal comfort and environmental variables for Madrid and Newcastle.

| Variable | Pearson Correlation | |
|---|---|---|
| | Madrid | Newcastle |
| | Coef. Correlation | |
| Ta (°C) | 0.14 ** | 0.128 |
| HR (%) | −0.13 ** | 0.177 |
| Ws (m/s) | 0.10 * | −0.252 * |
| SVF | −0.03 | −0.06 |
| Trm (°C) | 0.24 ** | 0.176 |

* The correlation is significant at level 0.05 (2 tails); ** the correlation is significant at level 0.01 (2 tails). Ta = air temperature; RH = relative humidity; SVF = sky view factor; Trmt = mean radiant temperature.

Older people there might be better adapted to the microclimatic conditions of their place of residence. Furthermore, in dense cities with heavy traffic and uneven distribution of green areas, there are differences in the microclimate between the public spaces that are worth considering (Table 2), with temperature differences of 3.4 °C, 11.7% in relative humidity and 0.4 m/s in wind conditions among the public spaces in Madrid. On the other hand, we found differences of 2.6 °C in temperature, 6.1% in relative humidity and 0.3 m/s in wind among the public spaces in Newcastle. This confirms the existence of differentiated microclimates in the city [9] which influence the thermal comfort for older people.

### *3.5. Neutral Temperature and Comfort Zone*

Linear regressions to represent older people's mean thermal sensation (MTSV) as a function of the mean air temperature (Ta) were obtained to identify the 'neutral temperature' (Tn) (MTSV = 0) and thermal sensitivity. The two regression equations passed the goodness-of-fit (R2 > 0.5). Both variables were different among both cities; in Madrid, the neutral temperature was 20.4 °C, whilst in Newcastle it was 17 °C; a difference of 3.4 °C between both climates. Figure 7 presents these equations for both climates. The slopes represent thermal sensitivity to temperature changes; it was found to be higher in Newcastle. This could be understood, as older people in Madrid were found to be more tolerant than in Newcastle and this could be attributed to their adaptative behaviour, thus people in Madrid wore higher levels of clothing insulation [25].

There are no outdoor thermal comfort studies for older people in Madrid and Newcastle to compare our results. As a reference from the literature review, this range would be between 23.9–28.1 °C for the average adult's outdoor thermal comfort in Madrid (Csa climate). Whilst no thermal comfort zone was found in previous studies for Newcastle or similar climates [41], as a reference, we considered Nikolopoulou and Lykoudis [42], who assessed outdoor thermal comfort for different climatic zones in Europe for the average adult. They found a great variation of 10°C for neutral temperature across Europe. In Cambridge and Sheffield (Cfb climate), it was found that neutral temperatures in autumn were 23.2 °C and 16.7 °C, respectively. The one found in Newcastle was similar to Sheffield's, whilst in Athens (Csa climate) it was 19.4 °C, one degree lower compared to our findings for Madrid.

The thermal comfort zone is defined by ASHRAE as the range of air temperature where at least 80% of the space occupants are satisfied with the thermal environment. Some authors suggest that comfort zones should be considered within the TSV interval of −1 and +1 [34,43–48]. By applying these values to the linear regression equations (Figure 7), the thermal comfort zone for Madrid in autumn would be between 9.8–31.1 °C, whilst in Newcastle it would be between 12.9–21 °C.

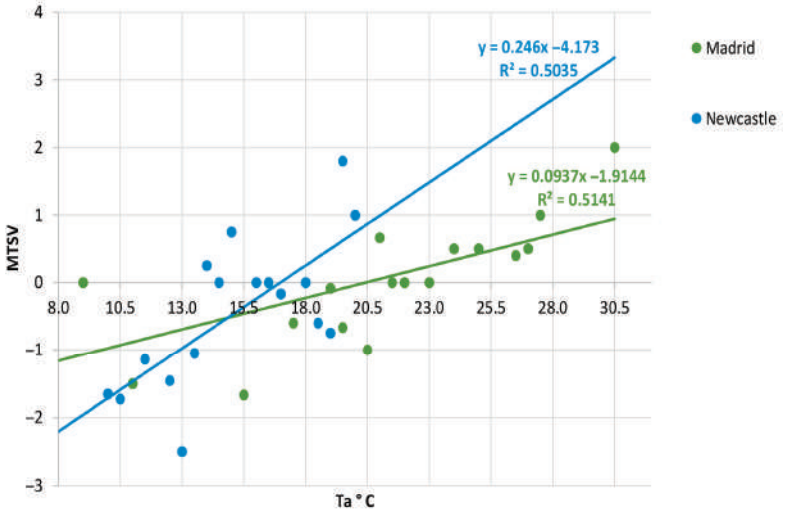


**Figure 7.** Linear regression air temperature vs. mean thermal sensation votes (MTSV) for Madrid and Newcastle.

The thermal comfort zone range was wider in Madrid. This could be explained because the thermal amplitude was greater during the experimental campaign in this city in autumn, with temperatures ranging from 8–31 °C. It would be necessary for people to adapt to these sudden changes in a few hours, which is even worse for the older population where adaptation is slower due to their metabolism and other physiological changes [5]. It is necessary to consider the differences between older adults in the perception of both cold and heat events during the autumn season that are becoming more usual with climate change [2], where it is necessary to know the comfort zone of these groups that are more vulnerable to both thermal extremes.

### *3.6. Thermal Comfort Indices (Physiological Equivalent Temperature) PET and Universal Thermal Index (UTC) vs. Thermal Sensation (TSV)*

According to the PET index, it was found that in Madrid, 32.9% of older people would be in thermal comfort and 21.4% would be in 'lightly warm, light heat stress', whilst in Newcastle, only 13.70% would be in thermal comfort and 86.3% would be between 'light cold stress' (34.25%), 'moderate cold stress' (31.5%) and 'strong cold stress' (20.55%).

Regarding UTCI, in Madrid, 75.7% of the older adults interviewed were within the wellness zone (9–26 °C) whilst 17.1% were within the 'moderate heat' zone (26–32 °C). In the case of Newcastle, 68.49% were within the wellness zone (9–26 °C) and 32.51% were within the 'light cold' zone where the physiological response would be the reduction of one degree of the temperature of the skin on the hands after 120 min of exposure [49].

Furthermore, the thermal sensation and thermal preference of older people interviewed were significantly correlated with the UTCI and PET indices ($p < 0.01$). In Madrid, 60.4% of people who were in 'well-being' according to the UTCI index had 'neutral' thermal sensations. Similarly, when analyzing the PET with the thermal sensation, it was found that the highest percentages of 'neutral' responses occurred within the 'comfort: no thermal stress' zone (65.2%).

In the case of Newcastle, it was found that the 'well-being' of the UTCI index corresponded to 84.4% of the 'neutral' responses, whilst regarding the PET index, the comfort zone corresponded to just 6.3% of the 'neutral' answers and 21.4% of 'no change' answers. It is important to note that the highest percentage of neutral TSV in older people would be within 'light stress due to cold' according to the PET index (Figure 8). Although most of them claimed to perceive the thermal environment as comfortable, they could be at risk

of thermal stress due to cold that could affect their health. This may be due to the loss of thermal sensitivity in both cities, especially in the case of Newcastle [37].

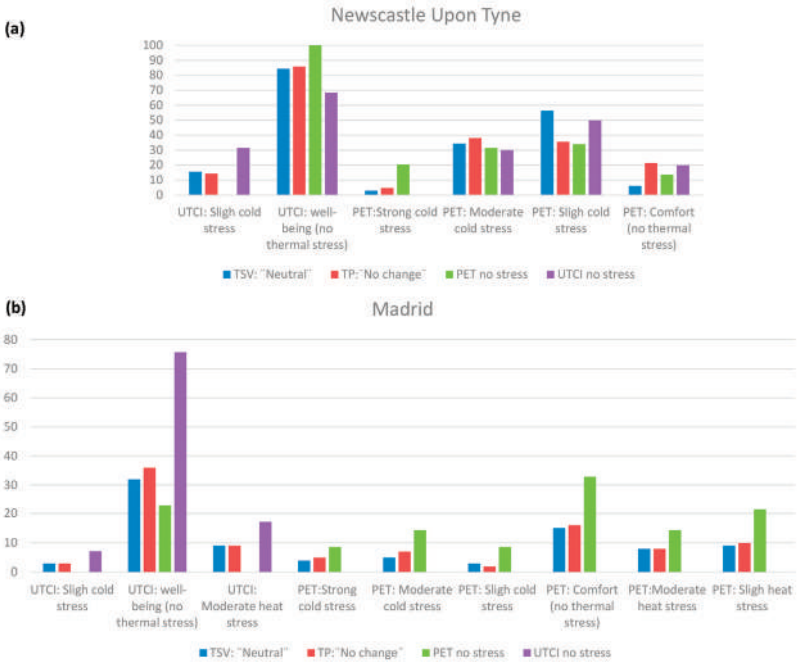


**Figure 8.** PET and UTCI and comparison with MTSV for (**a**) Newcastle upon Tyne and (**b**) Madrid.

The PET range for well-being (without thermal stress) was similar in both cities, being between 17.86–22.08 °C in Madrid and between 17.94–19.93 °C in Newcastle with a difference between $\pm 0.8 \pm 2.15$ °C. Just one previous study assessed the thermal comfort zone with the PET index in Madrid for the average adult in autumn [50], and it was found to be between 15.6–25.5 °C, whilst there is no evidence of similar studies for Newcastle. Figure 8 presents the PET and UTCI indices for each city and a comparison with TSV and TP.

## 4. Conclusions

The global trend of ageing populations and other challenges such as climate change that affect microclimate conditions for all the seasons led this research to analyse the outdoor thermal comfort of older adults in public spaces from two cities in Europe: Madrid in Spain and Newcastle upon Tyne in the United Kingdom, during autumn. As we have seen throughout this research, these are two very different cities in terms of size, density, climate, culture, etc.

The statistical influence of microclimatic variables on thermal comfort is evident in older people in both cities. Some differences in cultural behaviour and adaptation were identified. Older adults in Madrid wore higher levels of clothing insulation, were more tolerant and presented higher thermal comfort, and their thermal comfort range was wider due to the greater thermal amplitude (numerical difference between the minimum and maximum values observed during the day).

A difference of 3.4 °C was found in the neutral temperature between the cities; older people in Newcastle were shown to be more sensitive to climate changes.

In both cases, the risk of cold and heat stress was identified according to the PET index, although most of the older people perceived the environment as comfortable. The vulnerability of this population group to the effects of climate on their health is evident,

making further research on the subject necessary to establish mitigation and adaptation strategies for future extreme weather and climate change scenarios across Europe.

Additionally, some final considerations can be highlighted which are important for further research:

1. A dense city has significant microclimatic differences in the variables of temperature, relative humidity, and wind, which must be assessed at the pedestrian level to be able to establish the appropriate bioclimatic recommendations for healthier urban spaces.
2. Older people, the majority in most European cities, have intrinsic differences in their perception of both cold and heat. For this reason, both the definition of the comfort zone and the strategies must be qualified by considering age groups over 65 and over 80 years of age.
3. The final thermal comfort of a group must always combine external data with the real perception of the people in situ due to the wide number of variables that affect perception.

Therefore, considering that the European population is very old, it is necessary to establish spatial recommendations to improve the microclimatic conditions of public spaces, which should include sunny areas in winter and shaded areas in summer; green areas with deciduous trees and shrubs; areas protected from the winter wind thanks to walls, furniture or small windbreaks; and areas with fountains and clear paving. But at the same time, areas that are active but not noisy should be established. Older adults constitute a significant group in many urban neighbourhoods, which need to be considered so that they have spaces appropriate to their uniqueness and are not exposed to the risks of extreme heat or cold that they are not aware of, as has been reflected in this research.

Some limitations of this study are:

- Due to the small sample size, these results can only be taken as a reference.
- There was a wide climatic variability in both cities.
- The exposure time to microclimate conditions was not considered for the acclimatisation of older people. Future research should consider this to obtain more accurate results and to avoid biases, as some authors has suggested.

However, these results could be a starting point for the design of more comfortable and healthy public spaces that improve the quality of life of all citizens within the guidelines of active ageing and healthy cities.

**Author Contributions:** Conceptualisation, M.T.B.L. and E.H.G.; methodology, M.T.B.L.; software, M.T.B.L.; validation, M.T.B.L.; formal analysis, M.T.B.L.; investigation, M.T.B.L. and E.H.G.; resources, M.T.B.L.; data curation, M.T.B.L.; writing—original draft preparation, M.T.B.L.; writing—review and editing, M.T.B.L. and E.H.G.; visualisation, M.T.B.L.; supervision, E.H.G.; project administration, M.T.B.L.; funding acquisition, M.T.B.L. All authors have read and agreed to the published version of the manuscript.

**Funding:** This work was supported by *Secretaría de Educación Superior, Ciencia, Tecnología e Innovación del Ecuador*. SENESCYT under Grant [109-2017 (SENESCYT-SDFC-DSEFC-2017-4040-O)].

**Data Availability Statement:** The data presented in this study are available on request from the corresponding author. The data are not publicly available due to [privacy].

**Conflicts of Interest:** The authors declare no conflict of interest.

## References

1. IPCC. *Climate Change 2014*; Synthesis Report; Cambridge University Press: Cambridge, UK, 2014. [CrossRef]
2. Wang, J.; Guan, Y.; Wu, L.; Guan, X.; Cai, W.; Huang, J.; Dong, W.; Zhang, B. Changing Lengths of the Four Seasons by Global Warming. *Geophys. Res. Lett.* **2021**, *48*, e2020GL091753. [CrossRef]
3. Organización Iberoamericana de Seguridad Social. Boletín del Programa Iberoamericano de Cooperación Sobre Adultos Mayores. 2016. Available online: https://oiss.org/boletin-no-10-del-programa/ (accessed on 1 September 2022).
4. Comission on Social Determinants of Health. Closing the Gap in a Generation: Health Equity through Action on the Social Determinants of Health. Final Report of the Commission on Social Determinants of Health, Geneva. 2008. Available online: http://www.who.int/social_determinants/final_report/csdh_finalreport_2008.pdf (accessed on 1 September 2022).

5. Baquero Larriva, M.T.; Higueras García, E. Thermal comfort for the elderly: A systematic review of the scientific literature. *Rev. Esp. Geriatr. Gerontol.* **2019**, *54*, 280–295. [CrossRef]
6. Novieto, D.; Zhang, Y. Thermal comfort implications of the aging effect on metabolism, cardiac output and body weight. *Adapt. Chang. New Think. Comf.* **2010**, 1–9. Available online: https://acortar.link/UQQr7C (accessed on 1 September 2022).
7. Fariña, J.; Higueras, E.; Román, E. *Ciudad, Urbanismo y Salud. Criterios Generales de Diseño Urbano para Alcanzar los Objetivos de una Ciudad Saludable*; Envejecimiento Activo, Instituto Juan de Herrera: Madrid, España, 2019.
8. Erell, E.; Pearlmutter, D.; Williamson, T. *Urban Microclimate: Designing the Spaces between Buildings*, 1st ed.; Routledge: London, UK, 2011. [CrossRef]
9. Higueras, E. Urbanismo Bioclimático, GG, Barcelona. 2006. Available online: https://editorialgg.com/urbanismo-bioclimatico-libro.html (accessed on 1 September 2022).
10. Neila, J. *Arquitectura Bioclimática en un Entorno Construido*; Munilla-Lería: Madrid, Spain, 2004; ISBN 84-89150-64-8.
11. Kalmár, F. An indoor environment evaluation by gender and age using an advanced personalized ventilation system. *Build. Serv. Eng. Res. Technol.* **2017**, *38*, 505–521. [CrossRef]
12. Havenith, G.; Holmér, I.; Parsons, K. Personal factors in thermal comfort assessment: Clothing properties and metabolic heat production. *Energy Build.* **2002**, *34*, 581–591. [CrossRef]
13. Aghamolaei, R.; Lak, A. Outdoor Thermal Comfort for Active Ageing in Urban Open Spaces: Reviewing the Concepts and Parameters. *Ageing Int.* **2022**, 1–14. [CrossRef]
14. Oke, T.R. Street Design and Urban Canopy Layer Climate. *Energy Build.* **1988**, *11*, 103–113. [CrossRef]
15. Fernández, F.J.; Allende, F.; Rasilia, D.; Martilli, A. *Alcaide, Estudio de Detalle del Clima Urbano de Madrid*; Departamento de Geografía, Universidad Autónoma de Madrid: Madrid, Spain, 2016. Available online: https://acortar.link/tgKL6C (accessed on 1 September 2022).
16. Gagge, A.; Fobelets, A.; Berglund, L. A standar predictive index of human response of thermal environment. *ASHRAE Trans.* **1986**, *92*, 709–731.
17. Spagnolo, J.; de Dear, R. A field study of thermal comfort in outdoor and semi-outdoor environments in subtropical Sydney Australia. *Build. Environ.* **2003**, *38*, 721–738. [CrossRef]
18. Blazejczyk, K.; Epstein, Y.; Jendritzky, G.; Staiger, H.; Tinz, B. Comparison of UTCI to selected thermal indices. *Int. J. Biometeorol.* **2012**, *56*, 515–535. [CrossRef]
19. Mayer, H.; Höppe, P. Thermal comfort of man in different urban environments. *Theor. Appl. Climatol.* **1987**, *38*, 43–49. [CrossRef]
20. Innternational Sciety of Biometeorology. UTCI Universal Thermal Climate Index. 2004. Available online: http://www.utci.org/ (accessed on 12 July 2019).
21. Potchter, O.; Cohen, P.; Lin, T.; Matzarakis, A. Outdoor human thermal perception in various climates: A comprehensive review of approaches, methods and quantification. *Sci. Total Environ.* **2018**, *631–632*, 390–406. [CrossRef]
22. Manu, S.; Shukla, Y.; Rawal, R.; Thomas, L.; de Dear, R. Field studies of thermal comfort across multiple climate zones for the subcontinent: India Model for Adaptive Comfort (IMAC). *Build. Environ.* **2016**, *98*, 55–70. [CrossRef]
23. Frontczak, M.; Wargocki, P. Literature survey on how different factors influence human comfort in indoor environments. *Build. Environ.* **2011**, *46*, 922–937. [CrossRef]
24. Yang, W.; Wong, N.; Jusuf, S. Thermal comfort in outdoor urban spaces in Singapore. *Build. Environ.* **2013**, *2*, 426–435. [CrossRef]
25. Knez, I.; Thorsson, S. Thermal, emotional and perceptual evaluations of a park: Cross-cultural and environmental attitude comparisons. *Build. Environ.* **2008**, *43*, 1483–1490. [CrossRef]
26. Fong, C.; Aghamohammadi, N.; Ramakreshnan, L.; Sulaiman, N.; Mohammadi, P. Holistic recommendations for future outdoor thermal comfort assessment in tropical Southeast Asia: A critical appraisal. *Sustain. Cities Soc.* **2019**, *46*, 101428. [CrossRef]
27. Departamento de Producción de la Agencia Estatal de Meteorología de España y Departamento de Meteorología e Clima de Portugal, Atlas Climático Ibérico. Temperatura del Aire y Precipitación (1971–2000), Closas-Orc. 2011. Available online: http://www.aemet.es/documentos/es/conocermas/publicaciones/Atlas-climatologico/Atlas.pdf (accessed on 2 June 2020).
28. AEMET. Temperaturas Medias y su Comparación con las de los Últimos 30 Años. (Observatorio de Retiro), Banco Datos. Ayunt. Madrid Territ. y Medio Ambient. 2019. Available online: http://www-2.munimadrid.es/CSE6/control/seleccionDatos?numSerie=14020000020 (accessed on 22 March 2019).
29. Time and Date, Climate & Weather Averages in Newcastle upon Tyne, England, United Kingdom. Annual Weather Avergages Near Newcastle upon Tyne. 2015. Available online: https://www.timeanddate.com/weather/uk/newcastle-upon-tyne/climate (accessed on 29 June 2020).
30. International Standard Organization. *ISO 7726: Ergonomics of the Thermal Environment. Instruments and Methods for Measuring Physical Quantities*; International Standard Organization: Geneva, Switzerland, 1998.
31. Andrade, H.; Alcoforado, M. Microclimatic variation of thermal comfort in a district of Lisbon (Telheiras) at night. *Theor. Appl. Climatol.* **2008**, *92*, 225–237. [CrossRef]
32. Hwang, R.; Lin, T.; Matzarakis, A. Seasonal effects of urban street shading on long-term outdoor thermal comfort. *Build. Environ.* **2011**, *46*, 863–870. [CrossRef]
33. Martinelli, L.; Lin, T.; Matzarakis, A. Assessment of the influence of daily shadings pattern on human thermal comfort and attendance in Rome during summer period. *Build. Environ.* **2015**, *92*, 30–38. [CrossRef]

34. Hwang, R.; Chen, C. Field study on behaviors and adaptation of elderly people and their thermal comfort requirements in residential environments. *Indoor Air* **2010**, *20*, 235–245. [CrossRef]
35. ASHRAE. STANDARD 55—Thermal Enviornmental Conditions for Human Occupancy. 2020. Available online: https://www.ashrae.org/technical-resources/bookstore/standard-55-thermal-environmental-conditions-for-human-occupancy (accessed on 1 December 2017).
36. Mclntyre, D. A Guide to Thermal Comfort. *Appl. Ergon.* **1973**, *4*, 66–72. [CrossRef] [PubMed]
37. Larriva, M.B.; Higueras, E. Health risk for older adults in Madrid, by outdoor thermal and acoustic comfort. *Urban Clim.* **2020**, *34*, 100724. [CrossRef]
38. Karjalainen, S. Thermal comfort and gender: A literature review. *Indoor Air* **2012**, *22*, 96–109. [CrossRef] [PubMed]
39. Indraganti, M.; Rao, K. Effect of age, gender, economic group and tenure on thermal comfort: A field study in residential buildings in hot and dry climate with seasonal variations. *Energy Build.* **2010**, *42*, 273–281. [CrossRef]
40. Yao, F.; Fang, H.; Han, J.; Zhang, Y. Study on the outdoor thermal comfort evaluation of the elderly in the Tibetan plateau. *Sustain. Cities Soc.* **2022**, *77*, 103582. [CrossRef]
41. Larriva, M.B. Confort Térmico y Acústico para la Tercera edad en Espacios Públicos de la Ciudad Consolidada del Clima Mediterráneo Continental: Caso de Estudio Barrio Arapiles. Ph.D. Thesis, Universidad Politécnica de Madrid, Madrid, Spain, 2021. [CrossRef]
42. Nikolopoulou, M.; Lykoudis, S. Thermal comfort in outdoor urban spaces: Analysis across different European countries. *Build. Environ.* **2006**, *41*, 1455–1470. [CrossRef]
43. Wong, L.; Fong, K.; Mui, K.; Wong, W.; Lee, L. A field survey of the expected desirable thermal environment for older people. *Indoor Built Environ.* **2009**, *18*, 336–345. [CrossRef]
44. Bills, R.; Soebarto, V.; Williamson, T. Thermal experiences of older people during hot conditions in Adelaide. In Proceedings of the Revisiting the Role of Architectural Science in Design and Practice: 50th International Conference of the Architectural Science Association, Adelaide, Australia, 7–9 December 2016; pp. 657–664.
45. Fan, G.; Xie, J.; Yoshino, H.; Yanagi, U.; Hasegawa, K. Investigation of indoor thermal environment in the homes with elderly people during heating season in Beijing, China. *Build. Environ.* **2017**, *126*, 288–303. [CrossRef]
46. Ji, X.; Lou, W.; Dai, Z.; Wang, B.; Liu, S. Predicting thermal comfort in Shanghai's non-air-conditioned buildings. *Build. Res. Inf.* **2006**, *34*, 507–514. [CrossRef]
47. *ASHRAE Standar 55-1966*; Thermal Comfort Conditions. ASHRAE: Atlanta, GA, USA, 1966.
48. Feriadi, H.; Wong, N.; Chandra, S.; Cheong, K. Adaptive behaviour and thermal comfort in Singapore's naturally ventilated housing. *Build. Res. Inf.* **2010**, *31*, 37–41. [CrossRef]
49. Błazejczyk, K.; Broede, P.; Fiala, D.; Havenith, G.; Holmér, I.; Jendritzky, G.; Kampmann, B.; Kunert, A. Principles of the new Universal Thermal Climate Index (UTCI) and its application to bioclimatic research in European scale. *Misc. Geogr.* **2010**, *14*, 91–102. [CrossRef]
50. García, F.F.; Galán, E.; Cañada, R. Caracterización del régimen bioclimático medio del área metropolitana de Madrid, mediante la aplicación de la temperatura fisiológica (PET). *Territoris* **2012**, *8*, 83–101. Available online: https://raco.cat/index.php/Territoris/article/view/259755. (accessed on 5 February 2021).

*designs*

MDPI

*Article*

# Simulation and Analysis of Thermal Insulators Applied to Post-Disaster Temporary Shelters in Tropical Countries

**Bruno B. F. da Costa [1,*], Caio F. P. Silva [2], Ana Carolina F. Maciel [2], Herson D. P. Cusi [3], Gladys Maquera [3] and Assed N. Haddad [1,*]**

[1] Universidade Federal do Rio de Janeiro, Rio de Janeiro 21941-901, Brazil
[2] Universidade Federal de Uberlândia, Uberlândia 38400-902, Brazil; caio.civil.ufu@gmail.com (C.F.P.S.); anamaciel@ufu.br (A.C.F.M.)
[3] Universidad Peruana Unión, Juliaca 21100, Peru; hparic@upeu.edu.pe (H.D.P.C.); gladys.maquera@upeu.edu.pe (G.M.)
* Correspondence: bruno.barzellay@macae.ufrj.br (B.B.F.d.C); assed@poli.ufrj.br (A.N.H)

**Abstract:** Containers are fundamental elements for the development of international trade; however, it is estimated that there are more than 17 million retired containers stacked in ports around the world. Considering the high costs involved in the process of storing, transporting, or destroying these materials, in addition to their non-degradable nature, it is urgent to develop strategies for the sustainable use of these decommissioned containers. In this context, repurposing these containers into permanent structures is becoming a predominant trend. One solution is converting steel shipping structures into habitable spaces. However, due to the urgency with which Container Houses (CHs) are demanded in case of disasters, they are usually planned to be built as quickly as possible, serving as many people as possible, and do not consider the basic principles of energy efficiency. The performance of the CHs is, then, impaired, including risks of overheating, corrosion, and rust, among others, during service, making them an even more stressful experience for their users who are already in a vulnerable situation. Therefore, the objective of this study is to compare the performance of two thermal insulators applied to a temporary shelter container designed to promptly serve vulnerable populations. The model was developed in Building Information Modeling (BIM) software and simulated in Building Energy Simulation (BES) software, aiming to obtain subsidies for its technical and economic viability analysis. The results indicated that thermal insulators are able to generate significant savings in energy consumption, with mineral wool presenting better long-term performance.

**Keywords:** thermal analysis; BIM; BES; temporary shelter; container housing; computational simulation; thermal insulators

**Citation:** da Costa, B.B.F.; Silva, C.F.P.; Maciel, A.C.F.; Cusi, H.D.P.; Maquera, G.; Haddad, A.N. Simulation and Analysis of Thermal Insulators Applied to Post-Disaster Temporary Shelters in Tropical Countries. *Designs* **2023**, *7*, 64. https://doi.org/10.3390/designs7030064

Academic Editor: Farshid Aram

Received: 28 March 2023
Revised: 17 April 2023
Accepted: 24 April 2023
Published: 9 May 2023



## 1. Introduction

Every year, a surprising amount of people are forced to leave their homes in search of shelter and protection due to natural disasters. According to the Norwegian Refugee Council [1], in the year 2021 alone, 23.7 million people were affected by all kinds of geophysical and climatic catastrophes, such as earthquakes, volcanic eruptions, landslides, storms, floods, wildfires, droughts, and extreme temperature events. However, contrary to the unpredictable nature of climatic events, there is a constant increase in the occurrence of armed conflicts, political persecution, and other types of violence around the world, causing a significant rise in the number of people who move to preserve their lives [2]. Last year alone, 14.4 million people were displaced due to violence, the highest number over the past ten years. Thus, in 2021, adding natural and anthropogenic causes, 38 million refugees were accounted for, in 141 countries, with an estimated financial cost of around 21 billion dollars [1].

Indeed, the economic impact of this exodus is relevant, but the social and humanitarian damage is inestimable. Refugees are often forced to move with minimal resources, depending on all sorts of emergency aid, especially food, medicine, and shelter [2]. They are entire families who have no choice but to leave their cities, their jobs, and their lives. In this context, considering that the majority of those affected reside in underdeveloped countries where resources are already scarce, the situation becomes even more critical. According to [1], 74.7% of all displacements throughout 2021 were concentrated in Sub-Saharan Africa and the East Asia and Pacific regions, followed by South Asia. In these areas alone, there are over 34 million homeless people. Therefore, providing temporary shelter is a priority [3,4].

However, due to the urgency with which they are demanded, these shelters are usually provided in a rudimentary way with people being allocated to any available covered area, such as sports facilities, churches, or hangars. These places, in addition to not offering adequate basic infrastructure, steal the privacy of families who are compelled to sleep, store their belongings, clean themselves, and live with unknown people. In turn, in cases where international humanitarian aid is provided and where victims are taken to relief camps, the most used shelter structures are tents. This is an interesting and worthy option since families often own a private space. On the other hand, this type of structure, despite offering the minimum necessary protection, lacks comfort, and appears to be a campsite not a building. As a result, the feeling of protection against adverse thermal effects, strong winds, and suffocating dust, among others, is impaired. In this context, the use of shipping containers as temporary post-disaster shelters has drawn the attention of specialists in recent years [2,4–6].

Shipping containers compose the core of the world's cargo transportation system [7]. However, the rapid dissemination of this type of structure has always presented challenges regarding the sustainability of the logistic model used [8]. This is mainly because the lifecycle of containers is generally not constrained by their effective lifespan but rather by logistical constraints.

The beginning of the export process occurs when the container is put into operation when it is sent empty to the exporter (Figure 1). The cargo is then accommodated and the container is transported to the port of origin. After the maritime transit stage, the container is unloaded at the port of destination and forwarded to the importer's warehouse. After the completion of unloading, the empty container is transported back to the port terminal. At this point, the operator faces a dilemma. Upon arriving empty at the port, the container is stored awaiting return freight or round trip. The purpose of the last one is to use the containers disembarking at the port of destination for the export of other cargo after delivery to the final customer so that the containers do not return empty to the port of origin. Nevertheless, in recent years, there has been a significant slowdown in the flow of maritime transport [9] so making round trips is no longer so trivial. In this case, if it is impossible to reuse the container in a round trip, it must be returned empty to the port of origin. Yet, since the cost of retrieving empty containers back to their origin is almost as costly as moving a fully loaded container [7], it is too expensive and manufacturing new containers is considered more economical [10].

This strategic decision has contributed to the increase in the number of unused containers stored in seaports [11], causing problems associated with the allocation of space and requiring a great effort for their reallocation [9]. Currently, it is estimated that there are tens of millions of retired containers in ports around the world [8,12]. On the other hand, manufacturing new units does not eliminate the need to end the life cycle of out-of-service containers and, in this context, there are basically two options available. The first and most obvious is recycling, given the non-degradable nature of steel [11,12]. However, melting and remanufacturing the standard 3.63 ton container requires 8000 kWh of electrical energy [13–15], so this is not the most sustainable option. Thus, the second and most recent option has been the attempt to find new market niches in which these elements can be reused. Container housing is one of the most promising [9].

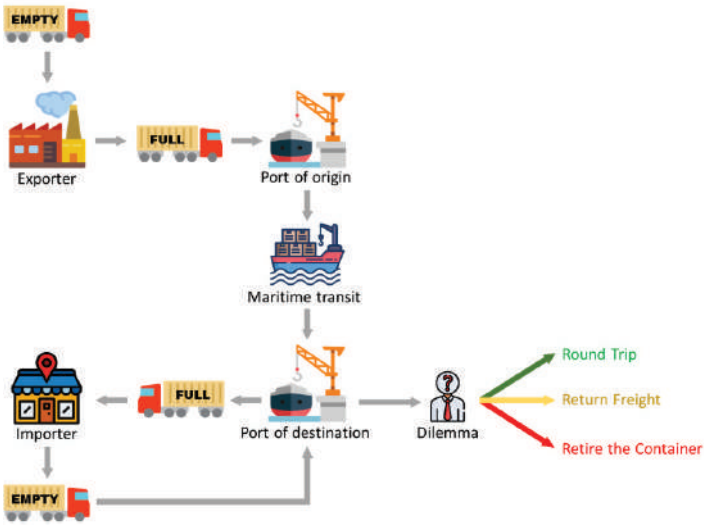


**Figure 1.** Export and import flow of goods using containers.

Shipping container buildings benefit from the intrinsic characteristics of modular construction [12] being economical and fast to build [16]. Furthermore, as they are made of corten steel alloy or weathered steel, the containers are highly resistant and durable, once they are designed to withstand many years in the salt air and spray on the ocean [17]. Nevertheless, regarding Container Houses (CH) for temporary shelters, portability is the most important feature of this system. In other words, the ease and speed with which they can be transported to the places where they are needed [6], providing immediate assistance to the victims. However, although the use of containers as buildings is not a recent concept, there is a gap in the technical literature available on the subject, especially concerning to their use as temporary shelters [14,16].

In fact, the technique has already been used successfully in countries, such as Korea, Japan, China, and Turkey to build relief camps for refugees and displaced populations [13]. Nonetheless, due to the urgency with which CHs are demanded in case of disasters, they are usually planned to be built as quickly as possible, serving as many people as possible, and not considering basic principles of comfort and sustainability [2]. The performance of the CHs is then impaired, including risks of overheating, corrosion, and rust, among others, during service, making them an even more stressful experience for their users who are already in a vulnerable situation.

Therefore, the objective of this study is the development of a novel standard Sustainable Container Housing (SCH) project, designed to promptly serve vulnerable populations with a focus on the analysis through computer simulation of the technical and economic viability of using two thermal insulators. The model will be developed in BIM software (Building Information Modeling) in order to allow the realization of thermo energetic simulation of the same, and the efficient survey of its cost, aiming to obtain subsidies for its technical and financial viability. It is proposed to obtain a versatile, cheap, and durable model, so that vulnerable populations can be promptly assisted in housing that, although temporary, allows them to live with dignity and comfort.

## 2. Theoretical Background

### *2.1. Modular Construction*

Modular construction has become a trend in the last two decades [5,11], and the technologies associated with its application have evolved significantly in the construction industry [13]. Also known as volumetric construction, modular building system, or mod-

ular architecture [3,18], there is still no formal definition for the terminology. However, the analysis of recent studies indicates the evolution and convergence of meanings for the term. Chatzimichailidou and Ma [19] define modular construction as a process where the units are built off site and, then, transported and assembled on-site. This concept is congruent with Lacey et al. [20] and Musa et al. [18] which complement it, indicating that this is a technique applicable to volumetric units which generally constitute the building's structural element. Ye et al. [21], Rakotonjanahary et al. [22], and Hong [3] go forward describing the components that compose the modular unit and that must be integrated in order to allow the transport of a complete module to the building installation site, that is, wall solutions, ceiling, frames, electrical and hydraulic installations, HVAC, and fixed furniture. Finally, Musa et al. [18] highlight the need to consider the logistical aspects as part of the modular construction process, as the use of the method only brings the expected results if executed in accordance with rigorous planning.

In this context, the increasing interest in the subject has generated an intense registration of the advantages of modular construction in the literature. Koke et al. [12] indicate that, when compared to the traditional construction method, modularization has a smaller environmental footprint. The information is confirmed by Cao et al. [23] who conclude that a traditional residential building consumes approximately 20% more energy and 36% more natural resources during construction. Bertolini and Guardigli [7] present positive environmental results regarding the use of modular elements in the construction industry through Life Cycle Analysis (LCA).

However, currently, the main benefits related to the use of modularization concern the greater productivity made possible by the system [11,24]. According to Jeong et al. [25], about 70% of the construction work for a modular unit is conducted off site, so little work is conducted during on-site assembly. As a result, most of the construction process can be carried out using the production line model, similar to that of the automobile industry, with well-defined workstations and less need for workers to move around the factory floor. This peculiarity, in addition to significantly reducing occupational risks [26], allows for optimizing internal finishing work and even facades, decreasing the construction schedule [20,21] as they are carried out in an industrial environment and not on the construction site which is subject to various adversities [22]. In addition, the use of specialized labor in a controlled environment favors a higher quality product delivery [18,21] and less waste generation [13,20].

Despite arousing great interest and the advantages of its use, the diffusion of modular construction has faced barriers [18]. Perhaps the most relevant is the difficulty in meeting the necessary technical criteria to guarantee user comfort and energy efficiency throughout its lifespan [12]. This is because the scope of modular construction is very broad, allowing the application of a wide variety of materials and construction techniques and making it difficult to develop comprehensive technical guides [20]. Among the various existing possibilities, the container house has stood out [11].

### *2.2. Shipping Containers*

Shipping containers are essentially large steel boxes that are used to transport cargo [27]. This element was idealized by Malcom McLean in the 1930s with the aim of rationalizing the transport of goods when he was still working as a driver of small trucks at the Port of Hoboken, in New Jersey, USA [6]. In 1958, Malcom patented containers as an "Apparatus for shipping freight" [28]. However, the product was intended to be a universal cargo transport solution [2]. After the patent registration, the possibility of transporting goods through standardized structures without the need for constant loading and unloading [6] caught the attention of the U.S. Military. The widespread use of this solution by the military influenced its acceptance by most shipping companies [28]. In this context, following the evolution of international trade, container production has expanded rapidly in recent decades [27], reaching unsustainable standards as shown in the Introduction section of this paper.

Containers use as buildings emerged as a way to reuse these structures and it is not being a new concept because only in the last twenty years has this constructive method achieved greater development [15,29]. This delay is due, at least in part, to the constant erroneous association of this kind of building with trailer houses, normally considered by the general population as unattractive and uncomfortable [18]. Currently, this solution is becoming a trend for several applications, such as hotels, healthcare facilities, low-income housing, and post-disaster settlements [11–13].

The shipping containers currently used in building construction can be divided into two main groups, the 20-ft container, with a length of 6.096 m, and the 40-ft container, with a length of 12.192 m [2,14], and both with a width of 2.438 m [28]. For architectural purposes, these containers offer a limited height, that is, 2.591 m of external height [11] which results in an internal ceiling height of just 2.385 m [28]. Although the International Residential Code (IRC) allows a ceiling height of 2.134 m [30], most national building codes require a minimum ceiling height of 2.40 m [10,11,15]. Therefore, a special subcategory of containers is more favorable, despite not being available on the market in the same quantity as the previous ones. High Cube (HC) containers have the same width and length as 20-ft and 40-ft containers but have an external height of 2.896 m, resulting in a minimum internal height of 2.655 m, attending to the national regulations requirements [9]. Table 1 presents the dimensions of the above described containers.

**Table 1.** Geometric characteristics of the most popular containers.

| Model | External Dimensions | | | Minimal Internal Dimensions | | | |
|---|---|---|---|---|---|---|---|
| | Length (m) | Width (m) | High (m) | Length (m) | Width (m) | High (m) | Floor Area ($m^2$) |
| 20-ft container | 6.096 | 2.438 | 2.591 | 5.710 | 2.352 | 2.385 | 13.430 |
| 40-ft container | 12.192 | 2.438 | 2.591 | 11.998 | 2.352 | 2.385 | 28.219 |
| 20-ft HC container | 6.096 | 2.438 | 2.896 | 5.710 | 2.352 | 2.655 | 13.430 |
| 40-ft HC container | 12.192 | 2.438 | 2.896 | 11.998 | 2.352 | 2.655 | 28.219 |

The shipping container standardization is a great advantage in terms of modularity, as it offers versatility in assembly options [10,11], besides facilitating the lifting, transport, and connection operations [14]. Considering a building as an articulation of properly combined spaces to meet the user needs [9], containers make it possible to arrange two or more elements in countless ways. Or even, the application of a single container holding all the infrastructure necessary for the user, which is the adopted approach in this study.

Although there are several container typologies, they must all be manufactured in accordance with the standards set by the International Organization for Standardization (ISO) and the International Convention for Safe Containers (CSC) [11,14]. Among the standards of greatest interest are ISO 668 [31], ISO 830 [32], ISO 6346 [33], ISO 1496-1 [34], ISO 1161 [35], ISO 2308 [36], and ISO 3874 [37] and also the guide provided by CSC [38]. These guidelines present the necessary specifications to ensure the uniformity of the geometric and mechanical properties of the containers for transportation purposes [9], but currently, there are no standards, guidelines, or codes for the use of containers as building materials [11]. Therefore, it is essential to know the main characteristics of these elements, so that the design and construction of the container house reach the required quality standard for use as a building.

The manufacturing process of shipping containers, following the modularization trend, is simple. This element consists of intrinsically structural components, such as corner posts, floor, and closure elements, such as walls, doors, and roofs. Once completed, they all become an integral part of the container's structural system. Initially, the walls are cut, corrugated, and welded together and then welded to the container floor. This is made up of a mesh of metal beams that will later be covered with a wooden floor [27]. The next step is to install the doors and corner posts which are welded to the walls and floor. Finally, the

roof is welded, completing the container's shell [27] and giving the element a high load capacity [2,9].

In addition to the great structural support, another characteristic that differentiates shipping containers as building materials is their durability [13]. This kind of container is designed to withstand extreme weather conditions during service, that is, they are elements that spend most of their life exposed to rain, wind, and sea air [2,9,28]. For this reason, they are built in Corten steel or weathering steel, a steel resistant to atmospheric corrosion which includes alloying elements that affect the corrosion process of materials and protect the steel integrity [27,28]. Corten steel has a weather resistance of four to eight times greater than ordinary steel, in addition to good weldability and workability [27]. In this context, this material promotes a great reduction in maintenance costs when applied in buildings, since these are generally located in less aggressive environments.

### *2.3. Shipping Containers for Post-Disaster Reconstruction*

The flexibility of modular construction and the benefits of using shipping containers as buildings, the so-called container architecture, have contributed to the development of the technique for various applications [11], including coffee shops, fast food kiosks, sales stands, public restrooms, hotels, residential buildings, field hospitals, information centers, leisure spaces, military barracks, scientific research laboratories, and educational buildings, among others. However, one of the most relevant applications of this technology is its use as post-disaster housing, due to its quick and easy installation [5]. More specifically, as a temporary shelter where victims are allocated before being moved to new homes [2]. In this sense, some studies have recently addressed the topic, especially in countries with a high occurrence of climate catastrophes and armed conflicts. Nevertheless, the literature is still limited.

Zafra et al. [39] applied Building Energy Modeling (BEM) to conduct a thermal performance assessment of container shelters in the Philippines. Two design models were created and simulated by changing the insulation material using the EnergyPlus engine. The authors concluded that, regardless of the design, the use of insulating materials is essential to obtain thermal comfort in containers in tropical climates. Obia [40] conducted several architectural and structural changes in temporary container shelters and concluded that all modifications were well accepted by respondents, confirming the technology's flexibility. Shen et al. [11] analyzed the effectiveness of climate-adaptive design for container buildings in three different climate zones, Stockholm, Berlin, and Rome. The results indicated that the integration of passive strategies and renewable technologies was the method that obtained the best results. Ling et al. [2] carried out a review of the feasibility of using containers as transitional shelters. The literature analysis indicated that the use of containers for this purpose has great potential, mainly due to its economic and operational advantages. However, the authors highlighted some system weaknesses that must be quickly mitigated, such as the lack of design guidelines and community acceptance. In fact, the analysis of this last topic was precisely the objective of the Wong et al.'s [41] research which sought to assess the level of acceptance of Malaysian citizens in relation to containerized houses. The used methodology was a questionnaire applied to 454 respondents. The results indicated that only 45% of the participants would consider living in a container house but that its use as a commercial establishment already has great approval.

The research of Tan and Ling [14] aimed to understand the current status of the technical aspect of the container for shelter provision. The authors found that this kind of building meets several technical criteria necessary for its use as a building, such as minimum internal area, ventilation, and fire safety. However, they concluded that further research is essential for this constructive technique to reach its full potential. Sun et al. [42] analyzed the advantages of using container construction in regions with very cold weather. The authors concluded that the system's versatility, combined with the ease of installation and customization possibilities make it adaptable to different locations. In cold weather regions where work schedules must be thought through to avoid periods when workers

are exposed to extreme temperatures, being able to do most of the work inside the factory can save time and money.

Elrayies [10] analyzed the thermal comfort of a container house in a hot and humid climate region. The study was performed through computer simulation, varying the external thermal insulation materials. Materials used were mineral wool, closed-cell spray polyurethane foam (ccSPF), and straw. The author concluded that the use of insulation is essential for habitable containers and that the type of material depends on the local climate. In this case, the most effective insulator was ccSPF. Bowley and Mukhopadhyaya [17] were dedicated to the development of an off-grid passive container house. Although the study is not directly related to temporary shelters, the sustainable design ideas presented are useful for this application, such as the photovoltaic power system, rainwater harvesting, and onsite wastewater treatment. A similar study was conducted by Dumas et al. [43] who developed a model of container housing heated by circulating geothermal water inside the building's outer walls called ZETHa (zero energy temporary habitation). The main objective of the system is to minimize thermal bridges in order to improve the building's internal comfort with less energy consumption. Zhang et al. [44] took a qualitative approach to analyze the societal factors that affect the suitability of containers as temporary post-disaster shelters with a focus on case studies following Hurricane Katrina in the US, the Christchurch Earthquake in New Zealand, and the 2009 Black Saturday bushfire-affected communities in Australia.

Finally, it is important to emphasize that there are other available technologies to be used as temporary post-disaster shelters. Caia et al. [45], for example, investigated the psychological effects suffered by victims of the earthquake in Italy in 1997. The study investigated people's satisfaction with temporary shelters, comparing a control group with people housed in shipping containers and dachas. The results indicated that the victims occupying the containers were very dissatisfied, while those allocated to the dachas felt only a little uncomfortable with the shelter. The authors attributed this feeling to the constructive typology of dachas, more similar to a "real home", that is, built-in wood, with large windows, and traditional sloped roofs. Unlike containers, which are made up of metal boxes with small windows and flat roofs. However, it must be considered that almost two decades have passed and container-building technology has evolved a lot. Currently, containers, despite still being made of metal, can receive thermoacoustic insulation, ensuring the comfort of their occupants. In addition, shipping containers can be customized to resemble traditional construction with large openings, different types of roofing, and even special elements, such as balconies and terraces. However, other technologies must be continuously explored, allowing the constant development of comfortable, cheap, and quick-to-execute solutions.

The analysis of the literature presented in this section shows that there are few studies dedicated to developing sustainability and energy efficiency concepts for temporary container shelters. Therefore, this study constitutes a starting point for a series of research focused on obtaining a standard design for a sustainable, energy-efficient, and autonomous container house to be used as a temporary shelter in tropical countries. In this context, it was decided to first analyze the two most used insulation materials in the cities of Macaé and Uberlândia where the Brazilian authors of the text reside since the next steps of the research will involve field measurements to assess the actual performance conditions of the containers. In future research, other types of containers, changes in architectural design, use of rainwater, photovoltaic and wind energy microgeneration, and the perception of users concerning this type of structure will also be considered. Indeed, when compared with the need to allocate people as quickly as possible, given their emergency use, these issues are usually considered of low importance [2,5]. However, they are fundamental aspects when related to user comfort and the life cycle of this type of building [5].

## 3. Materials and Methods

This research aims to evaluate the energy efficiency of a temporary shelter project built in a container through computer simulation. Therefore, a standard design was developed in a 40-ft HC container where two types of thermal insulating materials were simulated for two different climatic conditions. Figure 2 illustrates the research methodological framework.

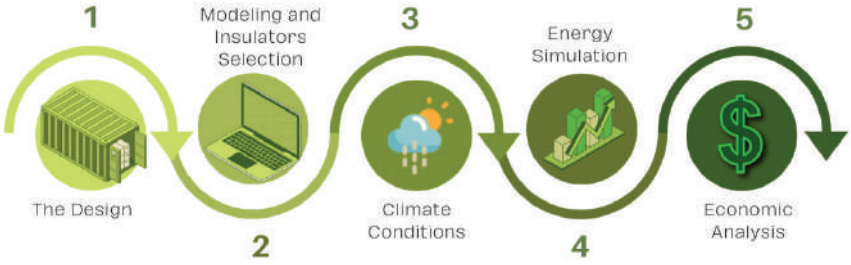


**Figure 2.** Research methodological framework.

### *3.1. The Design*

The proposed temporary shelter consists of a retrofitted 40-foot dry high cube (HC) shipping container module with external dimensions of 12.192 m in length, 2.438 m wide, and 2.590 m in height with an approximate area of 28.28 $m^2$ and an approximate volume of 76.99 $m^3$. The container is made of corten steel, has hinged doors at one end, and its walls are corrugated. This model was chosen because its area allows for greater layout flexibility and better spatial room arrangement in accordance with the recommended minimum dimensions for housing. Furthermore, this is the model that the researchers have at their disposal for carrying out future studies which will involve field measurements. Considering the container's dimensions, the sectorization of the layout began. A 6.98 $m^2$ kitchen integrated into the 7.36 $m^2$ living room, a 3.01 $m^2$ bathroom, and a 7.74 $m^2$ bedroom were defined. Figure 3 shows the final layout configuration.

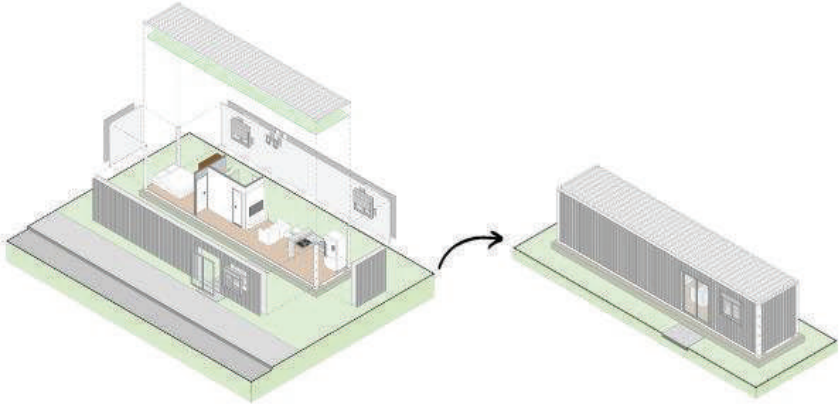

**Figure 3.** Final layout configuration.

### *3.2. Modeling and Insulation Material Selection*

Once the layout was defined, the project was modeled in Autodesk's Revit® 2023 software [46]. Building Information Modeling (BIM) is an information modeling technology that is integrated into a single file, and with that, it is possible to create associations between design, analysis, and documentation as well as communication between the systems that constitute the building. According to Eastman et al. [47], it is a digital model that contains

the exact geometry and information needed to support the design, construction, manufacture, and supply of resources necessary to produce a building. Parametric modeling allows the simulation and evaluation of different design solutions even during the design phase [48]. In addition, professionals from different areas can effectively participate in the design process, generating solutions that contribute to the definition of assertive and efficient choices, a situation that can also benefit the building's energy efficiency. Thus, the model has developed in such a way that each type of wall had its thermal characteristic configured, encompassing the properties of thermal conductivity, specific heat, and density.

Three scenarios for simulating thermal insulation were defined (Table 2). The first was considered a reference model in which thermal insulation was not used. In the other two scenarios, PET wool (polyethylene terephthalate) and mineral wool were used. All other project characteristics were maintained, including the type of connection between the container and the floor. Considering that this is the only uninsulated part of the structure, the option of positioning it on a large concrete base guarantees the reduction of thermal exchanges.

**Table 2.** Summary of the analyzed scenarios.

| Analyzed Scenario | Insulator Thickness (mm) | Insulator Type |
|---|---|---|
| 1 | 0 | No insulator |
| 2 | 50 | PET wool |
| 3 | 50 | Mineral wool |

PET wool is manufactured from plastic bottles and its development is specifically aimed at thermal and acoustic insulation in dry construction. It is a substance that does not absorb water or humidity, therefore, it does not mold and maintains its original characteristics for a long time with a lifespan of up to 100 years. Hence, PET wool is an excellent option for thermal insulation and can be used in several civil construction environments. Mineral wool is made from a volcanic rock called diabase. The manufacturing process starts with the production of fibers that are superheated to transform them into filaments that are agglomerated with resin solutions and result in products that can be light and flexible or very rigid, depending on the degree of compaction. The material is versatile and can be produced in different densities. In the three scenarios, the other materials were considered equal with the external coating painted directly on the container and the internal one in drywall (Figure 4). These two types of insulators are the most used in the regions where the model was simulated. Thus, considering that the future of this research will involve the purchase of this material and the construction of a prototype to perform field measurements, we chose to simulate only products that are easily found for sale in the local market.

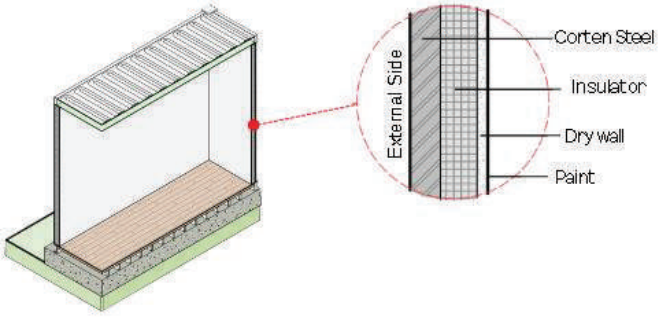


**Figure 4.** Assembly of the analyzed container walls.

The used PET wool was Wall 50 mm polyester blanket, from Ecofiber. This insulator is fully recyclable and being self-extinguishing, that is, it does not propagate flames and it is a lightweight material compared to other insulators. For mineral wool, the material from ISAR was selected. The product is THERMAX® PSL—32 of 50 mm with good thermal resistance, good acoustic insulation, chemical inertia, water resistance, incombustibility, and resilience. A thickness of 50 mm was chosen because it is the standard dimension for different suppliers of these two materials in our region.

Table 3 summarizes the properties of the materials proposed as thermal insulators.

**Table 3.** Insulating materials properties.

| Material | Insulator Thickness (mm) | Thermal Conductivity (W/m.K) | Thermal Resistance ($m^2$.K/W) | Density (Kg/$m^3$) | Thermal Transmittance (W/$m^2$.°C) |
|---|---|---|---|---|---|
| Mineral wool | 50 | 0.031 | 1.61 | 32 | 0.62 |
| PET wool | 50 | 0.041 | 1.20 | 30 | 0.83 |
| Wood floor | 30 | 0.12 | 0.25 | 450 | 4.00 |
| Drywall | 18 | 0.35 | 0.05 | 720 | 19.44 |
| Corten Steel | 2.6 | 55 | $4.72 \times 10^{-5}$ | 7800 | 21,153.85 |

Density, thermal conductivity, thermal resistance, and thermal transmittance are fundamental parameters in determining the efficiency of a thermal insulator, a low transmittance on the external walls of a residence is desirable, thus preventing the large amplitudes of the external environment from reaching the internal environment. In this context, the table above indicates that, despite the two materials having similar densities, the thermal characteristics of mineral wool are slightly superior to those presented by PET wool.

### *3.3. Climate Conditions*

Climate files from two Brazilian cities were selected to be loaded into the eQuest software (version 3.65) [49]. The equipment used to run the simulation was a notebook with 8 GB of memory, 1 TB HDD, Intel Core i7 processor, and 2 GB NVIDIA GEFORCE graphic card. The objective of this engine is to present results in a fast and objective way. Therefore, simulation results were obtained in a few minutes. Both are located in the southeast of Brazil, 1126 km apart. Uberlândia, which belongs to the State of Minas Gerais, is located at an altitude of 863 m and has a tropical high-altitude climate, with heavy rains in summer and droughts in winter. Macaé, belonging to the State of Rio de Janeiro, is located just 2 m above sea level and has a predominantly tropical climate, whose main characteristics are the large volumes of rainfall throughout the year, with summers and winters with high temperatures. These cities were selected because they had similar climatic characteristics in spring and autumn but with greater variations in the summer and winter months (Table 4). Therefore, considering that this paper aims to evaluate the energy efficiency of a container building project, based only on the insulation materials used, that is, disregarding the effects of other architectural decisions, it was considered pertinent to choose cities that present greater variations only in the most extreme temperature months.

**Table 4.** Average, maximum, and minimum temperatures of the analyzed cities.

| City | Medium Temperature | Jan. | Feb. | Mar. | Apr. | May | Jun. | Jul. | Aug. | Sep. | Oct. | Nov. | Dec. |
|---|---|---|---|---|---|---|---|---|---|---|---|---|---|
| Uberlândia | High | 28 °C | 28 °C | 28 °C | 28 °C | 26 °C | 25 °C | 26 °C | 27 °C | 29 °C | 29 °C | 29 °C | 28 °C |
| | Average | 23 °C | 24 °C | 23 °C | 23 °C | 21 °C | 19 °C | 20 °C | 21 °C | 23 °C | 24 °C | 23 °C | 23 °C |
| | Low | 20 °C | 20 °C | 20 °C | 18 °C | 16 °C | 15 °C | 15 °C | 16 °C | 18 °C | 19 °C | 20 °C | 20 °C |
| Macaé | High | 31 °C | 32 °C | 31 °C | 30 °C | 28 °C | 27 °C | 27 °C | 27 °C | 28 °C | 28 °C | 29 °C | 31 °C |
| | Average | 27 °C | 27 °C | 26 °C | 25 °C | 23 °C | 22 °C | 22 °C | 22 °C | 23 °C | 24 °C | 25 °C | 26 °C |
| | Low | 23 °C | 23 °C | 23 °C | 21 °C | 19 °C | 18 °C | 18 °C | 18 °C | 19 °C | 20 °C | 22 °C | 23 °C |

### *3.4. Energy Simulation*

The process of computational energy simulation in a building is known as Building Energy Simulation (BES). BES allows designers to conduct the necessary analyses in the various stages of building modeling in order to predict the real behavior of the building. This makes it possible to select the best design solution.

The BES software chosen for the analysis was the eQuest (Quick Energy Simulation Tool) developed by DOE.com. The software is free and allows calculating the energy consumption of a building throughout the year based on data from climate files in the region where the building is located. Interoperability between modeling (BIM) and energy simulation (BES) tools is usually achieved through data exchange protocols, such as Industry Foundation Classes (IFC) and Green Building Studio XML (gbXML). Existing BIM tools, such as Revit and ArchiCAD, as well as BES softwares, such as Green Building Studio, eQUEST, and IES-VE, support the IFC and gbXML format. As a BIM–BES exchange mechanism, Green Building Studio was applied which is used by Autodesk Revit.

After completing the project modeling in Revit, occupancy data, location, and all the parameters of the materials used were adjusted. The areas were defined as conceptual masses in a total of five (bedroom, bathroom, hallway, living room, and kitchen), and the reference floor was considered on the ground floor. Then, the necessary settings and adjustments were made, and the energy model was generated and exported in gbXML format which was created as an open-source project to facilitate data transfer between BIM files and building energy analysis (BES) software. To produce a Revit gbXML file, the Energy Analysis tool is used which builds an energy simulation model that can be loaded into Autodesk Green Building Studio (GBS), where it will be analyzed for errors, inconsistencies, or flaws in the export. After that, it is possible to export the gbXML file from the GBS cloud service and import it into a BES software that supports gbXML. The benefits of this energy analysis method are the accurate extraction of non-geometric data, such as occupancy, equipment, lighting, thermostat, daily weather data, and outside air information. After checks in Green Building Studio, the files were converted to DOE2 format and analyzed in eQuest software.

The occupancy of two people was considered for simulation, following the minimum pattern recommended by national standards. The use of one air conditioner per room was also considered except for the bathroom. The temperature of 23 °C was considered as the thermal comfort standard to be achieved by the model in the two analyzed cities. That is, the energy consumption for cooling simulated by the model was necessary to maintain the building's internal temperature at 23 °C. This value is within the operating temperature range considered by Brazilian regulations for both summer and winter [50]. To activate the HVAC system (Heating, Ventilation, and Air Conditioning), the recommendation of the ISO 17772-1:2017 [51] was adopted which provides suggestions for the occupancy schedule of single-family residences. Table 5 presents data from the occupancy schedule.

**Table 5.** Occupancy schedule.

| Hour | Devices Use | Lighting | Hour | Devices Use | Lighting | Hour | Devices Use | Lighting |
|---|---|---|---|---|---|---|---|---|
| 01:00 | 50 | 0 | 09:00 | 70 | 15 | 17:00 | 50 | 20 |
| 02:00 | 50 | 0 | 10:00 | 50 | 15 | 18:00 | 70 | 20 |
| 03:00 | 50 | 0 | 11:00 | 50 | 5 | 19:00 | 70 | 20 |
| 04:00 | 50 | 0 | 12:00 | 60 | 5 | 20:00 | 80 | 20 |
| 05:00 | 50 | 0 | 13:00 | 60 | 5 | 21:00 | 80 | 20 |
| 06:00 | 50 | 0 | 14:00 | 60 | 5 | 22:00 | 80 | 20 |
| 07:00 | 50 | 15 | 15:00 | 60 | 5 | 23:00 | 60 | 15 |
| 08:00 | 70 | 15 | 16:00 | 50 | 5 | 24:00 | 60 | 15 |

Source: ISO 17772-1:2017—Energy performance of buildings [51].

Table 6 shows the technical parameters adopted in the eQuest software to perform the simulations:

**Table 6.** Other parameters adopted in the eQuest.

| Parameter | Adopted Option |
|---|---|
| Heat transmission through opaque exterior surfaces | Delayed method via conduction transform functions. |
| Heat transmission through transparent surfaces | 84% glass solar factor |
| Weather data | Based on the Revit database for stations located in the analyzed cities. |
| Occupancy schedules | Based on ISO 17772-1:2017 [51] |
| HVAC System | Residential split/compact system gas residencial 14 SEER/0.9 AFUE < 5.5 ton. |

### *3.5. Economic Analysis*

The economic analysis aimed to identify the cost of each of the insulators used, and the energy savings resulting from its implementation. Initially, in the modeling software itself, the wall, and ceiling areas where the insulators will be applied were determined, totaling 114.60 $m^2$.

Then, the energy consumption (EC) of each simulated model (reference, mineral wool, and PET wool) was verified and multiplied by the cost of kWh in each analyzed city. In Uberlândia, R$0.65313/kWh and in Macaé, R$0.75411/kWh. Based on these data, the lag between the reference model and the models with insulators was calculated and multiplied by the tariff of the energy operators in each city. Monthly values were obtained and then summed to obtain annual consumption. Finally, the initial investment of each system was divided by the proportional annual savings of each one to discover the payback of each system. After determining the payback time, it was verified from which year the investment system would become profitable which would have the best cost–benefit in the long term. For this, the annual savings (AE) was subtracted from the initial investment (II) for a period of 20 years according to Table 7.

**Table 7.** Payback calculation.

| Year | PET Wool | Mineral Wool |
|---|---|---|
| 1 | II—AE1 | II—AE1 |
| 2 | II—(AE1 + AE2) | II—(AE1 + AE2) |
| ( . . . ) | ( . . . ) | ( . . . ) |
| 20 | II—(AE1 + ( . . . ) + AE20) | II—(AE1 + ( . . . ) + AE20) |

## 4. Results and Discussion

### *4.1. Results for Uberlândia*

The simulation was performed over a period of one year, a parameter that was defined in the e-Quest. The results of monthly and annual energy consumption in kWh of electrical energy for cooling were analyzed in the reference model and in the models with thermal insulation. Table 8 indicates that during the months of May, June, July, and August, the energy consumption of the systems using PET wool and mineral wool are virtually the same. This is because in these months the average temperatures are lower, therefore, the demand for cooling decreases and, consequently, the energy consumption. However, it is possible to state that both insulators produced much better results than the reference model (no insulation). In this context, mineral wool had the lowest consumption with savings of 17.13% compared to PET wool and 42.80% compared to the reference model.

**Table 8.** Annual electricity consumption results in each simulated model for Uberlândia.

| Month | Consumption (kWh) | | |
|---|---|---|---|
| | **No Insulation** | **PET Wool** | **Mineral Wool** |
| January | 178.20 | 119.60 | 98.50 |
| February | 175.50 | 119.90 | 95.30 |
| March | 239.60 | 172.90 | 127.20 |
| April | 216.40 | 145.80 | 113.40 |
| May | 126.60 | 79.60 | 79.60 |
| June | 107.90 | 70.10 | 75.60 |
| July | 94.30 | 62.50 | 68.50 |
| August | 133.60 | 88.20 | 90.30 |
| September | 200.00 | 142.20 | 117.10 |
| October | 201.40 | 146.70 | 110.10 |
| November | 178.40 | 127.30 | 98.60 |
| December | 229.70 | 161.90 | 116.40 |
| Annual consumption | 2081.60 | 1436.70 | 1190.60 |

The next step is to calculate the percentage reduction in primary energy consumption (RedCEP) of the housing unit in the real condition compared to the same housing unit in its reference condition. Applying Equation (1) in the scenarios with PET wool and mineral wool, the following results are obtained:

$$RedCEP = \frac{(CEP, ref \times Fce) - (CEP, real \times Fce)}{(CEP, ref \times Fce)} \times 100 \quad (1)$$

- *RedCEP* is the percentage reduction in primary energy consumption of the housing unit in the real model compared to the housing unit in the reference model;
- *CEP*, *ref* is the annual primary energy consumption of the housing unit in the reference model (kWh/year);
- *CEP*, *real* is the annual consumption of primary energy of the housing unit in the real model (kWh/year).
- *Fce* is the energy conversion factor.

After applying the conversion factor, there was a 30.98% reduction in energy consumption with PET wool and a 42.80% reduction with mineral wool (Table 9) when compared to the reference model without insulators. For the economic viability analysis, first, the annual expenditure on electricity was calculated, and, then, the cost of implementing each system. From these data, the payback time of each system was obtained. The cost per kWh used for the city of Uberlândia was R$0.65313. Thus, it was found that the annual cost of the system without insulation was R$1359.56; the PET wool system was R$938.35, and the mineral wool system was R$777.62. The average monthly cost of the system without isolation was R$113.30; in the system with PET wool, it was R$78.20, and in the system with mineral wool, it was R$64.80. Figure 5 shows the cumulative cost of consumption of each system over a year.

**Table 9.** Reduction in primary energy consumption (RedCEP).

| Material | CEP, Ref | CEP, Real | Fce | RedCEP |
|---|---|---|---|---|
| Mineral wool | 2081.60 | 1190.60 | 1.6 | 42.80% |
| PET wool | 2081.60 | 1436.70 | 1.6 | 30.98% |

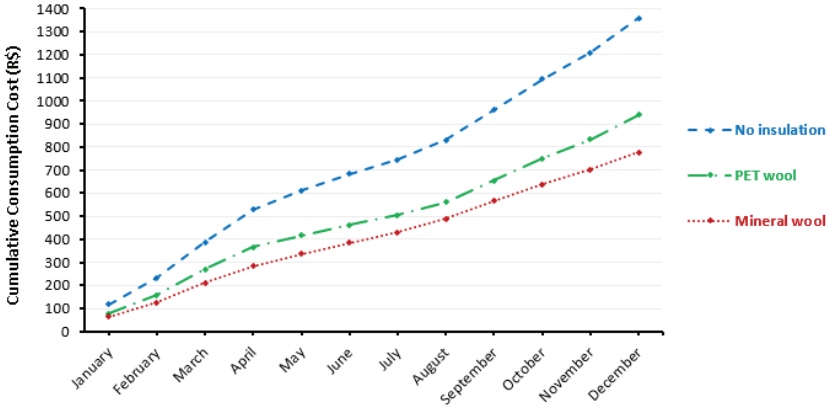


**Figure 5.** Cumulative consumption cost of each scenario for Uberlândia.

For the analyzed period of one year, the system with PET wool generated savings of R$421.20 compared to the system without insulation, and the mineral wool system generated savings of R$581.94, resulting in a difference between the two insulators of R$160.74. Table 10 shows the percentage of savings that each scenario achieved in relation to the scenario without insulation through the monthly comparison between the scenarios that used PET wool and mineral wool. PET wool achieved better results in June, July, and August which are the months with the lowest average temperatures. This is because the thermal resistance of PET wool is lower, so it "retains" less external heat.

**Table 10.** Percentage reduction in electricity costs between the simulated systems for Uberlândia.

| Month | PET Wool X No Insulator | Mineral Wool X No Insulator | Mineral Wool X PET Wool |
|---|---|---|---|
| January | 32.88% | 44.73% | 11.84% [1] |
| February | 31.68% | 45.70% | 14.02% [1] |
| March | 27.84% | 46.91% | 19.07% [1] |
| April | 32.62% | 47.60% | 14.97% [1] |
| May | 37.12% | 37.12% | 0.00% [2] |
| June | 35.03% | 29.94% | 5.10% [3] |
| July | 33.72% | 27.36% | 6.36% [3] |
| August | 33.98% | 32.41% | 1.57% [3] |
| September | 28.90% | 41.45% | 12.55% [1] |
| October | 27.16% | 45.33% | 18.17% [1] |
| November | 28.64% | 44.73% | 16.09% [1] |
| December | 29.52% | 49.33% | 19.81% [1] |

[1] Percentage of reduction that mineral wool achieved in energy costs compared to PET wool. [2] No difference between scenarios. [3] Percentage of reduction that PET wool achieved in energy costs compared to mineral wool.

In order to calculate the payback time, a market survey was carried out to obtain the $m^2$ value of each thermal insulator. The unitary value of each insulator was then multiplied by the areas of the walls and ceilings where the insulators were applied, obtaining the total value of the investment for each material (Table 11).

**Table 11.** Insulators cost.

| Material | Unit Cost (R$/$m^2$) | Area ($m^2$) | Total Cost (R$) |
|---|---|---|---|
| Mineral wool | 25.83 | 114.60 | 2960.12 |
| PET wool | 14.59 | 114.60 | 1672.01 |

It is, then, concluded that for a PET wool system, an investment of R$1671.98 in materials will be necessary, and for a mineral wool system, an investment of R$2960.12 will be required. Subsequently, these values were divided by the annual savings generated by each system, according to Equation (2).

$$Payback\ time = \frac{Initial\ Investment}{Annual\ Savings} \quad (2)$$

The payback time calculated for the scenario that used PET wool will be approximately four years (3.97 years), while in the mineral wool scenario, it will be about one year longer (5.09 years). Thus, Table 12 indicates that up to the eighth year of installation, PET wool is more economical, but from the eighth year onwards the situation is reversed. That is, mineral wool provides greater long-term savings for the city of Uberlândia.

**Table 12.** Annual savings and payback time for the city of Uberlândia over the next 20 years after installation.

| Year | PET Wool (R$) | Mineral Wool (R$) |
|---|---|---|
| 1 | −1250.78 | −2378.12 |
| 2 | −829.57 | −1796.18 |
| 3 | −408.37 | −1214.24 |
| 4 | 12.84 | −632.30 |
| 5 | 434.04 | −50.36 |
| 6 | 855.24 | 531.58 |
| 7 | 1276.45 | 1113.52 |
| 8 | 1697.65 | 1695.45 |
| 9 | 2118.85 | 2277.39 |
| 10 | 2540.06 | 2859.33 |
| 11 | 2961.26 | 3441.27 |
| 12 | 3382.46 | 4023.21 |
| 13 | 3803.67 | 4605.15 |
| 14 | 4224.87 | 5187.09 |
| 15 | 4646.07 | 5769.03 |
| 16 | 5067.28 | 6350.97 |
| 17 | 5488.48 | 6932.90 |
| 18 | 5909.68 | 7514.84 |
| 19 | 6330.89 | 8096.78 |
| 20 | 6752.09 | 8678.72 |

### *4.2. Results for Macaé*

For the city of Macaé, the format in which the analysis was carried out in the city of Uberlândia was repeated. Table 13 indicates that during the months of June, July, and August, the energy consumption of the systems using PET wool and mineral wool are virtually the same. This is because in these months the average temperatures are lower, therefore, the demand for cooling decreases and, consequently, the energy consumption. As in the analysis performed for the city of Uberlândia, it is possible to state that the two insulators produced better results than the reference scenario. Considering that the generated consumption was 2539.3 kWh for the reference model, 1810.7 kWh for the PET wool model, and 1396.8 kWh for the mineral wool model, the mineral wool had the lowest consumption among those analyzed with savings of 22.86% compared to PET wool.

**Table 13.** Annual electricity consumption results in each simulated model for Macaé.

| Month | Consumption (kWh) | | |
|---|---|---|---|
| | No Insulation | PET Wool | Mineral Wool |
| January | 269.60 | 202.50 | 142.00 |
| February | 298.00 | 221.10 | 149.60 |
| March | 307.20 | 223.90 | 153.30 |
| April | 209.10 | 141.30 | 112.00 |
| May | 163.80 | 107.70 | 96.50 |
| June | 103.90 | 63.30 | 68.40 |
| July | 110.70 | 71.80 | 74.10 |
| August | 125.30 | 85.40 | 85.70 |
| September | 170.60 | 120.60 | 103.60 |
| October | 183.60 | 131.30 | 106.00 |
| November | 300.20 | 222.50 | 154.30 |
| December | 297.30 | 219.30 | 151.30 |
| Annual consumption | 2539.30 | 1810.70 | 1396.80 |

The parameters for the calculation of primary energy consumption (RedCEP) for the city of Macaé according to Equation (1) are described in Table 14:

**Table 14.** Reduction in primary energy consumption (RedCEP).

| Material | CEP, Ref | CEP, Real | Fce | RedCEP |
|---|---|---|---|---|
| Mineral wool | 2539.30 | 1396.80 | 1.6 | 44.99% |
| PET wool | 2539.30 | 1810.70 | 1.6 | 28.69% |

After applying the conversion factor, there was a 28.69% reduction in energy consumption with PET wool and a 44.99% reduction with mineral wool when compared to the reference model without insulators. For economic viability analysis, the same process applied to the city of Uberlândia was used. The cost per kWh used for the city of Macaé was R$0.75411. Thus, it was found that the annual cost of the system without insulation was R$1941.91, the PET wool system R$1365.47, and the mineral wool system R$1053.34. The average monthly cost of the system without isolation was R$159.58, in the system with PET wool, it was R$113.79, and in the system with mineral wool, it was R$87.78. Figure 6 shows the cumulative cost of consumption of each system over a year.

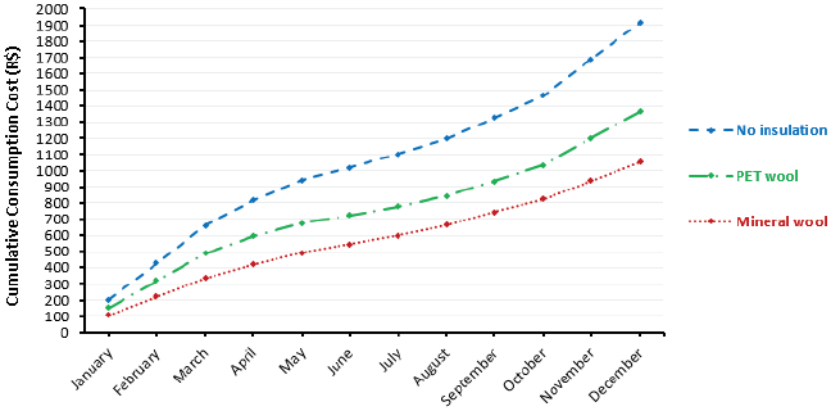


**Figure 6.** Cumulative consumption cost of each scenario for Macaé.

For the analyzed period of one year, the system with PET wool generated savings of R$549.44 compared to the system without insulation, and the mineral wool system

generated savings of R$861.57, resulting in a difference between the two insulators of R$312.13. Table 15 shows the percentage of savings that each scenario achieved in relation to the scenario without insulation through the monthly comparison between the scenarios that used PET wool and mineral wool. PET wool achieved better results in June and July which are the months with the lowest average temperatures. This is because the thermal resistance of PET wool is lower, so it "retains" less external heat.

**Table 15.** Percentage reduction in electricity costs between the simulated systems for Macaé.

| Month | PET Wool X No Insulator | Mineral Wool X No Insulator | Mineral Wool X PET Wool |
|---|---|---|---|
| January | 24.89% | 47.33% | 22.44% [1] |
| February | 25.81% | 49.80% | 23.99% [1] |
| March | 27.12% | 50.10% | 22.98% [1] |
| April | 32.42% | 46.44% | 14.01% [1] |
| May | 34.25% | 41.09% | 6.84% [1] |
| June | 39.08% | 34.17% | 4.91% [3] |
| July | 35.14% | 33.06% | 2.08% [3] |
| August | 31.84% | 31.60% | 0,24% [2] |
| September | 29.31% | 39.27% | 9.96% [1] |
| October | 28.49% | 42.27% | 13.78% [1] |
| November | 25.88% | 48.60% | 22.72% [1] |
| December | 26.24% | 49.11% | 22.87% [1] |

[1] Percentage of reduction that mineral wool achieved in energy costs compared to PET wool. [2] No difference between scenarios. [3] Percentage of reduction that PET wool achieved in energy costs compared to mineral wool.

The payback time calculation was performed based on Equation (2) and on the insulator installation values indicated in Table 11. The payback time calculated for the scenario that used PET wool will be approximately three years (3.04 years) while in the mineral wool scenario, it will be about five months longer (3.44 years). Thus, Table 16 indicates that up to the fourth year of installation, PET wool is more economical but from the fourth year onwards the situation is reversed. That is, mineral wool provides greater long-term savings for the city of Macaé.

**Table 16.** Annual savings and payback time for the city of Macaé over the next 20 years after installation.

| Year | PET Wool (R$) | Mineral Wool (R$) |
|---|---|---|
| 1 | −1122.54 | −2098.49 |
| 2 | −573.10 | −1236.92 |
| 3 | −23.66 | −375.35 |
| 4 | 525.78 | 486.22 |
| 5 | 1075.22 | 1347.79 |
| 6 | 1624.66 | 2209.36 |
| 7 | 2174.10 | 3070.93 |
| 8 | 2723.54 | 3932.50 |
| 9 | 3272.98 | 4794.07 |
| 10 | 3822.42 | 5655.64 |
| 11 | 4371.86 | 6517.21 |
| 12 | 4921.30 | 7378.78 |
| 13 | 5470.74 | 8240.35 |
| 14 | 6020.18 | 9101.92 |
| 15 | 6569.62 | 9963.49 |
| 16 | 7119.06 | 10,825.06 |
| 17 | 7668.50 | 11,686.63 |
| 18 | 8217.94 | 12,548.20 |
| 19 | 8767.38 | 13,409.77 |
| 20 | 9316.82 | 14,271.34 |

### *4.3. Comparison between Scenarios*

The comparison of energy consumption results between the analyzed scenarios for the two cities indicates that in Macaé where average monthly temperatures are higher, the use of thermal insulation becomes more advantageous, providing greater savings, especially in the medium and long term. Table 17 compiles the obtained results and highlights the difference between the analyzed scenarios.

**Table 17.** Difference in electricity consumption in kWh between the cities of Uberlândia and Macaé for the three analyzed scenarios.

| | Uberlândia (kWh) | Macaé (kWh) | Consumption Difference (kWh) | Consumption Difference (%) |
|---|---|---|---|---|
| No insulator | 2081.60 | 2539.30 | 457.70 | 18.02 |
| PET wool | 1436.70 | 1810.70 | 374.00 | 20.65 |
| Mineral wool | 1190.60 | 1396.80 | 206.20 | 14.76 |

Table 18 shows the comparison of the payback time. It is noticed that in Macaé, the payback time is shorter than in the city of Uberlândia, since the annual savings in electricity is greater and, consequently, the financial savings. In other words, in the city of Uberlândia, the investment with the installation is paid in four years for PET wool and five years and one month for mineral wool. In Macaé, both insulators pay for themselves in about three years. From the payback onwards, the application of the two insulators starts to generate passive savings for the system.

**Table 18.** Payback time for each system in the two cities.

| | Uberlândia | Macaé |
|---|---|---|
| PET wool | 4 years | 3 years |
| Mineral wool | 5 years and 1 month | 3 years and 5 months |

Regarding the cost-effectiveness of each system, it is noticed that in Uberlândia the PET wool system has a greater advantage over the mineral wool system up to the eighth year. After the eighth year, the relationship is inverted. In Macaé, very similar results were obtained, but this inversion occurs in the fifth year of installation. It is important to point out that the greater savings generated in Macaé are also due to the fact that the cost of kWh is higher in this city than in Uberlândia, that is, a difference of approximately 13.40%.

## 5. Conclusions

The main objective of this paper was to analyze alternatives for thermal insulation applied to the inner part of the envelope of a shipping container with the purpose of using it for construction of emergency housing construction. It is noticeable that in recent years the frequency and intensity of natural disasters have been increasing, influenced by the lack of urban planning, disorderly growth of cities, and climate change. Therefore, it is important that more studies are conducted both to mitigate the damage caused by disasters and to prevent them from recurring frequently over the years.

The results indicated that mineral wool had an advantage in reducing electricity consumption for cooling the housing unit. For the city of Uberlândia, the system with PET wool reduced the consumption of electricity by 30.98%, while the system with mineral wool achieved an annual reduction in consumption of 42.80%. In the city of Macaé, the reduction in electricity consumption with PET wool was 28.69%, and the system with mineral wool saved 44.99% within a year. Furthermore, the analysis of the scenarios when the average monthly temperatures are lower indicates that PET wool obtains better results when compared to mineral wool.

Regarding the life cycle of the materials, both PET wool and mineral wool do not suffer deformations and deterioration over the years, therefore, the insulators do not have

an estimated lifespan. Therefore, this criterion does not exempt the use of any material following the building life cycle. Concerning the installation cost, it was evident that mineral wool is the most expensive insulation option, being 45.52% more expensive than PET wool. However, in the long term, the mineral wool system is more cost-effective in both cities compared to PET wool.

The results indicate that in the city of Uberlândia, PET wool has a payback time of approximately four years while for mineral wool it is five years and one month. In turn, in the city of Macaé, the PET wool system had a payback time of three years while for mineral wool it is three years and five months. In this context, in Uberlândia, the mineral wool system obtained a better cost–benefit ratio from the eighth year onwards while in Macaé, from the 5th year onwards. Thus, in terms of energy efficiency, mineral wool stands out in relation to PET wool in both cities, however, in financial terms, the system with PET wool proved to be more efficient during the first eight years of installation in the city in Uberlândia and the first five years in the city of Macaé.

Although computer simulation is being increasingly used to analyze different alternative techniques and construction materials, thus guiding design decisions, this research is subjected to some limitations that should be considered, and some may serve as a stimulus for future work. First, this paper considers only two types of insulating material, PET wool and mineral wool which are the most common in the studied cities. Future research should consider a wider variety of insulators, thus expanding the validity of the results. Second, computer simulation has evolved a lot in recent years, but the reliability of the results directly depends on the parameters adopted during the modeling and simulation steps. In this context, the results of similar studies may vary according to the adopted material parameters, climatic data, and software used. It is suggested that future research analyze the effect of each of these characteristics on this model. Third, this research only considered the energy consumption related to the cooling of the housing unit due to the tropical climate of the analyzed cities which rarely requires heating of buildings aiming at thermal comfort. Future research should analyze the insulator's behavior in regions with different climatic conditions.

Finally, this research focused on analyzing the effect of insulating the inner surfaces of the container. Possible treatments related to the structure's external surface were not considered. Corten steel, the material that makes up the container's sides, has high thermal conductivity and reflectance. However, these two properties can be improved using special paints or coatings. Since the thermal conductivity of this material has a direct impact on the building's internal environment, its high reflectance can impact the entire surroundings. The re-emission of long-wave radiation from the sun reflected in containers can result in an unwanted increase in the temperature of the local microclimate, mainly in regions with a high concentration of buildings in containers. Future research should analyze the impact of changes in the outer covering of container houses and their influence on the surroundings. Therefore, current research can be extended in several directions, and one of them is the comparison of simulation results with field data. Research on the subject will follow this direction for this group.

**Author Contributions:** Conceptualization, C.F.P.S. and A.C.F.M.; methodology, C.F.P.S., A.C.F.M. and B.B.F.d.C.; software, C.F.P.S.; validation, H.D.P.C., G.M. and A.N.H.; formal analysis, H.D.P.C., G.M. and A.N.H.; investigation, B.B.F.d.C., C.F.P.S. and A.C.F.M.; resources, C.F.P.S., A.C.F.M. and B.B.F.d.C.; data curation, C.F.P.S.; writing—original draft preparation, B.B.F.d.C. and C.F.P.S.; writing—review and editing, B.B.F.d.C., A.C.F.M., H.D.P.C., G.M. and A.N.H.; visualization, B.B.F.d.C. and C.F.P.S.; supervision, B.B.F.d.C. and A.C.F.M.; project administration, B.B.F.d.C. and A.C.F.M. All authors have read and agreed to the published version of the manuscript.

**Funding:** This research received no external funding.

**Institutional Review Board Statement:** Not applicable.

**Informed Consent Statement:** Not applicable.

**Data Availability Statement:** Not applicable.

**Acknowledgments:** Assed Haddad would like to acknowledge Conselho Nacional de Desenvolvimento Científico e Tecnológico (CNPq), and Fundação Carlos Chagas Filho de Amparo à Pesquisa do Estado do Rio de Janeiro (FAPERJ), which helped in the development of this work. Bruno B. F. da Costa would like to acknowledge Prefeitura Municipal de Macaé which helped in the development of this work.

**Conflicts of Interest:** The authors declare no conflict of interest.

## References

1. Norwegian Refugee Council. *Children and Youth in Internal Displacement*, 1st ed.; The Internal Displacement Monitoring Centre: Geneva, Switzerland, 2022; p. 12.
2. Ling, P.C.H.; Tan, C.S.; Saggaff, A. Feasibility of ISO shipping container as transitional shelter—A review. *IOP Conf. Ser. Mater. Sci. Eng.* **2019**, *620*, 012056. [CrossRef]
3. Hong, Y. A study on the condition of temporary housing following disasters: Focus on container housing. *Front. Archit. Res.* **2017**, *6*, 374–383. [CrossRef]
4. Lin, H.; Cheng, J. A study of the simulation and analysis of the flow field of natural convection for a container house. *Sustainability* **2020**, *12*, 9845. [CrossRef]
5. Tanyer, A.M.; Tavukcuoglu, A.; Bekboliev, M. Assessing the airtightness performance of container houses in relation to its effect on energy efficiency. *Build. Environ.* **2018**, *134*, 59–73. [CrossRef]
6. Dumas, A.; Trancossi, M.; Madonia, M.; Bonnici, M. A novel concept of container house with zero energetic consumption. *SAE Int.* **2012**, *1*, 1507. [CrossRef]
7. Bertolini, M.; Guardigli, L. Upcycling shipping containers as building components: An environmental impact assessment. *Int. J. Life Cycle Assess.* **2020**, *25*, 947–963. [CrossRef]
8. Shi, M. Assessment of the impact of windows and building orientation on the energy intensity of container houses using BIM. *IOP Conf. Ser. Earth Environ. Sci.* **2021**, *769*, 022023. [CrossRef]
9. Pereira-de-Oliveira, L.A.; Bernardo, L.F.A.; Marques, A.R.A. Architectural building design with refurbished shipping containers: A typological and modular approach. *J. Eng. Res.* **2022**, *10*, 1–20. [CrossRef]
10. Elrayies, G.M. Thermal performance assessment of shipping container architecture in hot and humid climates. *Int. J. Adv. Sci. Eng. Inf. Technol.* **2017**, *7*, 1114–1126. [CrossRef]
11. Shen, J.; Copertaro, B.; Zhang, X.; Koke, J.; Kaufmann, P.; Krause, S. Exploring the potential of climate-adaptative container building design under future climates scenarios in three different climate zones. *Sustainability* **2020**, *12*, 108. [CrossRef]
12. Koke, J.; Schippmann, A.; Shen, J.; Zhang, X.; Kaufmann, P.; Krause, S. Strategies of design concepts and energy systems for nearly zero-energy container buildings (NZECBs) in different climates. *Buildings* **2021**, *11*, 364. [CrossRef]
13. Dara, C.; Hachem-Vermette, C.; Assefa, G. Life cycle assessment and life cycle costing of container-based single-family housing in Canada: A case study. *Build. Environ.* **2019**, *163*, 106332. [CrossRef]
14. Tan, C.S.; Ling, P.C.H. Shipping container as shelter provision solution for post-disaster reconstruction. *E3S Web Conf.* **2018**, *65*, 08007. [CrossRef]
15. Islam, H.; Zhang, G.; Setunge, S.; Bhuiyan, M.A. Life cycle assessment of shipping container home: A sustainable construction. *Energy Build.* **2016**, *128*, 673–685. [CrossRef]
16. Giiriunas, K.; Sezen, H.; Dupaix, R.B. Evaluation, modeling, and analysis of shipping container building structures. *Eng. Struct.* **2012**, *43*, 48–57. [CrossRef]
17. Bowley, W.; Mukhopadhyaya, P. A sustainable design for an off-grid passive container house. *Int. Rev. Appl. Sci. Eng.* **2017**, *8*, 145–152. [CrossRef]
18. Musa, M.F.; Yusof, M.R.; Mohammad, M.F.; Samsudin, N.S. Towards the adoption of modular construction and prefabrication in the construction environment: A case study in Malaysia. *ARPN J. Eng. Appl. Sci.* **2016**, *11*, 8122–8131.
19. Chatzimichailidou, M.; Ma, Y. Using BIM in the safety risk management of modular construction. *Saf. Sci.* **2022**, *154*, 105852. [CrossRef]
20. Lacey, A.W.; Chen, W.; Hao, H.; Bi, K. Structural response of modular buildings—An overview. *J. Build. Eng.* **2018**, *16*, 45–56. [CrossRef]
21. Ye, Z.; Giriunas, K.; Sezen, H.; Wu, G.; Feng, D. State-of-the-art review and investigation of structural stability in multi-story modular buildings. *J. Build. Eng.* **2021**, *33*, 101844. [CrossRef]
22. Rakotonjanahary, M.; Scholzen, F.; Waldmann, D. Summertime overheating risk assessment of a flexible plug-in modular unit in Luxemburgo. *Sustainability* **2020**, *12*, 8474. [CrossRef]
23. Cao, X.; Li, X.; Zhu, Y.; Zhang, Z. A comparative study of environmental performance between prefabricated and traditional residential buildings in China. *J. Clean. Prod.* **2015**, *109*, 131–143. [CrossRef]
24. Kristiansen, A.B.; Zhao, B.Y.; Ma, T.; Wang, R.Z. The viability of solar photovoltaic powered off-grid zero energy buildings based on a container home. *J. Clean. Prod.* **2021**, *286*, 125312. [CrossRef]

25. Jeong, G.; Kim, H.; Lee, H.; Park, M.; Hyun, H. Analysis of safety risk factors of modular construction to identify accident trends. *J. Asian Archit. Build. Eng.* **2022**, *21*, 1040–1052. [CrossRef]
26. Ahn, S.; Crouch, L.; Kim, T.W.; Rameezdeen, R. Comparison of worker safety risks between onsite and offsite construction methods: A site management perspective. *J. Constr. Eng. Manag.* **2020**, *146*, 05020010. [CrossRef]
27. Manuel, B.; Arif, B.T.K.T.; Thibaut, G.; Paul-George, I.; Joseph, R.; Kein, V.B. Sea Container Building. Bachelor's Thesis, Universitat Politècnica de Catalunya, Barcelona, Spain, 14 June 2017.
28. Moore, C.M.; Yildirim, S.G.; Baur, S.W. Educational adaption of cargo container design features. In Proceedings of the ASEE Zone III Conference, Springfield, IL, USA, 23–25 September 2015.
29. Su, M.; Yang, B.; Wang, X. Research on integrated design of modular steel structure container buildings based on BIM. *Adv. Civ. Eng.* **2022**, *2022*, 4574676. [CrossRef]
30. International Residential Code. Available online: https://archive.org/download/gov.law.icc.irc.2009/icc.irc.2009.pdf (accessed on 28 January 2023).
31. *ISO 668:1995*; Series 1 Freight Containers-Classification, Dimensions and Ratings. International Organization for Standardization: Geneva, Switzerland, 1995.
32. *ISO 830:1999*; Freight Containers-Vocabulary. International Organization for Standardization: Geneva, Switzerland, 1999.
33. *ISO 6346:1995*; Freight Containers Coding, Identification and Marking. International Organization for Standardization: Geneva, Switzerland, 1995.
34. *ISO 1496-1:1990*; Series 1 Freight Containers-Specification and Testing—Part 1: General Cargo Containers for General Purposes. International Organization for Standardization: Geneva, Switzerland, 1990.
35. *ISO 1161:1984/Cor 1:1990*; Technical Corrigendum 1:1990 to ISO 1161:1984. International Organization for Standardization: Geneva, Switzerland, 1990.
36. *ISO 2308:1972*; Hooks for Lifting Freight Containers of up to 30 Tonnes Capacity-Basic Requirements. International Organization for Standardization: Geneva, Switzerland, 1972.
37. *ISO 3874:1997*; Series 1 Freight Containers Handling and Securing. International Organization for Standardization: Geneva, Switzerland, 1997.
38. International Maritime Organization. *International Convention for Safe Containers*; International Maritime Organization: London, UK, 1996.
39. Zafra, R.G.; Mayo, J.R.M.; Villareal, P.J.M.; De Padua, V.M.N.; Castillo, M.a.H.T.; Sundo, M.B.; Madlangbayan, M.S. Structural and thermal performance assessment of shipping container as post-disaster housing in tropical climates. *Civ. Eng. J.* **2021**, *7*, 1437–1458. [CrossRef]
40. Obia, A.E. Architectural adaptation of the shipping container for housing the internally displaced persons in South-South Nigeria. *Int. J. Archit. Eng. Constr.* **2020**, *9*, 1–9. [CrossRef]
41. Wong, E.K.H.; Tan, C.S.; Ling, P.C.H. Feasibility of using ISO shipping container to build low cost house in Malaysia. *Int. J. Eng. Technol.* **2018**, *7*, 933–939. [CrossRef]
42. Sun, Z.; Mei, H.; Ni, R. Overview of modular design strategy of the shipping container architecture in cold regions. *IOP Conf. Ser. Earth Environ. Sci.* **2017**, *63*, 012035. [CrossRef]
43. Dumas, A.; Trancossi, M.; Madonia, M.; Coppola, M. Zero emission temporary habitation: A passive container house acclimatized by geothermal water. *J. Sol. Energy Eng.* **2014**, *136*, 044505. [CrossRef]
44. Zhang, G.; Setunge, S.; Elmpt, S. Using shipping containers to provide temporary housing in post-disaster recovery: Social case studies. *Procedia Econ. Financ.* **2014**, *18*, 618–625. [CrossRef]
45. Caia, G.; Ventimiglia, F.; Maass, A. Container vs. dacha: The psychological effects of temporary housing characteristics on earthquake survivors. *J. Environ. Psychol.* **2010**, *30*, 60–66. [CrossRef]
46. Revit: BIM Software for Designers, Builders, and Doers. Available online: www.autodesk.com (accessed on 15 January 2023).
47. Eastman, C.; Teicholz, P.; Sacks, R.; Liston, K. *BIM Handbook: A Guide to Building Information Modeling for Owners, Managers, Designers, Engineers and Contractors*, 1st ed.; Bookman: Porto Alegre, Brazil, 2014.
48. Filho, M.V.A.P.M.; da Costa, B.B.F.; Najjar, M.; Figueiredo, K.V.; Mendonça, M.B.; Haddad, A.N. Sustainability assessment of a low-income building: A BIM-LCSA-FAHP-based analysis. *Buildings* **2022**, *12*, 181. [CrossRef]
49. eQUEST: The Quick Energy Simulation Tool. Available online: www.doe2.com/equest (accessed on 15 January 2023).
50. *ABNT 16401-2:2008*; Central and Unitary Air Conditioning Systems. Part 2: Thermal comfort. Brazilian Association of Technical Standards: São Paulo, Brazil, 2008.
51. *ISO 17772-1:2017*; Energy Performance of Buildings—Indoor Environmental Quality—Part 1: Indoor Environmental Input Parameters for the Design and Assessment of Energy Performance of Buildings. International Organization for Standardization: Geneva, Switzerland, 2017.

MDPI
St. Alban-Anlage 66
4052 Basel
Switzerland
www.mdpi.com

*Designs* Editorial Office
E-mail: designs@mdpi.com
www.mdpi.com/journal/designs

Academic Open
Access Publishing

www.mdpi.com

ISBN 978-3-0365-8567-3